FIRE RESISTANT LIGHT WEIGHT SANDWICH COMPOSITES FOR MARINE APPLICATIONS

CHEN ZHOU

A thesis submitted to the University of Bolton in partial fulfilment of the requirements for the degree of Doctor of Philosophy

Institute for Materials Research and Innovation

University of Bolton

Deane Road, Bolton, BL3 5AB

United Kingdom

June 2020

Declaration of authorship

I declare that the work described in this PhD thesis has not been previously presented in any form to the University or to any other institutional body, whether for assessment or for other purposes. I confirm that the intellectual content of the work is the result of my own original research and of no other person.

Signed……

Date ……

Acknowledgements

Firstly, I would like to express my sincere appreciation and gratitude to my supervisor, Professor Baljinder K. Kandola, for giving me the opportunity to carry out this PhD research project and for her guidance, continuous support and motivation throughout my PhD. This work could have never been done without her valuable suggestions and patience.

I would also like to thank Professor John R. Ebdon for his valuable comments and help with the proofreading of my thesis during my writing up stage. I am very grateful to Professor Peter Myler for his invaluable assistance in this project. I am also very grateful to Professor Geoffrey Gibson for the opportunity to access the facilities in the fire laboratory at the University of Newcastle to carry out part of my experimental work.

Special thanks go to Dr John Milnes, Mr Akbar Zarei and Mr Ali A. Sharhani for their technical help and support with the experimental procedures. I would like to deliver my thanks also for the help given by Professor Richard Horrocks, Dr Mamadou Ndiaye, Dr Gill Smart and my friends, all of who were involved directly or indirectly in bringing this thesis to fruition. Also, I would like to extend my thanks to my colleagues: Awni, Nima, Sara, Rob, Maram, Mo, Gianmarco, Bartosz, Trishan, Fran, Annan, Raj, Katie and all other members of our Fire Materials Research Group at the IMRI, University of Bolton, for their guidance and support and in helping to facilitate this PhD project.

My special thanks go to my parents, Ming Zhou and Xingjuan Chen, for their endless love, care, support and encouragement. Finally, many thanks to my wife, Yawen Liu, for her love, support and great endurance during my PhD journey.

Thank you so much, all of you.

Abstract

Sandwich composites being lightweight materials, are increasingly being used in high-performance applications such as in transportation (aviation, marine and railway) due to their high specific stiffness, strength, fatigue, corrosion resistance and thermal insulation. Despite these favourable properties, their poor fire resistance is a major limiting factor for their usage in many engineering applications. Sandwich structures are generally composed of thin composite laminates as skins and thick, low-density materials (e.g. balsa, foam) as cores. Fibres such as glass/carbon used for reinforcement in composite skins are non-flammable and can retain their chemical and physical stability at relatively high temperatures. So, flammability of skins of composites arises mainly from the resin (matrix) part. Hence the preferred way to control the flammability of composites is to choose a resin of low flammability or reduce its flammability by adding additive or reactive flame-retardant chemicals. Blending of a flammable resin with an inherently flame-retardant resin is another simple and effective physical way to reduce its flammability.

The main aim of this research was to investigate the thermal properties and fire resistance of some light weight sandwich composites, that could be potentially used in marine applications. To achieve this, firstly, resins commonly used for marine and aerospace applications (unsaturated polyester (UP), vinyl ester (VE), epoxy) and some inherently fire-resistant resins (e.g. phenolic resins), which could be used alone or blended with UP and/or VE were selected. These resins were cast into plaques and characterised for their thermal properties via thermogravimetric analysis and fire performances by means of pyrolysis combustion flow calorimetry and cone calorimetry. The fire safety assessment diagram (total heat release plotted against the flashover propensity values, calculated by dividing peak heat release rate by time-to-ignition) from the cone tests gave an indication of the overall fire safety, the trend being phenolics followed by UP, VE and epoxy, in descending order of fire safety. The fire safety of blends was in between those of the respective phenolic and UP/VE resins. The correlations between several fire parameters collected from different test methods were also assessed.

In the second step, sandwich composites with similar components (glass fibre-reinforced UP composite laminates as skins and balsa wood as a core) but with different compositions were prepared. The design variables consisted of: two different thicknesses of core materials (12.7 mm (0.5 inch) and 25.4 mm (1 inch)), lay-ups (skins on one side or on both sides) and three different sample preparation techniques (resin infused laminates as skins on both sides, hand lay-up laminates as skins on both sides, and hand lay-up sandwich structure in one go). Their fire performances were evaluated by two different standard fire tests - cone calorimetry and propane burner testing at heat fluxes of 50 and 113 kW/m^2, respectively. In both tests, temperatures through the thickness of the samples were measured using thermocouples from which their thermal barrier performances could be studied. The results indicated that there was a minimal effect of the cone heater orientation or sample preparation technique, however,

samples containing thicker balsa core or composite laminates on both sides showed better thermal barrier performances (lower heat transfer), the behaviour in the former was due to the physical and thermal thickness of the thick core sample, giving rise to a larger volume of the charred wood. In spite of similar flammability of composite laminates on one side or on both sides, the glass fabric on rear side in the latter reduced the rate of burning, therefore resulted in a lower mass loss rate. Following these observations, the design selected for further study was: composite laminates on both sides, balsa core thickness of 25.4 mm (1 inch), and sample preparation technique involving hand lay-up sandwich structure in one go.

A number of sandwich composites were then prepared using different resins and resin blends/combinations impregnated as matrices for skins, keeping all other composition variables constant. This also included skins prepared from three layers of UP or UP/VE impregnated glass with a top glass fibre layer impregnated with a phenolic resin. Their fire and thermal barrier properties were studied and results analysed to select parameters that could be used to assess their overall fire-resistant properties. During cone and propane burner tests, the temperature differences in the top and back skin surfaces (measured using thermocouples) were used to calculate apparent thermal conductivities and resistivity values of the sandwich composite's charred residue, which gave an insight into the thermal barrier properties of the chars from different resin types. The overall fire performances indicated that introducing phenolic resins, either incorporated as blends with UP or VE, or applied as a top layer, helped in reducing the flammability of the composite, the latter approach giving the best results. Using cone parameters the same as those used for cast plaques, fire safety plots were obtained, from which overall flammability of different resin types and their blends could be ranked. However, this approach does not include heat transfer through the thickness of the samples, which affects the time to burn-through in a composite. Therefore, a novel thermal barrier efficiency index, including cone parameters of peak heat release rate, time-to-ignition, and also time taken for the back surface temperature to reach 300 °C in cone or propane burner test, was proposed to combine both the fire and thermal barrier properties, and plotted against total heat release values from cone tests for all sandwich composites. This changed the trend previously seen from cone parameters only. UP or VE/phenolic blended resins, while performing very well in cone and other flammability tests such as UL-94, show relatively poorer performance in the burn-through test. This was attributed to the higher thermal conductivity of the highly crosslinked char from the phenolic component. Hence, considering both fire and thermal barrier performances, while phenolic blends were still safer than UP or VE resins, the difference was less than that judged on the basis just the burning behaviour.

Among different designs, the best fire performance was exhibited by the sandwich composite prepared with both skins comprising one layer of phenolic resin on top of three UP or VE layered structures. The thin layer of phenolic skin seemed to be very effective in improving the overall flammability of the sandwich structure by either preventing or delaying ignition, whereas it had a minimal effect on the thermal barrier performance (burn-through property) of the composite.

Table of contents

List of Figures

List of Tables

Nomenclature

Abbreviations	Description
APP	Ammonium polyphosphate
ASTM	American Society for Testing and Materials
ATH	Alumina trihydrate
CFE	Critical flux at extinguishment
CO	Carbon monoxide
CO_2	Carbon dioxide
DMTA	Dynamic mechanical thermal analysis
DOPO	9,10-dihydro-9-oxa-10-phosphaphenanthrene-10-oxide
DSC	Differential scanning calorimetry
DTA-TGA	Differential thermal analysis-thermogravimetric analysis
EG	Expandable graphite
EHC	Effective heat of combustion
EP	Epoxy
FAA	Federal Aviation Administration
FIGRA	Fire growth rate
FO	Time-to-flame-out
FRP	Fibre-reinforced plastic
FTP	Fire Test Procedure
FTPC	Fire Test Procedure Code
FTT	Fire Testing Technology
GFRC	Glass fibre-reinforced composites
GRE	Glass fibre-reinforced epoxy
GRP	Glass reinforced plastic
HL	Hand lay-up laminates as skins on both sides
HLAll	Hand lay-up sandwich structure in one go
HRC	Heat release capacity
HRR	Heat release rate

HSC	High Speed Craft
IMO	International Maritime Organization
Int.	Intumescent
ISO	International Organization for Standardization
LOI	Limiting oxygen index
LVI	Low velocity impact
MARHE	Maximum average rate of heat emission
MMVF	Man-made vitreous fibres
MP	Melamine phosphate
N_2	Nitrogen
O_2	Oxygen
PCFC	Pyrolysis combustion flow calorimetry
PH	Phenolic
PH-Res	Phenolic resoles
PHRR	Peak heat release rate
PS	Polystyrene
PU	Polyurethane
PVC	Poly(vinyl chloride)
res.	residue
RI	Resin infused laminates as skins on both sides
RSR	Rate of smoke release
RT	Room temperature
RTM	Resin transfer moulding
SOLAS	International Convention for the Safety of Life at Sea
TBI	Thermal barrier efficiency index
TC	Thermocouple
Temp.	Temperature
TGA	Thermogravimetric analysis
THR	Total heat release
TSR	Total smoke release
TTI	Time-to-ignition

UP	Unsaturated polyester
UP-R	Unsaturated polyester, resin infusion purpose
VE	Vinyl ester
VE-Ep	Vinyl ester epoxy based
VE-Nov	Vinyl ester novolac phenolic based
wt	weight
w.r.t.	with respect to
3UP1M	UP; top one layer of Methylon
3UP/VE1M	UP/VE-Nov; top one layer of Methylon

Symbols	**Description**
Δ	Changes in parameters with respect to controls
ΔT	Temperature difference
H	Thickness
K	Thermal conductivity
K_{Comp}	Thermal conductivity of composite skins
K_{Ep}	Thermal conductivity of epoxy composite
K_f	Thermal conductivity of fibre
K_m	Thermal conductivity of matrix
K_{PH}	Thermal conductivity of phenolic composite
K_{UP}	Thermal conductivity of unsaturated polyester composite
K_{VE}	Thermal conductivity of vinyl ester composite
L	Thickness of the material
Q''	Heat flux per unit area
Qp	Peak heat release rate
Qsb	Heat for sustained burning
Qt	Total heat release
R	Thermal resistivity
R	Correlation coefficient
t	Time to reach
T_0	Top surface temperature
T_b	Back surface temperature

T_g	Glass transition temperature
T_{max}	The temperature at the maximum heat release rate
T_{max}	Time to reach maximum temperature
T_{onset}, $T_{10\%}$	The onset of decomposition temperature, at which 10% mass loss occurs
T_{PHRR}	Time to peak heat release rate
V_f	Fibre volume fraction of the composite
V_m	Matrix volume fraction of the composite

Chapter 1: Introduction and literature review

This PhD thesis, entitled “Fire resistant light weight sandwich composites for marine applications” mainly deals with sandwich structures, in which the skins consist of crosslinked thermoset glass fibre-reinforced composite layers from different types of resins and their blends. In order to understand the basics of sandwich structures, and the effects on flame retardance and other properties of different resins and co-blended resins used in their construction, this background survey of the relevant literature has been conducted. Gaps in the current understanding of the fire-resistant composites are identified, which form the basis for the research performed as part of this PhD project.

1.1 Sandwich composite structures

The need for innovative lightweight materials such as fibre-reinforced polymeric composites in transport and construction industries has rapidly increased in the last few years. This is due to their low weight-to-strength ratio, cost-effectiveness, high-strength and ease of processing [1,2]. A composite laminate is made of fibres (used for reinforcement) impregnated with a resin (matrix). Fibres usually used are glass or carbon and the resin could be unsaturated polyester, vinyl ester, epoxy or phenolic [3,4]. For marine application glass fibre-reinforced unsaturated polyester or vinyl ester composites are used. In rail applications, either these or epoxy composites are popular.

To increase the volume-to-weight ratio, quite often sandwich structures are used [2]. Sandwich-structured composites consist of two thin but stiff faces bonded to a lightweight but thick core. Faces are typically of some composite laminates with different types of resins as matrices and fibres as reinforcements. Polymer matrices can be classified under two types, 'thermoplastic' and 'thermosetting' according to the effect of heat on their properties.

1.1.1 Thermoset matrix resins

Thermoset resins are network-forming polymeric materials [5-8] and they are made from polymers that can form chemical cross links between reactive groups on their chains binding the polymer molecules together in three dimensional networks [6]. The process of cross linking is called “curing” and it is often an irreversible reaction. Before curing, the resin is in a liquid or viscous state and during the curing process, initially the resin will flow due to change in viscosity with heat, then the cross linking starts and finally it becomes a solid material after the completion of curing. Once the thermoset resin is completely cured, it cannot melt, deform and flow under the influence of heat like thermoplastic polymers [9]. The three-dimensional network can be formed in different ways such as condensation type polymerisation, use of cross-linking species and by addition polymerization of monomers containing two double bonds [9]. The curing

reaction or crosslinking reaction can be at ambient temperature or at high temperature with or without use of catalysts depending on the nature of the polymer.

There are certain important factors to be considered while handling and processing the thermoset resins, i.e., gel time, gel temperature and glass transition temperature (T_g). The gel temperature is the temperature at which the crosslinking of the resin starts (starting temperature of the cross-linking formation). Cured thermoset resins cannot melt like thermoplastic polymers when heated, even though above a certain temperature their mechanical properties will alter considerably. This temperature is the glass transition temperature (T_g) of the resin, a type of softening temperature, and it varies with respect to chemical structure of the resin system, degree of cure and the efficiency of mixing.

Thermoset resins are extensively used in various applications such as aerospace, automotive, marine and adhesives etc., owing to their strength, toughness and higher thermal resistance. Depending on the structure and properties of the thermoset resin, the application of each type of thermoset resin varies. The most widely used thermoset resin materials are discussed below.

Unsaturated polyester resins

Unsaturated polyester (UP) resins are one of the most commonly used thermosetting polymer types in the world [10,11]. UP resins contain internal double bonds that can be chain extended and crosslinked, and they are prepared by reaction of aliphatic diols with unsaturated and saturated diacids, and diluted with unsaturated co-reactant diluents, such as styrene, using a peroxide initiator [12]. The crosslinking reactions of unsaturated polyesters include radical polymerizations between a pre-polymer that contains unsaturated groups and styrene [13,14]. UP is widely used as coatings and constitutive matrices of chopped glass fibre-based composites of sheet moulding and bulk moulding compounds [10,11]. UP is used in various fields such as construction, electronic and transportation owing to their good mechanical properties, low density, low cost and easy processability characteristics [15]. In spite of UP having several good properties, it is highly flammable. Owing to its intrinsic chemical composition and molecular structure, it produces large quantities of smoke and toxic gases (e.g. from styrene) when burnt [16,17]. However, UP resin can be flame retarded by different methods.

Vinyl ester resins

Vinyl ester (VE) resins are most widely recognised as materials with excellent corrosion resistance mainly employed in anti-corrosion coatings of tanks, pipes and ducts. The vinyl ester molecules have good water resistance and resistance to many other chemicals. Sometimes they are used as a barrier or ‘skin’ coat for a polyester laminate that is to be immersed in water, such as in boat hulls.

Vinyl ester resins are generally formed initially by reaction of an epoxy resin precursor with acrylic or methacrylic acid, which provide unsaturated terminal sites [18-22] followed by reaction with styrene. As a result of the presence of reactive acrylate ester at the terminal ends of the molecular chain, the vinyl ester cross linking is at the ends of the molecular chain through the carbon – carbon double bonds (C=C) rather than throughout the chain as in unsaturated polyesters. Since this results in lower cross-linking density, vinyl esters are normally tougher than unsaturated polyester resins and the existence of fewer ester groups in vinyl ester resins helps in improving water and moisture resistance [23]. The vinyl ester resin contains 30 to 60% styrene by weight as a diluent and a bridging component in the curing process [18]. In vinyl ester resin, the crosslinking occurs by free–radical polymerisation with organic peroxides as initiators. During curing, the initiator opens up double carbon bonds on the vinyl ester and styrene molecules and forms cross linkages between them [18]. The rate of the cross linking/curing reaction mainly depends on the temperature and concentration of the monomer and initiator, which also determines the mechanical properties of the cured resin [24-27].

Epoxy resins

Epoxy (EP) resin is one of the most extensively used thermoset resins because of its excellent mechanical strength, low cure shrinkage, a relatively high maximum use temperature, excellent adhesion to glass fibres and good resistance to environmental degradation [28-31]. Based on their curing temperature, epoxy resins can be classified into room temperature resins and high temperature resins [32,33]. Uncured epoxy resins are generally in liquid form and are mixed with chemical additives (in significant amounts) known as curing agents or hardeners, both react with each other to become a part of the crosslinked network for chain extension and crosslinking of epoxy groups in the presence of curing agents. These curing agents can be amines (aliphatic or aromatic), or anhydrides [30]. Under the influence of heat the mixture eventually turns into a rigid three-dimensional network. On the other hand, for room temperature resins, heating is not required. The curing temperatures can vary from 5 °C to 260 °C, depending on the types of the base resin and the choice of curing agent [29,33]. Furthermore, depending on the chemical structure of the cured epoxy resin, its T_g varies from 120 - 220 °C [34].

Phenolic resins

Phenolic (PH) resin is generally known as an ‘inherently flame retardant’ resin owing to its high aromatic character. Phenolic resins are formed by the condensation reaction between phenol and formaldehyde of which water is the by-product [35]. Based on the type of phenol used, and the ratio of phenol to formaldehyde, phenolic resins are divided into two main types, resole type, which are inherently crosslinkable, and novolac type, to which a further source of formaldehyde needs to be added to bring about cure. When a cured phenolic resin is subjected to flame, it chars rather than melts or burns. So, it can be used in applications that are sensitive to flammability and smoke requirements, such as the interior of aircraft, rocket nozzles and

aerospace applications, etc. Phenolic resins can be used in plywood, printed circuit boards, foundry shells and cores, sandpaper, brake linings and grinding wheels. Owing to their low thermal conductivities, phenolic resins can be used for pan handles, bases for toasters, knobs for appliances and motor housings [35]. In addition, they have high electrical resistance, which is useful in electrical switches, circuit breakers, connectors and commutators, cabinets for radios and automotive electrical parts. The main drawbacks of phenolic resins are their brittleness and high curing shrinkage [36]. In addition, the great disadvantage of phenolic resin processes is that they are characterised by a complex process of polymerisation (cure) with generation of water and formaldehyde, with consequent formation of voids. Therefore, the processing of phenolic materials requires careful temperature control and gradual heating to allow continuous elimination of volatiles and to reduce the number of defects in final components [37].

In general, polymeric matrix resins in common use, and hence of importance as mentioned above, are unsaturated polyester, vinyl ester, epoxy and phenolic resins. Those were selected in common, and/or of potential, use on naval vessels/marine industry reported in a related EUCLID survey [38], indicating that the major resin in naval use is polyester based, which is relatively cheap but which shows poor fire properties. Polyester based materials were the dominant composites tested, as they constitute the bulk of naval composites. Vinyl ester resins show improved hydrolysis resistance and mechanical properties to polyester, but have similar poor fire properties. Epoxy resins have good ageing and mechanical characteristics, but again similar fire properties to polyester. Epoxy resins are used more extensively in rails/aerospace industry than naval applications. Other resins with good fire reaction properties are the phenolics, the drawback with these though are their poorer mechanical performance.

1.1.2 Thermoplastic matrix resins

Unlike thermosetting resins, which are crosslinked during curing, thermoplastics (polyethylene, polystyrene, polyester, nylon, acrylic, polypropylene, etc.) contain no crosslinking bonds and hence, move freely when the polymer reaches its melting/softening point [23]. Thermoplastics soften to a liquid in high heat, and then harden again when cooled. Hence, they can be moulded into a variety of shapes and structures, making thermoplastic resins applicable to many industries.

Reinforced thermoplastic composites are not as common as thermoset composites. The compounding operation tends to be more expensive for thermoplastics than for thermosets, and thermoset laminates normally offer better mechanical properties [39]. In recent years, however, interest in more environmentally friendly materials has led to a rise in the use of thermoplastic composites. Not only are thermoplastics recyclable, but they do not give off harmful emissions (e.g. styrene from UP and VE resins) when manufactured.

1.1.3 Fibre reinforcement

Fibres are the predominant reinforcing material used in advanced composites owing to their high strength and stiffness [40]. Fibres can be used in the form of continuous or discontinuous, depending on the application and manufacturing process (see Figure 1.1). The Figure 1.1 is adopted from [40]. In Figure 1.1, (a), (b) and (c) are continuous fibres and (d) and (e) are discontinuous fibres.

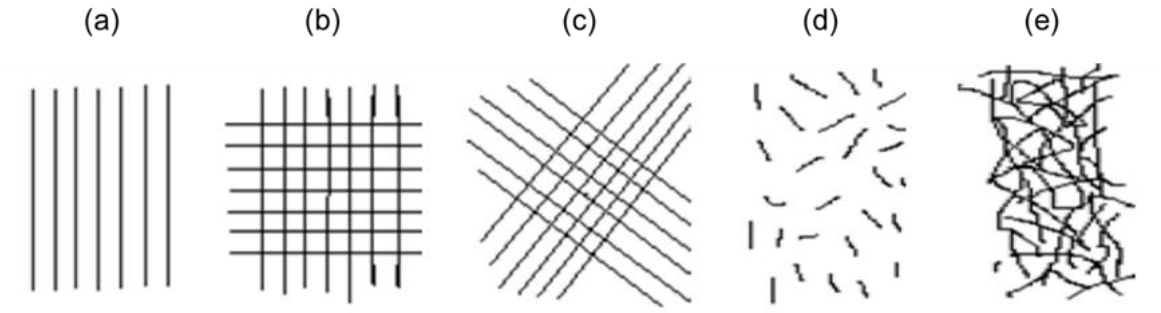

Figure 1.1: Fibre reinforcement types in composites; (a) unidirectional, (b) woven fabric, (c) roving, (d) chopped fibres, (e) fibre mat

In addition, properties of the composites are dependent on the certain fibre properties: the type of fibre, form of the fibre, fibre orientation, volume fraction of the fibre etc., In terms of cost, carbon fibres are the most expensive, followed by aramid, S-glass and E-glass [23].

Glass fibres

Glass fibres are most widely used in structural composites because of their good mechanical, chemical, electrical properties, low price and processability [41,42]. There are mainly three types of glass: E-glass (E for electrical) fibres possess low electrical conductivity, C-glass (C for corrosion) possess high corrosion resistance and chemical durability and S-glass (S for strength) usually have high strength. E-glass is the most commonly used type of glass fibre for polymeric composites. The main advantages of E-glass fibres are their good tensile and compressive strengths and stiffness, good electrical properties and low cost [33].

Carbon fibres

Carbon fibres are the most prevalent fibre forms used in high-performance composite structures. They generally exhibit superior tensile and compressive strength, have high moduli, excellent fatigue properties, high resistance to corrosion and creep [23]. Their impact strength, however, is lower than either glass or aramid, and they are brittle [33]. Some other disadvantages of carbon fibres are their low strains-to-failure, and higher cost than glass fibres [23].

Aramid fibres

Aramid fibres are man-made organic fibres with stiffness and strength intermediate between those of glass and carbon [23], Dupont's Kevlar fibre is the most prevalent para-aramid fibre. Aramid fibres are lightweight (low density) and have a combination of good tensile strength and modulus, excellent toughness, and outstanding ballistic and impact resistance. Moreover, they can absorb large amounts of energy during fracturing, which results from their high strain-to-failure values and their ability to undergo plastic deformation in compression [23]. The fibres also offer good resistance to abrasion and chemical and thermal degradation. However, the fibre can degrade slowly when exposed to ultraviolet light [33].

In summary, considering the overall cost, physical and mechanical performances of various fibres, E-glass fibre is more preferred in the marine industry because it is an affordable high-performance fibre.

1.1.4 Core materials

In order to reduce weight and save labour costs, core materials such as honeycombs, balsa, or foams are often used to produce sandwich composites [23]. The core is normally a low strength material, but its higher thickness provides the sandwich composite with high bending stiffness with overall low density [43]. The core materials of the sandwich structure are mainly of the following types: foam or solid, honeycomb, web and a corrugated or truss core [44]. In rail applications, balsa wood, honeycomb structures and polymer foams are prevalent as core materials. There are a large number of combinations and materials that can be used, each having its own specific pros and cons [45].

The most commonly used wood core is end-grain balsa. Balsa wood core's first usage was reported in the 1940s in flying boat hulls, made of aluminium skins and balsa-core, which could withstand the repeated impact of landing on water. This performance led the marine industry to begin using end-grain balsa as a core material in fibre-reinforced plastic (FRP) constructions. Balsa has high compressive properties, is a good thermal insulator offering good acoustic absorption, it will not deform when heated and acts as an insulating and ablative layer in a fire with the core charring slowly, allowing the non-exposed skin to remain structurally sound. It also offers positive flotation in the case of a boat hull [33]. Hence for marine applications usually balsa wood is used as a core [44], yet one of the disadvantages of balsa is that it is exacerbated by the fact that balsa can absorb large quantities of resin during lamination, although pre-sealing the surface of balsa can reduce this [33].

Another type of the core material, honeycomb, made of aluminium or aramid, can be processed into both flat and curved composite structures and can be made to conform to compound curves without excessive mechanical force or heating [33]. Properties of honeycomb materials depend

on the size of the cells and the thickness and strength of the web material. Honeycomb cores can give stiff and very light laminates; however, due to their very small bonding area, they are almost exclusively used with high-performance resin systems such as epoxies so that the necessary adhesion to the laminate skins can be achieved [33].

The foam core is frequently used in an adhesively bonded structure. Foams can be made from a variety of synthetic polymers including polystyrene (PS), polyurethane (PU), polyvinyl chloride (PVC), from which closed-cell polyvinyl chloride (PVC) foams are one of the most commonly used core materials for the construction of high-performance sandwich structures. Although the properties of foam cores are not as good as those of honeycomb cores, they are extensively used in commercial applications such as boat building and light aircraft construction. However, water absorption can be a problem in both open- and closed-cell foams [23].

A relative cost-performance comparison for different core materials shows that honeycomb cores are more expensive than foam cores but offer superior performance, which explains why many commercial applications use foam cores, which are also easier to work with, while aerospace applications use the higher-performance but more expensive honeycombs. Balsa wood's cost and performance are intermediate compared with the other two types, and is a popular choice for marine applications [23].

1.1.5 Fabrication techniques for sandwich structured composites

While composites can be prepared by several different techniques, such as use of pre-pregs, hand lay-up, resin transfer moulding, injection moulding, etc. in marine applications vacuum assisted resin infusion is commonly used. Resin infusion is a sophisticated and cost effective fabrication technique for manufacturing high performance, void-free composites even on large or complicated shaped composite structures [46]. By making use of this method, a high fibre volume fraction (between 43 and 60%) can be achieved at a vacuum pressure of the order of 1 bar [47-49]. This process is ideally suitable for the manufacture of composites used by professional manufacturers for the production of body panels of cars and in marine application for the production of boat hulls [50,51].

1.2 Properties and performances of sandwich composites

The performances and the properties of the sandwich composites are evaluated by various tests. The important properties of composites such as thermal properties and flammability are discussed in this section.

1.2.1 Application related fire performance challenges of sandwich structures

Applications of sandwich construction in the marine industry include ship funnels, masts,

propellers and secondary structures, which have increased over the past decades. However, the growing use of sandwich structures by the marine industry has led to many technical challenges, especially with regard to their fire performance that includes low softening temperatures of the resins and high flammability. The fire structural response of sandwich composites at elevated temperature and in fire depends on the heat-induced softening and damage to both the skins and core. Composites are reactive at high temperature due to the polymer matrix phase of the skins and the organic core, which can cause the sandwich material to decompose, ignite and burn [52]. However, distortion, creep and collapse often occur prior to flaming combustion due simply to heat-induced softening of the organic materials within sandwich composites [53-55].

A severe ship fire occurred on a Norwegian minesweeper in November 2002 that dramatically highlighted the fire hazard of sandwich composites [56]. The fire started in the propulsion system of KNM Orkla, which was built of sandwich composite material. The fire grew and spread rapidly due in part to the failure of the fire suppression system and lasted for more than 24 hours. The ship was totally destroyed. This incident has concerned many navies in terms of the fire safety of sandwich composites. For this reason, there is a need to understand the fire resistance of sandwich composites under typical ship fire conditions.

Studies on the fire performance of sandwich composites are focused on both fire reaction and fire resistance properties. Fire reaction describes the flammability and smoke toxicity of the combustible material. Some of the important fire reaction properties that affect growth of fire are heat release rate, time-to-ignition, flame spread rate, and oxygen index. Other reaction properties relate to the fire hazard, such as smoke density and gas toxicity. Fire resistance describes the burn-through resistance and mechanical integrity of a loaded material or structure during and after fire exposure. Resistance to fire also defines the ability of a material or structure to limit the spread of fire from room to room. These fire parameters can be evaluated using small, intermediate or full-scale test methods. These tests are able to provide information on the mechanical integrity and burn-through resistance of the sandwich structural design for a specific fire test condition.

1.2.2 Fire resistant properties of sandwich composites under fire scenarios

Introduction to composites in fire

The response of composite laminates to fire is complex and depends on many parameters, including the temperature and oxygen content of the fire, and the composition and thermal properties of the fibre reinforcement and polymer matrix. Figure 1.2 shows the basic processes involved in the thermal decomposition of a laminate in fire [56]. The polymer matrix and organic fibres will soften and thermally decompose when the laminate is heated above a critical temperature. Volatile gases and smoke are released as by-products of the decomposition

reaction process. The gases flow out from the decomposing composite into the flame zone where the flammable volatiles (mostly low molecular hydrocarbons) react with oxygen to cause the composite to ignite and burn. Ignition can only occur when there is a sufficient concentration of flammable decomposition gases released into the fire and the oxygen in the fire environment is above a minimum concentration (typically 10 - 12%). When insufficient oxygen is present, then smouldering ignition (i.e. non-flaming combustion) of the composite can occur. The combustion process at the boundary between the fire and composite involves a complex number of exothermic reactions which generate heat. The heat released by the combustion of flammable gases adds to the fuel load of the fire, causing a rise in flame temperature and flame spread rate.

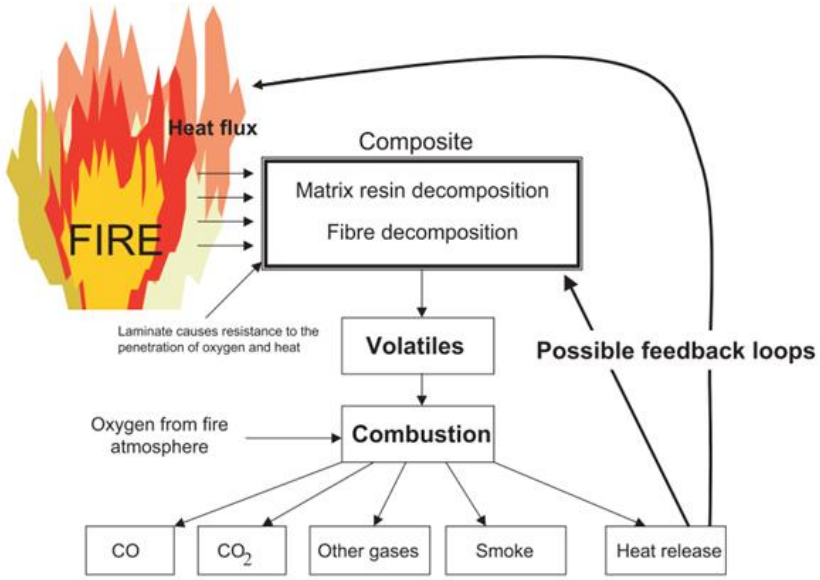

Figure 1.2: General processes for a composite in fire [56]

The fire response of sandwich materials is more complicated than for composite laminates because the temperature, damage and residual properties are controlled by the multi-material configuration of the skins and core. The general processes shown in Figure 1.2 also occur for sandwich composite materials, and the only significant difference is the contribution of the core. Organic core materials such as polymer foam or balsa wood can thermally decompose with the release of flammable volatiles that can increase the heat release rate of the composite. Understanding the reduction to the structural properties of laminates and sandwich composites in fire requires an in-depth understanding of the thermal, chemical (decomposition), physical damage, softening and failure mechanisms [52]. Figure 1.3 shows the processes involved for a hot decomposing polymer laminate exposed to one-sided radiant heating by fire [56].

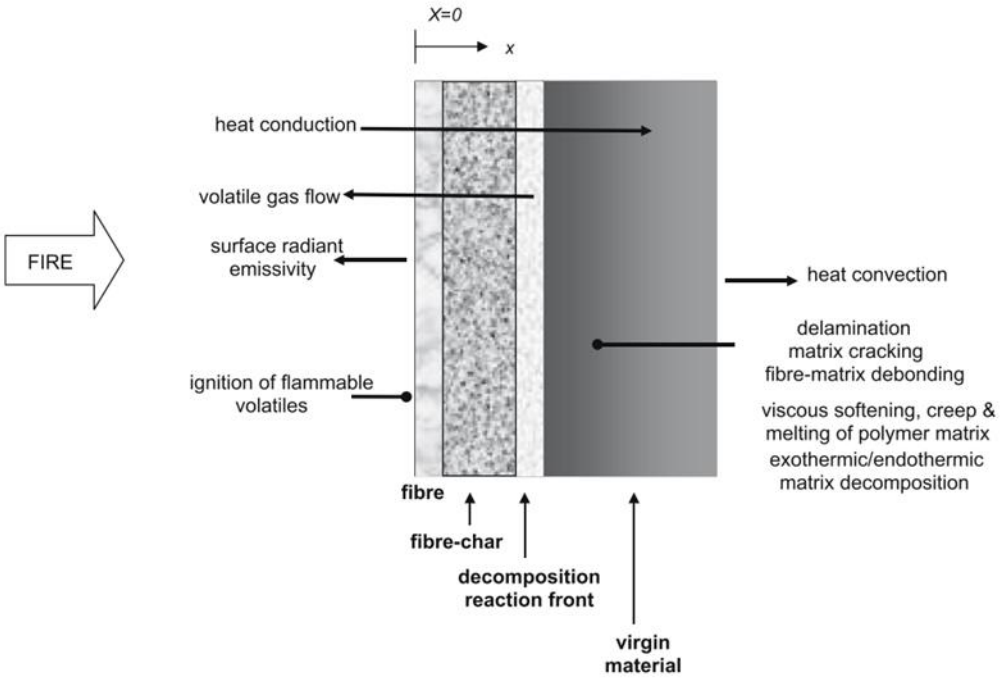

Figure 1.3: Schematic of the reaction processes of laminates exposed to fire [52]

Fire reaction and fire resistance of composites

Fire reaction is a general term in fire science that defines the flammability and combustion properties of materials, including laminates and sandwich composites. Certain fire reaction properties influence the growth and spread of fire. Other fire reaction properties are critical to human survival in fire. Some of the most important fire reaction properties are time-to-ignition, heat release rate, peak heat release rate, smoke density, limiting oxygen index (LOI), and flame spread rate [57]. The fire reaction properties of many types of laminates and several types of sandwich composites have been characterised, and lots of reaction data for different fire (heat flux) conditions has been published [57-62].

Fire resistance is different to fire reaction, which describes the physical and mechanical resistance of materials to fire attack. Fire resistance defines the softening and damage caused to materials, including the loss of mechanical properties during fire and the post-fire properties after the flame has been extinguished. Fire resistance also defines the ability of a material or structure to limit burn-through. Fire resistance is critical to the safe use of load-bearing composites in aircraft, ships, rails and buildings as their structures may collapse or fail due to losses in strength, stiffness and creep resistance.

Figure 1.3 shows the major thermal, chemical and physical processes that occur in composites exposed to fire. The thermal response of a composite is determined by heat conduction from the fire into the material together with surface radiation and convection effects. The internal temperature of the composite is also affected by ignition of flammable volatiles released by decomposition of the polymer matrix and organic fibres, the mass flow of volatiles from the

decomposition zone to the fire, and also the endothermic or exothermic heat resulting from the decomposition reactions of the matrix. Various physical changes occur when composites are exposed to fire, such as viscous softening; melting and vaporisation of the polymer matrix; softening and melting of glass fibres; oxidation of carbon fibres, growth and oxidation of char; char-glass fibre reactions; and matrix and delamination cracking [56]. All of the processes shown in Figure 1.3 can affect the structural integrity of composites in fire. Many of the processes occur simultaneously, thus make the modelling/simulation of a composite material in fire a complex problem. Understanding these processes and how they interact is crucial to understanding the effects of fire on composite structures.

The response of composites to fire can be generally described as follows. In the initial stage of fire, the radiant heat flux emitted by the flame is partially absorbed (with some reflected) and then conducted through the composite. The rate of heat conduction is determined by the incident heat flux (source of heat) and the thermal conductivity of the composite. Due to the relatively low thermal conductivity of most composite materials, a steep thermal gradient can occur in thick materials. The thermal gradient is often greater in sandwich composites than in laminates due to the low heat conduction of the low-density core. As the composite heats-up it will expand, and below the glass transition temperature (T_g) the amount of expansion is determined by the coefficient of the thermal expansion of the composite which can change with increasing temperature as the material undergoes phase changes.

As the composite heats-up it will eventually reach the decomposition temperature of the polymer matrix. The decomposition temperature depends on the chemical composition of the matrix and the heating rate and oxygen content of the fire. Most organic resin systems used in structural composites (e.g. unsaturated polyesters, vinyl esters, epoxies) decompose over the range of 250 - 500 °C. The long molecular chains of the polymer network break-down via a complex series of chain scission reactions. The decomposition process yields low molecular weight hydrocarbons, carbon monoxide and other volatiles as well as yielding a porous carbonaceous solid char. The volatiles flow from the heated surface of the composite outwards and this has a convective cooling effect that partially counteracts the heat conduction process. The flow of volatiles also stops air from diffusing into the decomposing composite, and therefore the decomposition process occurs in the absence of air. For this reason, many of the chain scission reactions are endothermic (rather than exothermic), and this reduces the internal temperature. The polymers commonly used in engineering composites lose about 70 - 95% of their mass as volatiles during the decomposition process, and the residual mass is transformed into char.

Physical processes involve thermal expansion and contraction; development of thermally-induced strains; internal pressure build-up due to volatiles and vaporised moisture; formation of gas-filled pores; matrix cracking; fibre-matrix interfacial debonding; delamination damage; surface ablation; and softening, melting and fusion of fibres [52]. These physical processes influence the structural behaviour of composites in fire along with the heat flux and duration of

the fire; the magnitude and type of load (tension, compression, bending, torsion, etc.); and the geometry of the composite structure [52].

The approximate temperatures over which the processes described above occur in glass fibre-reinforced composites are shown in Figure 1.4 [52,56]. A similar condition occurs for carbon fibre composites, although fibre oxidation must be considered and this commences at temperatures above 500 °C [63]. The condition for sandwich composite will be different and more complex due to the core material. Cracks and other damage within the decomposing core need to be taken into account as it will change the thermal behaviour of the sandwich composite under load. As a result, the internal temperature of the core may depend on the stress applied to the sandwich composite.

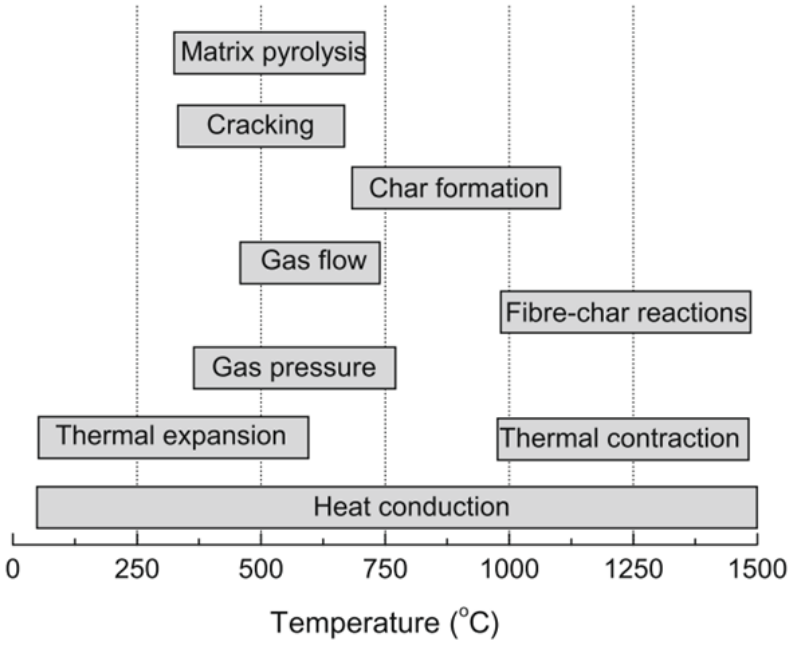

Figure 1.4: Various responses of glass fibre-reinforced composites to temperatures (The temperatures are approximate, and will depend on the polymer matrix type and fire conditions) [52]

Heat transfer in composite laminates/sandwich structures and heat transfer modelling of composites in fire

Accurate modelling of the heat transfer through the composite is a critical part of assessing the structural response of a composite laminate and/or sandwich composites exposed to fire. In the investigation of heat transfer in solid materials, three distinct modes of thermal energy transfer are usually considered, i.e., thermal conduction, convection and radiation. However, for simplicity in the analysis, almost all mathematical models for composites have only considered the effect of heat conduction under the condition of one-sided heating. The influence of heat transfer by external convection, such as airflow across the hot surface of a composite, is not usually considered. Similarly, the radiation of heat from a composite is also not usually taken into account [56]. The rate of heat conduction is determined by the incident heat flux (source of

heat) and the thermal conductivity of the composite, which could give more insight into thermal properties of each component in a sandwich structure. Main important parameters affecting the thermophysical properties in sandwich composites, such as thermal conductivity, specific heat capacity, density of each component, are discussed and some existing models for heat transfer are reviewed in the following sections.

Thermophysical properties of different components in sandwich structures

Thermal conductivity is an important physical property and it is the ability of a material to conduct heat. It represents the energy (quantity of heat) transferred per unit area and time under a temperature gradient of 1 kelvin per metre [64]. Thermal conductivities of different components (resin matrices, balsa wood, glass fibres) at room temperature are given in Table 1.1.

Table 1.1: Thermal conductivities of components in sandwich composites

	Thermal conductivity (W/m.K)	References
E-glass at 20 °C, – parallel to fibre direction	1.04 - 1.09	[65,66]
Unsaturated polyesters	0.2	[65]
Vinyl esters	0.2	[39,65]
Epoxy	0.1	[65]
Phenolics	0.21 - 0.35	[67-70]
Balsa wood 150 Kg/m^3 at 24 °C	0.0649	[71]
Rigid and contourable end-grain balsa core materials	0.0509 - 0.0890	[72]
Polypropylene	0.2	[65]

It can be observed from the table above that in general thermoset resins such as unsaturated polyesters and vinyl esters and the thermoplastic such as polypropylene have similar thermal conductivities at room temperature. Epoxy has a lower value, whereas different types of phenolic resins have a higher range of thermal conductivity values. Different types of balsa wood have a much lower range of thermal conductivity compared to all thermoset and thermoplastic resins. Glass fibre, however, has a much higher value than either resins or wood.

Specific heat capacity of a material is the amount of energy required to raise the temperature of 1 kg of the substance by 1 °C. It is of importance as it can give an indication of the energy needed to heat up or cool down a substance of a given mass to the desired temperature.

It is well known that the thermal conductivities and specific heat capacities of materials are temperature and material state dependent [56], which is an important factor while modelling heat transfer in composite laminates or sandwich composites [73]. These properties may vary considerably at high temperatures due to changes in resin volume fraction, and also as a consequence of pyrolysis reactions [74-76]. Within the composite skins also while density will change, thermal conductivity and specific heat capacity of components, will be changing

constantly as decomposition progresses through the composite. However, temperature dependent thermal conductivity and specific heat capacity values of different resins and core materials are not available in the open literature. Only a few experimental studies are cited. One example is work reported by Dimitrienko [77], shown here in Figure 1.5 as the variation in the through-thickness thermal conductivity of a glass/epoxy composite with temperature. Composite laminates manufactured were of dimensions 200 × 200 mm^2 and thickness 10 mm. Measurement of the transverse thermal conductivity of the composite was performed by using the static method with a constant gradient of temperature. In static methods, it is necessary to determine the heat flow and the temperature gradient along the specimen, measuring the temperature at two or more different places [78]. The interval of temperatures investigated was from 20 to 800 °C in air (plotted as x-axis in Figure 1.5). When glass fibre-reinforced epoxy composites are initially heated above room temperature, their thermal conductivity rises due to increases in the thermal conductivities of both the fibres and polymer matrix. When the pyrolysis temperature of the polymer matrix is reached, the thermal conductivity drops substantially due to the formation of a porous char network. After completion of the pyrolysis reactions, the thermal conductivity rises again due to the increasing thermal conductivity of the char with temperature [56].

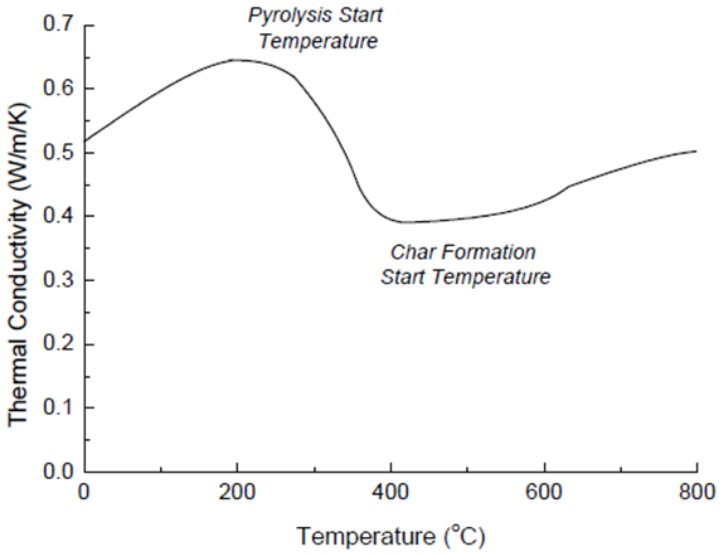

Figure 1.5: Effect of temperature on the through-thickness thermal conductivity of a glass/epoxy composite [77]

It is not easy to experimentally measure these thermophysical properties (thermal conductivity, specific heat capacity, density, etc.) of individual components in a sandwich structure over the broad temperature range of interest. Some available methods include infrared flash thermography, and measurement of the rate of heat conduction over a fixed distance during non-uniform heating of a composite by thermocouples [56].

The main limitation and challenge for the heat transfer modelling is the inadequacy of experimental data as mentioned above especially with thermal conductivity and specific heat

capacity values at high temperatures for the materials to be considered. Although some empirical equations have been proposed [77,79,80] to determine the thermal conductivities of components, these are only applicable to specific materials and require experimental data. As explained previously in Section 1.2.2, due to more complicated structure of sandwich composites than composite laminates, i.e., the thermophysical, chemical (decomposition), temperature, physical damage and residual properties are controlled by multi-material configuration of the skins and core. Core materials can also thermally decompose with the release of flammable volatiles that can increase the heat release rate of the composite [52].

Generally, the main heat transfer models predict the temperature profile within the materials on exposure to defined one-sided heat/fire conditions. While it is outside the scope of this thesis to review heat transfer models, selected processes considered in various heat transfer models are summarised in Table 1.2.

Table 1.2: Summary of the main processes when a composite is exposed to one-sided heating by fire. The numbers refer to the references that described the models. The symbols mean that the model considers (√) or does not (x) consider the process [52].

Main processes	References				
	[81]	[82]	[83]	[77]	[84]
Heat conduction through virgin material and char	√	√	√	√	√
Decomposition of polymer matrix and organic fibres	√	√	√	√	√
Flow of gases from the reaction zone through the char zone	√	√	√	√	√
Thermal expansion/contraction	x	√	√	√	x
Pressure rise (due to formation of combustion gases and vapourisation of moisture)	x	√	√	√	x
Formation of delamination, matrix cracks and voids	x	x	x	x	x
Reactions between char and fibre reinforcement	x	x	x	x	x
Ablation	x	x	√	x	x

According to the literature, the initial work of heat transfer modelling of composites in fire can be dated back to mid-1940s, commencing with the fire behaviour of wood [85-90]. The processes of the burning wood are similar to burning composites. Burning wood is modelled as a two-phase material consisting of the residual char and virgin (unpyrolysed) material, as schematically illustrated in Figure 1.6.

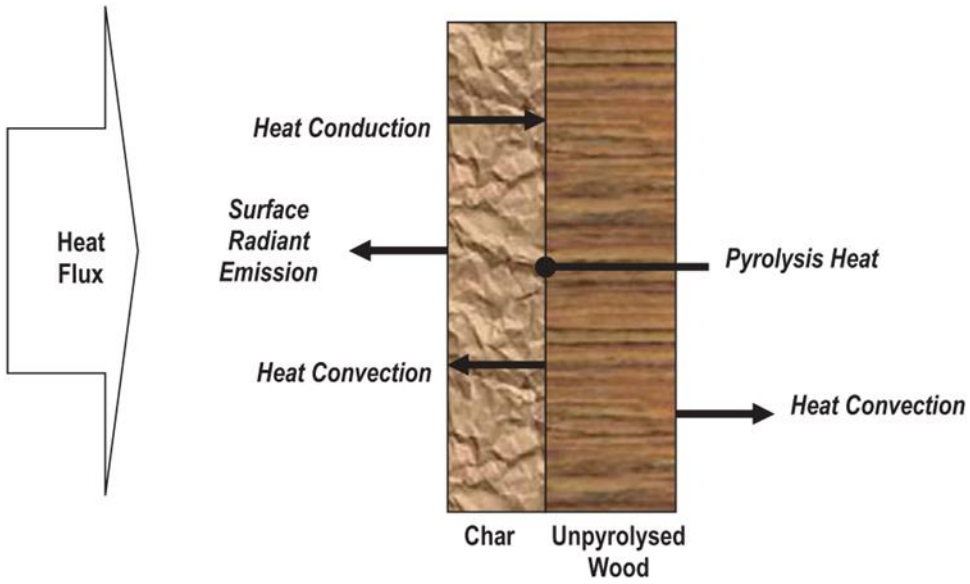

Figure 1.6: Schematic of the thermal decomposition of wood [56]

And then in 1972, the research by Kung [87] modelled wood pyrolysis, including transient heat conduction, internal heat convection of volatiles, decomposition of wood into volatiles and residual char, variable properties (density, specific heat and thermal conductivity), and the endothermic reaction of the decomposition process. In 1977, Kansa et al [89] developed a model that considered the temperature-dependent thermal properties of wood, and this improved the accuracy of modelling. These models have been adapted for composites by Henderson et al [79,81,91], Sullivan and Salamon [82,92], Springer et al [83,93], Dimitrienko [77,94], and Gibson et al [84]. The models have the capability to calculate the temperature profile distribution. The validation of the model by experimental fire tests has shown that the thermal equations can predict the temperature at any location in polymeric laminate and sandwich composites, which values are in good agreement with the experimental results [53,54,81,84,95-99]. The experimental work for heat transfer within sandwich composites will be discussed later on in Chapters 4 and 5, respectively.

1.3 Fire safety regulations and flammability evaluation of composites

Due to widespread usage of polymeric composites in offshore platforms, the transport and construction industries, where fire risks are of main concern, fire regulations are constantly evolving [96,100,101]. There are many national and international fire regulations. The current regulations used for maritime industry provided are briefly adopted by the International Maritime Organization (IMO). The emphasis is on the fire safety requirements for composite materials, and in particular as applicable to High Speed Craft (HSC). The International Maritime Organization (IMO) is responsible for the development and promulgation of the “International Convention for the Safety of Life at Sea” (SOLAS) [102,103]. For marine applications, all ships sailing in international waters must meet the demands of IMO/SOLAS [104,105]. Depending upon the end-use of a product, a number of the marine fire tests may be required: Fire Test to

Marine Equipment according to IMO FTPC (short for Fire Test Procedure Code) [104,105]. In the HSC Code [102] methods used for determining the characteristics that qualify a material as "fire-restricting" include the ISO 9705 (full-scale room fire test (room/corner test)) [106] and the ISO 5660 (small scale test (cone calorimeter)) [107], those test data in conjunction with mathematical models could be used to predict full scale performance [108]. However, it is important to emphasise that there are no residual strength requirements currently included in this test procedure. For rail applications, main fire testing standards are as follows: ISO 5658-2 [109], ISO 5660-1 [107], ISO 4589-2/3 [110], [111], ISO 9239-1 [112], EN 45545-2 [113] and BS 476 [114]. These standards describe test procedures and fire protection measures. They also define which test methods are required to qualify a material for a particular application. Most of the above regulations involve the use of small-scale fire reaction tests along with large-scale fire resistance tests so as to fully characterise a material's response.

1.3.1 Flammability evaluation of components

For flammability evaluation of components to be used in sandwich composites, tests such as limiting oxygen index and UL-94 are used.

Limiting oxygen index (LOI, ISO 4589-2)

The limiting oxygen index (LOI) is the minimum concentration of oxygen in an oxygen-nitrogen mixture required to just sustain burning [110], expressed as:

$$\text{LOI } (O_2 \text{ concentration, \% by volume}) = \frac{100 \times [O_2]}{[O_2] + [N_2]} \quad \text{(Equation 1.1)}$$

Where $[O_2]$ and $[N_2]$ are the concentrations of oxygen and nitrogen, respectively.

The test requires a bar shaped 80 - 150 mm long × 10 mm wide × ~3 mm thick sample held vertically within a transparent chimney containing a known, adjustable, concentration of nitrogen and oxygen. The sample is ignited at the top of specimen by using an ignition gas flame (16 ± 4 mm). The burning time of the ignited specimen at different oxygen concentrations is recorded in order to determine the minimum oxygen concentration that the specimen requires to sustain burning for at least 3 minutes after removal of the ignition flame [110].

LOI tests can give an indication of the combustibility of polymers, with 21% being the standard concentration of oxygen in the air, polymers with LOI values of 21 or below with burning continuously under normal conditions. Therefore, the higher the LOI value, the less flammable the material is. From literature, LOI values of commonly used - cured cast thermoset resins (well-known polymer matrices, widely used in composites, especially for glass fibre-reinforced composites (GFRC) applications) are compiled and given in Table 1.3.

Table 1.3: Flammability of selected thermoset cast resins in terms of LOI values [115]

Polymers	LOI (%)
Unsaturated polyester (UP)	20-22
Vinyl ester (VE)	20-23
General purpose epoxy (EP)*	22-25
Resole type phenolic (PH)	25-33

Note: * - The LOI values of epoxy resin reported in the table are for general purpose grade, which is low temperature curing type.

UL-94 (ASTM D 3801-00, ASTM D 635-03)

The UL-94 is one of the most commonly used small scale test for studying the flammability of the materials, especially for industrial applications. The test can be performed on samples clamped in both vertical or horizontal orientation. For both orientations, bar-shaped samples of 125 mm long × 13 mm wide × ~3 mm thick are ignited with a 20 mm high small flame using a Bunsen burner. The flame is applied at the free end of the specimen for 30 s or as soon as the flame front reaches the 25 mm reference mark (if less than 30 s) in the horizontal burning test or 10 s twice in the vertical mode, the interval between applications being the time taken for the burning of the specimen to cease. Average results of five specimens for each sample should be reported. The flammability by ranking the classifications of V-0, V-1 and V-2 in a vertical mode is that during the test, whether or not the cotton indicator is ignited by the flaming drops or particles from the tested specimen, should be recorded. A breakdown of the vertical rating classification requirements of the specimen is given in Table 1.4. The classifications given to the samples are: V-0, the material self-extinguishes within 10 s after each ignition and there are no flaming drippings igniting the cotton; V-1, it self-extinguishes within 30 s with no flaming drippings; V-2, it self-extinguishes within 30 s, however, flaming drippings which ignite the cotton indicator are allowed to present; “Failed”, if the specimen burns longer than 30 s or burns up completely to the sample holding clamp after removal of the flame applications.

Table 1.4: UL-94 classification requirements for vertical rating [116]

	V-0	V-1	V-2
Burning time after flame application	≤10 s	≤30 s	≤30 s
Total burning time (10 flame applications)	≤50 s	≤250 s	≤250 s
Burning and afterglow time for specimens after the second flame application	≤30 s	≤60 s	≤60 s
Specimens completely burnt up to the holding clamp	No	No	No
Cotton indicator ignited by flaming particles or drops	No	No	Yes

In the case of that material cannot be ranked in the vertical classifications, the horizontal mode - rate of burning of tested materials is then determined [117]. The sample is marked off at 25 mm and 100 mm from its exposed end to enable measurement of the burning length. After removal of the Bunsen burner flame, if the flame extinguishes before reaching the first timing mark, the sample is termed as “self-extinguished”; If the specimen continues to burn with a flame

or glowing combustion (visible glow without flame), the time when the flame front reaches each timing mark and the burnt length are recorded [118], and then the burning rate in a horizontal position can be calculated as:

$$\text{Burning rate (V, mm/min)} = \frac{\text{Burnt length (L, mm)}}{\text{Burning time (t, s)}} \times 60 \quad \text{(Equation 1.2)}$$

1.3.2 Flammability evaluation of composites

The flammability of sandwich composites are mainly tested by burning tests [119]. The burning characteristics and the burning rate are generally measured in these tests. Some main test methods used are summarised here:

Cone calorimeter (ISO 5660-1, ASTM E 1354)

Cone calorimetry is one of such tests, it is a piece of testing equipment used as part of the standardised tests [107]. A cone calorimeter can provide material "reaction to fire" information for use in evaluating the fire hazard of materials. The cone calorimeter is able to measure time-to-ignition (TTI), time-to-flame-out (FO), mass loss, smoke density, carbon dioxide (CO_2) and carbon monoxide (CO) concentrations and also to calculate heat release, including heat release rate (HRR), peak heat release rate (PHRR), total heat release (THR), through a relationship between oxygen consumption and energy output (to be discussed in Chapter 2, Section 2.4.5). This makes the cone calorimeter a very useful bench-scale test [120]. The standardised size for specimens to be tested is 100 mm × 100 mm. Longer TTI and lower heat outputs are preferable for flame retardant composites, as a longer TTI allows for more time to escape and lower heat output also increases the chances of survivability. The smoke output in a fire is also an important factor and generally the lower the value, the lower the fire gas toxicity. Along with measuring those burning characteristics mentioned above, thermal (fire resistance) properties from tested samples can also be measured by inserting thermocouples and recording the temperature profiles through the thicknesses of the composites.

Propane burner test (Measurement of fire resistance)

Small-scale fire testing is used for the assessment of the fire performance of composite materials. It offers an inexpensive and quick option with regard to sample preparation and test operation compared to other widely used fire tests, such as the full-scale furnace test, whilst allowing for a prompt evaluation of the heat transfer and flame resistance characteristics of composites [121]. The propane burner test, a fire test tool mainly carried out by the aeronautical industry to measure and assess the fire resistance of composite materials, using a constant heat flux test with a calibrated propane burner, can also be performed, and the front and back surface temperature of tested samples can be measured as reported elsewhere initially by

Tranchard et al [122] and then also demonstrated by Gibson et al [123,124]. A conventional small-scale Bullfinch burner connected to a propane gas tank provides regulated gas flow at a constant level [122,124], the heat flux parameter is adjustable so that it is possible to simulate fire scenarios of much higher intensity or much less severity. The specimen is held upright by a steel frame at a specified distance from the burner so that the burner flame strikes the sample surface perpendicular to the flame direction. The sample has insulation around the edges to avoid heat loss [121]. The propane flame produces a combustion zone at the front of the specimen which can be characterised through its field temperature, monitored by thermocouples to check consistency and record any anomalies, whereas on the back surface, additional thermocouples used for assessing the specimen's thermal performance. The field temperature is one possible way of characterising the severity of the flame during the small-scale fire test, however, a more controlled option is to perform the burner test at constant heat flux level with heat flux defined as the amount of thermal energy penetrating a specific area. It offers advantages over simple temperature-controlled tests in that it accounts not only for the radiative contribution of the flame which is sensed by thermocouples but also for the convective element. This is necessary because the propane burner used in the test produces a flame of high velocity with the convective characteristics becoming more dominant towards higher heat flux levels. Additionally, any energy feedback from the material into the combustion zone due to ignition and endothermic reactions will impair the field temperature measurements, distorting the level of adjustments necessary to maintain constant heat flux [121]. The two main parameters influencing the detectable field temperature and thus the heat flux at the specimen surface during the burner test are the propane gas pressure and the distance between the specimen front and burner itself, i.e., increasing the gas pressure results in higher heat flux whereas a greater distance lowers the heat flux.

From above, between those two test methods, the fire scenario of propane burner test differs from cone calorimetry, since the heat flux in the former is composed of both radiation and convection contributions, whereas the latter is a pure radiant heat flux (i.e., purely radiative heat transfer conditions) based on ISO 5660-1 standard.

Surface spread of flame test (IMO Resolution MSC.307(88) Part 5, ISO 5658-2)

Low flame spread is one of most important international maritime organization (IMO) test requirements required for composites in marine applications. According to IMO/Fire test procedure (FTP) code, passenger carrying vessels made of composites should have a high resistance to fire and smoke propagation [104]. Composites, in particular sandwich structured composites, are evaluated using the tests in accordance with IMO standards, as specified in IMO Resolution MSC.307(88) [104], or ISO 5658-2 [109]. The test apparatus, except the equipment for measurement of heat release (i.e., via a fume stack and thermocouples only for the IMO test), is specified in standard ISO 5658-2 [109]. These tests are commonly used to determine the ignitibility and the spread of flame across the surface of a specimen for the rail

and marine industries. The IMO test method involves mounting the conditioned specimen in a well-defined flux field and measuring the time of ignition, spread of flame and its final extinguishment, together with a stack thermocouple signal as an indication of heat release by the specimen during burning.

For this test, samples used are rectangular in size, 795 - 800 mm long × 150 - 155 mm wide, maximum 50 mm thick. The sample is marked with a horizontal line centrally at half height along the length, vertical marks are drawn every 50 mm intervals along the line to facilitate the observation of flame spread. Prior to mounting in the sample holder, the back and edges of the sample are wrapped in a single sheet of aluminium foil of 0.02 mm thickness. When mounted in the sample holder the sample is backed by a cool backing board. As can be seen from Figure 1.7, the sample is inserted to the test apparatus in a vertical position so that its longer side is horizontal. The properly-conditioned sample (at a temperature of 23 ± 2 °C, and a relative humidity of 50 ± 5 %) is held in a cool holder at a 15 ° angle to a radiant heating panel, the highest intensity of heat radiation being at the nearest end of the specimen, i.e., the irradiance along the sample varies from a maximum of 50.5 kW/m^2 at 50 mm along the sample to a minimum of 1.5 kW/m^2 at 750 mm towards the far end of the panel. The sample is exposed to a pilot flame (230 ± 20 mm high in the vertical orientation, the adjusted propane gas and air flow rates to about 0.4 and 1 L/min, respectively) at the start of the test. Throughout the test, the time the flame front crosses each 50 mm vertical reference line is recorded, both the time and the position on the specimen at which the progress of flaming combustion ceases, as well as fume stack signals, recorded and continued until test termination; The test is terminated when the specimen fails to ignite after a 10 minutes exposure, or 3 minutes have passed since all flaming from the specimen has ceased, whichever is longer. Additionally, visual observations on the behaviour of the specimen comprising the following phenomena are noted: flashing, transitory flaming (i.e., unstable flame front), sparks, glowing, charring, melting, flaming drips, fissures, fusion, intumescence, changes in form, debris falling away from the specimen, etc.

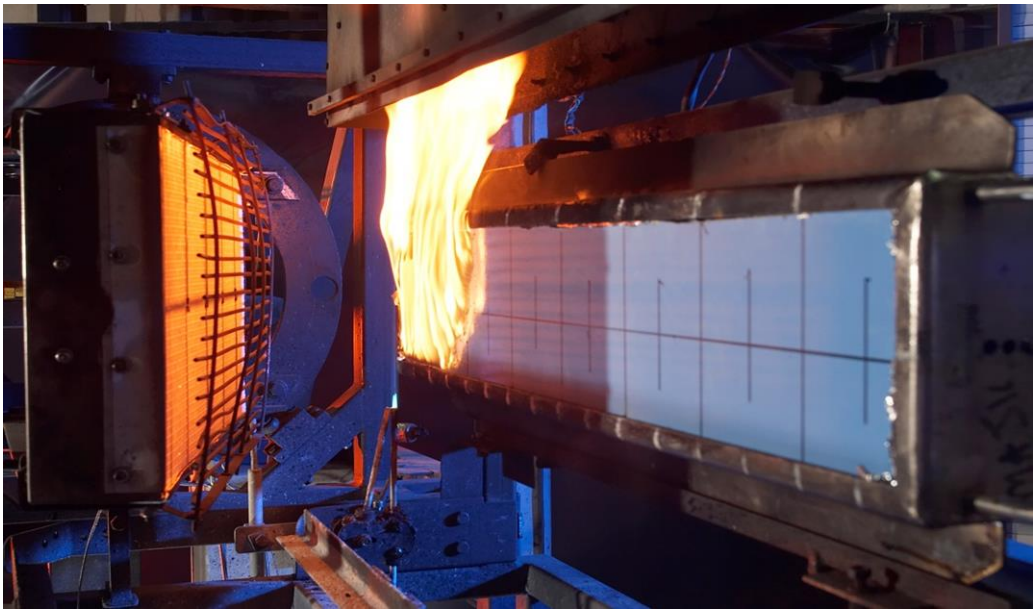

Figure 1.7: IMO FTP Code: Part 5 - spread of flame test apparatus [125]

During burning, the time of ignition, spread of flame, final extinguishment of flame, heat for sustained burning, together with a stack thermocouple signal as an indication of heat release by the specimen are measured. Samples tested using this standard and its surface flammability criteria are given in Table 1.5.

Table 1.5: IMO FTP Code: Part 5 - Surface flammability criteria [104]

	Bulkhead, wall and ceiling linings	Floor coverings	Primary deck coverings
CFE (kW/m^2)	≥20.0	≥7.0	≥7.0
Qsb (MJ/m^2)	≥1.5	≥0.25	≥0.25
Qt (MJ)	≤0.7	≤2.0	≤2.0
Qp (kW)	≤4.0	≤10.0	≤10.0
Burning droplets	Not produced	No more than 10 burning drops	Not produced

Where:

CFE = Critical flux at extinguishment
Qsb = Heat for sustained burning
Qt = Total heat release
Qp = Peak heat release rate

As shown in Table 1.5, composites giving average values for all the surface flammability criteria not exceeding those listed above are considered to meet the requirement for ‘low flame spread’.

1.4 Methods used to flame retard composites

Sandwich composites have excellent properties such as high stiffness-to-weight and bending strength-to-weight ratio and low density, however, the poor fire resistance of the sandwich structures is a critical problem in engineering applications [126]. In the sandwich structure, the skins on both sides should behave similar to the composite laminates. Flammability of composites is mainly caused by the resinous matrix (polyester, vinyl ester, epoxy resin) part. Fibres such as glass and carbon used for reinforcement in structural composites are non-flammable and can retain chemical and physical stability at relatively high temperatures [56]. Hence the preferred way to control the flammability of composites is to reduce the flammability of the resin. Epoxies in general are less flammable than unsaturated polyester or vinyl ester and polyester resins [127]. Although phenolic resins are inherently flame retardant and have excellent charring tendencies resisting fire ignition [58,59,128], they are not generally considered for structural applications due to their brittleness and lower mechanical properties compared to those of unsaturated polyesters and vinyl esters. However, due to their superior fire performance phenolics are used in some applications where fire performance criteria are important [4,129]. The performance of phenolics has been reported also to be superior from the

viewpoint of residual strength following fire [130]. The core material (polymeric foam, balsa wood, honeycomb), in some cases, is also flammable depending on the materials used in the structure [131], which also needs to be taken into account for lowering the flammability of the sandwich composite. In the presence of fire or high temperature, components of sandwich structures will decompose, ignite and burn, releasing heat, smoke, toxic gases, which can cause serious injury and death [132,133]. Therefore, the fire resistance of the sandwich structures should be improved if they are to be used in structural applications.

Flame retardants have been used for several years to improve the flame retardancy of composites [134]. The main routes to flame retard composites include:

Resin part -

a) Flame retardant additives
b) Chemical modification of resin
c) Resin blending

Composite laminates -

Protective coatings on composites

Sandwich composites -

a) Methods used in resin parts and composite laminates given above
b) Lower the flammability of the core material
c) Incorporate both (a) and (b) methods

Those main solutions available are discussed in detail in the following subsections:

1.4.1 Flame retardancy of resin part

Use of flame retardant additives is a common method to impart flame retardancy to the resins [134,135]. Flame retardant additives such as zinc borate and antimony oxide have been used with halogenated polyester, vinyl ester or epoxy resins [136,137]. Alumina trihydrate (ATH), ammonium polyphosphate (APP), melamine phosphate (MP), red phosphorus, 9,10-dihydro-9-oxa-10-phosphaphenanthrene-10-oxide (DOPO), magnesium hydroxide, calcium carbonate, expandable graphite (EG), nanoparticles (such as nanoclays, carbon nanotubes) are some other examples used for polyester and vinyl ester resin systems [138-140]. Zinc borate and stannates are most often used as smoke suppressants [140]. Combination of both nanoparticles and flame-retardant additives can be another alternative [139]. Many studies in the literature have illustrated the effect of additives on improvement in fire reaction properties of composites [141-144]. The concentration of flame-retardant additives is dependent on the flame-retardant type. However, to achieve a certain level of flame retardancy, high loading levels of flame retardants could be required, which may lead to poorer physical and mechanical properties of composites [127,145,146]. Another problem associated with flame retardant additives is that they are not suitable for resin infusion, since the mixture will often separate during infusion

leading to uneven distribution of the flame retardant in the composite [147]. To avoid this, those flame-retardant strategies are preferred which rule out the inclusion of flame-retardant additives in the polymeric matrix.

Chemical modification of the resin is another means through which the resin portion of the composite may be made more flame retardant. Brominated unsaturated polyester and vinyl ester resins are commonly used for glass/carbon fibre composites in marine structures [148]. Bromine imparts a fire-resistant property to the composite. The main drawback to the use of a halogenated resin is that it may release toxic and corrosive gases on exposure to fire. Due to the increasing environmental awareness and strict environmental legislation, their alternatives are being sought [140,148].

Blending of a flammable resin with an inherently flame-retardant resin in the matrix is another approach and considered as a simple and effective physical way to reduce the flammability of the former. In a recent work at Bolton, in order to reduce the flammability of the unsaturated polyester (UP) resin, it has been demonstrated that UP resins could be co-blended with less combustible and char-forming resins such as phenolic (phenol-formaldehyde), melamine-formaldehyde and furan resins [135,140,149-152]. The resultant blended and co-cured resins have seen to be significantly more flame retardant with no detrimental effect to physical and mechanical properties, than the UP resin. The fire risk assessment based on cone calorimetric data was conducted for different blend types and it was observed that resole phenolic resins and their blends with UP achieved the highest fire safety rating than those of melamine-formaldehyde and/or furan resins [140]. This technology was then extended to almost equally flammable vinyl ester resins. Composites based on VE/phenolic blends, whilst having mechanical properties slightly inferior to those of composites based on vinyl esters alone, had better flame retardance performance, particularly in a horizontal UL-94 flame spread test in which they “self-extinguished” [153,154]. Some of the resins from these studies have been chosen for further study in this project.

1.4.2 Flame retardancy of composite laminates

Use of flame-retardant coatings or thermally insulative materials on the heat-exposed surfaces of the composites is one of the commonly used methods of imparting flame retardance. These coatings are applied on the top to protect the composites from the heat source during burning and slow down or stop the combustion process. One well-known example of coating used to flame retard materials is an intumescent coating, which swells to form a foamed carbonaceous char layer and which works as an insulative barrier to underlying materials against flame and heat when heated [155]. The performance of an intumescent coating depends on the thickness of the coating since the thicker coating provides better flame retardant properties to underlying materials [134]. The other one is a flame retardant coating, which generally contains flame retardant chemicals, such as halogenated or phosphorus-based compounds, dispersed in a

binder. In most cases, a flame retardant coating is used to inhibit a flame spread of burning materials by the action of flame retardants contained in the coating [156,157]. Flame retardant coatings are generally not as effective as intumescent coatings. These methods can provide passive protection to the structure by acting as heat barriers, insulating and reflecting the radiant heat back towards the heat source which delays the heating-up rate and reduces the overall temperature on the reverse side of the substrate [140].

Thermal barrier surface coatings are used to reduce the heat transfer, so that the temperature of the resin does not reach its glass transition/decomposition temperature. Luangtriratana et al [158] have reported the use of five types of ceramic particulates (i.e., yttria doped zirconia (Zirconia), a low melting silicate glass (Glass flake), aluminium titanate, nanoclay and nanosilica), applied on the surface of glass fibre-reinforced epoxy (GRE) composites by dispersing in an inherently flame retardant phenolic resin and then coating on the GRE surfaces. All ceramic particles showed good performance as thermal barriers. When exposed to 35 and 50 kW/m^2 heat fluxes, the coatings were very effective in increasing TTI, reducing PHRR and increasing time to PHRR (T_{PHRR}), however they could not stop ignition. All ceramic coatings also reduced heat transfer, seen by the delay in temperature rise at the back surface of the sample.

Kandare et al [159,160] used fire-retardant intumescent mats containing vitreous fibres (MMVF), silicate, expandable graphite, an organic binder together with or without borosilicate glass on the surfaces of glass fibre-reinforced polyester composites. These mats of varied thicknesses (0.5 to 4 mm) while had no effect on TTI, could provide efficient thermal barrier protection in terms of significant reduction in PHRR and THR values in a cone calorimetric test.

1.4.3 Flame retardancy of sandwich composites

Other than those approaches discussed above to flame retard resin or composite laminates, the only other one for sandwich composites is to improve the flammability and thermal insulation performance of the core material. Application of flame-retardant fillers in the honeycomb or foam core, and combination with one of the other methods used for resins and skins have been reported in the literature.

Kandare et al [161] demonstrated that a thin glass-fibre veil impregnated with ammonium polyphosphate (APP) when bonded onto the composite surface of flax/epoxy laminates and their corresponding balsa-core sandwich composites, helped in reducing peak and total heat release rates of the composites in a cone calorimetric test at 50 kW/m^2 heat flux as well as in minimising heat transfer through the structure. The presence of APP and a glass veil at the heat-exposed surface of composites promoted the formation of a highly consolidated physical and thermal barrier by the rigid carbonaceous char, which reduced heat conduction and/or mass transport of combustible volatiles and oxygen into the pyrolysis zone thus reducing the flaming combustion intensity.

Sorathia et al [162] demonstrated the use of different intumescent coatings on sandwich composites made of 6 mm thick glass fibre-reinforced brominated vinyl ester resin skins and 76 mm thick balsa wood core. Depending on the coating type, thickness of the coating was 1.3 or and 5 mm. When tested in a cone calorimeter at 50 kW/m^2 heat flux, all coatings reduced flammability of the composites.

Zhu et al [163] used expandable graphite (EG) to flame retard sandwich composites made of skins from carbon fibre/epoxy resin prepregs and Nomex honeycomb core by either coating on the surface of the composite or filling in the honeycomb core. For coating on the surface, EG particles were sprayed by hand on the prepregs of the skin and adhered by resin of the prepreg before vacuum bagging and curing process. For filling in the honeycomb, EG particles were evenly distributed by hand. Surface coated samples showed delayed TTI, much reduced FO, PHRR and THR values in the cone calorimetric test at 35 kW/m^2. However, smoke production increased. In samples where EG was filled in the core, although the flammability decreased, but not to the same extent as in the surface coated ones, smoke production though was less in these. From this study, it can be concluded that by applying a flame retardant on the surface of the skin (or in resin) and in the core, significant flame-retardant effects can be obtained.

1.4.4 A combination of different flame retard strategies

In order to have very efficient fire-resistant properties for specific applications, usually different flame retard solutions are combined. As an example, the fire-resistant composite structure used for masts in naval ships [140] is shown in Figure 1.8. The layered composite structure consists of two glass/resin (GRP) laminates (typically, and most probably a flame-retardant halogenated resin) with a balsa core sandwiched in between these two skins, coated with an intumescent (Int.) layer and then with a phenolic foam layer bonded to it. While this structure's performance is satisfactory with respect to regulations, this is a far from ideal solution in terms of weight and cost. The manufacturing process needs three distinct stages, i.e., lamination, painting and foam application, this requires time and resources to complete. Furthermore, the overall density and hence weight of the layered composite structure is quite high compared to that of the unprotected GRP structure, hence the ineffective attraction of using lightweight advanced composites.

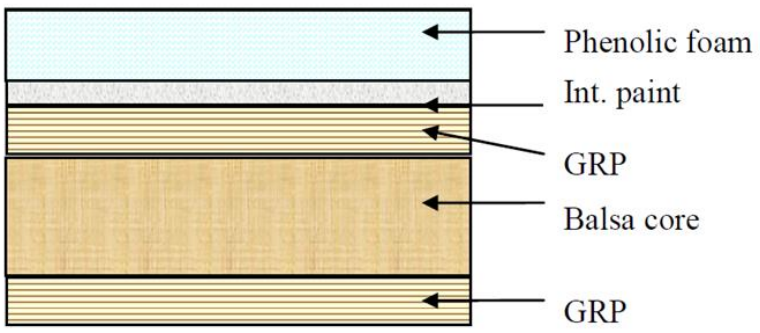

Figure 1.8: Schematic of the layered composite structure used for masts in naval ships [140]

1.5 Post-fire/heat mechanical properties of composites

Other than those factors mentioned in the previous sections, the one which could restrict the use of polymeric composites in structural applications is the reduction in strength and stiffness of the structure following heat/fire. The loss of mechanical properties (tension, flexure, compression, and interlaminar shear properties) of fibre-reinforced polymeric composites (polyester, vinyl ester, phenolic) occurs mainly due to resin softening when heated, chemical degradation, thermal decomposition, combustion and damage of the resin matrix that can form a char. When the resin part (e.g. vinyl ester) softens, up to 50% of the mechanical property of a composite laminate could be reduced at temperatures as low as 120 °C. On degradation/burning, the reduction could be up to 90% or completely lost depending on the resin type [1,2,134,164]. After a fire is extinguished, it is of importance to analyse the post-fire mechanical properties in order to assess and evaluate the residual integrity and safety of the structure for composites.

Sorathia et al [165] measured the post-fire percent residual flexural strength for a wide variety of composites after exposure to 25 kW/m^2 heat flux for 20 minutes. Graphite/PEEK and graphite/phenolic composites retained 75 and 53% strength, respectively, whereas glass/epoxy ones delaminated during the fire exposure retaining no strength. All composites treated with an intumescent coating and ablative protective material however could retain higher residual strength.

According to Mouritz and Mathys [1,164], glass/resole phenolic composites, despite having outstanding fire retardant properties, have low retentions of mechanical properties [164]. They exposed glass/phenolic laminates to different heat fluxes (25, 50, 75 and 100 kW/m^2) for times up to 1800 s in a cone calorimeter and studied the post-fire tensile and flexural properties. Even after exposure to low heat fluxes (<30 kW/m^2) for a short time and with no apparent signs of charring, the mechanical properties were reduced by 30%. On exposure to high heat fluxes, the composite charred, but by the time it ignited, it had lost up to 50% of its original stiffness and strength due to chemical degradation of the phenolic resin matrix. The char formed is usually very porous and brittle and provides minimal structural support to the fibres. Fire-induced delamination cracks beneath the char also contributed to the reduction in properties of the composites. Hence, the post-fire tension and flexural properties of phenolic composites are similar to other composites despite superior fire resistance of the former [1].

Mouritz and Mathys have also studied the effect of thermal barrier coatings on post-fire mechanical (flexural) properties of glass-reinforced polyester composites [2]. Four types of coatings, 0.5 mm intumescent paint, 3 mm intumescent mat, 3.2 mm ceramic fibre mat containing vitreous aluminosilicates, and 0.5 mm layer of a fire-retardant polyester-based coating containing halogens were applied to the composites. Composites were tested in a cone calorimeter at 25, 50, 75 and 100 kW/m^2 heat fluxes for a heat-exposure time of 325 s and also

tested at 50 kW/m^2 heat flux for different times up to 1800 s. The post-fire flexural properties of a composite with thermal barrier coating remained unchanged (or increased slightly) compared to the composite with no thermal barrier. When a coated composite (with one of four thermal barrier materials) ignited, it suffered much less fire damage compared to the material without a coating, and as a result, their post-fire mechanical properties reduced at a noticeably lower rate with increasing heat-exposure time and heat flux compared to the composite without a coating.

Luangtriratana et al [158] studied the effect of ceramic particulate surface coatings on heat-induced mechanical properties of glass fibre-reinforced epoxy composites. All samples were exposed to 25 kW/m^2 heat flux for 120 s and 50 kW/m^2 for 30 s. The flexural moduli of all heat-exposed samples were reduced; however, the reduction was much less in coated samples.

Mouritz and Gardiner [166] studied the compression properties of fire-damaged sandwich composites of glass/vinyl ester (VE) face sheets with poly(vinyl chloride) (PVC) and phenolic foam cores. The laminate with phenolic foam core had superior fire resistance properties, however, post-fire residual properties of both laminates degraded substantially even before they ignited and started burning.

Ulven and Vaidya [167] studied the effect of fire on the low velocity impact (LVI) response of glass/vinyl ester (VE) laminates and balsa wood core sandwich composites with glass/VE face skins. The LVI response parameters, peak force and contact stiffness decreased by 20 - 30% for the laminate and by 65 - 75% for sandwich composite, when both were subjected to a 100 s period of fire exposure. Greater reductions in post-fire properties in sandwich structures occurred due to burning of the resin in the skin and burning/charring of the balsa wood. The residual char was very porous and brittle with very low structural integrity. A lower density balsa wood core was observed to insulate the face sheet more than that by the one with higher density. Insulation provided by the core resulted in accumulation of heat in the face sheet, causing greater thermal damage and hence, less retention of stiffness.

1.6 Research aims and objectives

The main aim of this research is to investigate the thermal properties and fire resistance of some light weight sandwich composites, that could be potentially used in marine applications. To achieve this aim for the project, the following objectives have been identified as needing to be fulfilled.

1. To identify inherently fire-resistant resins which can be blended with UP and/or VE and processed by the resin infusion and hand lay-up methods.
2. To design layered composite structures (e.g. resin blends or layers of different resins as matrices) informed by existing fire results for individual resins and other components (e.g., balsa wood core) in sandwich composites.
3. Based on the results from objective (2), prepare composite laminates and sandwich

structures of different compositions, lay-ups, thicknesses of core materials, sample preparation techniques (resin infusion and hand lay-up), etc.

4. To test the laminates and sandwich structures for both fire and thermal properties.

In order to present this project in a clear manner, a brief description of contents in each chapter is given below.

This chapter (Chapter 1) presents background information and a comprehensive literature review, overview of the project aims and objectives. The literature review mainly covers the applications and the properties of important thermoset resins, properties of fibre-reinforced materials, performances and fabrication techniques used for glass fibre-reinforced composite laminates and sandwich structures, methods of testing flame retardancy, fire performance requirements for marine and rail applications, and post-fire mechanical properties for composites.

Chapter 2 summarises the experimental techniques used in this work, consisting of all materials used and their details, the details of different sample preparation techniques, the characterisation methods used for cast resins, glass fibre-reinforced composites and sandwich structures to test their flame retardancy/flammability, physical and chemical properties. This also includes the test methods introduced to evaluate the fire and thermal performances of sandwich composites and detailed descriptions of experimental setup and temperature profile measurement by means of two standard fire tests (cone calorimeter at 50 kW/m^2 and a propane burner test at 113 kW/m^2 heat flux).

Chapter 3 discusses the physical, chemical, morphological, thermal properties and fire performances of various components that can be used for sandwich composites, from which materials are selected for making sandwich composites for this work. The knowledge gained is also used for analysing the fire behaviours of the composites in later chapters. Their properties related to morphology, curing, thermal stability and fire performances are discussed in detail.

Chapter 4 demonstrates the thermal behaviour and fire performance of balsa wood via two fire tests as mentioned in Chapter 2. Burning behaviours of selected neat resins, composite laminates and sandwich structures from cone data are compared. Sandwich composites with similar components but different compositions are prepared and their fire performances evaluated by two standard fire tests. The variables include cone heater orientations, thicknesses of core materials, composite laminates on one/both sides and different sample preparation techniques, the effects of these variables on fire performances of composite structures are evaluated. In both tests, thermocouples are inserted at various locations of the samples, and temperature profiles exposed to different heat fluxes and fire conditions are plotted and analysed for the purpose of comparing their burn-through resistance and seeing if there is any potential correlation between these two tests.

Chapter 5 investigates sandwich composites of skins made with different types of neat resins, resin blends, and with a top layer of phenolic resin. Comparative fire performances and thermal barrier effects of sandwich structures are evaluated by cone and propane burner testing. Top and back surface temperatures for sandwich composites via two test methods are monitored and analysed, from which samples with lower heat transfer (i.e., better burn-through resistance) compared with those of controls are identified, indicating varied conductive nature of their char.

Chapter 6 focuses on the overall fire safety of materials used in this research, summarises and draws overall conclusions for sandwich composites in terms of better combinations of fire performance and burn-through properties derived from the analysis of results obtained in previous chapters. The recommendations that could be undertaken in this field for further work aimed at achieving a balanced fire and thermal barrier properties for sandwich composites are also included.

1.7 References

[1] A. P. Mouritz and Z. Mathys, “Post-fire mechanical properties of marine polymer composites,” *Composite Structures*, vol. 47, no. 1–4, pp. 643–653, Dec. 1999.

[2] A. P. Mouritz and Z. Mathys, “Post-fire mechanical properties of glass-reinforced polyester composites,” *Composites Science and Technology*, vol. 61, no. 4, pp. 475–490, Mar. 2001.

[3] M. Mohan, “The advantages of composite material in marine renewable energy structures,” *RINA, Royal Institution of Naval Architects International Conference - Marine Renewable Energy Conference 2008*, 2008.

[4] E. P. Gellert and D. M. Turley, “Seawater immersion ageing of glass-fibre reinforced polymer laminates for marine applications,” *Composites Part A: Applied Science and Manufacturing*, vol. 30, no. 11, pp. 1259–1265, Nov. 1999.

[5] R. B. Prime, *‘Thermosets’ in Thermal characterization of polymeric materials*, Chapter 6. San Diego: Academic Press, 1997.

[6] C. Zweben, A. Kelly, J. A. Manson, and R. Talreja, Eds., *‘Fibre-reinforcement and general theory of composites’ in Comprehensive composite materials*, Chapter 1. Amsterdam: Elsevier, 2000.

[7] D. Ratna, *Handbook of thermoset resins*, Chapter 2. UK: Smithers Rapra, 2009.

[8] D. Tilbrook. and H. M. Colquhoun, *Thermosets 2011 - From monomers to components*. Germany: Fraunhofer IRB Verlag, 2011.

[9] M. J. Forrest, *Analysis of thermoset materials, precursors and products*, Chapter 2. UK: Smithers Rapra, 2003.

[10] J. P. Pascault, H. Sautereau, J. Verdu, and R. J. J. Williams, *Thermosetting polymers*. New York: Marcel Dekker, 2002.

[11] H. Dodiuk and S. H. Goodman, *Handbook of thermoset plastics*, 3rd ed. Oxford: Elsevier, 2013.

[12] D. S. Sadafule and S. P. Panda, “Photocrosslinkable unsaturated polyesters,” *Journal of Applied Polymer Science*, vol. 24, no. 2, pp. 511–521, 1979.

[13] B. K. Kandola, A. R. Horrocks, P. Myler, and D. Blair, “The effect of intumescents on the burning behaviour of polyester-resin-containing composites,” *Composites - Part A: Applied Science and Manufacturing*, vol. 33, no. 6, pp. 805–817, 2002.

[14] S. Hörold, “Phosphorus flame retardants in thermoset resins,” *Polymer Degradation and*

Stability, vol. 64, no. 3, pp. 427–431, 1999.
[15] S. Cousinet, A. Ghadban, E. Fleury, F. Lortie, J. P. Pascault, and D. Portinha, “Toward replacement of styrene by bio-based methacrylates in unsaturated polyester resins,” *European Polymer Journal*, vol. 67, pp. 539–550, Jun. 2015.
[16] B. Z. Dholakiya, “Use of non-traditional fillers to reduce flammability of polyester resin composites,” *Polimeri*, vol. 30, pp. 10–17, 2009.
[17] Z. Bai, L. Song, Y. Hu, X. Gong, and R. K. K. Yuen, “Investigation on flame retardancy, combustion and pyrolysis behavior of flame retarded unsaturated polyester resin with a star-shaped phosphorus-containing compound,” *Journal of Analytical and Applied Pyrolysis*, vol. 105, pp. 317–326, 2014.
[18] S. Crawford and C. T. Lungu, “Influence of temperature on styrene emission from a vinyl ester resin thermoset composite material,” *Science of the Total Environment*, vol. 409, no. 18, pp. 3403–3408, 2011.
[19] C. A. Ittner Mazali and M. I. Felisberti, “Vinyl ester resin modified with silicone-based additives: III. Curing kinetics,” *European Polymer Journal*, vol. 45, no. 8, pp. 2222–2233, 2009.
[20] B. S. Rao, P. J. Madec, and E. Marechal, “Synthesis of vinyl ester resins - Evidence of secondary reactions by13C NMR,” *Polymer Bulletin*, vol. 16, no. 2–3, pp. 153–157, 1986.
[21] B. Gaur and J. S. P. Rai, “Curing and decomposition behaviour of vinyl ester resins,” *Polymer*, vol. 33, no. 19, pp. 4210–4214, 1992.
[22] B. Gaur and J. S. P. Rai, “Rheological and thermal behaviour of vinyl ester resin,” *European Polymer Journal*, vol. 29, no. 8, pp. 1149–1153, Aug. 1993.
[23] F. C. Campbell, *Structural Composite Materials*, Chapters 2,3,9. Ohio: ASM International publishing, 2010.
[24] J. S. Martin, J. M. Laza, M. L. Morra´s, M. Rodrı´guez, and L. M. Leo´n, “Study of the curing process of a vinyl ester resin by means of TSR and DMTA,” *Polymer*, vol. 41, no. 11, pp. 4203–4211, May 2000.
[25] W. D. Cook, G. P. Simon, P. J. Burchill, M. Lau, and T. J. Fitch, “Curing kinetics and thermal properties of vinyl ester resins,” *Journal of Applied Polymer Science*, vol. 64, no. 4, pp. 769–781, Apr. 1997.
[26] I. K. Varma, B. S. Rao, M. S. Choudhary, V. Choudhary, and D. S. Varma, “Effect of styrene on properties of vinyl ester resins, I,” *Die Angewandte Makromolekulare Chemie*, vol. 130, no. 1, pp. 191–199, 1985.
[27] V. M. Rosa and M. I. Felisberti, “Unsaturated polyester resin modified with poly(organosiloxanes). I. Preparation, dynamic mechanical properties, and impact resistance,” *Journal of Applied Polymer Science*, vol. 81, no. 13, pp. 3272–3279, Sep. 2001.
[28] B. K. Kandola and A. R. Horrocks, “Flame retardant composites, a review: the potential for use of intumescents,” in *Fire Retardancy of Polymers*, M. L. Bras, G. Camino, S. Bourbigot, and R. Delobel, Eds. UK: The Royal Society of Chemistry, 1998, pp. 395–417.
[29] M. A. Boyle, C. J. Martin, and J. D. Neuner, “Epoxy resins,” in *Composites Compendium*, H. Hansmann, Ed. ASM handbook / extraction: FB MVU, Werkstofftechnologien / Kunststofftechnik, 2003.
[30] L. S. Penn and H. Wang, “Epoxy resins,” in *Handbook of Composites*, Chapter 3., S. T. Peters, Ed. Boston, MA: Springer, 1998.
[31] K. K. Chawla, *Composite Materials*, 3rd ed. Chapter 3, New York, NY: Springer, 2012.
[32] I. Hamerton, *Recent Developments in Epoxy Resins*. Smithers Rapra Technology, 1996.
[33] “Composite engineering materials, guide to composites,” *SP Systems*. [Online]. Available: http://www.antonio.licciulli.unisalento.it/Corso_Ceramici/relazioni/materiali compositi.pdf. [Accessed: 12-Jun-2019].
[34] S. V Hoa, *Principles of the manufacturing of composite materials*, Chapter 2. Pennsylvania: DEStech Publications, 2009.
[35] A. Knop and L. A. Pilato, *Phenolic resins: chemistry, applications and performance*. Berlin Heidelberg: Springer-Verlag, 1985.

[36] W. F. Smith and J. Hashemi, *Foundations of materials science and engineering*, 4th ed. Boston: McGraw-Hill, 2005.
[37] J. C. Munoz, H. Ku, F. Cardona, and D. Rogers, “Effects of catalysts and post-curing conditions in the polymer network of epoxy and phenolic resins: Preliminary results,” *Journal of Materials Processing Technology*, vol. 202, no. 1–3, pp. 486–492, 2008.
[38] *EUCLID RTP3.8 TI-4115-9401*. 1994.
[39] J. Murphy, *The reinforced plastics handbook*. Oxford: Elsevier Advanced Technology, 1998.
[40] M. E. Tuttle, *Structural Analysis of Polymeric Composite Materials*, 1st ed. New York: Marcel Dekker, 2004.
[41] R. Bohlmann, M. Renieri, G. Renieri, and R. Miller, “Training course notes given to Thales in the Netherlands entitled ‘Advanced materials and design for integrated topside structures.’” Netherland, 2002.
[42] D. B. Miracle and S. L. Donaldson, *‘Introduction to composites’ in ASM Handbook - Composites*, Chapter 3., vol. 21. ASM International, 2001.
[43] E. Nilsson and A. C. Nilsson, “Prediction and measurement of some dynamic properties of sandwich structures with honeycomb and foam cores,” *Journal of Sound and Vibration*, vol. 251, no. 3, pp. 409–430, Mar. 2002.
[44] J. R. Vinson, *The behaviour of sandwich structures of isotropic and composite materials*, 1st ed. CRC Press, 1999.
[45] D. Wennberg, *Light-weighting methodology in rail vehicle design through introduction of load carrying sandwich panels*. Stockholm, 2011.
[46] T. S. Lundström and B. R. Gebart, “Influence from process parameters on void formation in resin transfer molding,” *Polymer Composites*, vol. 15, no. 1, pp. 25–33, Feb. 1994.
[47] C. Williams, J. Summerscales, and S. Grove, “Resin Infusion under Flexible Tooling (RIFT): a review,” *Composites Part A: Applied Science and Manufacturing*, vol. 27, no. 7, pp. 517–524, Jan. 1996.
[48] H. Tengler, “Vakuum-Injektionsverfahren. Z. Kunststoffe,” vol. 75, no. 2, pp. 73–75, 1985.
[49] J. M. Thirion, H. Girardy, and U. Waldvogel, “New developments in the production of composite high performance components by the RTM process,” *Composites (France)*, vol. 28, no. 3, pp. 81–84, 1988.
[50] S. Reuterlöv, “Cost effective infusion of sandwich composites for marine applications,” *Reinforced Plastics*, vol. 46, no. 12, pp. 30-32,34, Dec. 2002.
[51] A. Goren and C. Atas, “Manufacturing of polymer matrix composites using vacuum assisted resin infusion molding,” *Archives of Materials Science and Engineering*, vol. 34, no. 2, pp. 117–120, 2008.
[52] A. P. Mouritz, S. Feih, E. Kandare, Z. Mathys, A. G. Gibson, P. E. Des Jardin, S. W. Case, and B. Y. Lattimer, “Review of fire structural modelling of polymer composites,” *Composites Part A: Applied Science and Manufacturing*, vol. 40, no. 12, pp. 1800–1814, Dec. 2009.
[53] S. Feih, Z. Mathys, A. G. Gibson, and A. P. Mouritz, “Modeling compressive skin failure of sandwich composites in fire,” *Journal of Sandwich Structures and Materials*, vol. 10, no. 3, pp. 217–245, May 2008.
[54] S. Feih, Z. Mathys, A. G. Gibson, and A. P. Mouritz, “Modelling the tension and compression strengths of polymer laminates in fire,” *Composites Science and Technology*, vol. 67, no. 3–4, pp. 551–564, Mar. 2007.
[55] S. Feih, A. P. Mouritz, Z. Mathys, and A. G. Gibson, “Tensile strength modeling of glass fiber-polymer composites in fire,” *Journal of Composite Materials*, vol. 41, no. 19, pp. 2387–2410, Oct. 2007.
[56] A. P. Mouritz and A. G. Gibson, *Fire properties of polymer composite materials*. Solid Mechanics and its Applications, Dordrecht, The Netherlands: Springer, 2006.
[57] A. Tewarson and D. P. Macaione, “Polymers and composites - An examination of fire spread and generation of heat and fire products,” *Journal of Fire Sciences*, vol. 11, no. 5, pp. 421–441, Sep. 1993.

[58] G. T. Egglestone and D. M. Turley, “Flammability of GRP for use in ship superstructures,” *Fire and Materials*, vol. 18, no. 4, pp. 255–260, Jul. 1994.
[59] M. J. Scudamore, “Fire performance studies on glass-reinforced plastic laminates,” *Fire and Materials*, vol. 18, no. 5, pp. 313–325, Sep. 1994.
[60] A. T. Grenier, N. A. Dembsey, and J. R. Barnett, “Fire characteristics of cored composite materials for marine use,” *Fire Safety Journal*, vol. 30, no. 2, pp. 137–159, Mar. 1998.
[61] A. P. Mouritz, Z. Mathys, and A. G. Gibson, “Heat release of polymer composites in fire,” *Composites Part A: Applied Science and Manufacturing*, vol. 37, no. 7, pp. 1040–1054, Jul. 2006.
[62] D. M. Allison, A. J. Marchand, and R. M. Morchat, “Fire performance of composite materials in ships and offshore structures,” *Marine Structures*, vol. 4, no. 2, pp. 129–140, Jan. 1991.
[63] S. Feih and A. P. Mouritz, “Tensile properties of carbon fibres and carbon fibre–polymer composites in fire,” *Composites Part A: Applied Science and Manufacturing*, vol. 43, no. 5, pp. 765–772, May 2012.
[64] K. K. Chawla, *Composite Materials*, 3rd ed. Chapter 10, New York, NY: Springer, 2012.
[65] H. Derek, *An introduction to composite materials*, 1st ed. Cambridge Solid State Science Series, Cambridge: Cambridge University Press, 1981.
[66] B. T. Lattimer, J. Ouellette, and J. Trelles, “Thermal response of composite materials to elevated temperatures,” in *Modeling of Naval Composite Sturctures in Fire*, L. S. Couchman and A. P. Mouritz, Eds. Cooperative Research Centre for Advanced Composite Structures, 2006, pp. 1–46.
[67] “Thermal conductivity of phenolic.” [Online]. Available: https://www.makeitfrom.com/material-properties/Phenol-Formaldehyde-PF-Phenolic. [Accessed: 01-Jul-2019].
[68] J. D. Monk, E. W. Bucholz, T. Boghozian, S. Deshpande, J. Schieber, C. W. Bauschlicher, and J. W. Lawson, “Computational and experimental study of phenolic resins: Thermal–mechanical properties and the role of hydrogen bonding,” *Macromolecules*, vol. 48, no. 20, pp. 7670–7680, Oct. 2015.
[69] J. T. Mottram and R. Taylor, “Thermal conductivity of fibre-phenolic resin composites. Part II: Numerical evaluation,” *Composites Science and Technology*, vol. 29, no. 3, pp. 211–232, 1987.
[70] R. D. Patton, C. U. Pittman, L. Wang, J. R. Hill, and A. Day, “Ablation, mechanical and thermal conductivity properties of vapor grown carbon fiber/phenolic matrix composites,” *Composites - Part A: Applied Science and Manufacturing*, vol. 33, no. 2, pp. 243–251, 2002.
[71] *End grain balsa core, FLEXOKORE, Property Table Data sheet*. West Walpole Street, NE33 5BY, UK: East Coast Fibreglass Supplies Ltd, 2016.
[72] D. Rosato and D. Rosato, *Reinforced Plastics Handbook*, 3rd ed. Oxford: Elsevier, 2005.
[73] J. Lua and J. O’Brien, “Fire simulation for woven fabric composites with temperature and mass dependent thermal-mechanical properties,” in *Proceeding of composites in fire*, vol. 3, Newcastle upon Tyne, England, 2003.
[74] M. L. Potocki, M. E. Tuttle, and A. M. Mescher, “Behavior of polymeric composites exposed to a heat flux simulating fire,” *Mechanical behavior of advanced materials*, pp. 325–332, 1998.
[75] C. S. Vatikiotis and D. Salinas, “Heat transfer in a fibrous composite with combustion,” in *American Society of Mechanical Engineers and American Institute of Chemical Engineers, Joint National Heat Transfer Conference*, Orlando, Florida, 1980.
[76] G. S. Springer and S. W. Tsai, “Thermal conductivities of unidirectional materials,” *Journal of Composite Materials*, vol. 1, no. 2, pp. 166–173, Apr. 1967.
[77] Y. I. Dimitrienko, “Thermomechanical behaviour of composite materials and structures under high temperatures: 1. Materials,” *Composites Part A: Applied Science and Manufacturing*, vol. 28, no. 5, pp. 453–461, Jan. 1997.
[78] M. A. Llavona, R. Zapico, F. Blanco, L. F. Verdeja, and J. P. Sancho, “Methods for

measuring thermal conductivity," *RDM Revista de Minas*, vol. 6, pp. 89–98, 1991.
[79] J. B. Henderson and T. E. Wiecek, "A mathematical model to predict the thermal response of decomposing, expanding polymer composites," *Journal of Composite Materials*, vol. 21, no. 4, pp. 373–393, 1987.
[80] M. R. E. Looyeh and P. Bettess, "A finite element model for the fire-performance of GRP panels including variable thermal properties," *Finite Elements in Analysis and Design*, vol. 30, no. 4, pp. 313–324, 1998.
[81] J. B. Henderson, J. A. Wiebelt, and M. R. Tant, "A model for the thermal response of polymer composite materials with experimental verification," *Journal of Composite Materials*, vol. 19, no. 6, pp. 579–595, 1985.
[82] R. M. Sullivan and N. J. Salamon, "A finite element method for the thermochemical decomposition of polymeric materials-I. Theory," *International Journal of Engineering Science*, vol. 30, no. 4, pp. 431–441, 1992.
[83] H. L. N. Mcmanus and G. S. Springer, "High temperature thermomechanical behavior of carbon-phenolic and carbon-carbon composites, I. Analysis," *Journal of Composite Materials*, vol. 26, no. 2, pp. 206–229, 1992.
[84] A. G. Gibson, Y. S. Wu, H. W. Chandler, J. A. D. Wilcox, and P. Bettess, "A model for the thermal performance of thick composite laminates in hydrocarbon fires," *Revue de l'Institut Français du Pétrole*, vol. 50, no. 1, pp. 69–74, Jan. 1995.
[85] C. H. Bamford, J. Crank, and D. H. Malan, "The combustion of wood. Part I," *Mathematical Proceedings of the Cambridge Philosophical Society*, vol. 42, no. 2, pp. 166–182, 1946.
[86] T. R. Munson and R. J. Spindler, "Transient thermal behaviour of decomposing materials: Part 1 general theory and application to convective heating," RAD-TR-61-10, AVCO Corporation, 1961.
[87] H. C. Kung, "A mathematical model of wood pyrolysis," *Combustion and Flame*, vol. 18, no. 2, pp. 185–195, 1972.
[88] A. M. Kanury, "Thermal decomposition kinetics of wood pyrolysis," *Combustion and Flame*, vol. 18, no. 1, pp. 75–83, 1972.
[89] E. J. Kansa, H. E. Perlee, and R. F. Chaiken, "Mathematical model of wood pyrolysis including internal forced convection," *Combustion and Flame*, vol. 29, pp. 311–324, 1977.
[90] B. Fredlund, "Modelling of heat and mass transfer in wood structures during fire," *Fire Safety Journal*, vol. 20, no. 1, pp. 39–69, 1993.
[91] M. R. Tant, J. B. Henderson, and C. T. Boyer, "Measurement and modelling of the thermochemical expansion of polymer composites," *Composites*, vol. 16, no. 2, pp. 121–126, 1985.
[92] R. M. Sullivan and N. J. Salamon, "A finite element method for the thermochemical decomposition of polymeric materials-II. Carbon phenolic composites," *International Journal of Engineering Science*, vol. 30, no. 7, pp. 939–951, 1992.
[93] H. L. N. Mcmanus and G. S. Springer, "High temperature thermomechanical behavior of carbon-phenolic and carbon-carbon composites, II. Results," *Journal of Composite Materials*, vol. 26, no. 2, pp. 230–255, 1992.
[94] Y. I. Dimitrienko, "Thermal stresses and heat-mass transfer in ablating composite materials," *International Journal of Heat and Mass Transfer*, vol. 38, no. 1, pp. 139–146, Jan. 1995.
[95] M. R. E. Looyeh, K. Rados, and P. Bettess, "Thermochemical responses of sandwich panels to fire," *Finite Elements in Analysis and Design*, vol. 37, no. 11, pp. 913–927, 2001.
[96] N. Dodds, A. G. Gibson, D. Dewhurst, and J. M. Davies, "Fire behaviour of composite laminates," *Composites Part A: Applied Science and Manufacturing*, vol. 31, no. 7, pp. 689–702, 2000.
[97] M. R. E. Looyeh, P. Bettess, and A. G. Gibson, "A one-dimensional finite element simulation for the fire-performance of GRP panels for offshore structures," *International Journal of Numerical Methods for Heat and Fluid Flow*, vol. 7, no. 6, pp. 609–625, 1997.
[98] S. Feih, Z. Mathys, A. G. Gibson, and A. P. Mouritz, "Modelling the compression strength

of polymer laminates in fire," *Composites Part A: Applied Science and Manufacturing*, vol. 38, no. 11, pp. 2354–2365, 2007.
[99] C. Konstantis, "Structural behaviour of composite sandwich panels in fire," PhD thesis, Newcastle University, 2014.
[100] B. R. Kirby, "Recent developments and applications in structural fire engineering design - A review," *Fire Safety Journal*, vol. 11, no. 3, pp. 141–179, 1986.
[101] B. R. Kirby, "The application of BS5950: Part 8 of fire limit state design to the performance of 'old' structural mild steels," *Fire Safety Journal*, vol. 20, no. 4, pp. 353–376, 1993.
[102] *IMO Resolution MSC.97(73): International Code of Safety for High-Speed Craft, 2000 (2000 HSC Code, 2008 Edition)*. International Maritime Organization, 2000.
[103] H. Hoppe, "International regulations for high-speed craft an overview," in *International Conference on Fast Sea Transportation*, 2005.
[104] *IMO Resolution MSC.307(88): International Code for Application of Fire Test Procedures*. International Maritime Organization, FTP Code, 2010.
[105] *ISO, EN. 1716:2010 Reaction to fire tests for products — Determination of the gross heat of combustion*. 2010.
[106] *ISO 9705:1993 Fire tests - Full-scale room test for surface products*. International Organization for Standardization (ISO), 1993.
[107] *ISO, EN. 5660-1:2015 Reaction-to-fire tests — Heat release, smoke production and mass loss rate — Part 1: Heat release rate (cone calorimeter method) and smoke production rate (dynamic measurement)*. 2015.
[108] V. Babrauskas and R. D. Peacock, "Heat release rate: The single most important variable in fire hazard," *Fire Safety Journal*, vol. 18, no. 3, pp. 255–272, Jan. 1992.
[109] *ISO, EN. 5658-2:2006 Reaction to fire tests — spread of flame — Part 2: Lateral spread on building and transport products in vertical configuration*. 2006.
[110] *ISO, EN. 4589-2:1996 Plastics — Determination of burning behaviour by oxygen index — Part 2: Ambient-temperature test*. 1996.
[111] *ISO, EN. 4589-3:1996 Plastics — Determination of burning behaviour by oxygen index — Part 3: Elevated-temperature test*. 1996.
[112] *ISO, EN. 9239-1:2010 Reaction to fire tests for floorings — Part 1: Determination of the burning behaviour using a radiant heat source*. 2010.
[113] *CEN, TS. EN 45545-2 Railway applications – Fire protection on railway vehicles Part 2, requirements for fire behaviour of materials and components*. 2004.
[114] *BS 476: Part 7: 1997, Fire tests on building materials and structure, Part 7, Method of test to determine the classification of the surface spread of flame of products*. London, UK: British Standards Institution, 1997.
[115] P. Joseph and J. R. Ebdon, "Recent developments in flame-retarding thermoplastics and thermosets," in *Fire Retardant Materials*, Chapter 7., A. R. Horrocks and D. Price, Eds. Cambridge, UK: Woodhead Publishing Ltd., 2001, pp. 220–263.
[116] *ASTM D 3801-00 UL 94 Vertical: Standard test method for measuring the comparative burning characteristics of solid plastics in a vertical position*. ASTM International, 2001.
[117] "Understanding UL 94 certifications and limitations," *The Code Authority newsletter, Underwriters Laboratories Inc.*, no. 3, pp. 1–2, 2007.
[118] *ASTM D 635-03 UL 94 Horizontal: Standard test method for rate of burning and/or extent and time of burning of plastics in a horizontal position*. ASTM International, 2003.
[119] L. A. Utracki, Ed., *Polymer Blends Handbook*. Dordrecht, The Netherlands: Kluwer Academic Publishers, 2003.
[120] D. Marquis, E. Guillaume, and D. Lesenechal, "Accuracy (trueness and precision) of cone calorimeter tests with and without a vitiated air enclosure," *Procedia Engineering*, vol. 62, pp. 103–119, 2013.
[121] S. Christke, "Multi-layer polymer-metal laminate as fire protection for lightweight transport structures," PhD thesis, Newcastle University, UK, 2016.
[122] P. Tranchard, F. Samyn, S. Duquesne, M. Thomas, B. Estèbe, J.-L. Montès, and S. Bourbigot, "Fire behaviour of carbon fibre epoxy composite for aircraft: Novel test bench

and experimental study," *Journal of Fire Sciences*, vol. 33, no. 3, pp. 247–266, 2015.
[123] A. G. Gibson, W. W. Jusoh, G. Kotsikos, P. Di Modica, S. Christke, K. Yi, A. P. Mouritz, and E. Kandare, "Model for the characterisation and design of Passive Fire Protection (PFP) systems for steel structures," in *ECCM 2016 - Proceeding of the 17th European Conference on Composite Materials*, 2016.
[124] A. G. Gibson, W. N. B. Wan-Jusoh, and G. Kotsikos, "A propane burner test for passive fire protection (PFP) formulations containing added halloysite, carbon nanotubes and graphene," *Polymer Degradation and Stability*, vol. 148, pp. 86–94, Feb. 2018.
[125] "Marine fire testing." [Online]. Available: https://www.warringtonfire.com/testing-services/reaction-to-fire-testing/marine-fire-testing. Warringtonfire, UK. [Accessed: 25-Apr-2020].
[126] A. Hörold, B. Schartel, V. Trappe, M. Korzen, and J. Bünker, "Fire stability of glass-fibre sandwich panels: The influence of core materials and flame retardants," *Composite Structures*, vol. 160, pp. 1310–1318, 2017.
[127] A. R. Horrocks and B. K. Kandola, "Flammability and fire resistance of composites," in *Design and manufacture of textile composites*, Chapter 9., Cambridge England: Woodhead Publishing, 2005, pp. 330–363.
[128] A. G. Gibson and J. Hume, "Fire performance of composite panels for large marine structures," *Plastics, Rubber, and Composites Processing and Applications*, vol. 23, no. 3, pp. 175–183, 1995.
[129] G. Marsh, "Fire-safe composites for mass transit vehicles," *Reinforced Plastics*, vol. 46, no. 9, pp. 26–30, Sep. 2002.
[130] U. Sorathia, C. Beck, and T. Dapp, "Residual strength of composites during and after fire exposure," *Journal of Fire Sciences*, vol. 11, no. 3, pp. 255–270, May 1993.
[131] J. P. Vitale, G. Francucci, and A. Stocchi, "Thermal conductivity of sandwich panels made with synthetic and vegetable fiber vacuum-infused honeycomb cores," *Journal of Sandwich Structures and Materials*, vol. 19, no. 1, pp. 66–82, 2017.
[132] M. Kim, J. Choe, and D. G. Lee, "Development of the fire-retardant sandwich structure using an aramid/glass hybrid composite and a phenolic foam-filled honeycomb," *Composite Structures*, vol. 158, pp. 227–234, Dec. 2016.
[133] A. Anjang, V. S. Chevali, B. Y. Lattimer, S. W. Case, S. Feih, and A. P. Mouritz, "Post-fire mechanical properties of sandwich composite structures," *Composite Structures*, vol. 132, pp. 1019–1028, 2015.
[134] B. K. Kandola and E. Kandare, "Composites having improved fire resistance," in *Advances in Fire Retardant Materials*, Chapter 15., A. R. Horrocks and D. Price, Eds. Cambridge, UK: Woodhead Publishers, 2008, pp. 398–442.
[135] B. K. Kandola, L. Krishnan, and J. R. Ebdon, "Blends of unsaturated polyester and phenolic resins for application as fire-resistant matrices in fibre-reinforced composites: Effects of added flame retardants," *Polymer Degradation and Stability*, vol. 106, pp. 129–137, 2014.
[136] H. J. Gabrisch and G. Lindenberger, "The use of thermoset composites in transportation: their behaviour," *SAMPE Journal*, vol. 29, no. 6, pp. 23–27, 1993.
[137] J. L. Sevart, O. H. Griffin, Z. Gürdal, and G. A. Warner, "Flammability and toxicity of composite materials for marine vehicles," *Naval Engineers Journal*, vol. 102, no. 5, pp. 45–54, Sep. 1990.
[138] P. Georlette, "Applications of halogen flame retardants," in *Fire Retardant Materials*, Chapter 8., A. R. Horrocks and D. Price, Eds. Cambridge: Woodhead Publishing, 2001, pp. 264–292.
[139] B. K. Kandola and J. R. Ebdon, "Recent developments in fire retardation and fire protection of fibre-reinforced composites," *Materials China*, vol. 35, no. 5, pp. 333–344, 2016.
[140] B. Kandola and L. Krishnan, "Fire performance evaluation of different resins for potential application in fire resistant structural marine composites," in *Proceedings of the 11th International Symposium on Fire Safety Science (IAFSS)*, 2014, vol. 11, pp. 769–780.

[141] F. Laoutid, L. Bonnaud, M. Alexandre, J. M. Lopez-Cuesta, and P. Dubois, “New prospects in flame retardant polymer materials: From fundamentals to nanocomposites,” *Materials Science and Engineering R: Reports*, vol. 63, no. 3, pp. 100–125, 2009.
[142] M. Rakotomalala, S. Wagner, and M. Döring, “Recent developments in halogen free flame retardants for epoxy resins for electrical and electronic applications,” *Materials*, vol. 3, no. 8, pp. 4300–4327, 2010.
[143] E. D. Weil, “Fire-protective and flame-retardant coatings - A state-of-the-art review,” *Journal of Fire Sciences*, vol. 29, no. 3, pp. 259–296, 2011.
[144] M. Bar, R. Alagirusamy, and A. Das, “Flame retardant polymer composites,” *Fibers and Polymers*, vol. 16, no. 4, pp. 705–717, 2015.
[145] E. Kandare, B. K. Kandola, P. Myler, and G. Edwards, “Thermo-mechanical responses of fiber-reinforced epoxy composites exposed to high temperature environments. Part I: Experimental data acquisition,” *Journal of Composite Materials*, vol. 44, no. 26, pp. 3093–3114, 2010.
[146] E. Kandare, B. K. Kandola, E. D. McCarthy, P. Myler, G. Edwards, Y. Jifeng, and Y. C. Wang, “Fiber-reinforced epoxy composites exposed to high temperature environments. Part II: Modeling mechanical property degradation,” *Journal of Composite Materials*, vol. 45, no. 14, pp. 1511–1521, 2011.
[147] W. S. Chow, L. N. Chang, and M. Jaafar, “Flame retardant epoxy hybrid composite laminates prepared by vacuum-assisted resin infusion technique,” *Journal of Composite Materials*, vol. 49, no. 12, pp. 1471–1481, May 2015.
[148] K. N. Shivakumar, G. Swaminathan, and M. Sharpe, “Carbon/Vinyl ester composites for enhanced performance in marine applications,” *Journal of Reinforced Plastics and Composites*, vol. 25, no. 10, pp. 1101–1116, Jul. 2006.
[149] D. Deli, B. K. Kandola, J. R. Ebdon, and L. Krishnan, “Blends of unsaturated polyester and phenolic resins for application as fire-resistant matrices in fibre-reinforced composites. Part 1: identifying compatible, co-curable resin mixtures,” *Journal of Materials Science*, vol. 48, no. 20, pp. 6929–6942, Oct. 2013.
[150] B. K. Kandola, L. Krishnan, D. Deli, and J. R. Ebdon, “Blends of unsaturated polyester and phenolic resins for application as fire-resistant matrices in fibre-reinforced composites. Part 2: Effects of resin structure, compatibility and composition on fire performance,” *Polymer Degradation and Stability*, vol. 113, pp. 154–167, 2015.
[151] B. K. Kandola, J. R. Ebdon, and K. P. Chowdhury, “Flame retardance and physical properties of novel cured blends of unsaturated polyester and furan resins,” *Polymers*, vol. 7, no. 2, pp. 298–315, 2015.
[152] B. K. Kandola, L. Krishnan, D. Deli, P. Luangtriratana, and J. R. Ebdon, “Fire and mechanical properties of a novel free-radically cured phenolic resin based on a methacrylate-functional novolac and of its blends with an unsaturated polyester resin,” *RSC Advances*, vol. 5, no. 43, pp. 33772–33785, 2015.
[153] C. Zhou, “Optimization of the matrix material for fibre reinforced composites used in fire situations,” MSc thesis, University of Bolton, UK, 2015.
[154] B. K. Kandola, J. R. Ebdon, and C. Zhou, “Development of vinyl ester resins with improved flame retardant properties for structural marine applications,” *Reactive and Functional Polymers*, vol. 129, pp. 111–122, 2018.
[155] B. K. Kandola and A. R. Horrocks, “Composites,” in *Fire Retardant Materials*, Chapter 5., A. R. Horrocks and D. Price, Eds. Cambridge, UK: Woodhead Publishing Ltd., 2001, pp. 182–203.
[156] S. Liang, N. M. Neisius, and S. Gaan, “Recent developments in flame retardant polymeric coatings,” *Progress in Organic Coatings*, vol. 76, no. 11, pp. 1642–1665, Nov. 2013.
[157] T. J. Ohlemiller and J. R. Shields, “The effect of surface coatings on fire growth over composite materials in a corner configuration,” *Fire Safety Journal*, vol. 32, no. 2, pp. 173–193, Mar. 1999.
[158] P. Luangtriratana, B. K. Kandola, and P. Myler, “Ceramic particulate thermal barrier surface coatings for glass fibre-reinforced epoxy composites,” *Materials and Design*, vol.

68, pp. 232–244, 2015.
[159] E. Kandare, C. Chukwudolue, and B. K. Kandola, “The use of fire-retardant intumescent mats for fire and heat protection of glass fibre-reinforced polyester composites: Thermal barrier properties,” *Fire and Materials*, vol. 34, pp. 21–38, 2010.
[160] E. Kandare, A. K. Chukwunonso, and B. K. Kandola, “The effect of fire-retardant additives and a surface insulative fabric on fire performance and mechanical property retention of polyester composites,” *Fire and Materials*, vol. 35, no. 3, pp. 143–155, Apr. 2011.
[161] E. Kandare, P. Luangtriratana, and B. K. Kandola, “Fire reaction properties of flax/epoxy laminates and their balsa-core sandwich composites with or without fire protection,” *Composites Part B: Engineering*, vol. 56, pp. 602–610, 2014.
[162] U. Sorathia, T. Gracik, J. Ness, A. Durkin, F. Williams, M. Hunstad, and F. Berry, “Evaluation of intumescent coatings for shipboard fire protection,” *Journal of Fire Sciences*, vol. 21, no. 6, pp. 423–450, 2003.
[163] C. Zhu, J. Li, F. Ji, X. Yi, C. Rudd, and X. Liu, “Sandwich structure composite with expandable graphite filled or coated: Evaluation of flame retardancy and mechanical performances,” *Open Journal of Safety Science and Technology*, vol. 9, pp. 7–21, 2019.
[164] A. P. Mouritz and Z. Mathys, “Mechanical properties of fire-damaged glass-reinforced phenolic composites,” *Fire and Materials*, vol. 24, no. 2, pp. 67–75, Mar. 2000.
[165] U. Sorathia, C. Beck, and T. Dapp, “Residual strength of composites during and after fire exposure,” *Journal of Fire Sciences*, vol. 11, no. 3, pp. 255–270, 1993.
[166] A. P. Mouritz and C. P. Gardiner, “Compression properties of fire-damaged polymer sandwich composites,” *Composites Part A: Applied Science and Manufacturing*, vol. 33, no. 5, pp. 609–620, May 2002.
[167] C. A. Ulven and U. K. Vaidya, “Impact response of fire damaged polymer-based composite materials,” *Composites Part B: Engineering*, vol. 39, no. 1, pp. 92–107, 2008.

Chapter 2: Experimental

In this chapter, materials, sample preparation and experimental methodologies used for designing fire resistant light weight composites for marine applications are discussed. First of all, materials used in this work are given in detail. Establishment of curing conditions and sample preparation for cast resin samples, glass fibre reinforced composite laminates and sandwich structured composites are described. Experimental techniques used involving DSC, DMTA, TGA, PCFC and fire performances are introduced. Two standard fire tests, cone calorimetry at 50 kW/m^2 and propane burner test at 113 kW/m^2 have been used, for which detailed experimental setup and methodology for temperature profile measurement during the tests are described.

2.1 Materials

2.1.1 Thermoset resins

2.1.1.1 Unsaturated Polyester resins (UP) *(Sourced from Scott-Bader, UK)*

- Crystic® 2-406PA: containing the mixture of phthalic anhydride-based unsaturated polyester, cobalt octoate (<0.2 wt%), and styrene (35-40 wt%) [1], hereinafter referred to simply as UP.
- Crystic® 702PAX: a pre-accelerated, orthophthalic polyester resin with low viscosity and controlled exotherm characteristics, suitable for resin infusion techniques, hereinafter referred to simply as UP-R.
- UP resin catalyst: Butanox® M-50 (Sourced from Akzo Nobel), containing dimethyl phthalate (55-70 wt%) and methyl ethyl ketone peroxide (30-37 wt%) [2], 1-2 wt% with respect to (w.r.t.) UP.

2.1.1.2 Vinyl Ester resins (VE) *(Sourced from Scott-Bader, UK)*

- Crystic® VE676: an epoxy Bisphenol-A-based vinyl ester resin, containing methacrylic acid (<2 wt%) and styrene (45-50 wt%) [3], hereinafter referred to simply as VE-Ep.
- Crystic® VE673: an epoxy Novolac-based vinyl ester resin, containing 35-40 wt% of styrene [4], hereinafter referred to simply as VE-Nov.
- VE resin catalyst: Trigonox® 239, a free-radical catalyst for curing the VE samples, cumyl hydroperoxide [5], sourced from Akzo Nobel, 2 wt% w.r.t. VE.
- Redox accelerator: 12% cobalt octoate, sourced from Sigma-Aldrich, 0.25 wt% w.r.t. VE.

2.1.1.3 Epoxy resin (Ep) *(Sourced from Huntsman Advanced Materials Ltd.)*

- Epoxy resin: Araldite® LY 5052, containing epoxy phenol novolac (60-72 wt%) and butanedioldiglycidyl ether (34-42 wt%) [6], hereinafter referred to simply as Ep.
- Hardener: Aradur® 5052 CH, containing isophorone diamine (30-42 wt%), 2,2-dimethyl-4,4 methylenebis(cyclohexylamine) (50-56 wt%), and 2,4,6-tris(dimethylaminomethyl) phenol (1-7 wt%) [7], 30 wt% w.r.t. Ep.

2.1.1.4 Resole Type Phenolic Resins (PH-Res) (Sourced from Sumitomo Bakelite Europe NV)

- Durez® 33156: Alcohol soluble ethanol-based phenolics resole containing 20-29 wt% ethanol [8], hereinafter referred to simply as Durez.
- Methylon® 75108: a solvent-free, allyl-functionalised phenolic resole [9], hereinafter referred to simply as Methylon.

2.1.2 Thermoplastic resins

2.1.2.1 Elium resin (Elium) (Sourced from Arkema, France)

- Elium® 150: a low viscosity liquid, thermoplastic resin, containing 2-Propenoic acid, 2-methyl-, methyl ester (50-85 wt%) and acrylic copolymers (10-50 wt%) [10], hereinafter referred to simply as Elium.
- Initiator: >75.0% Benzoyl Peroxide (wetted with ca. 25% Water), BPO [11], sourced from Tokyo Chemical Industry Co., Ltd., 2 wt% w.r.t. Elium.

All the materials were used as received.

2.1.3 Glass fabric

Glass woven plain fabric of E-glass type with area density of 300 g/m^2 was sourced from Glasplies, UK.

2.1.4 Core materials

25.4 mm (1 inch) and 12.7 mm (0.5 inch) thick end grain balsa wood core materials as sheets of size 1220 mm × 610 mm and with nominal density of 150 kg/m^3 were sourced from East Coast Fibreglass Supplies Ltd. (manufactured by FLEXOKORE Ltd., UK). The samples were dried at 80 °C for 12 hours to get rid of moisture prior to making samples.

The balsa wood was used as this is the most widely used core material for marine applications. Sandwich structures with end grain balsa result in a particularly lightweight and sturdy end

product, as the balsa wood is cut perpendicular to the grain direction it has optimum physical properties due to its honeycomb-like cell structure.

2.2 Establishment of curing conditions

Curing of thermosetting resins is difficult because it involves the interaction between chemical kinetics and changes in physical properties [12]. In order to develop a better quality of cast resin plaque without any voids, the curing condition of the resin needs to be properly monitored. The curing conditions of some of the UP, VE and their blends with phenolic resins were adapted from the previous work conducted in Fire Materials Laboratory at Bolton [13-15]. These curing conditions were established based on Differential Scanning Calorimeter (DSC) study on uncured resins [13,14]. At least one DSC run for each resin sample was conducted again to validate the results with those from the previous work. If they were within a certain margin of variability, i.e., peak temperatures within 10 °C compared with the previous results, then it did not impact on the proposed curing conditions; if not, then another DSC test was conducted and the results taken from the two closer ones were used to establish curing conditions for that sample. The curing reaction is an exothermic reaction, i.e., heat is released during the reaction. Information from the DSC curves of uncured resins can be used to establish the curing conditions for neat and blended resins. In addition, it can also be used to study the compatibility of the component resins in the blends. According to the information provided on the datasheet by the manufacturer and DSC results obtained from the cured samples, initial curing conditions were established. If a small exothermic peak could be observed, which implied that the thermoset resin was not completely cured, it needed to be post-cured again. However, if the DSC curve showed a single flat line, it indicated that the sample was completely cured. On the basis of those, DSC results were taken as guidance to establish the optimum curing conditions for the cast resin samples. For the purpose of getting a good cast resin sample without voids, several curing conditions were tried under the guidance of DSC results and other factors, such as rate of curing, etc. After a few trial and error attempts, curing conditions for cast resins were established to generate uniform and void-free samples.

Figure 2.1 shows the DSC traces for VE-Ep cast resin sample, before and after curing. In the cases of the VE samples, Trigonox® 239 (2 wt%) was added as the curing catalyst with 12% cobalt octoate (0.25 wt%) as an accelerator; Butanox® M-50 (2 wt%) was added as the curing catalyst in the cases of the UP samples; no catalyst is required to assist curing of the phenolic resoles. As can be seen from Figure 2.1, curing of VE-Ep gives rise to two exothermic peaks, the first one starting at room temperature and with maximum at 74 °C and the maximum of the second peak at 143 °C, respectively. This suggests that the curing of VE-Ep can be conducted at room temperature, but for complete curing, additional post-curing at 140 °C will be required.

Using this method, optimum curing conditions for all the neat, blended resins were established, from which all neat resins were cast. Curing conditions for composite laminates and sandwich structure samples had to be slightly modified, the details are discussed in the following section.

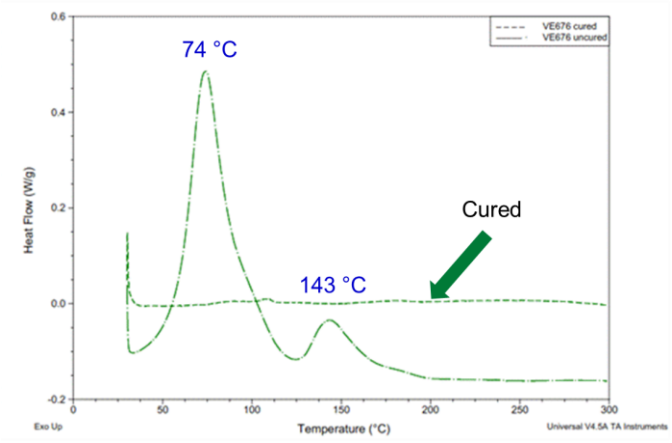

Figure 2.1: DSC traces for uncured and cured samples of VE-Ep before and after curing

2.3 Sample preparation

2.3.1 Cast resin preparation

2.3.1.1 Neat resins

Circular plaques of cured resins were prepared by mixing the resin with an appropriate catalyst, accelerator, initiator and/or hardener (see Table 2.1) using a mechanical stirrer (IKA_RW 16 overhead electric, four bladed propeller stirrer) in a 100 mL beaker for 3-5 minutes [13-15]. These mixtures were then poured into 55 mm diameter circular aluminium open moulds to a depth of 3 mm. Except for both phenolic resins, Durez and Methylon, they were directly transferred to the moulds. It is to be noted that both resins are usually stored in the freezer, it is better to unfreeze them for some time to allow the required amount of resin to reach room temperature and reduce their viscosity for easier handling. The samples were then cured in an oven using optimum curing conditions given in Table 2.1. During the curing in the oven, the heating ramp was set up at 3 °C/minute for all samples. The lower ramp rate helps in removal of any volatiles (e.g. water vapour in case of phenolics) being generated during curing, leading to void-free samples. In the case of phenolics, multiple curing steps were needed in order to evaporate the water at lower temperatures first and also completely curing the sample.

Table 2.1: Optimum curing conditions for neat resins

Resin	Catalyst/Accelerator/Initiator/Hardener	Curing conditions
UP	2 wt% Butanox® M-50	Room temperature (RT) 24 h, 80 °C 6 h
UP-R	2 wt% Butanox® M-50	RT 24 h, 80 °C 6 h
VE-Ep	0.25 wt% cobalt octoate (12%), 2 wt% Trigonox® 239	RT 24 h, 80 °C 3 h, 140 °C 3 h
VE-Nov	0.25 wt% cobalt octoate (12%), 2 wt% Trigonox® 239	RT 24 h, 80 °C 3 h
Ep	30 wt% Aradur® 5052 CH	RT 24 h, 80 °C 6 h
Durez	N/A	50 °C 6 h, 80 °C 12 h, 160 °C 3 h, 180 °C 2 h
Methylon	N/A	100 °C 8 h, 120 °C 6 h, 130 °C 6 h, 150 °C 2 h, 180 °C 2 h, 220 °C 3 h
Elium	2 wt% Benzoyl Peroxide (>75%) (wetted with ca. 25% water)	RT 1 h, 90 °C 1 h

Note: N/A - not applicable.

2.3.1.2 Blended resins

Appropriate quantities of blends of the UP and VE resins with the phenolic resoles, Durez and Methylon [13,14] and also blends of UP and VE resins, were prepared in the ratios of 70/30 and/or 50/50 wt% with vigorous mixing using a mechanical stirrer but at high shear (900 rpm) in a 100 mL beaker for 10 minutes or so until forming a homogeneous solution. In order to produce void-free samples, the resin was degassed under vacuum for 5 minutes. After that, the required quantities of catalyst and/or accelerator were added to the resin mixtures, which were then stirred for a further 5 minutes. For the blends with poor processability, additional solvent such as ethanol was added to reduce the viscosity, which also helped in improving their compatibility. A detailed study of the compatibility of UP/phenolic resin blends is reported elsewhere [13]. The resin mixtures were finally transferred to 55 mm diameter moulds to depths of 3 mm, cured, and then post-cured. The details are given in Table 2.2. It must be noted that these curing conditions are acceptable in the research environment, however, to be exploited for industrial applications, the appropriateness in terms of time, cost, etc. needs to be considered and hence to be optimised further for reduced total curing hours or fewer multiple curing steps.

Table 2.2: Optimum curing conditions for blended resins

Resin	Catalyst/Accelerator	Curing conditions
UP/Durez:70/30	2 wt% Butanox® M-50 w.r.t. UP	50 °C 6h, 80 °C 24h, 90 °C 9h, 130 °C 1h, 160 °C 1h, 180 °C 2h
UP/Durez:50/50	2 wt% Butanox® M-50 w.r.t. UP	80 °C 24h, 100 °C 1h, 130 °C 1h, 160 °C 1h, 180 °C 2h
UP/Metyhlon:70/30	2 wt% Butanox® M-50 w.r.t. UP	50 °C 6h, 80 °C 12h, 100 °C 8h, 120 °C 6h, 130 °C 6h, 150 °C 2h, 180 °C 2h
UP/Metyhlon:50/50	2 wt% Butanox® M-50 w.r.t. UP	50 °C 6h, 80 °C 12h, 100 °C 8h, 120 °C 6h, 130 °C 6h, 150 °C 2h, 190 °C 2h
VE-Ep/Durez:70/30	0.25 wt% cobalt octoate (12%), 2 wt% Trigonox® 239 w.r.t. VE	80 °C 10 h, 100 °C 6 h, 130 °C 1 h, 160 °C 1 h, 180 °C 2 h
VE-Ep/Durez:50/50	0.25 wt% cobalt octoate (12%), 2 wt% Trigonox® 239 w.r.t. VE	80 °C 24 h, 100 °C 1 h, 130 °C 1 h, 160 °C 1 h, 180 °C 2 h; one specimen was further post-cured at 230 °C 3 h
VE-Ep/Methylon:70/30	0.25 wt% cobalt octoate (12%), 2 wt% Trigonox® 239 w.r.t. VE	80 °C 2 h, 100 °C 6 h, 150 °C 6 h, 180 °C 3 h
VE-Ep/Methylon:50/50	0.25 wt% cobalt octoate (12%), 2 wt% Trigonox® 239 w.r.t. VE	RT 24 h, 80 °C 6 h, 110 °C 6 h, 140 °C 6 h, 180 °C 3 h
VE-Nov/Durez:70/30	0.25 wt% cobalt octoate (12%), 2 wt% Trigonox® 239 w.r.t. VE	80 °C 2 h, 130 °C 1 h, 160 °C 1 h, 180 °C 2 h
VE-Nov/Durez:50/50	0.25 wt% cobalt octoate (12%), 2 wt% Trigonox® 239 w.r.t. VE	80 °C 24 h, 100 °C 1 h, 130 °C 1 h, 160 °C 1 h, 180 °C 2 h
VE-Nov/Methylon:70/30	0.25 wt% cobalt octoate (12%), 2 wt% Trigonox® 239 w.r.t. VE	80 °C 2 h, 100 °C 6 h, 150 °C 6 h, 180 °C 3 h
VE-Nov/Methylon:50/50	0.25 wt% cobalt octoate (12%), 2 wt% Trigonox® 239 w.r.t. VE	RT 24 h, 80 °C 6 h, 110 °C 6 h ,140 °C 6 h, 180 °C 3 h
UP/VE-Nov:50/50	2 wt% Butanox® M-50 w.r.t. UP; 0.25 wt% cobalt octoate (12%), 2 wt% Trigonox® 239 w.r.t. VE	RT 24 h, 80 °C 6 h

2.3.2 Glass fibre reinforced composite laminates preparation

In order to prepare the glass fibre reinforced composite laminates, two different methods: hand lay-up and vacuum bagging, and resin infusion techniques were used. After some initial experimentation, for UP resins and UP/phenolic blends, the amount of catalyst Butanox® M-50 used was reduced from 2 wt% to 1 wt%. Similarly, for VE resins and VE/phenolic blends, the amount of catalyst Trigonox® 239 used was reduced from 2 wt% to 1 wt% to increase gel times and the amount of the accelerator cobalt octoate (12%) solution used was similarly reduced from 0.25 wt% to around 0.1 wt%. For Elium resin, the amount of initiator Benzoyl Peroxide (wetted with ca. 25% water) added was reduced from 2 wt% to 1 wt%.

2.3.2.1 Hand lay-up and vacuum bagging

Glass fibre reinforced composite (GFRC) laminates were prepared by using 500 mm × 500 mm × 12 mm sized aluminium square metal plates, wrapped with green film and coated with release agent to enable easy removal of the cured laminate. Four plies of E-glass fabric of size 300 mm × 300 mm were used in GFRC preparation by wet hand lay-up method. The glass fabric with resin ratio used was 1:1 by weight. Each ply of fabric was impregnated with the resin/resin mixture prepared by mixing with a mechanical stirrer (IKA_RW16 overhead electric, four bladed propeller stirrers at high shear 900 rpm) in a beaker for 10-15 minutes depending on forming homogeneous solution by using a roller shown in Figure 2.2. All four plies of fabrics were stacked together to form a consolidated wet laminate. The top mould was positioned on the wet laminate, covered with another metal plate on top of the laminate and then wrapped with a breather fabric to prevent the leakage of the resin all over the plate at high temperature but allowing the vacuum to penetrate and also helping to remove volatiles produced during the curing of resin. It was noted that the sealant tape could not be placed around all sides of the wet laminate because the sealant tape is thicker and higher than prepared laminates, hence the pressure was applied on the sealant tape rather than the laminate itself.

A vacuum valve was fitted on the centre of the top plate, and connected through a hose to the vacuum controller. The whole arrangement was sealed using a nylon vacuum bagging tape. The bag was then placed inside the vacuum oven under 1 bar pressure and cured under the conditions optimised from cast resins established before.

The GFRC laminates of neat resole type phenolic resins could not be prepared because of their low viscosities at high temperatures and excessive leakage could be observed during post-curing. The methodology is shown in Figure 2.2.

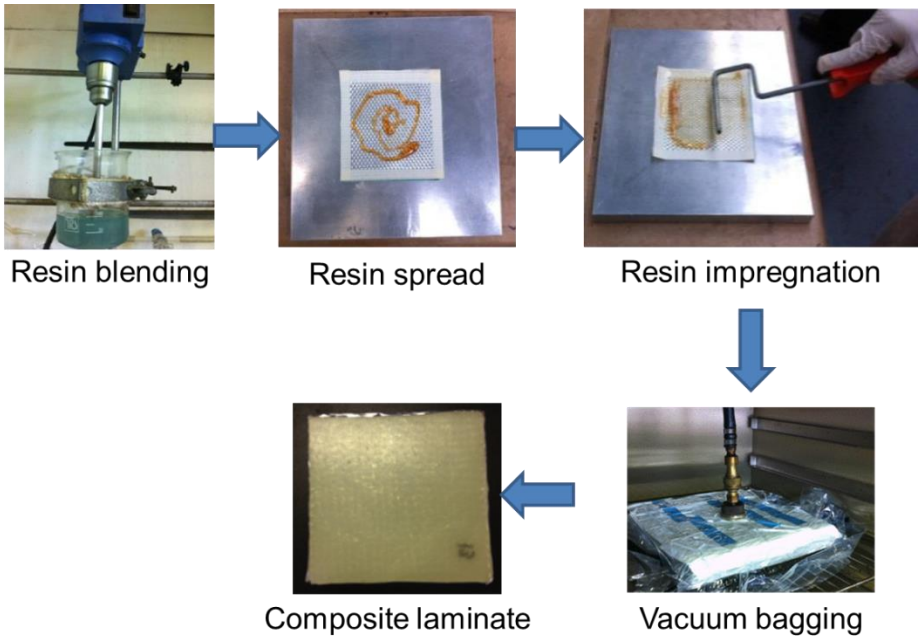

Figure 2.2: Preparation process for glass fibre-reinforced composite laminates by hand lay-up and vacuum bagging technique

2.3.2.2 Resin infusion

Resin infusion is a sophisticated technique for manufacturing high performance, void-free composites. The key to successful resin infusion is the preparation process. A 500 mm × 500 mm × 12 mm sized aluminium square metal plate was wrapped with green film and coated with mould release agent to enable easy removal of the laminate after curing. Four plies of E-glass fabric of size 350 mm × 350 mm were cut as reinforcement for the moulding to make the final laminate size of 300 mm × 300 mm, which were positioned in the centre of the plate. A layer of peel ply was applied to completely cover the whole areas of reinforcement. This helped to easily peel off the finished part after curing. Infusion mesh, resin flow channels, vacuum connectors, resin feed connector and bagging film were set up at required position to be enclosed in a configured stack of bagging materials and subjected to vacuum pressure using a vacuum pump. Once all the air was removed from the bag and the glass fibre reinforcement was fully compressed, liquid resin mixed with hardener was introduced to the reinforcement through a tube which then infused through the reinforcement under the vacuum. Once the resin had fully infused through the reinforcement, the supply of resin was cut off by using a pipe clamp and the resin was left to cure, still under vacuum pressure (See Figure 2.3).

All phenolic resins and their blends with UP or VE while could be resin infused but since they needed to be post-cured at elevated temperatures, the materials used for resin infusion technique could not withstand such high temperatures. Even replacing PVC vacuum hose by silicone vacuum hose and another high temperature resistance film that can resist 204 °C in the infusion bagging system did not help. Losing vacuum or having a leak during the post-curing period at high temperatures in the bag ruined the sample, hence this technique is not ideal to carry out when post-curing at high temperatures, hence could not be used for these samples.

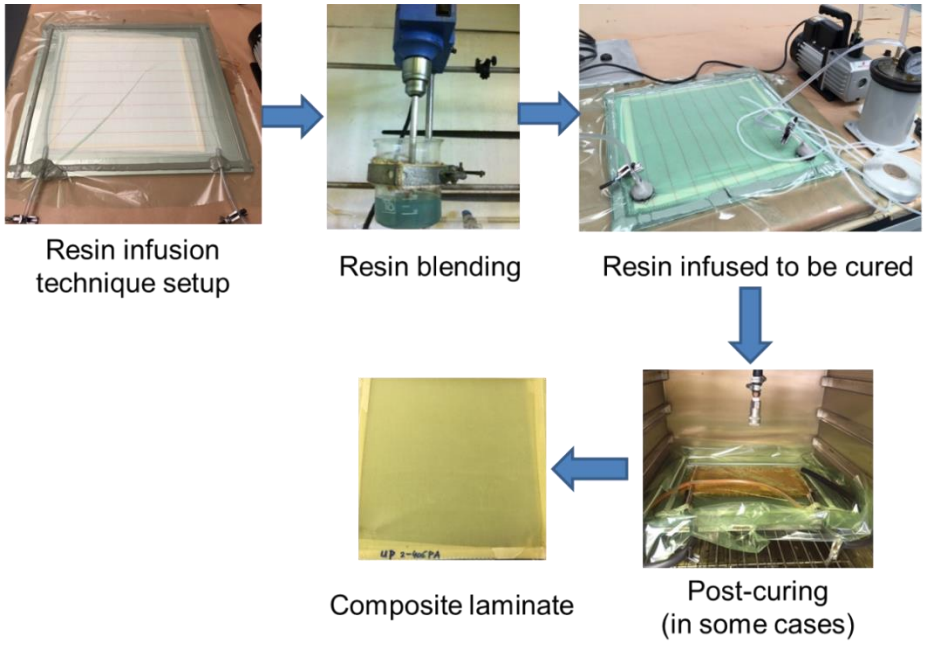

Figure 2.3: Preparation process for glass fibre-reinforced composite laminates by resin infusion technique

2.3.3 Sandwich structure samples preparation

To make sandwich structure samples, the same methodology to prepare GFRC laminates was used. 25.4 mm (1 inch) and/or 12.7 mm (0.5 inch) balsa wood sheet with the size of 300 mm × 300 mm was used as a core material, which was dried in the oven at 80 °C for 12 hours (to lose around 8% moisture by calculation) prior to making sandwich structure samples.

Two techniques were used to prepare sandwich structure samples:
(1) Laminates were made by hand lay-up or resin infusion technique and then stuck to both sides of balsa core with glue.
(2) Hand lay-up sandwich structure: all in one go.

In order to clarify different techniques used to prepare different sandwich structures, the schematics and flow charts are shown in Table 2.3.

- Resin infused laminate only on top: One laminate was prepared using the resin infusion technique and glued on one side of the balsa core.
- Resin infused laminate on both sides: Two laminates were prepared using the resin infusion technique and glued on both sides of the balsa core.
- Hand lay-up laminates on both sides: Two laminates were prepared using the hand lay-up technique and glued on both sides of the balsa core.
- Hand lay-up sandwich structure: in one go, as can be seen from the flow chart shown below, for the bottom skin, 4 layers of resin impregnated glass fabric layers were stacked (wet laminate) first, the balsa core was placed on top of the prepared wet laminate, and then

another wet laminate prepared separately on another metal plate was placed on top of balsa core to make the wet sandwich structure. The assembly was then vacuum bagged as for the hand lay-up structure (Section 2.3.2.1) and cured.

In some cases, due to the delamination of the core and laminate, epoxy resin was used as an adhesive for all VE and VE blended sandwich structured samples.

The differences among all of these techniques will be discussed later on in Chapter 4.

Table 2.3: Different techniques for sample preparation of sandwich structures

Samples	Laminates (4 plies)	Sandwich preparation	Finished samples
Resin infused laminates, only on top	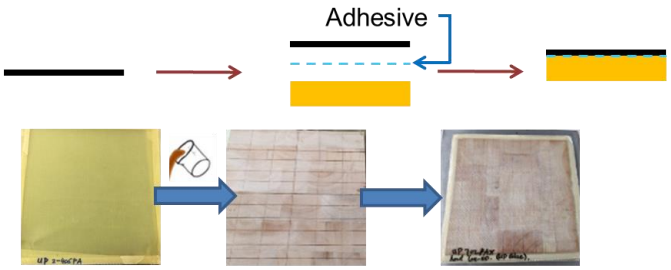		
Resin infused laminates on both sides	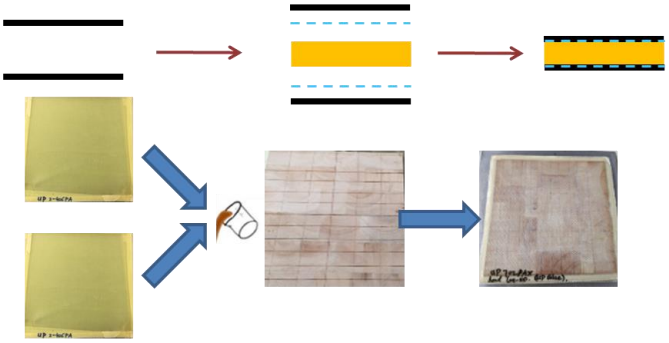		
Hand lay-up laminates on both sides	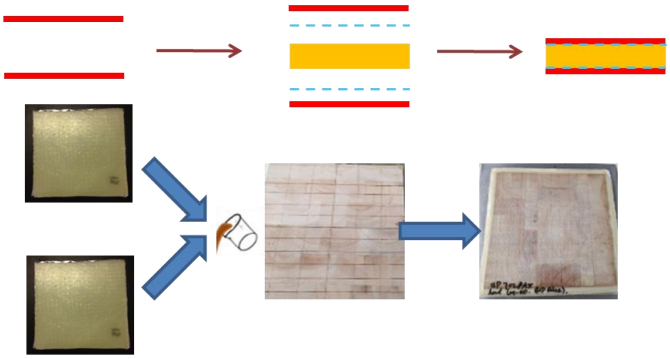		
Hand lay-up, sandwich structure (In one go)	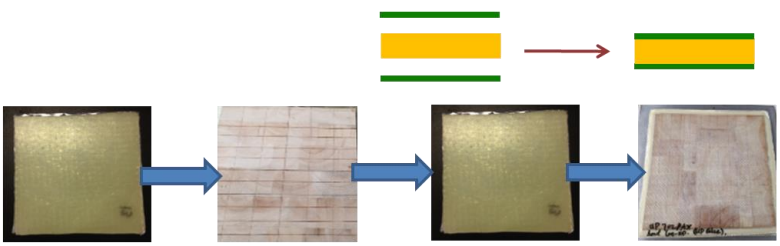		

2.3.3.1 Sandwich structure composites with similar components but different compositions

A number of sandwich composites containing similar components but different compositions were prepared. The variables included thicknesses of core materials, composite laminates on one/both sides and different sample preparation techniques. The effects of these variables on fire performances of the composite structures were evaluated.

In order to see how balsa wood burns in comparison to plywood, cone calorimetric tests were carried out at 50 kW/m^2 heat flux on 6 mm thick plywood and 12.7 mm thick balsa wood. The results given in Appendix 1 (Figure A1-1 and Table A1-1) indicated that balsa wood ignited early due to its porous structure, but burnt for a lesser time despite being double in thickness (12.7 mm) compared to plywood (6 mm). Both wood samples though burnt in a similar manner, i.e., with two peaks of heat release, however, the plywood had higher PHRR, THR and TSR values, indicating lower flammability of the balsa wood. The reproducibility of the results though was similar in both cases. Hence, end grain balsa was the best choice for this research work considering its cost and performance.

For these composites, UP-R resin was selected because of its commercial importance, and this resin showed better performances than UP in the resin infusion technique. Six samples were prepared using different arrangements as shown in Table 2.4. Two thicknesses of 12.7 mm (0.5 inch) and 25.4 mm (1 inch) balsa core were used. UP-R resin also was used as an adhesive to stick composite laminates on the balsa core for the whole set. The assembly of sandwich structures was then cured by vacuum bagging under 1 bar pressure. The size of prepared samples was 300 × 300 mm^2 and cut to the desired size for testing respectively. Details of the sample are given in Table 2.4.

Table 2.4: Sandwich structure samples – UP-R set (Crystic® 702PAX)

Sample Name	Sample ID	Thickness (mm)
Resin infused laminates (Top side) - 1 inch	RI-Top UP-1	26.8
Resin infused laminates (Both sides) - 1 inch	RI-UP-1	27.9
Hand lay-up laminates - 1 inch	HL-UP-1	27.7
Hand lay-up sandwich structure: in one go - 1 inch	HLAll-UP-1	27.4
Resin infused laminates (Both sides) - 0.5 inch	RI-UP-0.5	15.2
Hand lay-up sandwich structure: in one go - 0.5 inch	HLAll-UP-0.5	14.7

2.3.3.2 Sandwich structure composites with different resin types and combinations

All sandwich composite structures were prepared using the 25.4 mm (1 inch) balsa core and composite laminates on both sides, but the composite laminates were from different resin types or resin blends. All samples prepared are given in Table 2.5. Hand lay-up sandwich structure in one go (HLAll) technique was used for these composites because of less time consumption and easier handling during sample preparation. In total eighteen samples were prepared using UP, VE, Ep, Elium, UP/PH-Res, VE/PH-Res, UP/VE and UP/VE/PH-Res resins. Only VE resins and VE/Methylon blends were prepared, owing to the incompatibility between VE with Durez reported in our previous studies [14] and so VE/Durez blends were discarded here. Some initial experiments for UP-R with PH-Res blends were tried, as a result of extraordinary performances of UP-R's commercial importance in resin infusion technique mentioned in Section 2.3.3.1 than UP, but again incompatibility between UP-R/PH-Res blends was observed, hence UP was used. Furthermore, due to the excellent flame retardancy of PH-Res, especially Methylon based on our previous work [13-15], in two samples (Samples 17 and 18, Table 2.5), top one layer of Methylon and other three layers made of UP/VE blends or UP, namely 3UP/VE1M or 3UP1M, respectively, were used to design sandwich structure composites.

As already mentioned in Section 2.3.2 above, after some preliminary experimentation, the amount of catalyst, accelerator and initiator for all of UP, VE, Elium resins and their blends used were significantly reduced to increase gel times. The catalyst Trigonox® 239 reduced from 2 to 1 wt%, accelerator cobalt octoate from 0.25 to 0.1 wt%, catalyst Butanox® M-50 from 2 to 1 wt% and Benzoyl Peroxide from 2 to 1 wt%, respectively.

Details of the samples and adhesive used for all samples are given in Table 2.5. During sandwich structure preparation, for most of the samples in this set, neat resin or blended resins themselves were used as adhesives to bind wet laminates on the balsa core. Only in Samples 3 (VE-Ep), 4 (VE-Nov), 11,12 (VE-Ep/Methylon blends) and 13,14 (VE-Nov/Methylon blends), an epoxy resin (Araldite® LY 5052) was used as an adhesive to stick composite laminates onto balsa core. This was because if the base resin was used, the delamination between VE skin and core occurred, indicating their incompatibility. Moisture on the surface of the balsa core would have a detrimental effect on the strength and durability of the adhesive bond, hence balsa wood was thoroughly dried in an oven before bonding with the composite laminates.

All sandwich structures were cured under vacuum with 1 bar pressure using curing conditions given in Table 2.5. The size of prepared samples was 300 × 300 mm^2, thicknesses of which were slightly varied from 26.9 to 27.6 mm, from which coupons of the desired sizes for fire testing.

Table 2.5: Sandwich structures with balsa core thicknesses of 25.4 mm for UP, VE, Ep, Elium, UP/PH-Res, VE/PH-Res, UP/VE and UP/VE/PH-Res resins as skins

Sample No.	Samples (skin types)	Adhesive	Thickness (mm)	Curing conditions
	Neat resin + Glass woven plain fabric			
1	UP	UP	27.4	RT 24h, 80 °C 6h
2	UP-R	UP-R	27.4	RT 24h, 80 °C 6h
3	VE-Ep	Ep	27.2	RT 24h, 80 °C 3h, 140 °C 3h
4	VE-Nov	Ep	27.3	RT 24h, 80 °C 3h
5	Ep	Ep	27.3	RT 24h, 80 °C 6h
6	Elium	Elium	27.6	RT 4h, 90 °C 6h
	Blended resins + Glass woven plain fabric			
7	UP/Durez:70/30	UP/Durez:70/30	27.2	50 °C 6h, 80 °C 24h, 90 °C 9h, 130 °C 1h, 160 °C 1h, 180 °C 2h
8	UP/Durez:50/50	UP/Durez:50/50	27.3	80 °C 24h, 100 °C 1h, 130 °C 1h, 160 °C 1h, 180 °C 2h
9	UP/Methylon:70/30	UP/Methylon:70/30	27.2	50 °C 6h, 80 °C 12h, 100 °C 8h, 120 °C 6h, 130 °C 6h, 150 °C 2h, 180 °C 3h
10	UP/Methylon:50/50	UP/Methylon:50/50	27.2	50 °C 6h, 80 °C 12h, 100 °C 8h, 120 °C 6h, 130 °C 6h, 150 °C 2h, 190 °C 3h
11	VE-Ep/Methylon:70/30	Ep	27.2	RT 2h, 80 °C 6h, 100 °C 6h, 150 °C 6h, 180 °C 6h
12	VE-Ep/Methylon:50/50	Ep	27.2	RT 2h, 80 °C 6h, 110 °C 6h, 140 °C 6h, 180 °C 6h
13	VE-Nov/Methylon:70/30	Ep	26.9	RT 2h, 80 °C 6h, 100 °C 6h, 150 °C 6h, 180 °C 6h
14	VE-Nov/Methylon:50/50	Ep	27.2	RT 2h, 80 °C 6h, 110 °C 6h, 140 °C 6h, 180 °C 6h
15	UP/VE-Nov:50/50	UP/VE-Nov:50/50	27.3	RT 24h, 80 °C 12h
16	UP/VE-Nov/Methylon:35/35/30	UP/VE-Nov/Methylon:35/35/30	27.2	50 °C 2h, 80 °C 12h, 100 °C 6h, 120 °C 6h, 130 °C 6h, 150 °C 2h, 180 °C 4h, 190 °C 6h
17	UP/VE-Nov:50/50; top one layer of Methylon (3UP/VE1M)	UP/VE-Nov:50/50	27.4	RT 12h, 80 °C 12h, 100 °C 8h, 120 °C 6h, 130 °C 6h, 150 °C 2h, 180 °C 6h
18	UP; top one layer of Methylon (3UP1M)	UP	27.3	RT 24h, 80 °C 12h, 100 °C 8h, 120 °C 6h, 130 °C 6h, 150 °C 2h, 180 °C 6h

2.4 Experimental techniques

2.4.1 Differential scanning calorimetry (DSC) – Curing behaviour study

DSC was used to study the thermal curing behaviour of neat resins and their blends, and some DSC, DMTA and TGA results in Sections 2.4.1 - 2.4.3 were taken from my colleague's and my previous work [13-15]. The rest were carried out especially for this work using a DSC (Q2000, TA instruments) to monitor the curing of the resin and resin blend samples (2-10 mg). The curing peak and heat of reaction during curing (J/g) from the curves were measured. Around 5 mg of each uncured resin and resin blends, including appropriate curing agents, was placed in an aluminium pan (standard pan) fitted with an aluminium lid (standard lid) that had a pin hole to ensure that any volatiles could escape during dynamic temperature scanning from 30 °C to 300 °C with a heating rate of 5 °C/minute under nitrogen at a gas flow rate of 100 mL/minute into DSC cell. During the curing procedure, each sample cured in the oven was taken out to run the DSC again to see if it was cured. After curing, the sample was tested again to find out whether the resin was completely cured or any further post-curing was required.

2.4.2 Dynamic mechanical thermal analysis (DMTA) – Compatibility study

A DMA Q800 from TA instruments was used to test cast resin samples with a single cantilever clamp and multi-frequency-strain experiment set up (0.1% strain and 1 Hz frequency). The test specimen was clamped between the movable and stationary fixture of the single cantilever clamp and was placed in an enclosed thermal chamber. The specimen size of 17.5 × 13 × 3 mm^3 was heated at 5 °C/minute within the temperature range 30 - 300 °C. Poisson's ratio was set to 0.36. Poisson's ratio is a measure of the Poisson effect, the phenomenon in which a material tends to expand in directions perpendicular to the direction of compression. In general, the fully cured thermoset resins display Poisson's ratio values in between 0.2 - 0.36 at room temperature depending on the resin type, hence it was set to 0.36. Tan delta, storage modulus and loss modulus were measured and recorded. The temperature at the peak on the Tan delta curve was taken as the glass transition temperature (T_g) of the material, which might be slightly different from the value determined by DSC. DMTA was used to confirm whether cast resins were fully cured or not, also to study the compatibility of blended resins and figure out their glass transition temperatures (T_g).

2.4.3 Thermogravimetric analysis (TGA) – Thermal stability analysis

Thermogravimetric Analysis (TGA) measures weight changes in a material as a function of temperature or time under a controlled atmosphere either in air or nitrogen and also measures thermal stabilities of materials. Some results were taken from our group's previous work [13-15], the rest of neat resins and/or their resin blends were subjected to TGA studies by using an SDT

2960 from TA instruments. A resin sample (using 10 ± 1 mg) was placed in a platinum sample pan that was supported by a precision balance and heated over a temperature range from room temperature to 900 °C at a constant heating rate of 10 °C/minute under air or nitrogen with flow rate 100 ± 5 mL/minute.

2.4.4 Pyrolysis combustion flow calorimetry (PCFC) – Combustion behaviour analysis

A pyrolysis combustion flow calorimeter is a small-scale tool to study the flammability of materials using 3-10 mg sample size. The technique involves controlled pyrolysis of the sample in an inert gas stream followed by high temperature oxidation of the volatile pyrolysis products. Oxygen consumption theory is used to measure the heat of combustion of the pyrolysis products. The maximum amount of heat released per unit mass per degree of temperature (J g^{-1} K^{-1}) is a material property that can be a good predictor of flammability. The heat release capacity (HRC), defined as the maximum heat release rate divided by the constant heating rate in the test, and the temperature at the maximum heat release rate (T_{max}), are the principle results obtained from the PCFC.

In this work a PCFC, Fire Testing Technology Ltd., UK, was used for flammability assessment of different cured neat resins and their blended samples. The heating rate used in the pyrolysis zone was 1 °C/s to 750 °C. The pyrolysis was conducted under flowing nitrogen (80 cc/min). The combustion temperature was set at 900 °C under flowing gas with a mixture of O_2/N_2 at 20/80 cc/minute flow rate by volume, and the sample weight was 3-5 ± 0.5 mg. The results, the heat release capacity (HRC), peak value of heat release rate (PHRR), total heat release (THR) and PHRR temperature (Peak Temperature) of tested samples, presented are averages of three experiments.

2.4.5 Cone calorimetry – Fire performance study

For cone calorimetric tests, a cone calorimeter instrument (Fire Testing Technology, UK) was used to evaluate the flammability and fire performance of cast resin samples, GFRC laminates and sandwich structure samples in accordance with ISO 5660. For cast resins circular samples of 55 mm diameter with a thickness of 3 mm were used. Whereas, for composite laminates 75 mm × 75 mm square specimens with a thickness of approximately 1 mm were used, and for sandwich structure samples 75 mm × 75 mm square specimens with a thickness of approximately 15-28 mm were used. Before cone calorimeter testing, the bottom surface and the edges of the samples were wrapped with aluminium foil of approximately 0.04 mm thickness as per ISO 5660, with the shiny side towards the specimen to ensure that only the top surface would be exposed to the radiant heat source directly. The fundamental principle behind cone calorimetry is that the amount of oxygen consumed during the combustion of polymeric material is proportional to the amount of heat released [16,17]. When the sample is heated, volatiles are

ignited and extracted through the exhaust duct with a set orifice flow rate of 24 L/s fed into an oxygen analyser, which measures the amount of oxygen consumed. The consumption of oxygen by the sample during the test is measured and converted into a heat release value, as approximately 13.1 MJ of heat is released per kilogram of oxygen consumed during combustion. The rate of smoke released every second is measured from the liberated smoke opacity in the exhaust duct with respect to light transmittance from a laser (632.8 nm wavelength) to a photocell detector located across the duct. The transmittance is recorded using the cone software (ConeCalc, Fire Testing Technology). The higher the smoke opacity means the lower the light transmission. The total smoke production is obtained by summing up the rate of smoke release over the burning period.

From these data, the primary fire properties (i.e., main cone parameters) can be measured and obtained by the cone calorimeter including time-to-ignition (TTI), time-to-flame-out (FO), peak heat release rate (PHRR), total heat release (THR), total smoke release (TSR) and residual mass (%). Those parameters were recorded and used to evaluate the fire performances for different types of cast resins, composite laminates, core materials and sandwich structures. The data collected from this bench scale real fire test can be used for fire modelling and prediction of large-scale fire behaviour.

Figure 2.4: Fire Testing Technology (FTT) Cone calorimetry

The sample holder and methodology were slightly modified compared to those described in ISO 5660. The limitation in the quantity of samples available resulted in the use of specimens with a reduced sample size of 75 mm × 75 mm rather than using the normal 100 mm × 100 mm sizes as outlined in ISO 5660. In previous work in our laboratories, the use of reduced size gave similar relative trends (similar PHRR, THR and EHC results of same sample were obtained) to those observed using 100 mm × 100 mm specimens [18]. Cone calorimetry was conducted at

an incident heat flux of 50 kW/m^2 with a minimum of three replicates for each formulation in both horizontal and vertical orientations. Spark ignition was used as the ignition source.

Methodology used for two cone orientations is as:

2.4.5.1 Horizontal orientation

(1) Normal cone testing in horizontal orientation

The specimen was wrapped in the usual way and placed on a 75 mm × 75 mm dimensions metal sample holder according to ISO 5660, which was then placed on the load cell to detect and record the weight of the sample during the experiment, and then exposed to a radiant heat source in horizontal orientation at a predetermined heat flux. An electric spark igniter was situated around 13 mm right above the top surface of a specimen and below the cone heater, which ignited the flammable gases leaving the sample when the sample was heated. The distance between front face of the specimen and the cone heater face was adjusted to 25 mm. When the sample ignited, the igniter was turned off and moved to the side.

(2) Cone testing in horizontal orientation with thermocouples

In order to understand the temperature profiles through the thickness and of various components of sandwich structures during the cone calorimetric tests, thermocouples were inserted in samples. The experimental methodology is same as described in Section 2.4.5.1 (1), but of three specimens tested for each sample, one contained thermocouples. For three different types of tested samples, the experimental setup for temperature measurements was different. The thermocouples' setup is shown in Figure 2.5.

a) Composite laminates – two K-type thermocouples were inserted in each sample; one was on the top of surface and the other was on back surface of sample.
b) Core material – four K-type thermocouples were placed in each sample, one was on the top of surface, two were inserted at even distances in the core material and the last one was inserted on the back surface of sample.
c) Sandwich structures – five K-type thermocouples were placed in each sample, in which: (I) on top of the upper surface (II) just underneath the upper surface (III) within centre of the core material (balsa wood) interior (IV) just underneath core material (balsa wood) and (V) underneath the lower surface.

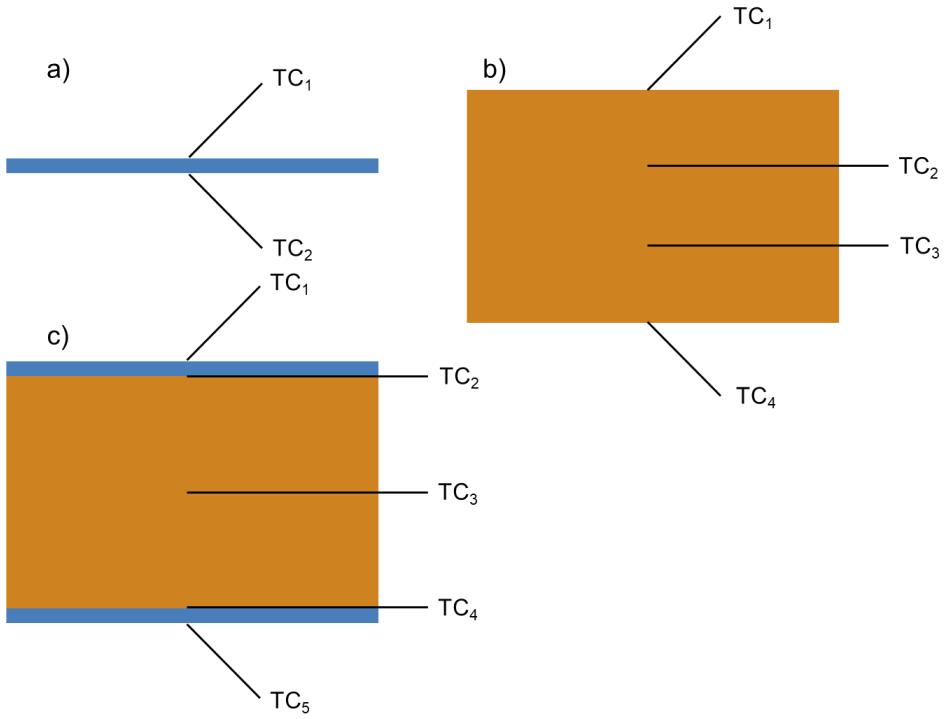

Figure 2.5: Experimental setup for temperature measurements in horizontal orientation in a cone calorimeter of (a) composite laminates, (b) core material and (c) sandwich structures

To insert the thermocouples within the sandwich composites (Figure 2.5 (c)), holes were drilled in the core material at required positions (one at each end of the interface (TC_2, TC_4) and one in the middle (TC_3)) using a 0.5 mm diameter twist drill bit. A small amount of an epoxy adhesive (Araldite® Rapid) was applied on the tips of thermocouples before being pushed through the core to the centre of the sample. For the back surface of the sample, one thermocouple (TC_5) with epoxy glue on its tip was directly attached to the surface. The samples were left for at least 30 minutes to let the adhesive resin cure prior to testing. The thermocouple for the top surface (TC_1) was tilted, passed through the hole of the cone heater frame and placed on the top surface of the sample at a 30-degree angle to ensure that a downwards force is applied and the thermocouple remains in place during the test. On the top surface thermocouple, TC_1, epoxy glue was not applied as it would have become source of ignition.

2.4.5.2 Vertical orientation

In this case, the cone heater was moved into the vertical orientation and a special sample holder was constructed ‘in house’ from 1.5 mm mild steel sheet; 25 mm side right angle pieces were folded and cut to the required length and depth and welded up to hold samples of 75 mm × 75 mm dimensions. This yielded a frame without a rear central area with the view that if this was omitted then temperature measurements could be made from the rear face of the sample. The sample holder was provided with an internal backing board of 6 mm thick calcium silicate (Duratec® 750) followed by a layer of calcium silicate wool immediately behind the sample which was wrapped in the usual way. Further backing boards were cut and drilled with 1 mm diameter holes for mineral insulated thermocouples (type 310 stainless steel sheath). The backing board

was marked with a vertical centre line, the position of the sample determined and holes for the thermocouple were drilled to match the centre of the sample, and another two points 10 mm above and 10 mm below the centre of the sample. The thermocouples were pushed through the calcium silicate wool and aluminium foil to make contact with the sample. The whole assembly was held in place using thin stainless-steel wires wrapped around and twisted on the back surface. The sample holder setup is shown in Figures 2.7 and 2.8. Tests were conducted at a heat flux of 50 kW/m^2. Since a high irradiance was applied to the sample, a mild steel shutter was constructed with calcium silicate card insulation on the side facing the cone radiator in order to reduce preheating of the sample and operator. Spark ignition was as in standard orientation and at approximately 10 mm in the front of the front surface of the sample when the test was initiated. The spark igniter was in the idle position before the test began and was removed immediately once the ignition was done. Figure 2.6 indicates experimental setup in vertical orientation in a cone calorimeter.

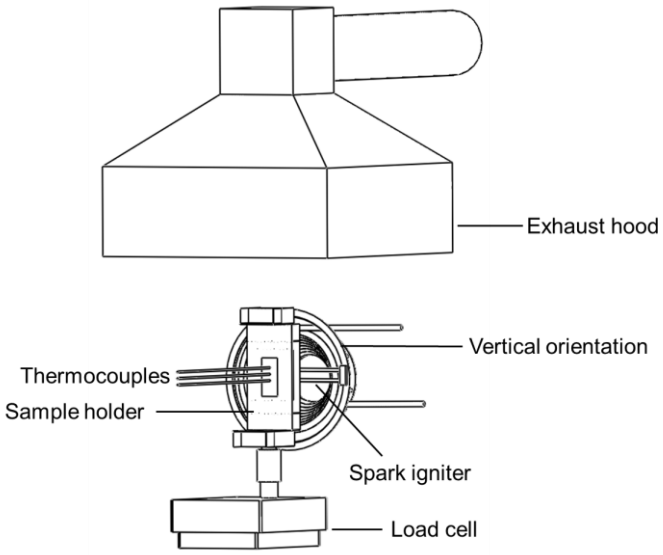

Figure 2.6: Experimental setup in vertical orientation in a cone calorimeter (not to scale)

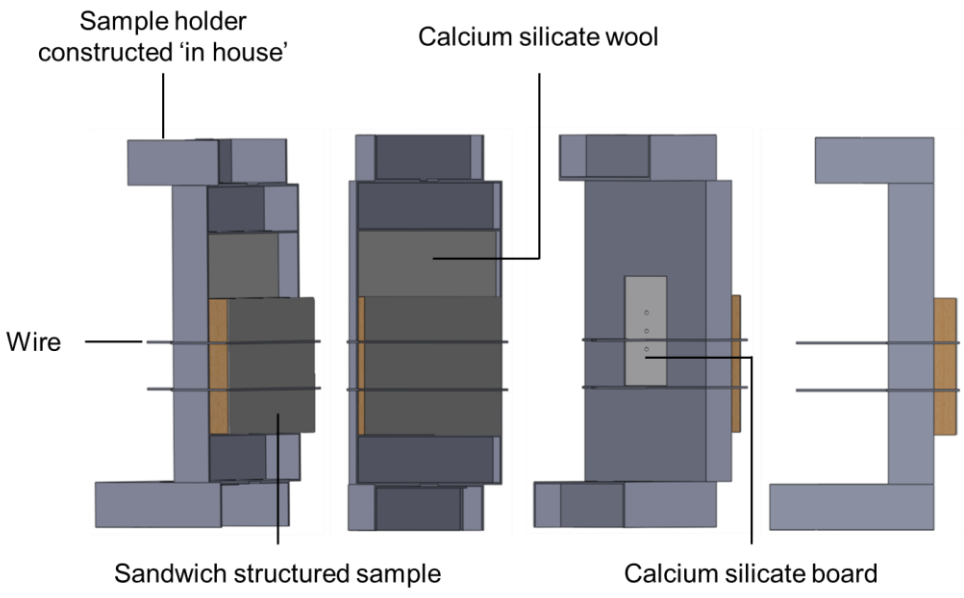

Figure 2.7: Various views (45°, front, back and side views) of sample holder setup

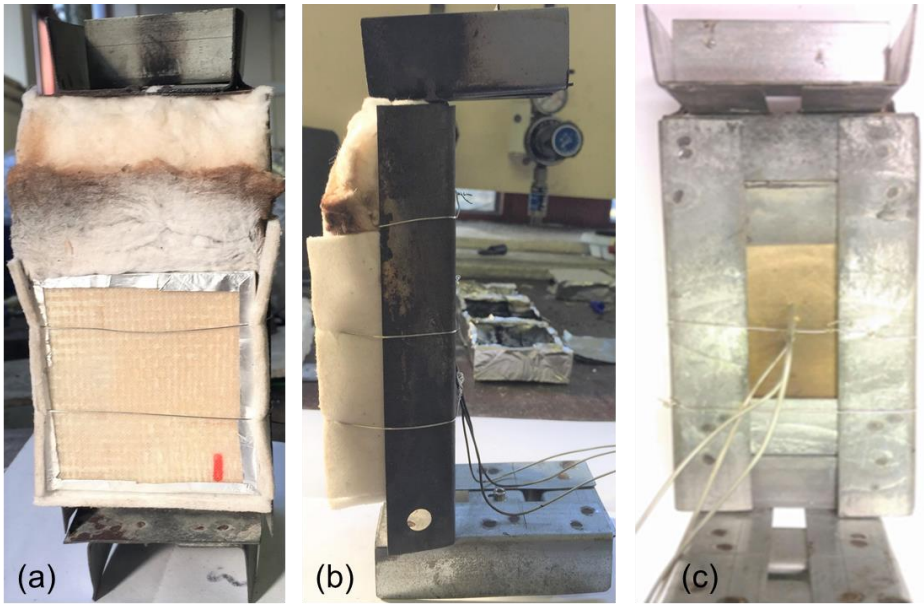

Figure 2.8: Digital images of sample holder assembly (a) front view, (b) side view, and (c) back view in a cone calorimeter in vertical orientation

Temperature versus time plots of different components in sandwich structures - composite laminates (skin), balsa wood (core) and sandwich structures during the tests were recorded in both horizontal and vertical orientations by a data logger and plotted, respectively. This experiment was repeated five times, three for normal horizontal cone calorimetric tests and another two - one for each orientation with thermocouples.

2.4.6 Propane burner testing – Fire performance study

The propane burner test was carried out in the Fire Lab at the University of Newcastle. The test facility at Newcastle was previously developed based on a test reported elsewhere [19] aiming to study the fire behaviour of composites designed for aircraft industry. This test is compliant with two aeronautical certification fire tests: ISO 2685:1998(E) [20] from the International Organization for Standardization and FAR 25.856(b):2003 [21] from the Federal Aviation Administration (FAA). ISO 2685:1998(E) provides guidance for the test method to determine the fire resistance of all structures located in zones designated as ‘fire zones’. As described in the standard, the material has to be ‘capable of withstanding the application of heat by a standard flame for 5 minutes’. During the test, the specimen is placed in a vertical orientation and at a distance of 75 mm from the burner nose. A standard flame calibrated at a temperature of 1100 °C and with a heat flux of 116 kW/m^2 and delivered by a propane gas burner is applied on the specimen. Another standard FAR 25.856(b):2003 defines a method to determine the burn-through resistance characteristics of the material when exposed to a high intensity open flame. This specification permits demonstration of the non-penetration of the flame through the thermal insulation materials. Based on the two fire tests standards mentioned above, methodology for propane burner test was modified than those described in ISO 2685:1998(E) and FAR 25.856(b):2003 by Gibson et al [22].

The propane burner test was performed by exposing 150 mm × 150 mm samples (GFRC laminates, balsa core and sandwich structures) to a propane flame (sourced from Calor Gas Ltd.). The temperature measurements were carried out using a constant heat flux test with a calibrated propane burner (sourced from Bullfinch), as shown in Figure 2.9. The sample was mounted on a 10 mm thick steel substrate, protected around the edges and side by Kaowool ceramic fibre insulation. The temperature rises at the reverse faces of the samples were continuously monitored during the tests by two thermocouples placed and glued using epoxy adhesive resins (Araldite® 2014) on the rear centre face of the samples and fully insulated by Kaowool. A burner-to-sample distance of 350 mm was used throughout the tests. Another thermocouple for hot face temperature measurement was placed and maintained 10 mm in front of the tested sample front face, following the procedure proposed by Gibson [22]. The hot face temperature in the test was controlled at a constant value by adjusting propane burner gas pressure measured with a k-type thermocouple maintained at a point 10 mm in front of the test sample to ensure that temperature was 1000 ± 50 °C. The propane burner applied at the sample surface was at a constant heat flux of 113 kW/m^2, the test parameters of the heat flux were slightly adjusted from those given in two standards mentioned above so that the results obtained could be directly compared with Gibson team's work [22]. The ventilation system (extraction/exhaust hood) was on at all times during the test.

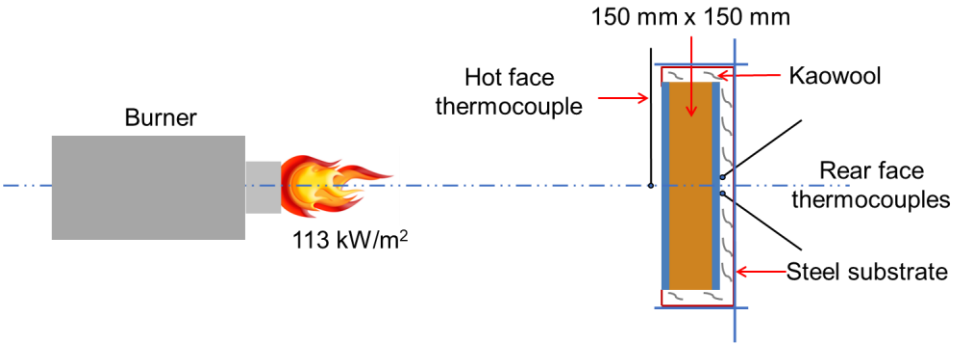

Figure 2.9: A schematic (side view) of propane burner testing (not to scale)

The images of the setup for testing are shown in Figure 2.10. It should be noted that tests were stopped manually when the back-surface temperature reached 300 °C, this is because resin started decomposing and the propane flame burnt through the whole sample above that temperature along with heavy smoke being observed from the back.

Figure 2.10: (a) Propane burner testing setup for temperature measurements on sandwich composites; (b) Propane burner testing in progress

2.5 References

[1] Crystic® 2-406PA, Scott Bader, Material Safety Data Sheet
[2] Butanox® M-50, Akzo Nobel, Material Safety Data Sheet
[3] Crystic® VE676, Scott Bader, Material Safety Data Sheet
[4] Crystic® VE673, Scott Bader, Material Safety Data Sheet
[5] Trigonox® 239, Akzo Nobel, Material Safety Data Sheet
[6] Araldite® LY 5052, Huntsman, Material Safety Data Sheet
[7] Aradur® 5052 CH, Huntsman, Material Safety Data Sheet
[8] Durez® 33156, Sumitomo Bakelite Europe NV, Material Safety Data Sheet
[9] Methylon® 75108, Sumitomo Bakelite Europe NV, Material Safety Data Sheet
[10] Elium® 150, Arkema, Material Safety Data Sheet
[11] Benzoyl Peroxide (wetted with ca. 25% Water), Tokyo Chemical Industry, Material Safety Data Sheet
[12] M.V. Alonso, M. Oliet, J.M. Perez, F. Rodrıguez, and J. Echeverrıa, “Determination of curing kinetic parameters of lignin–phenol–formaldehyde resole resins by several dynamic differential scanning calorimetry methods,” *Thermochimica Acta*, vol. 419, pp. 161–167, 2004.
[13] D. Deli, B.K. Kandola, J.R. Ebdon, and L. Krishnan, “Blends of unsaturated polyester and phenolic resins for application as fire-resistant matrices in fibre-reinforced composites. Part 1: identifying compatible, co-curable resin mixtures,” *Journal of Materials Science*, vol. 48, pp. 6929–6942, 2013.
[14] B.K. Kandola, J.R. Ebdon, and C. Zhou, “Development of vinyl ester resins with improved flame retardant properties for structural marine applications,” *Reactive and Functional Polymers*, vol. 129, pp. 111–122, 2018.
[15] B.K. Kandola, L. Krishnan, D. Deli, and J.R. Ebdon, “Blends of unsaturated polyester and phenolic resins for application as fire-resistant matrices in fibre-reinforced composites. Part 2: Effects of resin structure, compatibility and composition on fire performance,” *Polymer Degradation and Stability*, vol. 113, pp. 154–167, 2015.
[16] V. Babrauskas, “Specimen heat fluxes for bench-scale heat release rate testing,” *Fire and Materials*, vol. 19, no. 6, pp. 243–252, 1995.
[17] ISO 5660-1:1993. Fire tests on building materials and structures – Part 15: Method for measuring the rate of heat release of products.
[18] B. Biswas and B.K. Kandola, “The effect of chemically reactive type flame retardant additives on flammability of PES toughened epoxy resin and carbon fiber-reinforced composites,” *Polymers for Advanced Technologies*, vol. 22, no. 7, pp. 1192–1204, 2011.
[19] P. Tranchard, F. Samyn, S. Duquesne, M. Thomas, B. Estebe, J-L Montes, and S. Bourbigot, “Fire behaviour of carbon fibre epoxy composites for aircraft: Novel test bench and experimental study,” *Journal of Fire Sciences*, vol. 33, no. 3, pp. 247–266, 2015.
[20] ISO 2685:1998(E). Aircraft — Environmental test procedure for airborne equipment — Resistance to fire in designated fire zones. International Organization for Standardization, 1998.
[21] FAR 25.856(b):2003. Title 14 code of Federal – test methods to determine the burnthrough resistance of thermal/acoustic insulation materials (Appendix F, Part VII).
[22] A.G. Gibson, G. Kotsikos, P. DiModica, S. Christke, W.W. Jusoh, K. Yi, A.P. Mouritz, and E. Kandare, “Model for the Characterisation and Design of Passive Fire Protection (PFP) Systems for Steel Structures,” *Composite Fire Protection ECCM 2016*, 2016.

Chapter 3: Material characterisation

In this chapter the physical, chemical, morphological, thermal properties and fire performances of various components to be used for sandwich composite structures have been discussed, based on which materials were selected for making sandwich composites. The knowledge gained has also been used for analysing the fire behaviours of the composites in later chapters. As mentioned previously the sandwich composite structure is made of two fibre-reinforced polymeric composite laminates as skins and a core, usually balsa for marine structures. The composite laminates used in this work are made of glass fibre and different resins/resin blends. Since the glass fibre is not flammable, this was not tested further. All generic properties available from the manufacturer or literature for the glass fibre, different resins and balsa wood have already been given in Chapter 2, Section 2.1. Here their properties related to morphology, curing, thermal stability and fire performances have been discussed in detail. Some of the data have been taken from previous studies undertaken within the Fire Materials Group at Bolton [1-3], while some studies were carried out specially for this work.

3.1 Rationale for choice of the resins

Unsaturated polyester (UP) and vinyl ester (VE) resins are commonly used in marine applications [4,5], hence are the focus of this study. Other resins of interest are epoxy (Ep), and phenolics (PH-Res). Epoxy though not very common for marine applications, is preferentially used in aerospace, trains, automotive, etc, hence chosen for comparison. Phenolics were chosen because they are inherently flame retardant and are used in ship interiors or other parts where fire performance is a major issue. Recently, a new low-cost resin has been developed by Arkema [6], which is a liquid thermoplastic acrylic resin (Elium) and is suitable for resin transfer moulding and resin infusion processes. It has mechanical properties similar to epoxy resin and also presents major advantages of being post-thermoformable and recyclable [6]. Hence, this resin is also studied.

3.2 Physical, chemical and morphological properties

3.2.1 Neat resins

Unsaturated polyesters (UP) are condensation polymers formed by the reaction of polyols (also known as polyhydric alcohols), organic compounds with multiple alcohol or hydroxy functional groups, with saturated or unsaturated dibasic acids [4,7]. The use of unsaturated polyesters and additives such as styrene lowers the viscosity of the resin. The initially liquid resin is converted to a solid by cross-linking of chains. This is done by creating free radicals at unsaturated bonds, which propagate in a chain reaction via other unsaturated bonds in adjacent molecules, linking them in the process. The initial free radicals are induced by adding a compound that easily

decomposes into free radicals. This compound is known as the initiator; commonly used initiators are generally organic peroxides such as benzoyl peroxide or methyl ethyl ketone peroxide [5,8]. Cobalt salts are often used as catalysts. Unsaturated polyesters offer ease of handling, low cost, dimensional stability, as well as good mechanical, chemical-resistance and electrical properties, which provide the most economical way to incorporate resin, filler and reinforcement. Two UP resins, Crystic® 2-406PA (UP) and Crystic® 702PAX (UP-R) were sourced from Scott-Bader (see Section 2.1.1.1, Chapter 2). UP was selected because it is commercially used for marine applications. UP-R was chosen because it is suitable for use in the resin infusion technique. Both UP resins were cured with a methyl ethyl ketone peroxide-based radical catalyst (Butanox® M-50, Akzo Nobel).

Vinyl ester resin (VE), is a resin produced by the esterification of an epoxy resin with acrylic or methacrylic acids [9-13]. The "vinyl" groups refer to these ester substituents, which are prone to polymerize. The diester product is then dissolved in a reactive solvent, such as styrene, to approximately 35-45 percent content by weight. Polymerization is initiated by free radicals, which are generated by UV-irradiation or peroxides [9]. This thermoset material can be used as an alternative to polyester and epoxy materials as the thermoset polymer matrix in composite materials, where its chemical characteristics, strengths, mechanical properties, and bulk cost are intermediate between those of polyester and epoxy [12,13]. Vinyl ester has lower resin viscosity (~ 200 cps) than polyester (~ 500 cps) and epoxy (~ 900 cps). Vinyl ester resin is a common resin in the marine industry due to its corrosion resistance and ability to withstand water absorption. It is usually initiated with methyl ethyl ketone peroxide.

VE resins are similar to UP resins as both systems contain carbon-carbon double bonds, which can copolymerize with styrene monomer. However, the physical properties of VE are, in general, superior to those of UP due to the fact that VE resins have reactive double bonds at the ends of short polyester chains, while UP resins have internal double bonds distributed along the chains. Hence VE provides better control over the degree of crosslinking of the resin [14]. Two VE resins, one epoxy (bisphenol A) based (VE-Ep) and another phenolic novolac based (VE-Nov) were sourced, which were cured by a free-radical catalyst Trigonox® 239 together with a redox accelerator, cobalt octoate. VE-Ep was selected because it is commonly used in the marine industry. VE-Nov was selected because of the presence of the novolac structure as it was expected that this would be less readily flammable than VE-Ep and also that it would be more compatible with phenolic resins.

Epoxy resin is one of the most extensively used thermoset resins because of its excellent mechanical strength, low cure shrinkage, a relatively high maximum use temperature, excellent adhesion to glass fibres and good resistance to environmental degradation [15-18]. Uncured epoxy resins are generally in liquid form and are mixed with chemical additives known as curing agents or hardeners. Under the influence of heat the mixture eventually turns into a rigid three-dimensional network [19]. In rail applications, epoxy composites are popular. Hence one epoxy

resin (Ep) sourced from Huntsman was selected as a reference material.

Phenolic resins are formed by the condensation reaction between phenol and formaldehyde, of which water is the major by-product [20]. Phenolic resin is generally known as an 'inherently flame retardant' resin due to its high aromatic content. When phenolic resin is subjected to flame, it chars rather than melting or burning. Hence it can be used in applications that are sensitive to flammability and smoke reduction requirements. The main disadvantages of phenolic resins are their brittleness and high curing shrinkage [21]. In addition, the curing processes of phenolic materials require careful temperature control and gradual heating to allow continuous elimination of volatiles in order to reduce the number of defects in final components [22]. Two phenolic resins (PH-Res) were selected based on our experience of their blends with unsaturated polyester resins as well as vinyl ester resins [1-3]. The phenolic resins were an alcohol-soluble resole (Durez) and an allyl-functional resole (Methylon), both from Sumitomo Bakelite Europe NV.

One commercialised liquid thermoplastic acrylic resin - Elium (Arkema, France) was also chosen to compare with different resin systems. Elium is a low-cost thermoplastic resin, recently developed by Arkema for manufacturing composites with mechanical properties similar to the thermosetting resins. This resin is suitable for resin transfer moulding (RTM) and resin infusion processes. It has mechanical properties similar to the epoxy resin and also presents major advantages of being post-thermoformable and recyclable.

3.2.2 Resin blends

The blending or intimate mixing of two resins is a well-recognized and useful method for preparing new materials that combine the excellent properties of more than one resin [1]. For example, blending of epoxy resin with phenolic resin, in which the phenolic resin can co-cure with the epoxy, allows low temperature curing [23]. In the context of improving the flame retardancy of unsaturated polyester (UP) or vinyl ester (VE) resins, one simple physical way is to co-cure them with inherently fire-retardant and char-forming phenolic resoles (PH-Res).

The homogeneous blending of two different polymeric materials/resins is a big challenge due to the absence of a significant entropic advantage associated with the mixing of one macromolecule with another; only if there is a significant negative enthalpy of mixing, i.e. a specific positive interaction between the two components, is mixing readily achieved [24]. In the case of pairs of crosslinkable polymeric resins there is an additional requirement: to complete the simultaneous curing of both resins. In the case of blending UP or VE with conventional phenolic resins the main challenge is the different curing mechanisms of these two resin types. Phenolics cure by condensation reactions with the elimination of water (incompatible with UP and VE) and formaldehyde at temperatures of up to 180-200 °C [25], whilst UP and VE resins cure with styrene by a free radical process at temperatures typically below 80 °C [7]. Thus, whilst

mixtures of low molecular weight resin precursors may be miscible, once chain extension and crosslinking begin, immiscibility may develop leading to significant phase separation and resulting in brittle, non-homogeneous, blends. With crosslinkable polymers, however, gross phase separation may be prevented and domain sizes kept small if the two resins co-cure to form a semi- or fully interpenetrating polymer network [26]. Well interpenetrated networks can behave as homogeneous materials, for example, they can display a single glass transition temperature (T_g). This can be achieved by adding different functional groups in one of the resins. This aspect has been extensively explored in previous research at Bolton [1,3,27-29]. To overcome the challenge of UP/PH-Res and VE/PH-Res incompatibility, arising from their different chemical structures and curing mechanisms (radical versus condensation), phenolic resins of different functionalities were explored.

It has been demonstrated that the flammability of UP-phenolic blends was significantly reduced compared to that of the UP resin [1,3,27-29]. This work was also extended to the almost equally flammable VE resin, and it was shown that the VE/PH-Res blends were less flammable than VE [2].

Based on above experience, here two phenolic resoles, an ethanol-soluble (Durez), and allyl-functionalised (Methylon) have been selected to be blended with UP or VE and the blends then used to make sandwich composite structures.

3.2.3 Physical appearances of cured neat resins and resin blends

Digital images of optimally cured and post-cured cast samples of neat resins and resin blends are shown in Figure 3.1 (a)-(h) and Figure 3.2 (a)-(m), respectively.

It can be seen from Figure 3.1 (a)-(e) and (h) that corresponding UP, UP-R, VE-Ep, VE-Nov, Ep and Elium sample plaques are relatively flat, smooth and uniform, without voids after curing, as expected in view of the homogeneity of these single materials. Although the cured Durez and Methylon samples are similarly clear and uniform without any voids after curing, see Figure 3.1 (f) and (g), plaques of both samples are slightly curved owing to differential mould shrinkage. Significant darkening of the phenolic samples, especially for Durez, takes place during curing probably owing to some chemical degradation and rearrangement leading to increased conjugated unsaturation and hence light absorption [2].

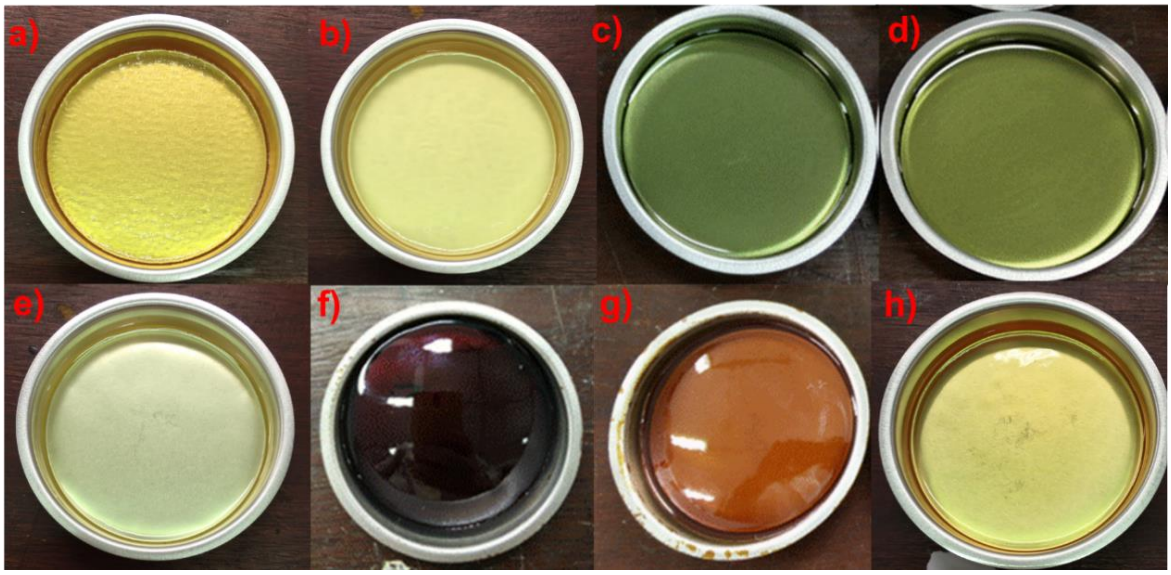

Figure 3.1: Digital images of cured neat resin samples of (a) UP; (b) UP-R; (c) VE-Ep; (d) VE-Nov; (e) Ep; (f) Durez; (g) Methylon; and (h) Elium

For UP/PH-Res blends, images of UP/Durez blends given in Figure 3.2 (a) and (b) show that in both 70/30 and 50/50 wt% of blends of UP/Durez some air bubbles can be observed, but there are no visible signs of inhomogeneity. Whereas in UP/Methylon blends, both cured 70/30 and 50/50 wt% blends appear from their images to be homogeneous, clear, flat and only few tiny bubbles on the bottom of the 70/30 wt% plaque (Figure 3.2 (c) and (d)). The compatibilities of UP/Durez and UP/Methylon blends have been discussed in detail in our group's previous publication [1].

In the case of VE/PH-Res blends, for the VE/Durez blends, those of the VE-Ep/Durez blends the digital images of cured resin plaques (Figure 3.2 (e) and (f)) showed some phase separation but not complete separation. These samples are not as homogeneous and clear as those of the individual resins (Figure 3.1 (c) and (f)). There are some blemishes and bubbles within the cured samples. Darkening in the 50/50 wt% blend can be clearly seen in Figure 3.2 (f), which may be due to some degradation resulting from curing at a high temperature of 230 °C. However, the images of VE-Nov/Durez blends show clear evidence of phase separation in the 70/30 wt% blend (Figure 3.2 (g)), which is even worse in the 50/50 wt% blend (Figure 3.2 (h)), in which voids exist in this sample and a large globule of phenolic resin suspended in the VE can be noticed. This is unexpected as VE-Nov was expected to be more compatible than VE-Ep with the phenolic resin owing to the presence of the novolac structure in it.

For VE/Methylon blends, all cured blended mixtures appear from their images to be homogeneous, clear, flat and free of bubbles (Figure 3.2 (i)-(l)), except for VE-Ep/Methylon:70/30 wt% (shown in Figure 3.2 (i)), in which some phase separation can be seen in the cured sample. This sample was prepared again by adding additional ethanol to lower the viscosity of the blended resin and improve homogeneity. One more additional step was added prior to the established curing conditions to remove the solvent curing at 50 °C for 6 hours, in

order to evaporate solvent. But phase separation was still there.

For UP/VE-Nov:50/50 blend shown in Figure 3.2 (m), it can be observed that the blended resin mixed well; the cured plaque looks homogeneous, it is flat and uniform, and without voids.

Figure 3.2: Digital images of cured resin blended samples of (a) UP/Durez:70/30; (b) UP/Durez:50/50; (c) UP/Methylon:70/30; (d) UP/Methylon:50/50; (e) VE-Ep/Durez:70/30; (f) VE-Ep/Durez:50/50; (g) VE-Nov/Durez:70/30; (h) VE-Nov/Durez:50/50; (i) VE-Ep/Methylon:70/30; (j) VE-Ep/Methylon:50/50; (k) VE-Nov/Methylon:70/30; (l) VE-Nov/Methylon:50/50 and (m) UP/VE-Nov:50/50

3.3 Thermal properties of neat resins and resin blends

Thermal behaviour evaluation of different cured resins and resin blends, carried out by dynamic mechanical thermal analysis (DMTA) and differential thermal analysis-thermogravimetric analysis (DTA-TGA), is discussed in this section.

3.3.1 DMTA – Compatibility study

The glass transition temperature (T_g), where on raising temperature the polymer transits from a hard, glassy material to a soft, rubbery material, is one of the most important properties in thermosetting polymers. The higher T_g value of a resin indicates that it can go through higher processing temperature and the cured resin can retain its mechanical integrity up to a higher temperature. The peak values of tan delta *vs*. temperature curves were used to determine the Tan delta, T_g values of different resins. Tan delta represents the ratio of the viscous to elastic response of a viscoelastic material, or in other words, the energy dissipation potential of the material, it quantifies the way in which a material absorbs and disperses energy, and it is also known as the Loss Factor.

Plots of tan delta *vs.* temperature for cured samples are given in Figure 3.3 and T_g values derived from these plots are given in Table 3.1.

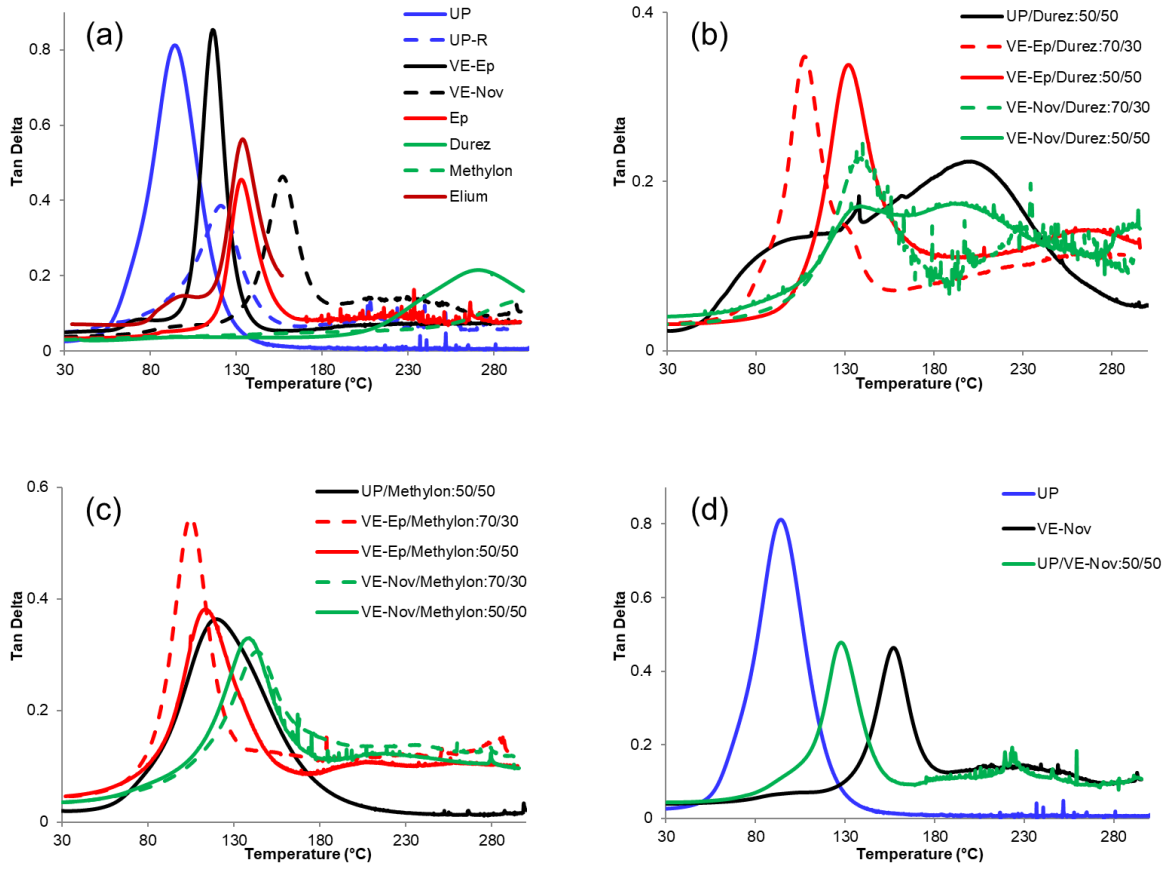

Figure 3.3: Plots of tan delta *vs.* temperature for cured samples of (a) all neat resins; (b) UP, VE blends with Durez; (c) UP, VE blends with Methylon; (d) UP/VE blends for comparison. - Results of UP, VE-Ep, VE-Nov, Durez, Methylon, UP or VE blends with Durez and/or Methylon taken from Ref [2]

As can be observed from Figure 3.3 and Table 3.1, all neat cast resins display single T_g values as expected. On comparing T_g values of UP and VE, UP-R and VE-Nov show higher T_g values than those of UP and VE-Ep. It can be also seen that VE resins have higher T_g values (116,

157 °C) than UP resins (92, 121 °C) in general. Ep and Elium resins also show higher T_g values, 133 and 134 °C, respectively than UP and VE resins except for the VE-Nov resin. It should be noted that because Elium is a thermoplastic resin, the test for that sample was run only up to 160 °C otherwise when heated, the Elium sample would have softened and damaged the single cantilever cell, whereas the rest of the resins are thermosets, and could be safely tested up to 300 °C. Two phenolic resins, Durez and Methylon, showed much higher T_g values (277 and 295 °C, respectively) than the rest of UP, VE, Ep and Elium neat resins (92-157 °C), which is as expected due to the greater degree of crosslinking of phenolic resins.

Table 3.1: Glass transition temperatures (T_g) derived from the peak values of tan delta *vs*. temperature curves from DMTA results for cured neat resins and resin blends

Resin	T_g (°C)
UP	92
UP-R	121
VE-Ep	116
VE-Nov	157
Ep	133
Durez	277
Methylon	295
Elium	134
UP/Durez:70/30	149, 235
UP/Durez:50/50	92, 197
UP/Methylon:70/30	114
UP/Methylon:50/50	119
VE-Ep/Durez:70/30	107, 264
VE-Ep/Durez:50/50	132, 259
VE-Nov/Durez:70/30	138, 231
VE-Nov/Durez:50/50	133, 198
VE-Ep/Methylon:70/30	105
VE-Ep/Methylon:50/50	113
VE-Nov/Methylon:70/30	143
VE-Nov/Methylon:50/50	139
UP/VE-Nov:50/50	128

Within resin blends, UP/Durez, VE-Ep/Durez, VE-Nov/Durez blends show two clear maxima indicative of two glass transition temperatures (T_g), indicating poor compatibilities between those two resin combinations and that there are phase separations within these blends as seen from their physical appearances in Section 3.2.3. Blends of UP/Methylon, VE-Ep/Methylon and VE-Nov/Methylon on the other hand all appear to form homogeneous single-phase materials, i.e. compatible blends with a single T_g in all cases. On comparing these UP/phenolic results with VE/phenolic blends, it can be seen that UP/Durez showed phase separation as reported elsewhere [1] but not as noticeable as in VE/Durez and in particular VE-Nov/Durez blends [2]. UP/Methylon and two different VE/Methylon blends are similarly compatible, indicating some interactions between two components, shown by a single T_g in both cases. UP/VE-Nov blends

showed only a single T_g at 128 °C, indicating their good compatibilities as well as a T_g value in between those of the two individual resins.

3.3.2 TGA – Thermal stability analysis

Thermal and thermo-oxidative stabilities of cured resins and resin blends were assessed by thermogravimetric analysis of approximately 10 mg of each sample under both nitrogen and air atmospheres, respectively, at a heating rate of 10 ºC/min from room temperature to 900 ºC. TGA data for various cured neat resins and resin blends recorded under nitrogen and air atmospheres are reported in detail elsewhere [2,30], some neat samples and UP/VE-Nov blends were prepared, tested especially for this work and derived data for all samples are given in Table 3.2. Residues obtained under nitrogen would comprise both carbonaceous (char) and inorganic contents while under air the carbonaceous content is oxidised. The onset of decomposition temperature is represented as $T_{10\%}$, the temperature at which 10% mass loss occurs. The residual mass at 550 °C is given. This temperature has been chosen because both UP and VE resins undergo complete degradation at this temperature and any additional char residue at this temperature for the other neat resins or blended resins would indicate increased thermal stability, and hence their lower flammability.

The temperature of onset of thermal degradation, $T_{10\%}$, i.e., temperature at which the polymer starts decomposing and volatiles begin to be released has a bearing on the time-to-ignition, TTI in the cone calorimeter, as demonstrated previously [28]. It is interesting to investigate to what extent the thermal degradation behaviours of these polymers observed from the TGA data are consistent with the fire performance as assessed by cone calorimetry. This aspect will be discussed later in the cone calorimetry experiments (Section 3.4.2).

It is well known that the char-forming tendency of a polymer is a measure of its flame retardancy [31] as char is formed at the expense of the formation of combustible volatiles. Since flaming combustion is a gas-phase process, any combustible material needs first to degrade to yield combustible volatiles to fuel the conflagration. Polymers that crosslink during degradation produce less volatile material but more crosslinked char, and as a consequence are less flammable than those that undergo primarily chain scission or chain stripping to produce more volatile fragments, most of which will be flammable. Within organic matrix resins, higher char forming resins such as phenolics are inherently more fire-retardant, which indicate their higher crosslinking tendency on thermal decomposition and hence, lower flammability.

It can be seen from Table 3.2 that both UP resins (Crystic® 2-406PA (UP) and Crystic® 702PAX (UP-R)) have onset of decomposition temperatures around 325 °C in N_2, leaving 4.4 and 4.7% char at 550 °C, respectively. Both VE resins have onset of decomposition temperatures around 380 °C in N_2, VE-Ep and VE-Nov, leaving 5.0 and 18.9% char at 550 °C, respectively. Similar to UP and UP-R, VE-Ep decomposes in air completely, leaving no char. VE-Nov on the other hand has 7.3% residue left, which indicates that VE-Nov has more char forming tendency and better thermal stability, i.e., a probable lower flammability than the rest of three.

Table 3.2: Data extracted from TGA traces recorded under N_2 and air atmospheres for cured neat resins and resin blends

Resin	N_2 atmosphere		Air atmosphere	
	$T_{10\%}$ (°C)	Residue remaining at 550 °C (wt%)	$T_{10\%}$ (°C)	Residue remaining at 550 °C (wt%)
UP	325	4.4	310	0
UP-R	326	4.7	316	0
VE-Ep	380	5.0	358	0
VE-Nov	377	18.9	365	7.3
Ep	356	12.0	357	10.8
Durez	323	60.9	308	60.0
Methylon	424	42.9	438	43.8
Elium	294	1.1	293	0
UP/Durez:70/30	338	21.1 (21.3)	316	36.8 (18.0)
UP/Durez:50/50	344	38.1 (32.6)	296	48.7 (30.0)
UP/Methylon:70/30	347	20.1 (15.9)	326	20.8 (13.1)
UP/Methylon:50/50	356	27.5 (23.6)	338	19.2 (21.9)
VE-Ep/Durez:70/30	311	24.6 (21.8)	319	12.0 (18.0)
VE-Ep/Durez:50/50	386	34.8 (33.0)	391	37.9 (30.0)
VE-Nov/Durez:70/30	259	29.2 (31.5)	266	24.0 (23.5)
VE-Nov/Durez:50/50	353	37.8 (39.9)	369	43.0 (35.5)
VE-Ep/Methylon:70/30	374	21.6 (16.4)	385	24.0 (13.1)
VE-Ep/Methylon:50/50	391	32.1(23.9)	394	35.0 (21.9)
VE-Nov/Methylon:70/30	377	30.7 (26.1)	379	29.6 (18.6)
VE-Nov/Methylon:50/50	383	33.6 (30.9)	397	35.4 (27.4)
UP/VE-Nov:50/50	340	9.1 (11.6)	333	2.1 (3.6)

Note: Figures in parentheses are the residual mass yields that might be expected for the resin blends assuming they behave as simple mixtures of the individual component resins. i.e. that a blend would have a char yield which is the weighted average of the char yields for the component resins. For instance, under N_2, UP/Durez:70/30 = 4.4 × 70% + 60.9 × 30% = 21.3, and so on.

Epoxy resin has an onset of decomposition temperature of 356 and 357 °C in N_2 and air, respectively, which is in between those of UP and VE resins, and hence its TTI in cone tests is expected to be similar to those of VE resins. The char forming tendency of epoxy is much more than both UPs and VE-Ep, whereas compared to VE-Nov, epoxy resin forms less char in N_2 but more in air at 550 °C.

Within the two phenolic resins, Durez, whilst having an onset of decomposition temperature of 323 °C in N_2 and 308 °C in air, has a much higher thermal stability in terms of retention of mass at 550 °C due to high aromatic content hence forming more char as expected, i.e., 60.9% in N_2 and 60.0% in air. On the other hand, Methylon has a $T_{10\%}$ value of 424 °C in N_2 and 438 °C in air, indicating that it should have a higher time-to-ignition in fire tests, but has a less charring tendency (42.9% residue in N_2) than the Durez resin (60.9% in N_2).

Elium resin shows an onset of decomposition temperature of 294 and 293 °C in N_2 and air, respectively, with the lowest temperature values of $T_{10\%}$ among all neat resins, leaving 1.1% char in N_2, and complete degradation, leaving no residual char, in air atmosphere at 550 °C. Thermal stability in terms of mass remaining of Elium resin at 550 °C is the lowest.

It can also be observed from Table 3.2 that the resin blends under both N_2 and air atmospheres give residual masses at 550 °C with values intermediate between those of base UP/VE and phenolic resins as expected. However, in all but the VE-Nov/Durez:70/30 and 50/50 wt% blends, the residual mass yields are greater than those that would be expected assuming the blends to behave as simple mixtures of the resin components, i.e. that the blend would give a residual mass which is the weighted average of the residual masses for the component resins. The reason for this may be that in those cases in which the resins in the blend are truly or nearly compatible, both components in the matrix are properly blended and cured to be regarded as a homogeneous material, and the phenolic component in the matrix provides a thermally protective effect [2] around the UP or VE component to form more char residue, hence producing overall more char. However, in cases in which compatibility is poor, for example, the VE-Nov/Durez blends here, curing is less efficient and such a protective effect is not established; thus they decompose separately and hence form less residue than the calculated values shown in Table 3.2, as seen previously in our group's work on UP/phenolic blends [1].

The compatibilities and thermal stabilities of UP/phenolics and VEs/phenolics blends have been discussed in detail in our group's previous publications [1-3]. Good compatibilities of the UP/Methylon, VE-Ep/Methylon and VE-Nov/Methylon resins reported before and shown here (Figure 3.2 (c,d,i-l)) giving homogeneous materials with a single T_g (see Table 3.1), indicate that these materials are worth investigating further. The poor compatibilities of the VE-Ep/Durez and VE-Nov/Durez resins, and to some extent of the UP/Durez blends, can be seen visually in Figure 3.2 (a,b,e-h) and also from DMTA results in Table 3.1, which show two clear T_g values.

It can also be noted from the $T_{10\%}$ values, that the cured Durez and Durez resin blends are less thermally stable than the corresponding Methylon and Methylon resin blends, i.e. Methylon and Methylon blends show higher $T_{10\%}$ (°C) values than those of Durez and Durez blends, suggesting that the Methylon-based materials would be expected to have higher TTI values in cone calorimetric fire tests than those of Durez-based materials.

For UP/VE-Nov blends, $T_{10\%}$ value and residue remaining at 550 °C (wt%) in both N_2 and air atmospheres are between those of the individual UP and VE-Nov resins, and thus TTI in cone tests is expected to be intermediate between those of the individual resins. Residues remaining from UP/VE-Nov blends are slightly lower than calculated ones in both nitrogen and air atmospheres. This indicates that these resins do not interact on decomposition and the flammability of the blend will not be an average of both resins, but still better than that of UP. This is surprising as both UP and VE resins are similar in that both contain carbon-carbon double bonds, which can copolymerize with styrene monomer, initiated by free radicals, their compatibility can be seen visually in Figure 3.2 (m) and a single T_g value by DMTA results in Table 3.1.

Overall, the higher residual masses of all blends at 550 °C indicate their higher and improved thermal stability with respect to those of the individual UP, VE-Ep and VE-Nov resins.

3.4 Flammability studies – fire performances evaluation

3.4.1 Pyrolysis combustion flow calorimetry (PCFC) for cast resins – flammability study

Plots of heat release rate (HRR) *vs*. temperature for all of the neat resins, and blends are shown in Figures 3.4 and 3.5 respectively and derived parameters are given in Table 3.3 (a) and (b). The maximum value of heat release rate (PHRR) divided by the heating rate of PCFC test gives a value of heat release capacity (HRC), which can be used as a reliable indicator of a polymer's flammability [32,33]. All resins show a single peak, the intensity of which determines their HRC, and hence flammability. The THR is the amount of heat released throughout the decomposition, in a PCFC run, and can be indicative of the total amount of heat generated.

3.4.1.1 Cast neat resins

The PCFC parameters of cured neat resins are given in Table 3.3 (a). It can be observed that among the neat resins, on comparing UP with UP-R from Figure 3.4 (a), UP shows a single broad peak whereas UP-R shows a single narrow peak and PHRR is slightly higher than that for UP. However, areas under the curves are similar for both UPs indicating their similar THR. UP shows lower HRC, THR and slightly higher peak temperature than UP-R (370 *vs.* 467 J/g-

K, 26.5 *vs.* 27.5 kJ/g and 408 *vs.* 395 °C, respectively), which means that UP is less flammable than UP-R.

Similarly, on comparing VE-Ep and VE-Nov, VE-Ep shows a single sharp and prominent peak whereas VE-Nov shows a single but lower PHRR. VE-Ep shows much higher HRC, THR and slightly higher peak temperature than VE-Nov (621 *vs.* 402 J/g-K, 30.1 *vs.* 25.1 kJ/g and 445 *vs.* 436 °C, respectively), which means that VE-Ep is more flammable than VE-Nov. This is expected as novolac helps in reducing the flammability of the vinyl ester.

Within UPs and VEs, it can be concluded in terms of HRC that UP and VE-Nov are less flammable than UP-R and VE-Ep, the flammability of UPs and VEs can be ranked as:

VE-Ep > UP-R > VE-Nov > UP.

On comparing Ep with UPs/VEs, Ep shows two peaks - a first PHRR at 375 W/g followed by a second lower peak value of 156 W/g, indicating a two-step decomposition of this epoxy resin. Ep shows values of HRC, THR and peak temperature (375 J/g-K, 25.9 kJ/g and 392 °C, respectively), similar but in between those of UP and VE-Nov, which means the flammability of Ep is expected to be in between of UP and VE-Nov resins.

Comparing the two phenolics - Durez and Methylon curves, Durez shows a relatively low broad PHRR at 61 W/g and some tiny peaks at temperatures between 200 and 400 °C whereas Methylon shows a single smooth peak and PHRR is much higher than Durez. Durez shows much lower HRC, THR and significantly higher peak temperature than Methylon (62 *vs.* 323 J/g-K, 8.9 and 17.7 kJ/g, 523 and 468 °C, respectively), which indicates that Durez should be less flammable than Methylon. Both phenolic resins demonstrate lower flammability than the two UPs and two VEs via showing lower HRC, THR values as well as relatively higher peak temperature.

Elium shows similar behaviour to Ep, with HRC, THR and peak temperature as 394 *vs.* 375 J/g-K, 26.0 *vs.* 25.9 kJ/g and 387 *vs.* 392 °C, respectively. On comparing Elium with UPs/VEs, Elium shows one peak and the values of HRC, THR are in between and a slightly lower peak temperature compared with UP and VE-Nov, which means the flammability of Elium is expected to be in between those of UP and VE-Nov.

Based on the HRC among all cast resins, the flammability of all neat resins can be ranked from high to low flammability ranking as follows:

VE-Ep > UP-R > VE-Nov > Elium > Ep > UP > Methylon > Durez.

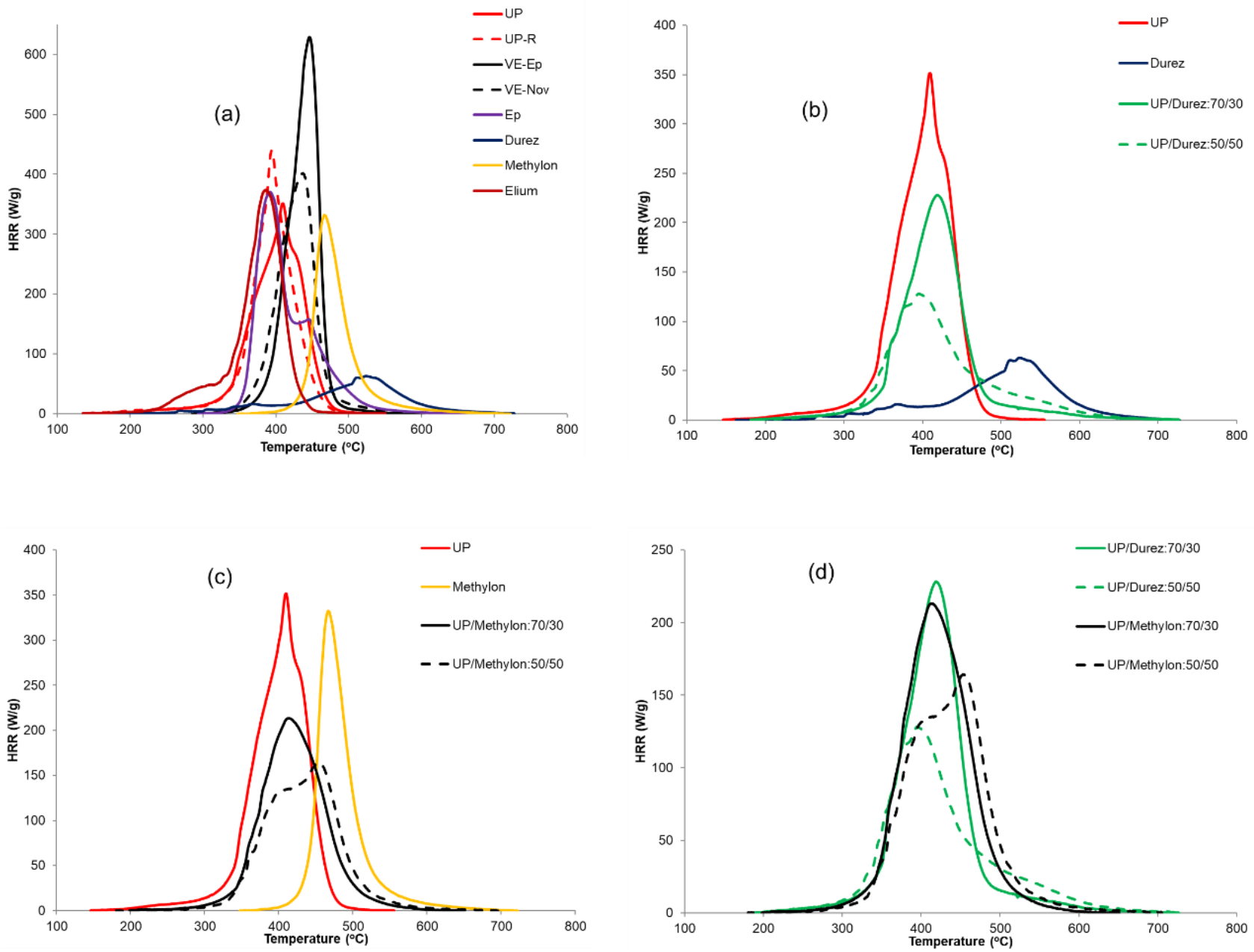

Figure 3.4: PCFC traces (HRR *vs.* Temp) recorded for (a) neat resins, (b) UP/Durez blends, (c) UP/Methylon blends, (d) UP/Durez and UP/Methylon blends

Table 3.3 (a): PCFC results of cured neat resins

Resin	HRC (J/g-K)	PHRR (W/g)	THR (kJ/g)	Peak Temperature (°C)	Heating Rate (°C/s)
UP	370±8	352±9	26.5±0.7	408±2	0.95±0.01
UP-R	467±8	440±7	27.5±0.7	395±1	0.94±0
VE-Ep	621±20	619±19	30.1±0.7	445±2	1.00±0
VE-Nov	402±5	402±5	25.1±0.3	436±1	1.00±0
Ep	375±8	375±7, 156±2	25.9±0.5	392±5	1.00±0
Durez	62±2	61±2	8.9±0.1	523±5	0.99±0
Methylon	323±11	325±12	17.7±0.4	468±1	1.01±0
Elium	394±6	373±2	26.0±0.3	387±1	0.95±0.01

Table 3.3 (b): PCFC results of resin blends

Resin	HRC (J/g-K)			PHRR (W/g)			THR (kJ/g)			Peak Temperature (°C)			Heating Rate (°C/s)
	Expt.	Calc. Av*	% change w.r.t. control**	Expt.	Calc. Av*	% change w.r.t. control**	Expt.	Calc. Av*	% change w.r.t. control**	Expt.	Calc. Av*	Change w.r.t. control** (°C)	
UP/Durez:70/30	232±1	278	*-37.3*	230±1	265	*-34.7*	20.7±0.6	21.2	*-21.9*	419±1	443	*+11*	0.99±0
UP/Durez:50/50	125±8	216	*-66.2*	124±8	207	*-64.8*	15.1±0.5	17.7	*-43.0*	394±9	466	*-14*	0.99±0
UP/Methylon:70/30	221±6	356	*-40.3*	218±5	344	*-38.1*	22.5±0.9	23.9	*-15.1*	414±2	426	*+6*	0.99±0
UP/Methylon:50/50	171±8	347	*-53.8*	168±8	339	*-52.3*	19.9±0.7	22.1	*-24.9*	455±2	438	*+47*	0.99±0
VE-Ep/Methylon:70/30	347±18	532	*-44.1*	338±16	531	*-45.4*	23.3±1.1	26.4	*-22.6*	446±2	452	*+1*	0.97±0.01
VE-Ep/Methylon:50/50	305±8	472	*-50.9*	296±8	472	*-52.2*	20.8±0.6	23.9	*-30.9*	451±2	457	*+6*	0.97±0.01
VE-Nov/Methylon:70/30	285±0	378	*-29.1*	278±0	379	*-30.8*	20.9±0.2	22.9	*-16.7*	436±1	446	*+0*	0.98±0
VE-Nov/Methylon:50/50	232±14	363	*-42.3*	227±13	364	*-43.5*	19.0±0.6	21.4	*-24.3*	441±1	452	*+5*	0.98±0
UP/VE-Nov:50/50	386±12	386	*+4.3*	365±9	377	*+3.7*	26.3±0.5	25.8	*-0.8*	432±1	422	*+24*	0.95±0.01

Notes:

- HRC = heat release capacity, PHRR = peak heat release rate, THR = total heat release.
- * calculated averages from parameters of individual components (Table 3.3 (a)) assuming they behave as simple mixtures of component resins
- ** % change with respect to (w.r.t.) respective control (UP or VE), for Peak Temperatures, the change is expressed in °C.
- The reproducibility in pyrolysis combustion flow calorimetry is ±5%.

3.4.1.2 Cast resin blends

The PCFC parameters of the blends are given in Table 3.3 (b), the calculated average values from the individual components have also been provided to see whether these blends are acting as physical mixtures of respective two components or there is some interaction between the components. The percentage change in each parameter with respect to the respective control (UP or VE) is also presented in Table 3.3 (b) where negative values show reduction and positive indicates increase. For the Peak Temperatures, the change with respect to the respective control resin is expressed in °C.

UP/Phenolic resin blends

As seen from Figure 3.4 (b), the HRR of neat UP resin has a peak at 408 °C, whereas Durez resin shows a PHRR peak at much higher temperature of 523 °C. The HRC of UP/Durez blends are in between those of the respective resins, which are much lower than average calculated values, indicating some interaction between two components. Both UP/Durez:70/30 and UP/Durez:50/50 show greater reductions in HRC and THR than that of UP (Table 3.3 (a), (b)). The peak temperature in 70/30 blend also increases indicating good flame retardant properties of this blend. The peak temperature in UP/Durez:50/50 blend is however, much lower compared to calculated average, as well as with respect to the control UP, which is not as expected due to higher phenolic content in the latter, this erratic behaviour could be due to poorer compatibility between two components in 50/50 wt% blend, seen previously by their physical appearances (some phase separation) and DMTA results [1].

Similarly, from Figure 3.4 (c) it can be seen that HRR of Methylon starts rising at a much higher temperature (> 350 °C) and it reaches a peak at 468 °C. Good compatibility has been observed between UP and Methylon resin, as discussed before (Sections 3.2.3 and 3.3.1). As can be seen from Table 3.3 (a), (b), the flammability of UP/Methylon blends in terms of their HRC values are in between those of the respective resins and THR significantly reduced compared to that of UP. It should also be noted from Figure 3.4 (c) that UP/Methylon:50/50 presents a small peak at 400 °C before the main peak, in which the former indicates the combustion of UP resin and the latter of Methylon resin. Both UP/Methylon:70/30 and UP/Methylon:50/50 show reductions in HRC, THR, and increases in peak temperatures, the effect is more pronounced in the 50/50 blend as expected, i.e., by increasing the proportion of phenolic resins into the blends, the flammability is lowered.

The flammability of UP/Phenolic resin blends and individual UP resin in terms of their HRC can be ranked as follows:

UP > UP/Durez:70/30 > UP/Methylon:70/30 > UP/Methylon:50/50 > UP/Durez:50/50.

VEs/Phenolic resin blends

Due to the incompatibility of both types of VE resins - VE-Ep and VE-Nov resins with Durez, the cast resin blends were not tested in PCFC tests. From the good compatibility between both VE and Methylon resin (Sections 3.2.3 and 3.3.1), it is expected that the blends should have intermediate properties of the respective resins. It can be observed from Figure 3.5 (a) and Table 3.3 (a), (b) that HRC values for VE-Ep/Methylon blends are significantly reduced indicating their sharply decreased PHRR values compared to respective value for VE-Ep, with a similar trend for THR. The values of VE-Ep/Methylon blends are in between those of the respective resins as expected. For VE-Nov/Methylon blends, similar trends can be observed from Figure 3.5 (b) that the flammability of VE-Nov/Methylon blends is reduced compared to VE-Nov, which is more pronounced in respective 50/50 wt% blends, i.e., the reduction for parameter values of HRC, THR is higher in 50/50 blend are as expected. It can also be noticed that both VE-Ep/Methylon and VE-Nov/Methylon blends show reduced flammability than those of corresponding control resins (VE-Ep or VE-Nov).

The flammability of VEs/Phenolic resin blends and VE resins in terms of their HRC can be ranked as follows:

VE-Ep > VE-Nov > VE-Ep/Methylon:70/30 > VE-Ep/Methylon:50/50 > VE-Nov/Methylon:70/30 > VE-Nov/Methylon:50/50.

UP/VE resin blends

For the UP/VE blend, good compatibility between UP and VE resin components has been observed (Sections 3.2.3 and 3.3.1), hence it is expected that the UP/VE resin blend will show flammability intermediate of the two neat resins. As can be seen from Figure 3.5 (d) and Table 3.3 (a), (b), the HRC, THR and peak temperature (386 J/g-K, 26.3 kJ/g and 432 °C, respectively) are in between those of the two neat resins, indicating that UP/VE-Nov:50/50 is slightly less flammable than VE-Nov and slightly more flammable than UP.

The flammability of UP/VE resin blends and individual UP and VE in terms of their HRC can be ranked as follows:

VE-Nov > UP/VE-Nov:50/50 > UP.

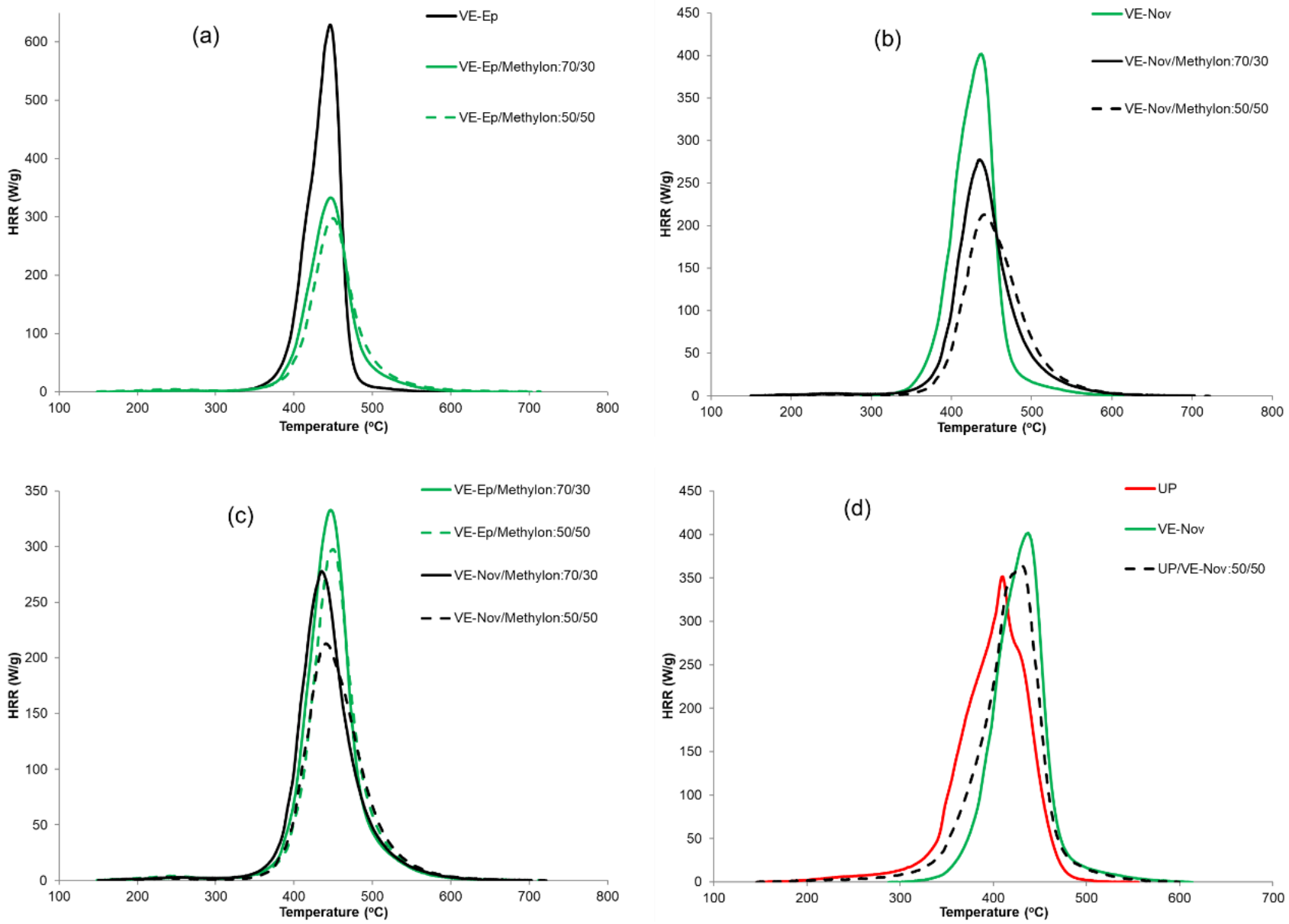

Figure 3.5: PCFC traces (HRR *vs.* Temp) recorded for (a) VE-Ep/Methylon blends, (b) VE-Nov/Methylon blends, (c) VE-Ep/Methylon and VE-Nov/Methylon blends, (d) UP/VE-Nov blends

3.4.1.3 Fire safety assessment

The relative overall fire performance of different resins and resin blends are evaluated by plotting the total heat release (THR) against the heat release capacity (HRC) values obtained in PCFC tests, as shown in Figure 3.6. Fire safe materials should have low THR and HRC values; i.e. such materials should fall close to the coordinates (0;0) on a 2-D plot.

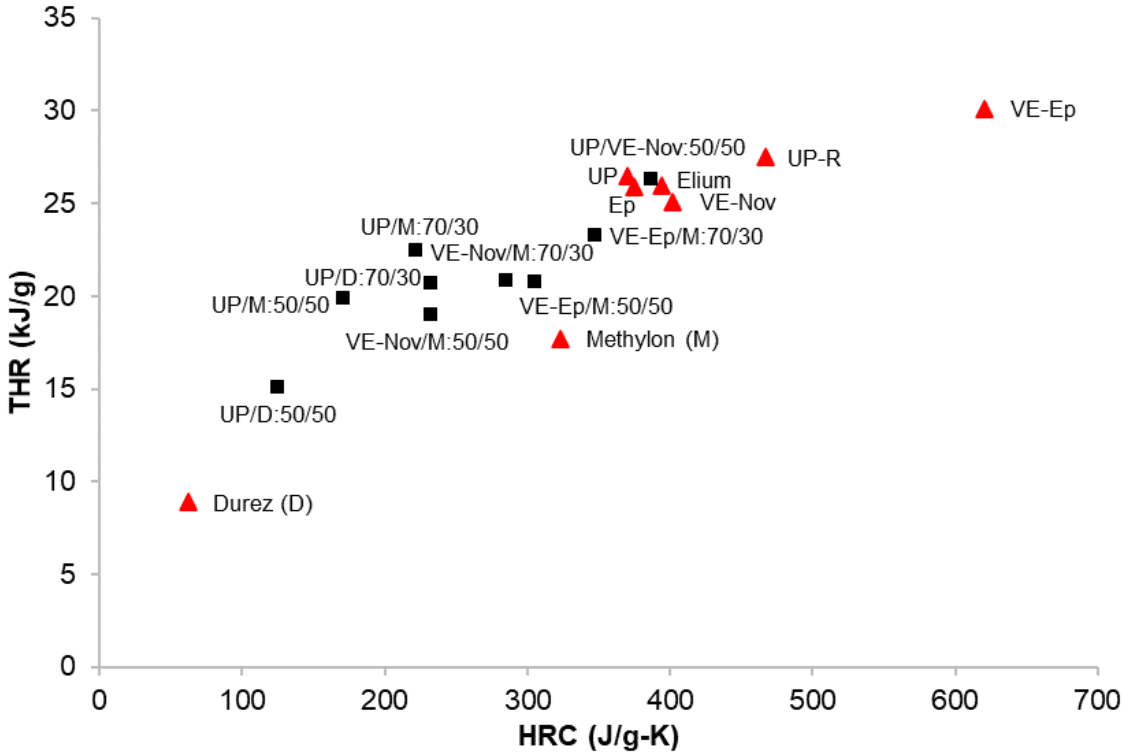

Figure 3.6: A 2-D fire safety assessment grid for all resins and their blends tested in PCFC tests

It can be observed that both UPs, VEs, Ep and Elium are at right upper corner of the graph, indicating their high flammability and low fire safety, as deduced from PCFC tests. Both phenolics, Durez and Methylon, however are closer to the 0,0 origin, especially Durez, which is the closest to 0;0, indicating the lowest flammability and high fire safety among all neat resins, and much less flammable than Methylon. Whereas VE-Ep shows the highest flammability indicating lowest fire safety among all resins and resin blends. UP is slightly less flammable than UP-R by showing lower THR as well as HRC values. Similarly, VE-Ep is more flammable than VE-Nov. Ep is slightly less flammable than Elium, and in between with UP and VE-Nov resins in terms of its HRC and THR.

All neat UP, VE, Ep and Elium resins are considered as having low fire safety measures, whereas both phenolic resins, Durez and Methylon, can be regarded as relatively fire safe.

Within resin blends, it can be seen from Figure 3.6 that UP/VE-Nov:50/50 blends are the most flammable, assessed by the highest coordinate values (of HRC, THR) among all resin blends.

Values of THR against HRC for blended resins fall within the region in between with those respective individual resins, which can be considered as having higher fire safety than neat UP or VE-Ep or VE-Nov. Both UP/Durez blends show intermediate fire safety compared with neat UP and Durez resins. UP/Durez:50/50 shows lower flammability than 70/30 blend and fire safety of both blends has been greatly improved compared to UP on its own. A similar trend can be seen for UP/Methylon blends, with THR values and HRC values of 50/50 blends significantly reduced. Also, surprisingly, it can be noted that HRC values for UP/Methylon blends are lower than those of both components.

For both VE-Ep/Methylon and VE-Nov/Methylon blends, 50/50 wt% blends show higher fire safety than those of 70/30 wt% blends as expected. Their fire safety has been greatly improved compared to the individual VE resins. VE-Ep/Methylon and VE-Nov/Methylon blends in both 70/30 and 50/50 wt% show intermediate values of THR compared to those of the respective neat resins. In VE-Ep/Methylon blends, the HRC value of the 70/30 wt% blend is in between those of the two individual components, whereas for the 50/50 wt% blend it is lower than those of both components. Whereas in VE-Nov/Methylon blends, HRC values of both blend proportions are lower than two corresponding individual components. In the case of VE-Nov/Methylon blends, the reason for lower HRC values (PHRR/heating rate) could be a higher extent of cross-linking/interaction between the two resin components, the blend behaving as one entity and hence, showing a lower HRC during the decomposition stage [2]. This effect probably also applies to the case of UP/Durez blends by displaying greatly reduced THR and HRC values, despite some incompatibility being observed [1]. The flammability/fire safety of UP/VE-Nov:50/50 is in between those of the individual VE-Nov and UP as indicated by the intermediate THR against HRC values.

Overall, it can be noted that blending UP or VEs resins with phenolic resoles leads to significant improvements in fire safety. Blending UP with VE resins shows quite similar results compared to those of neat resins (UP or VE) due to similar fire safety behaviours of both resins (Figure 3.6). It should also be noted (see Table 3.3, also shown in Figure 3.6) that there is a large improvement in the fire safety aspect of VE-Ep/Methylon blends relative to that of VE-Ep compared with the corresponding UP/Methylon systems.

3.4.2 Cone calorimetry – flammability study

Cone calorimetry was carried out on cured neat UP-R, Ep, Elium plaques of the resins and UP/VE-Nov resin blends under a radiant heat flux of 50 kW/m^2, the rest of cone results were taken from our previous work [2]. Plots of heat release rate (HRR) and mass loss *vs*. time for all neat resins and their respective blends are shown in Figures 3.7, 3.10 and 3.11, respectively. Derived cone calorimetric results of neat resins and resin blends are given in Table 3.4.

3.4.2.1 Cast resins

As can be seen from Figure 3.7 (a) and Table 3.4, both UP resins ignited around 37 - 40 s. Of these two, UP shows slightly lower peak heat release rate, PHRR than UP-R, (1053 *vs*. 1214 kW/m^2), lower total heat release, THR (78.9 *vs*. 97.4 MJ/m^2), lower total smoke release, TSR (4090 *vs*. 5435 m^2/m^2), which means that UP resin shows slightly lower flammability compared to UP-R resin. Both resins burnt completely, leaving no char residue. A similar trend can be seen from PCFC results discussed above in Section 3.4.1.1, i.e., HRC (heat release capacity) and THR values for UP were lower than that of UP-R.

Both VE resins ignited at around 42 - 46 s, slightly higher than UP resins (37 - 40 s). A similar trend can be seen from TGA results where onset of decomposition temperature ($T_{10\%}$) of VE resins was higher than those of both UPs (see Table 3.2). The charring tendency and higher thermal stability of VE-Nov shown in the TGA section, in Table 3.2, indicated its lower flammability than VE-Ep, and this is reflected here in cone tests by lower PHRR, (914 kW/m^2), THR, (99.2 MJ/m^2), TSR, (4536 m^2/m^2) and higher char residue (11%) of the VE-Nov compared to the values for VE-Ep (1275 kW/m^2, 110 MJ/m^2, 5547 m^2/m^2 and 1%, respectively). A similar trend for the values of HRC and THR is also observed from PCFC results shown in Table 3.3. VE-Ep also seems to be slightly more flammable than the UP and UP-R resins, showing a slightly higher PHRR and producing more total heat release and slightly more smoke (Table 3.4), which could be due to different styrene contents in two different resin types. The exact amounts of styrene in these resins are not known owing to the commercially sensitive information. VE-Nov resin seems to be least flammable compared to the other three resins in cone tests, shown by slightly higher TTI and highest charring tendency (11%) with intermediate THR and smoke production. This was expected from TGA results (Section 3.3.2, Table 3.2) of VE-Nov with higher values of $T_{10\%}$ and higher yield of residue, that this should be more thermally stable and less flammable compared to UP, UP-R and VE-Ep resins.

Ep has a quite high TTI (58 s), but burns producing very high PHRR (1779 kW/m^2) and THR (118.6 MJ/m^2) values and only 5% char residue. On comparing with two UPs and VEs, it can be observed that Ep has higher TTI, but much higher PHRR and THR indicating that Ep is more flammable than all UPs and VEs. Surprisingly, this trend was not seen in PCFC test where Ep shows a slightly higher HRC than UP resin but lower than UP-R and both VE resins, its THR is slightly higher than VE-Nov resin but lower than the other three resins. This erratic behaviour of Ep resin tested in cone and PCFC tests might be due to the different extents of pyrolysis and/or different combinations of pyrolysis products in the two different test methods, i.e., in cone calorimetry and PCFC, considering that it is complete combustion in cone calorimetry and incomplete combustion in a PCFC chamber with mixed gas flow [34].

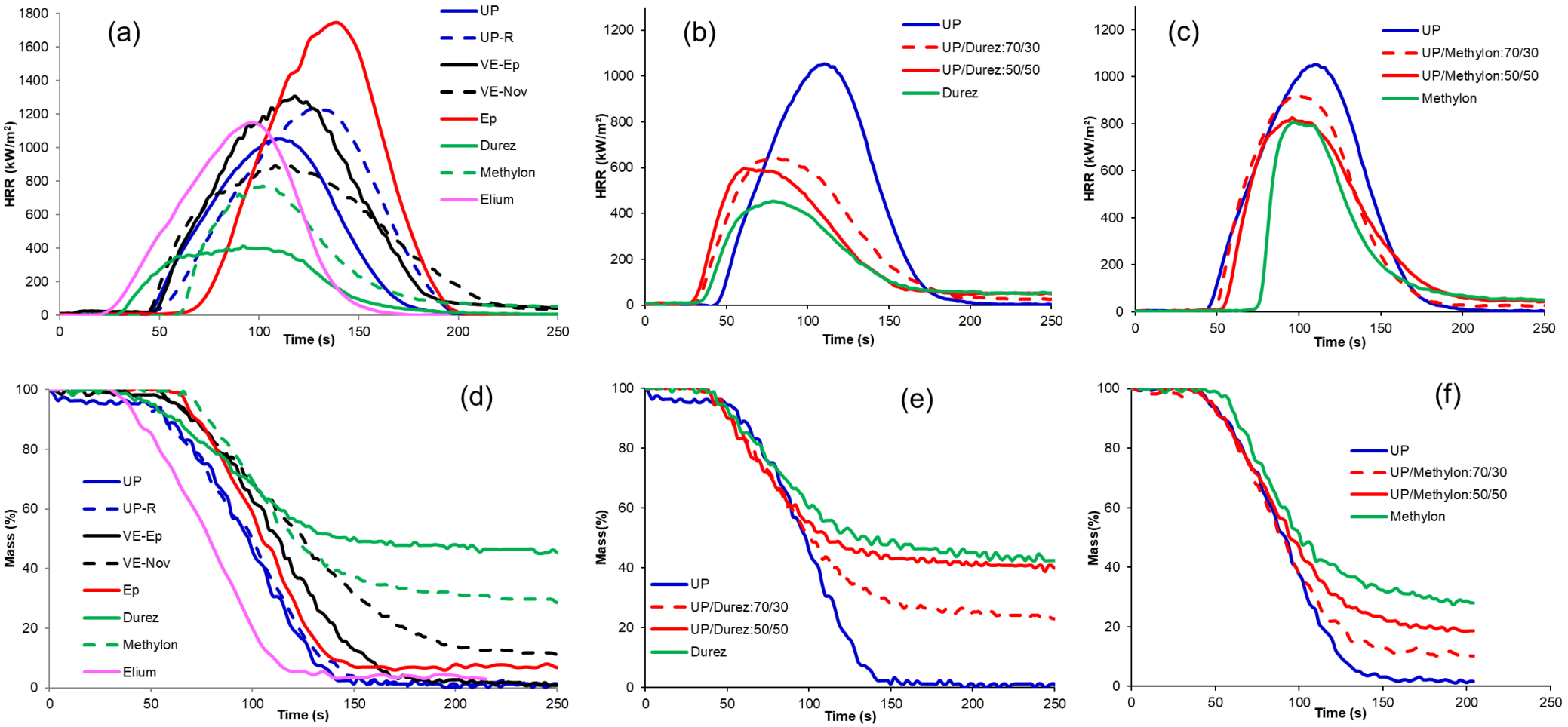

Figure 3.7: Plots of (a-c) HRR and (d-f) mass loss *vs.* time for (a, d) all neat resins and blends of (b, e) UP/Durez, (c, f) UP/Methylon [Partly taken from Ref [2]]

Table 3.4: Summary of cone calorimetric results for UP, UP-R, VE-Ep, VE-Nov, Ep, phenolics, Elium, UP/phenolic, VE-Ep/phenolic, VE-Nov/phenolic, UP/VE-Nov blends and for the constituent resins

Sample	TTI (s)	FO (s)	PHRR (kW/m^2)	FIGRA ((kW/m^2)/s)	THR (MJ/m^2)	TSR (m^2/m^2)	Residue (wt%)
UP	40	178	1053	26.3	78.9	4090	1
UP-R	37	164	1214	32.8	97.4	5435	0
VE-Ep	46	173	1275	27.7	110.0	5547	1
VE-Nov	42	212	914	21.8	99.2	4536	11
Ep	58	154	1779	30.7	118.6	4033	5
Durez	38	171	445	11.7	41.6	1392	45
Methylon	68	216	728	10.7	59.4	2675	32
Elium	20	125	1094	54.7	77.9	4714	2
UP/Durez:70/30	31 *(-9)*	178	630 *(-40.2)*	20.3	62.3 *(-21.0)*	2307 *(-43.6)*	24 *(+23)*
UP/Durez:50/50	31 *(-9)*	156	568 *(-46.1)*	18.3	48.4 *(-38.6)*	1357 *(-66.8)*	37 *(+36)*
UP/Methylon:70/30	54 *(+14)*	179	955 *(-9.3)*	17.7	70.7 *(-10.4)*	3819 *(-6.6)*	11 *(+10)*
UP/Methylon:50/50	57 *(+17)*	201	828 *(-21.4)*	14.5	61.0 *(-22.7)*	3166 *(-22.6)*	14 *(+13)*
VE-Ep/Durez:70/30*	51 *(+5)*	163	937 *(-26.5)*	18.4	63.7 *(-42.2)*	3638 *(-34.4)*	14 *(+13)*
VE-Ep/Durez:50/50*	47 *(+1)*	147	893 *(-29.9)*	19.0	56.5 *(-48.6)*	2320 *(-58.2)*	14 *(+13)*
VE-Nov/Durez:70/30*	59 *(+17)*	191	1025 *(+12.1)*	17.4	78.4 *(-21.0)*	3124 *(-31.2)*	18 *(+7)*
VE-Nov/Durez:50/50*	51 *(+9)*	161	1046 *(+14.4)*	20.5	63.7 *(-35.8)*	2314 *(-48.9)*	24 *(+13)*
VE-Ep/Methylon:70/30	50 *(+4)*	151	1120 *(-12.1)*	22.4	65.2 *(-40.7)*	3187 *(-42.5)*	9 *(+8)*
VE-Ep/Methylon:50/50	51 *(+5)*	199	1091 *(-14.4)*	21.4	72.1 *(-34.4)*	3472 *(-37.4)*	14 *(+13)*
VE-Nov/Methylon:70/30	59 *(+17)*	160	1173 *(+28.3)*	19.9	70.5 *(-28.9)*	3028 *(-33.2)*	15 *(+4)*
VE-Nov/Methylon:50/50	46 *(+4)*	167	1188 *(+29.9)*	25.8	68.2 *(-31.2)*	3130 *(-31.0)*	16 *(+5)*
UP/VE-Nov:50/50	48 *(+8)*	180	1074 *(+2.0)*	22.4	93.9 *(+19.0)*	5394 *(+31.9)*	3 *(+2)*

Notes:

- TTI = time-to-ignition, FO = time to flame out, PHRR = peak heat release rate, THR = total heat release, TSR = total smoke release.
- PHRR, THR, TSR and residue values in parentheses and in italic fonts are the changes in a percentage (%) in cone calorimetric parameters between the blends and values from the constituents (UP or VEs resins), negative if reduced or positive if increased. Except for TTI, where the difference is expressed in s.
- The reproducibility in cone parameters is ±5%.
- * These blends showed phase separation by visual observation and DMTA.

Of the two phenolic resins, Durez has a lower TTI, 38 s, similar to that of the UP resins, whereas Methylon, has the highest TTI among all neat resins (68 s). This is consistent with the pattern observed in $T_{10\%}$ values, i.e., a higher value of Methylon (424 *vs.* 323 °C), seen in the TGA results (Table 3.2), corresponding to a higher TTI here in cone tests. In general, although phenolics are expected to have inherent flame-retardant properties, their TTI values are quite low. However, once ignited, they burn slowly with lower PHRR and total heat release (THR) compared with those of UP and VE resins, as can be seen from Figure 3.7 (a). The lower flammability of phenolics is due to the greater number of relatively stable aromatic benzene rings in their chemical structures [35-37], which on heating crosslink and form stable char, whereas the UP or VE resins decompose into combustible volatiles, which burn. This is also evident from mass loss *vs.* time curves in Figure 3.7 (d), where phenolic resins show lower mass loss and produce more char at the end of the experiment, especially for Durez compared to both UP and VE resins. Both UP resins and VE-Ep resin are burnt away after cone tests, VE-Nov, leaving 11% char residue, which is much lower than those of two phenolic resins (45 and 32%). Durez shows lower PHRR (445 kW/m^2), THR (41.6 MJ/m^2), TSR (1392 m^2/m^2), and produces a higher char residue (45%) compared to the values for Methylon (728 kW/m^2, 59.4 MJ/m^2, 2675 m^2/m^2, 32%, respectively), which indicates that Durez is less flammable than Methylon resin despite its low TTI. Similar trends in HRC and THR from PCFC results can be noticed (see Section 3.4.1.1, Table 3.3). Both phenolic resins show much lower PHRR, THR, TSR compared to UP and VE resins, also the charring tendency of both phenolics (32 - 45%) is much higher than UPs and VEs (0 - 11%). The crosslinking tendency of Methylon resin is slightly less than Durez as seen from lower char yield value (32%) at the end of the tests.

Elium resin has a lowest TTI (20 s) as expected from TGA results, i.e., lowest $T_{10\%}$ value of 294 °C (see Table 3.2), whereas for the rest of the neat resins $T_{10\%}$ values are all above 310 °C. Elium has the shortest FO time (125 s) and an earliest start of mass loss and a relatively high mass loss rates compared to the other neat resins as can be seen in Figure 3.7 (a), (d) and Table 3.4. Compared to those of UP and VE resins, it can be observed that Elium has a similar PHRR to that of UP (1094 *vs.* 1053 kW/m^2), but a lower THR than both UPs and VEs. In fact, Elium shows the lowest THR (77.9 MJ/m^2) among all neat resins other than the two phenolics, and leaves only 2% of char residue indicating the low charring tendency of this thermoplastic resin.

The charring tendency is evident from the high residual char yield obtained at the end of the cone tests. The charring tendency of different neat resins from this experiment can be ranked as:

Durez > Methylon > VE-Nov > Ep > Elium ≈ VE-Ep ≈ UP ≈ UP-R

This trend is similar to that observed for char yields in the TGA experiments. The values of residue remaining at 550 °C under air atmosphere from TGA results (taken from Table 3.2) against cone residue (Table 3.4) are plotted in Figure 3.8 to illustrate their correlation.

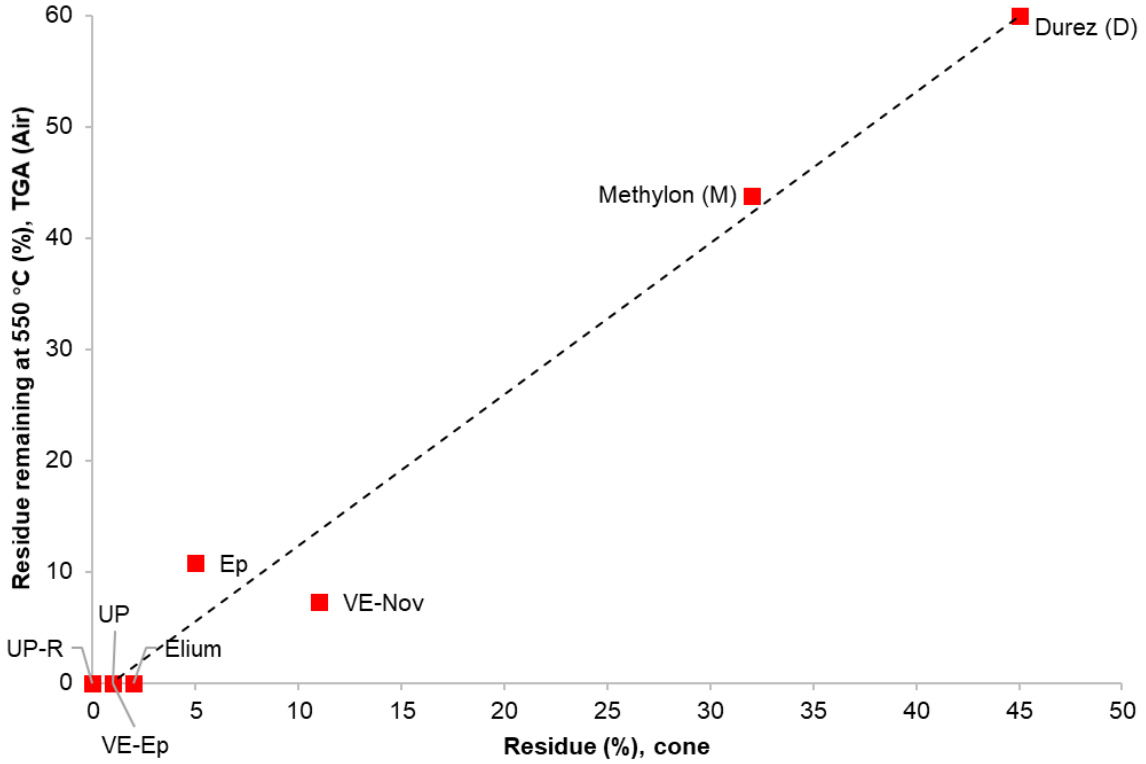

Figure 3.8: Plot of residue remaining at 550 °C under air from TGA data *vs.* residue from cone calorimetric data for cured neat resins

It is worth noting that, as expected, there is a reasonable correlation of the residue between char yields obtained in the TGA experiments (mass remaining at 550 °C in air) and final char yields in the cone calorimetric tests despite using different testing methods. Although TGA experiments were run under both air and nitrogen atmospheres (Table 3.2), the results plotted here were taken from the experiments under an air atmosphere for better comparison because in cone fire tests, samples were run under an air atmosphere. Residues obtained under air are the carbonaceous content prior to further oxidation at elevated temperatures.

Also, the time-to-ignition (TTI) in the cone calorimeter demonstrated in above section seems to show some correlation to the temperature of onset of thermal degradation, $T_{10\%}$ from the TGA data. In order to compare and investigate the correlation of different neat resins more straightforwardly, and to see whether or not the $T_{10\%}$ values from the TGA data are consistent with the fire performance as assessed by cone calorimetry, the $T_{10\%}$ values are plotted against the corresponding TTI values in Figure 3.9.

It can be seen from Figure 3.9 that the correlation between $T_{10\%}$ (T_{onset}) and TTI is reasonable, i.e., in general, those resins that have low $T_{10\%}$ have low TTI and vice versa.

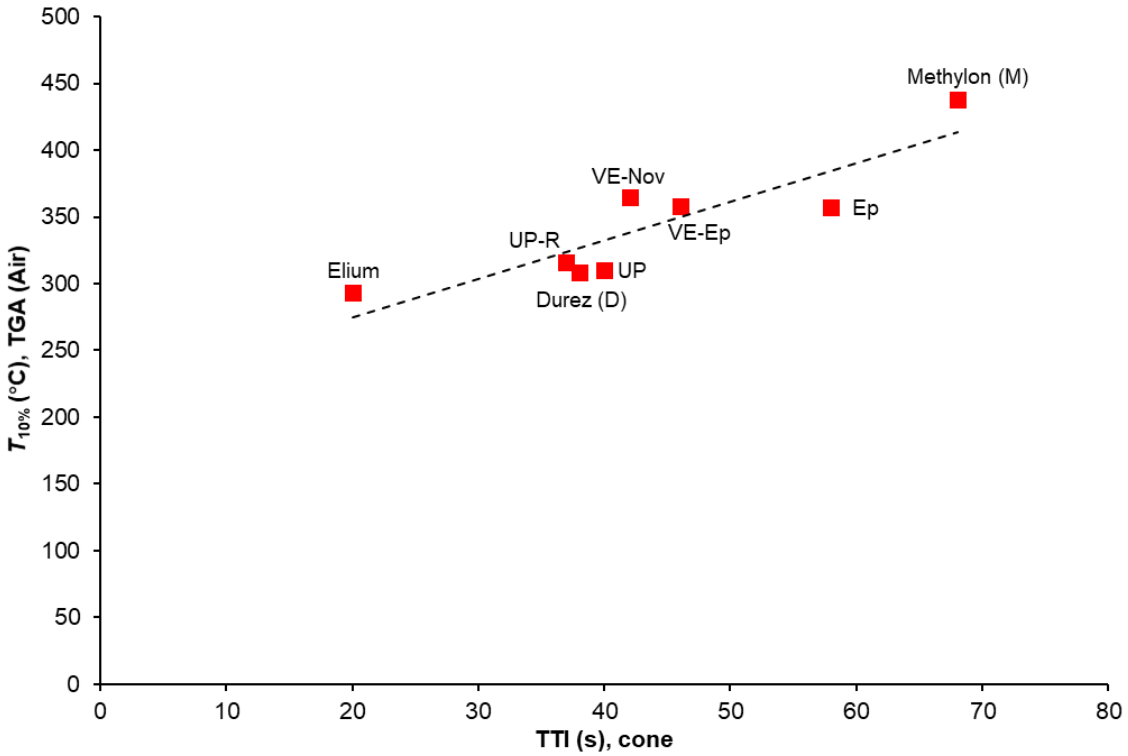

Figure 3.9: Plot of $T_{10\%}$ from TGA data under air *vs.* TTI from cone calorimetric data for cured neat resins

3.4.2.2 Resin blends

Within resin blends, although both VE-Ep/Durez and VE-Nov/Durez blends showed phase separation mentioned above in their physical appearance and DMTA results (Sections 3.2.3 and 3.3.1, respectively), they were subjected to cone experiments. It should be noted that this is an academic exercise for these samples in order to see whether or not the flammability of these phase separated blended resins can still be improved since inhomogeneous blends are not suitable for use as matrix resins in laminates or in making sandwich structured samples. For greater clarity to investigate the influence on resin blends, the percentage (%) changes in selected cone calorimetric parameters of PHRR, THR, TSR and residue values for all blends with respect to those of the constituent (UP or VEs) resins are given in Table 3.4, negative if reduced or positive if increased, except for TTI, where the difference is expressed in s.

UP/Phenolic resin blends

In UP/PH-Res blends, as can be seen from Figure 3.7 (b), (c) and Table 3.4, TTI is slightly affected by the presence of the phenolic resin. In the cases of UP/Durez blends, the values being slightly lower than that of UP. This is more clearly seen from the values in parentheses (Table 3.4) in which the difference between TTI for the blend and that of the UP is given. This indicates that since these blends are not intimately co-crosslinked, and that the UP ignites first. In the UP/Methylon blends, on the other hand, the TTI is much higher than that of UP. This could be due to the fact that the blend is co-crosslinked [1], and hence delays the ignition of a

homogeneous material.

Most other parameters for the blends are between those of the neat phenolics and neat UP resin, and the influence of the PH-Res increases with increasing PH-Res content, as can be seen from Figure 3.7 (b, e), (c, f) and Table 3.4. The UP/Durez blends, despite poor compatibility shown by DMTA results (Section 3.3.1), surprisingly show significant reduction in PHRR, THR and TSR values for the blends, which is unexpected. Whereas in UP/Methylon blends, although UP/Methylon blends are more compatible and probably more fully co-crosslinked [1], the reductions in various parameters are much less than those of UP/Durez blends, the flammability of UP/Methylon is greater than UP/Durez blends, however, still lower than that of individual UP. In terms of smoke production, UP/Durez blends produce lower TSR than respective UP/Methylon blends. The trend in TSR is similar to those of the other flammability parameters.

VEs/Phenolic resin blends

From Figure 3.10 (a) and (b), it can be seen that for the VE-Ep/Durez blends, TTI values are similar to that for VE-Ep. PHRR, THR and smoke values (Table 3.4) are reduced compared to those of VE-Ep, owing to the low flammability of Durez. In the case of VE-Nov/Durez blends, TTI and PHRR are slightly higher, but THR and smoke values are lower and reduced, compared to the corresponding values for VE-Nov, as well as more char residue due to the presence of phenolic resin, Durez. On comparing these VE/Durez results with those of the UP/Durez blends (Table 3.4), it can be noticed that Durez is more effective in reducing flammability of the UP than of the VE. This could be due to the fact that there is more phase separation in VE/Durez blends compared to UP/Durez blends, as indicated by physical appearance as well as DMTA results (Sections 3.2.3 and 3.3.1), which arises from less degree of crosslinking/interaction tendency during curing [2]. Hence in VE/Durez blends, VE and Durez components probably decompose/undergo combustion separately leading to less char residue and having higher flammability than those of UP/Durez blends [2].

From Figures 3.10 (c), 3.11 (a) and Table 3.4, it can be seen that, the trend for TTI for the blends of VE with Methylon is similar to those of VE-Ep/Durez and VE-Nov/Durez blends. TTI increase for VE-Nov/Methylon with respect to VE-Nov is noticeable, especially for 70/30 wt% blends, seen in Figure 3.11 (a) and Table 3.4. However, PHRR is only reduced in VE-Ep/Methylon, but significant reduction occurs in THR and TSR for both VE/Methylon blends. On comparing these results with respective UP/Methylon blends, this effect of the reduction in THR and TSR for both VE/Methylon blends is more noticeable than the respective effect can be seen in UP/Methylon resin blends (Table 3.4).

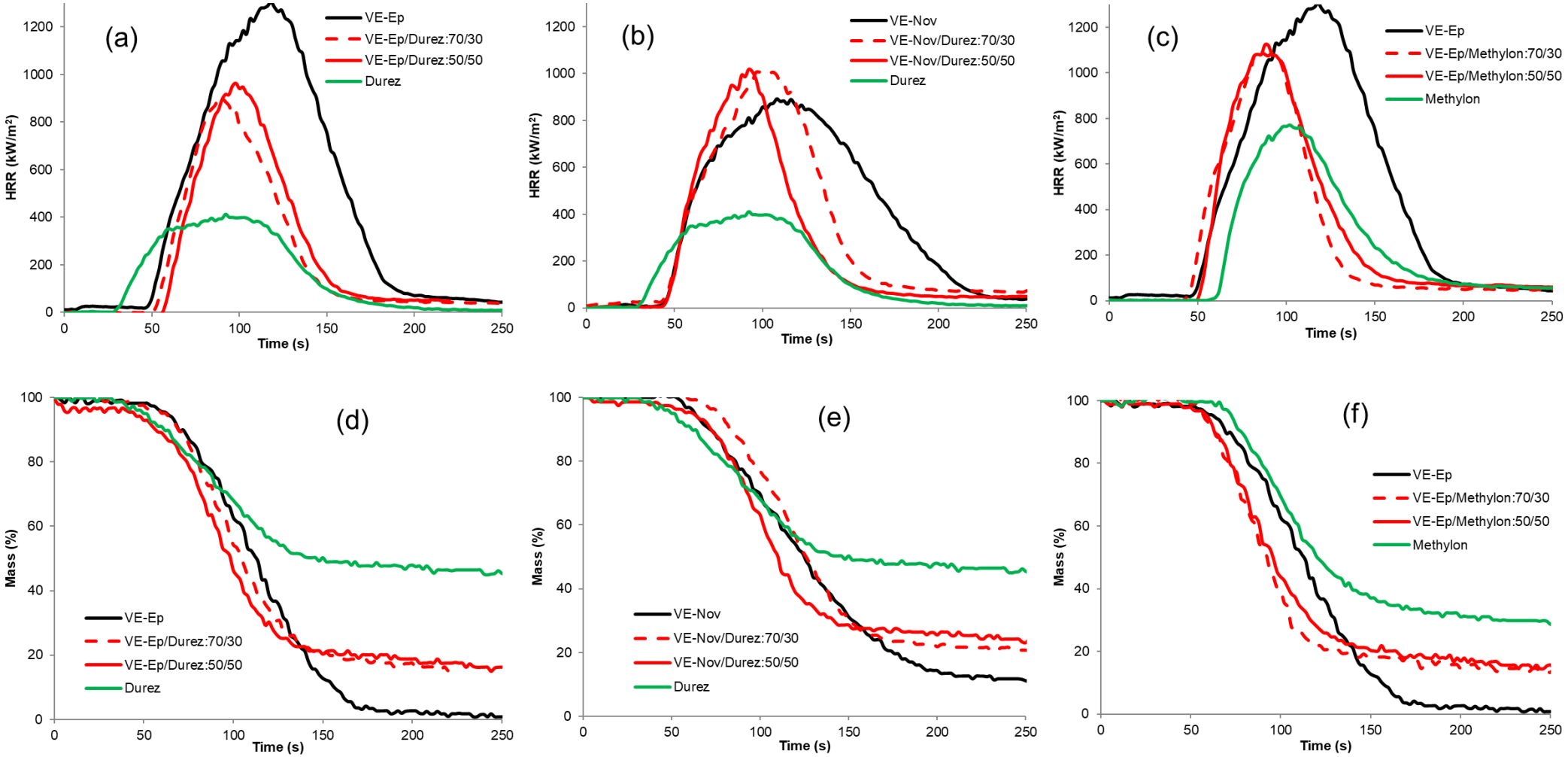

Figure 3.10: Plots of (a-c) HRR and (d-f) mass loss *vs*. time for constituent resins and blends of (a, d) VE-Ep/Durez, (b, e) VE-Nov/Durez, (c, f) VE-Ep/Methylon [Taken from Ref [2]]

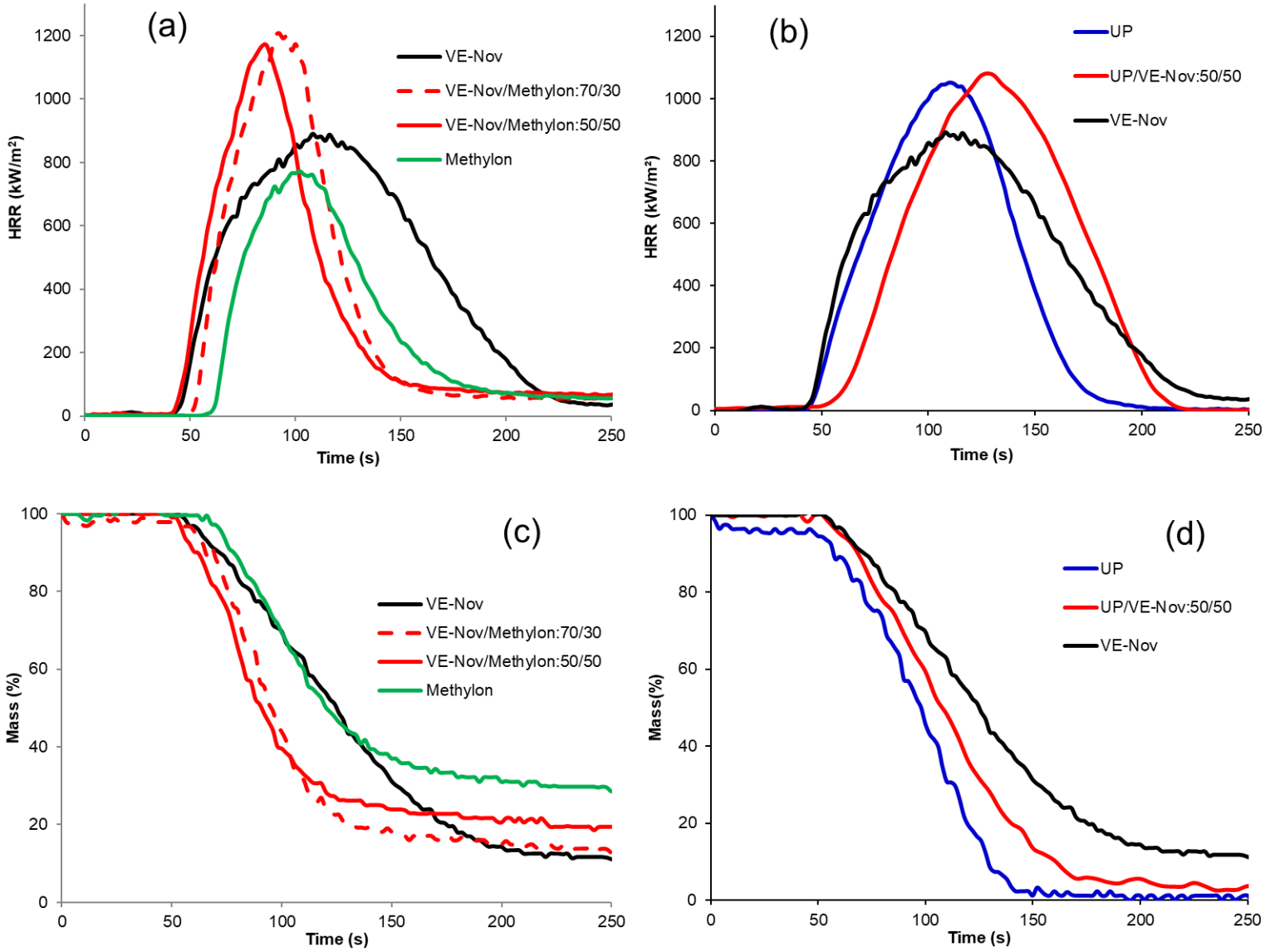

Figure 3.11: Plots of (a, b) HRR and (c, d) mass loss *vs*. time for constituent resins and blends of (a, c) VE-Nov/Methylon [Taken from Ref [2]], (b, d) UP/VE-Nov

UP/VE resin blends

TTI values for UP/VE-Nov:50/50 blends (48 s) were higher than those of two individual neat UP and VE resins (40 - 42 s). This could be due to the fact that the blend is well co-crosslinked [1], and hence the ignition behaviour of a homogeneous material is seen in this case. UP/VE-Nov:50/50 shows intermediate values of THR and char residue (93.9 MJ/m^2 and 3%, respectively) compared to those of the two individual components. In contrast, PHRR and TSR were slightly higher than both of individual UP and VE resins (1074 kW/m^2 and 5394 m^2/m^2, respectively). Based on those derived values presented in Table 3.4, the flammability of UP/VE-Nov:50/50 seems not to be much difference than UP or VE-Nov on their own and is between two neat resins.

Overall, the flammabilities and smoke production in all blends are between those of the neat resins (UP or VEs) and phenolic resin components.

3.4.2.3 Fire safety assessment

Fire safety of the materials can be ranked using the fire growth rate index (FIGRA), which is maximum quotient of HRR/elapsed time, *t*, often equals to PHRR/time to PHRR (T_{PHRR})) [38,39]. FIGRA is used for the evaluation of a product's reaction to fire properties, in other words, a measure of a product's fire hazard [40]. FIGRA is a combined rate parameter that shows the growth rate of a fire it reflects the response rate of a certain material or product in a given fire scenario.

National regulations at present in about 30 countries have adopted the FIGRA classification and adapted it to their national regulations. For example, the calculation of FIGRA values is used in the BS EN 13823 standard for a single burning item test [41]. Additionally, FIGRA has been shown elsewhere to predict well the tendency to fire growth for a number of different products in different scenarios [40].

The FIGRA indicates the burning propensity of a material. The lower the FIGRA value, the lower is the fire growth in a material [30]. It can be noticed that in terms of FIGRA values (see Table 3.4), within neat resins, both phenolic resins show relatively low values, hence higher fire safeties. Regarding UP and VE resins, VE-Nov shows the highest and UP-R the lowest fire safety among them. Elium, due to its highest FIGRA value, is the least fire safe material among all the neat resins. In resin blends, very clear trends can be seen in that UP/phenolic blends show higher fire safety (3 out of 4 within the top four fire safe blended materials) than those of VEs/phenolic blends, especially for UP/Methylon blends, due to the relatively high TTI and low PHRR values of Methylon. Whereas UP/VE-Nov blends show a low fire safety as expected as per their individual component of fire safety values. In addition, 50/50 wt% blends show relatively

lower FIGRA values than corresponding 70/30 wt% blends in general.

According to FIGRA values calculated and given in Table 3.4, the fire safety of different neat resins and resin blends can be ranked as follows:

Neat resins -

Methylon > Durez > VE-Nov > UP > VE-Ep > Ep > UP-R > Elium

Resin blends -

UP/Methylon:50/50 > VE-Nov/Durez:70/30 > UP/Methylon:70/30 > UP/Durez:50/50 > VE-Ep/Durez:70/30 > VE-Ep/Durez:50/50 > VE-Nov/Methylon:70/30 > UP/Durez:70/30 > VE-Nov/Durez:50/50 > VE-Ep/Methylon:50/50 > VE-Ep/Methylon:70/30 ≈ UP/VE-Nov:50/50 > VE-Nov/Methylon:50/50

The fire safety ranking however, depends upon many factors, such as TTI, THR, PHRR etc, which may not follow the same trend. In addition to FIGRA data presented above, the combined THR against flashover propensity values are also introduced, i.e., the relative overall fire performance of different resins and resin blends can be evaluated by plotting the total heat release (THR) against the flashover propensity values calculated by dividing PHRR by TTI [42], which can give a better understanding of the assessment of full-scale fire hazards, as shown in Figure 3.12. The parameter, PHRR/TTI, is a measure of the severity of the fire. The rationale for using PHRR/TTI as an indicator of flashover is that a short time-to-ignition (TTI) and a high peak heat release rate (PHRR) are considered to be necessary requirements for flashover to occur. The propensity to flashover potential, the higher PHRR/TTI values are associated with a greater propensity to flashover. The THR range reveals the total amount of heat that can be released by the fuel, i.e., the larger the value of THR, the more heat the material releases as it burns [42]. Here all neat resins and resin blends have been plotted by using selected parameters of great significance from the cone calorimetric testing rather than just one factor, hence a better picture can be obtained for all different resins and blended resin systems. It should be also noted that even though the 50/50 wt% blends are included in the plots; these proportions are not ideal for use because higher phenolic contents in the blends may reduce the mechanical properties of UP or VE resins [2]. Ideally, fire safe materials should have low THR and PHRR/TTI values. In other words, such materials should fall close to the coordinates (0;0) on a 2-D plot.

It can be seen from Figure 3.12 that within neat resins both UPs, VEs, Ep, and Elium resins have low fire safety, and moreover, that both VE resins (and especially VE-Ep) show lower fire safety than both UP resins. Ep shows the longest fire duration among all different resins and displays a relatively quicker growing fire. Elium demonstrates the fastest growing fire amongst all the different resins. Both phenolic resins, Durez and Methylon, show extraordinarily low flammability and hence have high fire safety among all resins and resin blends, especially Durez. Furthermore, the overall trend can be observed that while none of the resins falls within the

region close to the coordinates (0;0), all phenolic resins and their blends with UP or VEs fall within the region considered as having higher fire safety than corresponding individual UP or VEs. i.e., blending UP or VE resins with phenolic resoles (PH-Res) brings about significant improvements in fire safety. It can also be noted apparently that the large improvement in the fire safety aspect of the VE-Ep/Durez blends relative to that of VE-Ep compared with the lesser improvement in the corresponding UP resin systems arises in spite of the phase separation in the former blends.

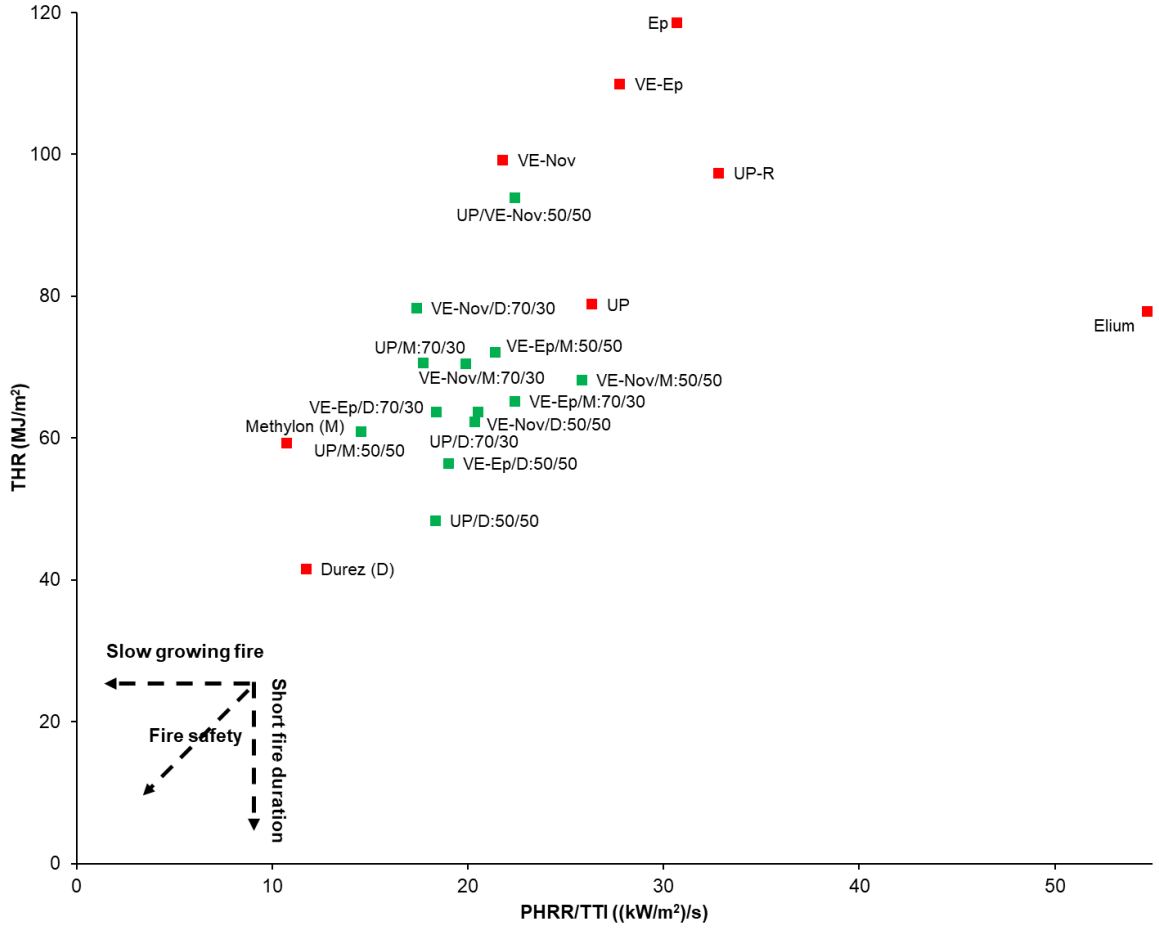

Figure 3.12: A 2-D fire safety assessment grid for UP, UP-R, VE-Ep, VE-Nov, Ep, Durez, Methylon and Elium resins and their blends, when exposed to 50 kW/m^2 heat flux

3.4.3 Correlation between PCFC and cone calorimetry

The reduction of the heat release rate as well as total heat release measured by the cone calorimeter could be clear-cut evidence for the efficiency of a resin's flame retardancy. PCFC, can provide same information on a much smaller sample and in less time for different resins and resin blends. It is interesting to investigate to what extent flammability behaviours of different resins and resin blends are consistent with the fire performance as assessed by PCFC and cone calorimetry. Percent reductions in PHRR and THR values with respect to respective UP/VE in all blends, obtained from two tests were used for comparison between PCFC and calorimetric data, the results are given in Table 3.5.

It can be observed from Table 3.5 that relative trends between PCFC and cone calorimetry are quite similar and reasonable, except for VE-Nov/Methylon blends where PHRR is reduced in the PCFC test but showed an increase in cone calorimetric results. These blends are compatible hence are expected to undergo combustion similarly in both tests and show similar trends. The reason could be due to the fact that test conditions are very different for the two different techniques [34], i.e., PCFC is non-sensitive to physical flame-retardant effects whereas both chemical and physical phenomena have a great effect on cone calorimetric results. Therefore, PHRR values obtained with both techniques do not always show a good correlation, VE-Nov/Methylon blends probably fall into this category here.

Table 3.5: PHRR and THR increase or reduction in PCFC and cone calorimetry for UP and VE with phenolic blends [expressed in (%) compared to that of UP or VE control]

Resin	PCFC		Cone calorimetry	
	PHRR (W/g)	THR (kJ/g)	PHRR (kW/m^2)	THR (MJ/m^2)
UP/Durez:70/30	*-34.7*	*-21.9*	*-40.2*	*-21.0*
UP/Durez:50/50	*-64.8*	*-43.0*	*-46.1*	*-38.6*
UP/Methylon:70/30	*-38.1*	*-15.1*	*-9.3*	*-10.4*
UP/Methylon:50/50	*-52.3*	*-24.9*	*-21.4*	*-22.7*
VE-Ep/Methylon:70/30	*-45.4*	*-22.6*	*-12.1*	*-40.7*
VE-Ep/Methylon:50/50	*-52.2*	*-30.9*	*-14.4*	*-34.4*
VE-Nov/Methylon:70/30	*-30.8*	*-16.7*	*+28.3*	*-28.9*
VE-Nov/Methylon:50/50	*-43.5*	*-24.3*	*+29.9*	*-31.2*
UP/VE-Nov:50/50	*+3.7*	*-0.8*	*+2.0*	*+19.0*

In order to investigate the correlation between PCFC and cone calorimetry, respective PHRR and THR values for both testing methods are plotted as in Figure 3.13 (a) and (b), and the correlation coefficients, R, were calculated. It can be observed from PHRR graph (Figure 3.13 (a), R = 0.64) that within UP/Durez and UP/VE-Nov blends, these values show good correlation, whereas UP/Methylon, both VE/Methylon blends do not show that trend, also can be seen in Table 3.5. By contrast, from the THR graph (see Figure 3.13 (b), R = 0.79), these THR results are quite comparable and showing relatively good correlation, except for VE-Ep/Methylon:70/30 blend, which is slightly out of the linear relationship compared to respective neat resins. It could be a good indication that fire performances of THR of different resins and resin blends are quite consistent as assessed by either PCFC or cone calorimetry, whereas PHRR obtained from two test methods were not showing as good a correlation as THR. The reason could be that in terms of THR, in a PCFC run, the THR is evaluated by the amount of heat released throughout the decomposition, which is indicative of the total amount of heat generated based on the oxygen consumption theory. Similarly, in cone tests, the fundamental principle behind it is that the amount of oxygen consumed during the combustion of polymeric material, which is proportional to the amount of heat released. Hence the expected good agreement of THR in both test techniques. Whereas as has been explained previously, due to different test conditions for two different testing techniques, PHRR values obtained from both techniques sometimes do not show a good correlation, hence the poorer correlation shown in the data in Figure 3.13 (a)

compared with that shown in Figure 3.13 (b) is not unexpected.

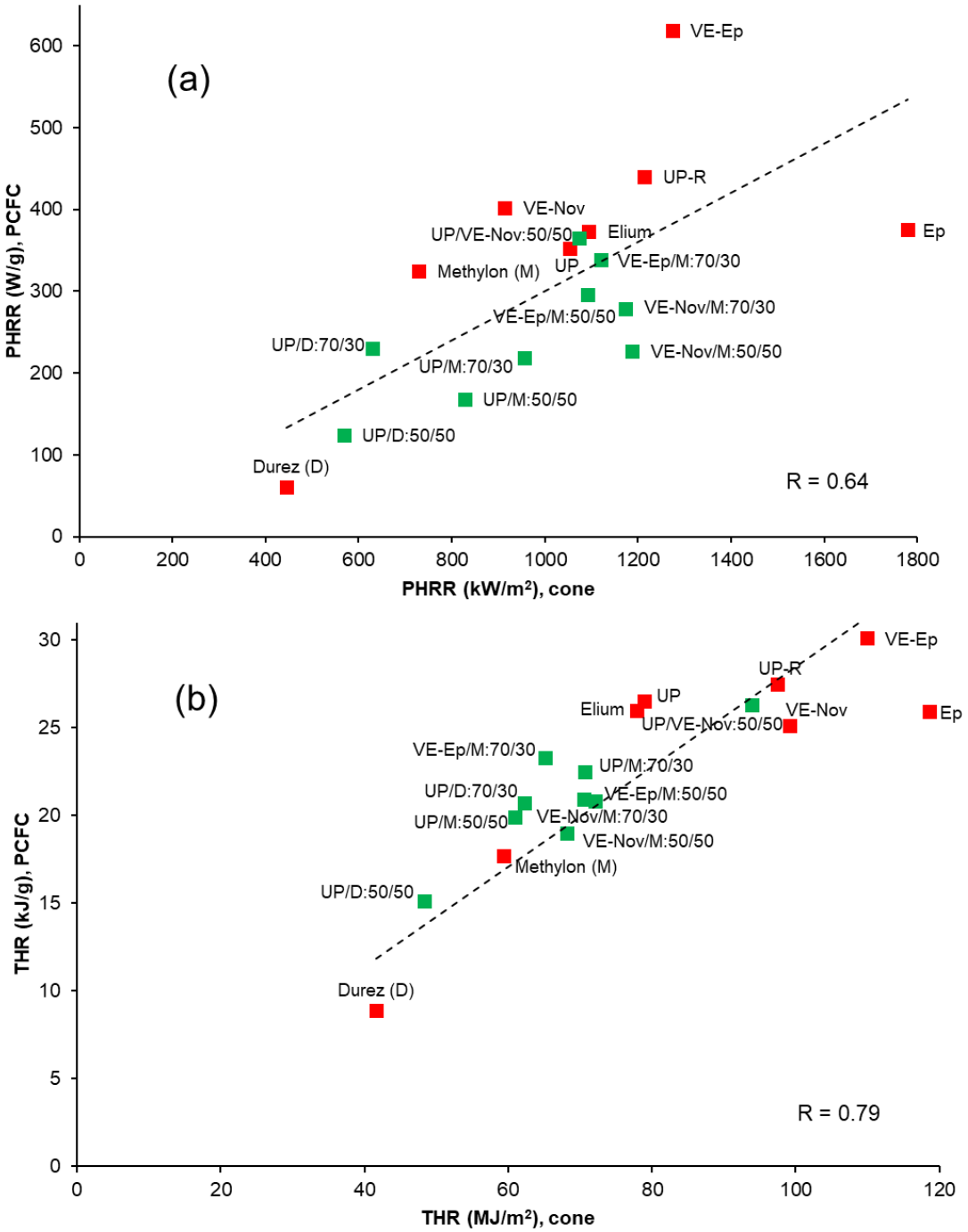

Figure 3.13: Plots of (a) PHRR and (b) THR from cone calorimetric data and PCFC tests for different cured neat resins and resin blends

3.5 Conclusions

In this chapter morphology, thermal stability and fire performances of resins commonly used for marine industry, UP and VE, were compared with those of other commonly used resins, including phenolics. All resins were cured after establishing their curing condition by DSC results. UPs, VEs, Ep and Elium were cured at room temperature, followed by post-curing at 80 - 90 °C for a few hours. Phenolics on the other hand needed curing at elevated temperatures, up to

220 °C. UP and VE were blended with two different phenolics and it was observed that UP and phenolics are more compatible than respective VE and phenolics. Methylon-based blends with UP or both VE showed better compatibility than Durez-based ones. UP and VE-Nov resins when blended, also showed good compatibility. The thermal stability of all resins and blends were studied by TGA, and their flammability by PCFC and cone calorimetry.

From their results as per fire safety assessment diagram from the cone, the overall fire safety from high to low could be ranked as follows:

Neat resins -

Durez > Methylon > UP > VE-Nov > UP-R > VE-Ep > Ep > Elium

Resin blends -

UP/phenolics > VE/phenolics > UP/VE-Nov

3.6 References

[1] D. Deli, B. K. Kandola, J. R. Ebdon, and L. Krishnan, “Blends of unsaturated polyester and phenolic resins for application as fire-resistant matrices in fibre-reinforced composites. Part 1: Identifying compatible, co-curable resin mixtures,” *Journal of Materials Science*, vol. 48, no. 20, pp. 6929–6942, 2013.

[2] B. K. Kandola, J. R. Ebdon, and C. Zhou, “Development of vinyl ester resins with improved flame retardant properties for structural marine applications,” *Reactive and Functional Polymers*, vol. 129, pp. 111–122, 2018.

[3] B. K. Kandola, L. Krishnan, D. Deli, and J. R. Ebdon, “Blends of unsaturated polyester and phenolic resins for application as fire-resistant matrices in fibre-reinforced composites. Part 2: Effects of resin structure, compatibility and composition on fire performance,” *Polymer Degradation and Stability*, vol. 113, pp. 154–167, 2015.

[4] A. Kandelbauer, G. Tondi, O. C. Zaske, and S. H. Goodman, “Unsaturated Polyesters and Vinyl Esters,” in *Handbook of Thermoset Plastics*, 3rd ed., H. Dodiuk and S. H. Goodman, Eds. William Andrew Publishing, 2014, pp. 111–172.

[5] F. A. Cassis and R. C. Talbot, “Polyester and Vinyl Ester Resins,” in *Handbook of Composites*, S. T. Peters, Ed. Springer, Boston, MA, 1998, pp. 34–47.

[6] “Elium® resins.” [Online]. Available: https://www.arkema.fr/fr/produits/product-finder/range/Resines-Elium/. [Accessed: 01-Nov-2018].

[7] P. Penczek, P. Czub, and J. Pielichowski, “Unsaturated polyester resins: Chemistry and technology,” in *Crosslinking in Materials Science, Advances in Polymer Science*, B. Ameduri, Ed. vol 184. Springer, Berlin, Heidelberg, 2005, pp. 1–95.

[8] K. G. Johnson and L. S. Yang, “Preparation, Properties and Applications of Unsaturated Polyesters,” in *Modern Polyesters: Chemistry and Technology of Polyesters and Copolyesters*, J. Scheirs and T. E. Long, Eds. John Wiley & Sons, Ltd, Chichester, UK, 2004, pp. 697–713.

[9] S. Crawford and C. T. Lungu, “Influence of temperature on styrene emission from a vinyl ester resin thermoset composite material,” *Science of The Total Environment*, vol. 409, no. 18, pp. 3403–3408, 2011.

[10] C. A. Ittner Mazali and M. I. Felisberti, “Vinyl ester resin modified with silicone-based additives: III. Curing kinetics,” *European Polymer Journal*, vol. 45, no. 8, pp. 2222–2233, 2009.

[11] B. S. Rao, P. J. Madec, and E. Marechal, “Synthesis of vinyl ester resins - Evidence of

secondary reactions by C-13 NMR," *Polymer Bulletin*, vol. 16, no. 2–3, pp. 153–157, 1986.
[12] B. Gaur and J. S. P. Rai, "Curing and decomposition behaviour of vinyl ester resins," *Polymer*, vol. 33, no. 19, pp. 4210–4214, 1992.
[13] B. Gaur and J. S. P. Rai, "Rheological and thermal behaviour of vinyl ester resin," *European Polymer Journal*, vol. 29, no. 8, pp. 1149–1153, 1993.
[14] H. Li, "Synthesis, Characterization and Properties of Vinyl Ester Matrix Resins," PhD Thesis Virginia Polytechnic, 1998.
[15] B. K. Kandola and A. R. Horrocks, "Flame retardant composites - A review - The potential for use of intumescents," in *Fire retardancy of polymers*, M. L. Bras, G. Camino, S. Bourbigot, and R. Delobel, Eds. Royal Society of Chemistry, London, 1998.
[16] M. A. Boyle, C. J. Martin, and J. D. Neuner, "Epoxy resins in compendium composites in ASM handbook / extraction," H. Hansmann and H. Wismar, Eds. FB MVU, Werkstofftechnologien / Kunststofftechnik, 2003.
[17] L. S. Penn and H. Wang, "Epoxy resins," in *Handbook of Composites*, 2nd ed., S. T. Peters, Ed. Chapman & Hall, Boston, MA, 1998, pp. 48–74.
[18] K. K. Chawla, "Composite materials: Science and engineering," 3rd ed., Springer Publishing, New York, 2012.
[19] I. Hamerton, "Recent developments in epoxy resins," Report No. 91, Rapra Technology Ltd., ISBN-1-85957-083-6, 1996.
[20] A. Knop and L. A. Pilato, *Phenolic resins: chemistry, applications and performance*. Springer-Verlag, Berlin Heidelberg, 1985.
[21] W. F. Smith and J. Hashemir, *Foundations of material science and engineering*. McGraw-Hill, New York, 2006.
[22] J. C. Munoz, H. Ku, F. Cardona, and D. Rogers, "Effects of catalysts and post-curing conditions in the polymer network of epoxy and phenolic resins: Preliminary results," *Journal of Materials Processing Technology*, vol. 202, pp. 486–492, 2008.
[23] C. S. Tyberg, K. Bergeron, M. Sankarapandian, P. Shih, A. C. Loos, D. A. Dillard, J. E. McGrath, J. S. Riffle, and U. Sorathia, "Structure-property relationships of void-free phenolic-epoxy matrix materials," *Polymer*, vol. 41, no. 13, pp. 5053–5062, 2000.
[24] W. J. MacKnight and F. A. Karasz, "Polymer Blends," in *Comprehensive Polymer Science*, S. L. Aggarwal, Ed. Volume 7, Pergamon Press, Oxford, 1989.
[25] A. Zinke, "The chemistry of phenolic resins and the processes leading to their formation," *Journal of Applied Chemistry*, vol. 1, no. 6, pp. 257–266, 1951.
[26] L. H. Sperling and V. Mishra, "The current status of interpenetrating polymer networks," *Polymers for Advanced Technologies*, vol. 7, no. 4, pp. 197–208, 1996.
[27] B. K. Kandola, L. Krishnan, and J. R. Ebdon, "Blends of unsaturated polyester and phenolic resins for application as fire-resistant matrices in fibre-reinforced composites: Effects of added flame retardants," *Polymer Degradation and Stability*, vol. 106, pp. 129–137, 2014.
[28] B. K. Kandola, J. R. Ebdon, and K. P. Chowdhury, "Flame retardance and physical properties of novel cured blends of unsaturated polyester and furan resins," *Polymers*, vol. 7, no. 2, pp. 298–315, 2015.
[29] B. K. Kandola, L. Krishnan, D. Deli, P. Luangtriratana, and J. R. Ebdon, "Fire and mechanical properties of a novel free-radically cured phenolic resin based on a methacrylate-functional novolac and of its blends with an unsaturated polyester resin," *RSC Advances*, vol. 5, no. 43, pp. 33772–33785, 2015.
[30] B. Kandola and L. Krishnan, "Fire Performance Evaluation of Different Resins for Potential Application in Fire Resistant Structural Marine Composites," *Fire Safety Science*, vol. 11, pp. 769–780, 2014.
[31] D. W. van Krevelen, "Some basic aspects of flame resistance of polymeric materials," *Polymer*, vol. 16, no. 8, pp. 615–620, 1975.
[32] R. Sonnier, H. Vahabi, L. Ferry, and J. M. Lopez-Cuesta, "Pyrolysis-combustion flow calorimetry: A powerful tool to evaluate the flame retardancy of polymers," in *Fire and*

Polymers VI: New Advances in Flame Retardant Chemistry and Science, A. B. Morgan, C. A. Wilkie, and G. L. Nelson, Eds. ACS Symposium Series 118: American Chemical Society, Washington, DC, USA, 2012, pp. 361–390.

[33] R. E. Lyon and R. N. Walters, “Pyrolysis combustion flow calorimetry,” *Journal of Analytical and Applied Pyrolysis*, vol. 71, no. 1, pp. 27–46, 2004.

[34] R. Sonnier, L. Ferry, C. Longuet, F. Laoutid, B. Friederich, A. Laachachi, and J. M. Lopez-Cuesta, “Combining cone calorimeter and PCFC to determine the mode of action of flame-retardant additives,” *Polymers for Advanced Technologies*, vol. 22, no. 7, pp. 1091–1099, 2011.

[35] B. K. Kandola and E. Kandare, “Composites having improved fire resistance,” in *Advances in Fire Retardant Materials*, A. R. Horrocks and D. Price, Eds. Woodhead Publishing Limited, Cambridge, UK, 2008, pp. 398–442.

[36] B. K. Kandola, D. Deli, and J. R. Ebdon, “Compatibilised polymer blends,” UK patent application, GB1121498.8, 2012.

[37] B. K. Kandola, A. R. Horrocks, P. Myler, and D. Blair, “Thermal characterisation of thermoset matrix resins,” in *Fire and polymers*, G. L. Nelson and C. A. Wilkie, Eds. ACS Symposium Series: American Chemical Society, Washington, DC, USA, 2001, pp. 344–360.

[38] B. Schartel and T. R. Hull, “Development of fire-retarded materials—Interpretation of cone calorimeter data,” *Fire and Materials*, vol. 31, no. 5, pp. 327–354, Aug. 2007.

[39] B. Schartel, C. A. Wilkie, and G. Camino, “Recommendations on the scientific approach to polymer flame retardancy: Part 2—Concepts,” *Journal of Fire Sciences*, vol. 35, no. 1, pp. 3–20, 2017.

[40] B. Sundström, “The Development of a European Fire Classification System for Building Products - Test Methods and Mathematical Modelling,” PhD thesis, Department of Fire Safety Engineering, Lund University, Sweden, 2007.

[41] “BS EN 13823:2010+A1:2014: Reaction to fire tests for building products. Building products excluding floorings exposed to the thermal attack by a single burning item.” BSI, The British Standards Institution, 2010.

[42] R. V. Petrella, “The Assessment of Full-Scale Fire Hazards from Cone Calorimeter Data,” *Journal of Fire Sciences*, vol. 12, no. 1, pp. 14–43, 1994.

Chapter 4: Designing sandwich structure composites with similar components but different compositions

In this chapter, sandwich structure composites with similar components but different compositions have been prepared and their fire performances evaluated by using two different standard fire tests - cone calorimetry and propane burner testing. The variables include cone heater orientation, thicknesses of core materials, composite laminates on one/both sides and different sample preparation techniques. The effects of these variables on fire performances of the composite structures were evaluated. In order to have relatively good comparison, the same type of neat resin, UP-R resin, was selected for this chapter's work. Curing conditions used for preparing all UP-R sandwich composite samples were RT for 24h and followed by 80 °C for 6h. Details of the samples are given in Table 4.1.

Table 4.1: Sandwich structure samples of balsa wood with thicknesses of 12.7 mm (0.5") and 25.4 mm (1") – UP-R resin

Sample	Sample ID
Resin infused laminates (Top side) (1")	RI-Top UP-1
Resin infused laminates (Both sides) (1")	RI-UP-1
Hand lay-up laminates (1")	HL-UP-1
Hand lay-up sandwich structure: in one go (1")	HLAll-UP-1
Resin infused laminates (Both sides) (0.5")	RI-UP-0.5
Hand lay-up sandwich structure: in one go (0.5")	HLAll-UP-0.5

The two fire tests were chosen based on two different standards, cone calorimetry based on the ISO 5660 [1] standard, widely used for marine applications, and a propane burner test based on ISO 2685:1998(E) [2], used in the aerospace sector. The propane burner test was chosen because it can produce a large and constant heat flux to simulate a severe fire condition. Heat fluxes used in these two standards were different. The heat flux in the propane burner test is 113 kW/m^2 heat flux and whereas in the cone calorimetry it is 50 kW/m^2. Since in the propane burner test the sample orientation is vertical and in cone calorimetry it is horizontal, the cone tests were also performed in vertical orientation as discussed in detail in Chapter 2, Section 2.4.5.

In this chapter firstly thermal degradation and burning behaviour of balsa wood has been investigated by thermogravimetry and cone calorimetry. The burning behaviour of the resin as a plaque (results taken from Chapter 3), in a composite laminate and in a sandwich structure has been evaluated to have an understanding of the effect of different components on the burning of the sandwich structure. Then in samples from Table 4.1, the effects of cone heater orientation, thicknesses of core materials, composite laminates on one/both sides and different sample preparation techniques have been investigated. From cone results time-to-ignition (TTI), flame-out time (FO), peak heat release rate (PHRR), total heat release (THR), total smoke

release (TSR) and wt% residue values were obtained. In both cone and propane burner tests, thermocouples were inserted on the back face of the samples and temperature profiles of the samples exposed to different heat fluxes and fire conditions in cone calorimetry and propane burner testing have been plotted, analysed and compared.

4.1 Thermal degradation and burning behaviour of balsa wood

4.1.1 Thermal degradation – study by thermogravimetric analysis (TGA)

Simultaneous DTA-TGA experiments were performed on as-received balsa wood (which contains moisture) and oven dried balsa wood in both air and nitrogen atmospheres. Due to the hydrophilic nature of balsa wood, its moisture content is 2 - 8% [3], depending on laboratory atmospheric conditions. In these samples ~8% moisture within the balsa was calculated from the averaged mass loss of 5 pieces of balsa block before and after drying at 80 °C for 12 h in an oven. Since moisture can affect the thermal degradation and hence, flammability behaviour of the wood, it is worthwhile to investigate its behaviour with/without moisture. Hence two balsa wood samples were prepared and tested, one was dried in an oven at 80 °C for 12 h prior to TGA testing, the other was tested as-received from the manufacturer. The DTA-TGA experiments were conducted from room temperature to 900 ºC using 3 - 5 mg of balsa wood samples heated at a constant heating rate of 10 ºC/min under air or nitrogen atmospheres with flow rate of 100 mL/min ± 5 mL/min. For each sample two test specimens were tested. As can be seen from Figure 4.1, there is only a small difference at the beginning of the thermal degradation mass loss behaviours of balsa wood samples with/without moisture, due to loss of moisture.

The analysed results are given in Table 4.2. There is not much difference between the two as can be expected. The TGA curve for the balsa shows that the dehydration of balsa occurs over the range RT - ~150 °C with 1 - 3% mass loss, mostly attributed with the evaporation of water from the balsa; there is slightly more mass loss from as-received wood than oven dried one, Figure 4.1. However, the mass loss in as-received balsa wood is less than 8%, as seen from mass change after heating the balsa wood block in an oven. Since in the large wood sample, there are more pores, more moisture is absorbed, whereas in TGA 3 - 5 mg pieces of the wood are sampled, which will not have so many pores, hence the difference in the results. And then the decomposition started at about 250 - 270 °C ($T_{10\%}$) in air and nitrogen, respectively and was largely completed by ~300 - 400 °C. The balsa wood has one stage of mass loss in N_2, indicating the decomposition, with about 80% of the original mass transformed into volatiles and the remaining 20% transformed into charred wood, leaving 20 - 22% char residue. In air the decomposition stage is followed by an oxidation of char stage, leaving ~2% residue. During decomposition, the balsa becomes highly porous due to the break-down of the organic constituents such as cellulose, hemicellulose and lignin [3], which is a typical behaviour of wood's decomposition [3-5].

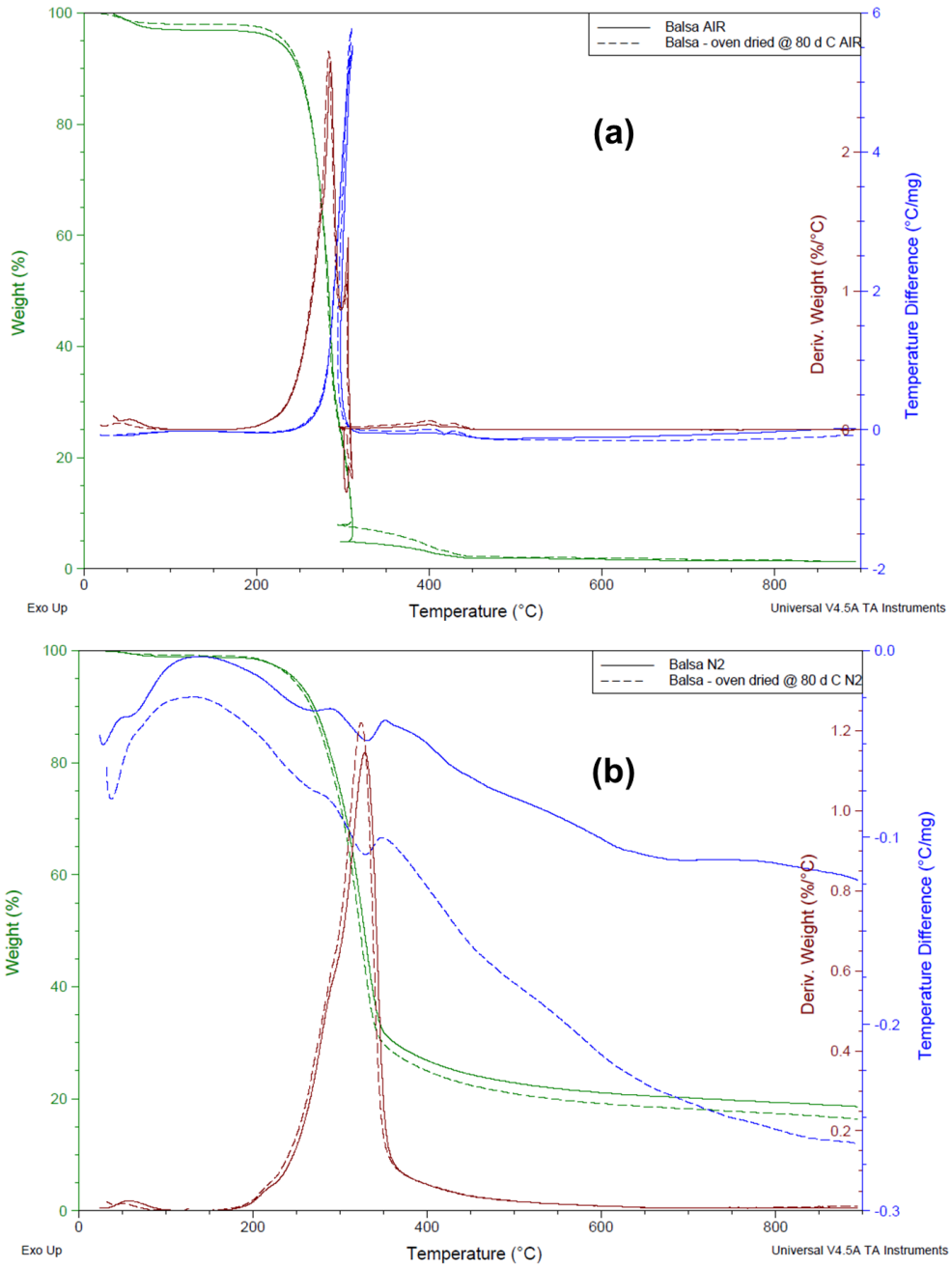

Figure 4.1: TGA-DTG-DTA curves for balsa wood (with moisture) and oven dried balsa wood in (a) air and (b) nitrogen atmospheres

Table 4.2: Data extracted from TGA traces recorded under N_2 and air atmospheres for balsa wood with/without moisture

Resin	N_2 atmosphere		Air atmosphere	
	$T_{10\%}$ (°C)	Char res. at 550 °C (wt%)	$T_{10\%}$ (°C)	Char res. at 550 °C (wt%)
Balsa (with moisture)	270	21.8	248	1.8
Balsa - oven dried at 80 °C	267	19.9	250	2.1

This study has shown the effect of adsorbed water on the thermal degradation is minimal. Hence, for fire testing and other experiments, the sandwich composite samples were not oven dried again.

4.1.2 Fire performance of balsa wood – cone calorimetry

Balsa wood samples of two different thicknesses 12.7 mm (0.5”) and 25.4 mm (1”) were tested as received (with moisture) via cone calorimeter at a heat flux of 50 kW/m^2. Since the wood burns for a long time, the major flame went out by 360 s for all wood samples and there was just glowing and smouldering. Hence the test was stopped after 10 minutes by taking the sample out of the load cell. The average density of the balsa used in this work was 150 kg/m^3, although there was a large amount of variability (a standard deviation of 45 kg/m^3) within a single panel of as-received wood, which is typical for balsa and should be taken into account. Hence for each sample, similar sample weights were selected to have similar nominal densities of balsa, and triplicates test specimens were conducted for comparison. HRR, RSR and mass loss *vs*. time for 12.7 mm (0.5”) and 25.4 mm (1”) thick balsa wood are plotted in Figure 4.2 (a-f, respectively) and derived results from cone calorimetry are given in Table 4.3 as well. Digital images before and after cone calorimetric tests were taken and are presented in Figure 4.3.

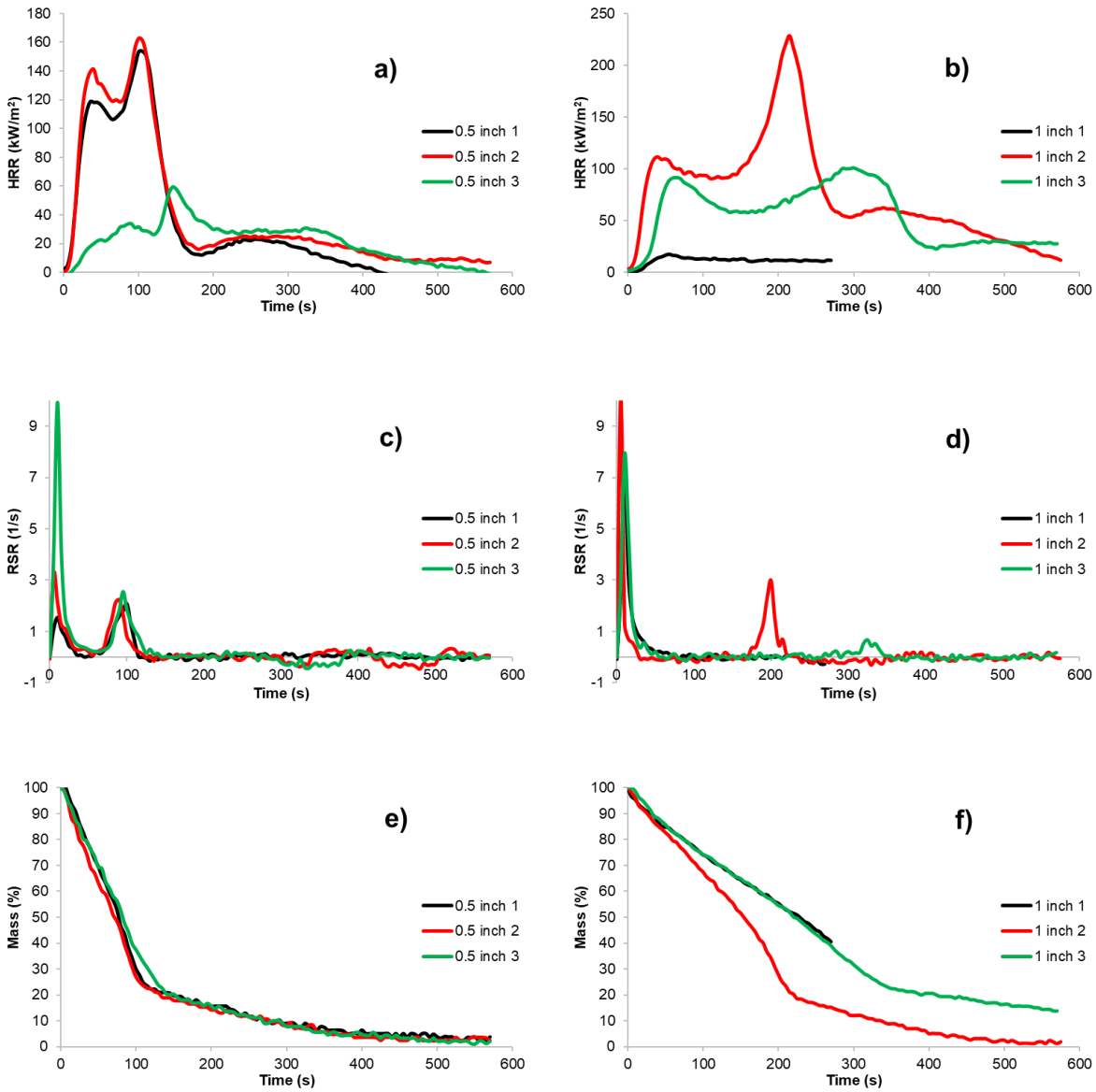

Figure 4.2: Plots of (a, b) HRR, (c, d) RSR and (e, f) mass loss *vs*. time for 12.7 mm (0.5”) and 25.4 mm (1”) thick balsa wood

Table 4.3: Derived cone calorimetric results of balsa wood with thicknesses of 12.7 mm (0.5”) and 25.4 mm (1”)

Sample ID	TTI (s)	FO (s)	PHRR (kW/m^2)	THR (MJ/m^2)	TSR (m^2/m^2)	Residue (wt%)
Balsa wood 0.5” 1	4	132	118,154	18.7	99	2
Balsa wood 0.5” 2	5	130	141,163	22.9	133	2
Balsa wood 0.5” 3	123	146	59	12.4	204	2
Balsa wood 1” 1	-	-	18	3.1	97	40
Balsa wood 1” 2	5	267	112,229	43.7	130	1
Balsa wood 1” 3	25	361	92,101	31.5	134	14

Notes: TTI = time-to-ignition, FO = time-to-flame-out, PHRR = peak heat release rate, THR = total heat release, TSR = total smoke release. The reproducibility in cone parameters was ±5% in general. “-” indicates the specimen did not ignite, hence TTI and FO time cannot be collected.

Figure 4.3: Digital images of balsa wood with thicknesses of (a) 12.7 mm (0.5”) and (b) 25.4 mm (1”) before and after cone calorimetric test

From the results, it can be observed that the burning behaviours of balsa wood of two different thicknesses varied a lot and also within the same thickness, the reproducibility of the results is very poor and so cannot be quantified in terms of a simple standard deviation measurement unless a larger number of specimens had been tested per sample. From the digital images of residue after the tests (Figure 4.3), it can be seen that for 12.7 mm (0.5”) thick samples, all three specimens burnt completely and at the end only a thin layer of glass fabric, some wood floc and aluminium foil remained. By contrast, large differences in the residues of 25.4 mm (1”) thick specimens can be observed, due to a big difference in their fire performances, seen from HRR *vs.* time curves (Figure 4.2 (b)). Due to the large variation for each individual result, averaged results with standard deviation are not presented here, rather individual results of each specimen are given in Table 4.3. Some of the balsa wood specimens ignited whereas some did not. The reason might be that balsa wood is a natural product with variable density along the block. Also, these samples are made of blocks, held together by gluing them to a thin glass woven fabric on one side, while the other side has gaps, as seen from Figure 4.3. The position of these gaps varies in different samples, which may affect their ignition and burning behaviours. All 12.7 mm (0.5”) specimens ignited, two specimens had similar TTI (4 - 5 s), whereas in the third one TTI was delayed to 123 s. Specimens with similar TTI have similar other cone parameters, i.e., PHRR, mass loss etc. One 25.4 mm (1”) did not ignite and the other two had different TTI values, hence quite a variation in all results.

In all the samples which ignited, no matter whether 12.7 mm (0.5”) or 25.4 mm (1”) thick, two peaks of HRR can be observed. A spark igniter facilitates the initial ignition of the combustible gases in the cone calorimeter test. The igniter is removed once sustained flaming of wood occurs. The cone calorimeter only measures the HRR if there is combustion of the volatile gases since it uses oxygen depletion to measure HRR. When the balsa wood ignited, it showed the start of the peak (corresponding to TTI), the first peak is when the wood burned and released heat, which reduced once the protective char layer forms as the result of the thermal degradation of the wood. And the second peak in the HRR curves occurs when the heat penetrates through the char and rest of the sample starts burning [6-10]. The time for the second peak HRR reflects the relative thickness of the specimens, i.e. physically thick samples take much longer time to reach the second peak (Figure 4.2 (a), (b)). Flameout time or FO time for the physically thick samples is much longer than the thin ones. As can be observed in Figure 4.2 (e), (f), mass loss started at the beginning of cone testing in both wood samples of different thicknesses, due to loss of moisture in the wood, and then the burning and charring of the wood, after that followed by a reduced mass loss rate due to smouldering of wood until complete mass loss. The mass loss rate of thick samples is slower than the thin ones because of the thermally thick behaviour [11], when the heat wave penetration depth is less than the physical depth such that an increase in physical thickness does not influence the time-to-ignition under a given set of conditions [11], resulting in slower degradation in thick wood. THR of thick samples are much higher than those of thin samples for those ignited as a result of their physical thickness effects, more wood

content in thick sample, which burns and smoulders, hence released more heat. Smoke production (Figure 4.2 (c), (d)) is consistent with mass loss prior to ignition and after the time for sustained ignition, and another apparent smoke release peaks are consistent with the second peaks in HRR curves. Also, by visual observation, it is noticed that while the main flame extinguished, glowing on the wood was seen in all wood samples. Based on the above results it can be seen that, 25.4 mm (1”) thick balsa wood can behave as a better thermal barrier to slow down burning than the 12.7 mm (0.5”) thick one.

4.1.3 Heat transfer (thermal gradients) during cone calorimeter and propane burner tests

In order to understand the heat transfer through the balsa, during the cone tests of 25.4 mm (1”) thick samples, thermocouples were inserted at the back-surface side of balsa to measure temperature profiles. These tests were conducted at both 35 and 50 kW/m^2 heat fluxes in the cone calorimeter and the results are presented in Figure 4.4, samples were run at a lower heat flux of 35 kW/m^2 in order to see the effect of slow burning, whereas 50 kW/m^2 is a standard value. The propane burner test at a 113 kW/m^2 heat flux was also conducted and temperature profiles obtained.

It can be seen in cone calorimetric testing, temperature profiles under 50 kW/m^2 heat flux are higher than that of 35 kW/m^2, due to a higher heat flow rate intensity as can be expected, i.e., lower heat flux could have higher TTI in cone tests, hence delayed ignition causing slowing down of the temperature rising at the beginning in 35 kW/m^2. Once the balsa wood ignited, the wood charred and oxidised, the wood with lower heat flux burns slower than the 50 kW/m^2 one, resulting in lower thermal degradation and heat release associated with char oxidation, hence the temperature rising trend is lower in the heat flux of 35 kW/m^2. Up to 350 s, there is a steady state in both heat fluxes under cone calorimetry, the reason could be the dehydration of balsa wood, in which adsorbed and absorbed water are lost. This also could be due to the fact that the wood chars at lower temperature and the formed charred protective layer slows down the temperature rising trends, until the surface temperature is high enough to cause ignition. Once wood samples ignited, the one with lower heat flux (35 kW//m^2) was expected to have higher TTI and slower burning. As mentioned in Section 4.1.2, see Figure 4.2 (b), the HRR increases to a second peak (starting after ~150 s in cone tests), consistent with the faster thermal degradation and higher heat release associated with char oxidation, hence temperature profiles on the back surface increased rapidly after 450 s. Following the exhaustion of volatiles, flaming combustion ends and the HRR returns to a steady baseline at the time of around 600 s (Figure 4.2 (b)). In the absence of a protective char, at the time of around 950 s (Figure 4.4), the temperature profiles become relatively stable because a complete charred wood has been formed. In general, temperature profiles for the heat flux of 50 kW/m^2 rise quicker and temperature is higher than that of 35 kW/m^2 indicating that higher burning rate and PHRR of the balsa wood at 50 kW/m^2 in cone tests. By contrast, temperature changes at 35 kW/m^2 are much

slower.

In propane burner tests, the test was stopped manually when the back-surface temperature reached 300 °C, at which temperature, it was defined that the whole sample was burnt through and heat was transferred to the back surface of tested sample. It can be noticed that temperature profiles trend of 50 kW/m^2 in cone calorimetry is similar as the one with 113 kW/m^2 heat flux in propane burner tests. Hence it is interesting to investigate whether or not the results obtained using different testing methods at different heat fluxes would show some correlation, which will be discussed in Section 4.3.

In Figure 4.4, it can be seen from the curves obtained from propane burner tests (in red) that there is a steady state up to 100 s, indicating the dehydration of wood and probably charred protective layer of wood formed before ignition. After that, while the surface temperature of wood reached its thermal degradation temperature, hence causing ignition, the wood started to burn and released heat, thus raising the temperature of the back surface. Finally, when the heat penetrates through the former char, often cracked and the rest of the sample starts burning more intensively due to the high heat flux of the propane gas flame, hence temperature profiles after 350 s increase very sharply till the end of tests (reaching 300 °C).

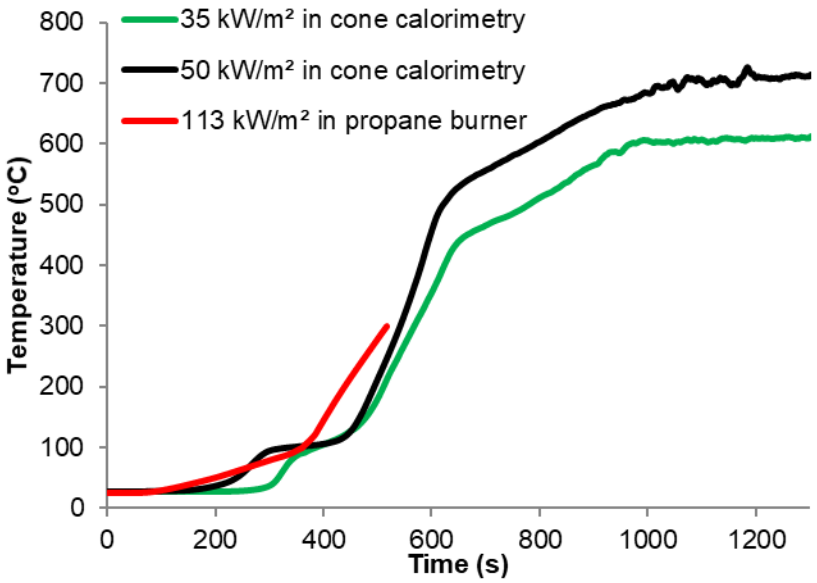

Figure 4.4: Temperature profiles on back surfaces of balsa wood in three different heat fluxes - 35, 50 kW/m^2 in cone calorimeter and 113 kW/m^2 in propane burner tests

In short, the HRR curves for the balsa wood (Figure 4.2 (b)) reflect the HRR curves for standard wood [6,12].

4.2 Burning behaviour of resin as a neat resin, in a composite laminate and in a sandwich structure

It is important to have an understanding of the fire performance of different resin systems used as a neat resin, in a composite laminate or in a sandwich structure and how do they perform and correlate with each other. Here samples of a standard cured UP resin (circular plaque, diameter 55 mm, thickness of ~3 mm), composite laminate (4 layers glass fabrics, made by resin infusion technique, size = 75 mm × 75 mm, thickness = ~1.1 mm) and sandwich structures (25.4 mm (1 inch) balsa core, skins of 4 layers glass fabrics on each side of samples, made by resin infusion technique, size = 75 mm × 75 mm, thickness = ~27.6 mm, i.e., RI-UP-1 sample in Table 4.1) were tested in the cone calorimeter at 50 kW/m^2 heat flux in horizontal mode and the results compared.

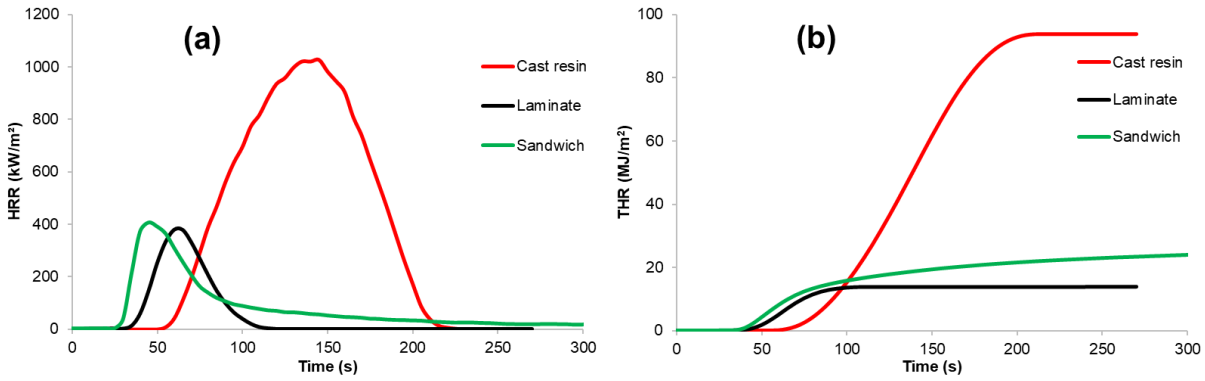

Figure 4.5: Plots of combined (a) HRR and (b) THR for cast UP resin, composite laminate and sandwich structure *vs.* time

Table 4.4: Summary of cone calorimetric results for UP cast resin, composite laminate and sandwich structure

UP Sample	Resin (wt%)	TTI (s)	FO (s)	PHRR (kW/m^2)	THR (MJ/m^2)	TSR (m^2/m^2)	Residue** (wt%)
Cast resin	100	44±6	179±6	1050±21	96.3±2.1	6044±256	0
Composite laminate	31	33±4	72±5	391±15	13.8±0.4	696±69	69±0 (0)
Sandwich structure	37*	28±2	1198±113	443±49	24.6±0.5	878±179	74±1 (40)

Notes:
TTI = time-to-ignition, FO = time-to-flame-out, PHRR = peak heat release rate, THR = total heat release, TSR = total smoke release.
* = Resin content in skin
** = Values in the parentheses are after compensating for glass content.

It can be observed from Figure 4.5 and Table 4.4 that the burning behaviours of composite laminate and the sandwich structures are very similar, the only difference is that the sandwich structure burns for a longer time. The burning behaviour of the resin however is different from composite laminate and the sandwich structure. There are some differences in TTI in different sample types. TTI depends on the amount of resin on the surface and the physical thickness of the sample. The composite laminate and sandwich structure showed slightly lower TTI values than that of UP cast resin alone, that is due to physical thicknesses of tested samples, i.e., the thicknesses of tested samples reduce from cast resin (3 mm) to composite laminate (1.1 mm) and skin on the top surface of sandwich structure (1.1 mm), hence cast resin has higher TTI. In general, both composite laminate and sandwich structure showed lower flammability than cast

resin alone by showing significantly reduced PHRR, THR and TSR, forming more charring residue.

Because 25.4 mm (1”) thick balsa wood was used as core material in sandwich structure, balsa wood would not ignite first. When the skin laminate ignited, the wood charred by forming a protective char layer, as discussed in Section 4.1.2, which behaved as a thermally thick barrier as expected. At the end of the cone experiment, all cast resin was totally burnt out and no residual char was left. The resin within the composite laminate was completely burnt out, only four layers of glass fabric remained after the test. Each layer of glass fabric was separate and could not hold together. Whereas, in the sandwich structure, all resin within the top laminate was burnt out exposing glass fabric layers, but the bottom layer of laminate had some charred residue and unburnt resin, and charred residue of balsa wood. By comparison with the burning behaviour of resin as a neat resin, in a composite laminate and in a sandwich structure, it can be concluded that sandwich structure flammability is similar/slightly higher compared to composite laminate when considering standard variation, i.e., similar/slightly increased PHRR, TSR etc. In the case of composite laminate and the sandwich structure, the TTI and PHRR are expected to be similar. The slightly higher PHRR value seen by the sandwich structure in Table 4.4 could be due to a different resin content on the surface of that specimen. The total heat release, THR of the composite sandwich structure, however, is much higher than that of the composite laminate due to the longer burning of balsa wood in the former.

4.3 Burning and heat transfer behaviours of composites under cone calorimetric and propane burner testing

The cone calorimetric tests of sandwich structure composites with similar components but different compositions were performed at 50 kW/m^2 heat flux in both horizontal and vertical orientations. Sample sizes were 75 × 75 mm^2, with varying sample thicknesses. Separations between the cone heater and front surface of samples were setup at 25 mm in both cases. The spark igniter was applied at the same distance to the top surface of the samples. Insulation conditions on both cone heater orientations were similar. The effects of cone heater orientation, thicknesses of core materials, composite laminates on one/both sides, different sample preparation techniques via two different standard fire tests - cone calorimetry at 50 kW/m^2 and propane burner tests at 113 kW/m^2 heat flux are discussed in the following sections.

4.3.1 Effect of cone heater orientation

The HRR as a function of time curves for sandwich composites in horizontal and vertical orientations at 50 kW/m^2 heat flux are plotted together in Figure 4.6 and analysed results given in Table 4.5. In the vertical orientation mass loss could not be recorded as the thermocouples interfered with the data collected.

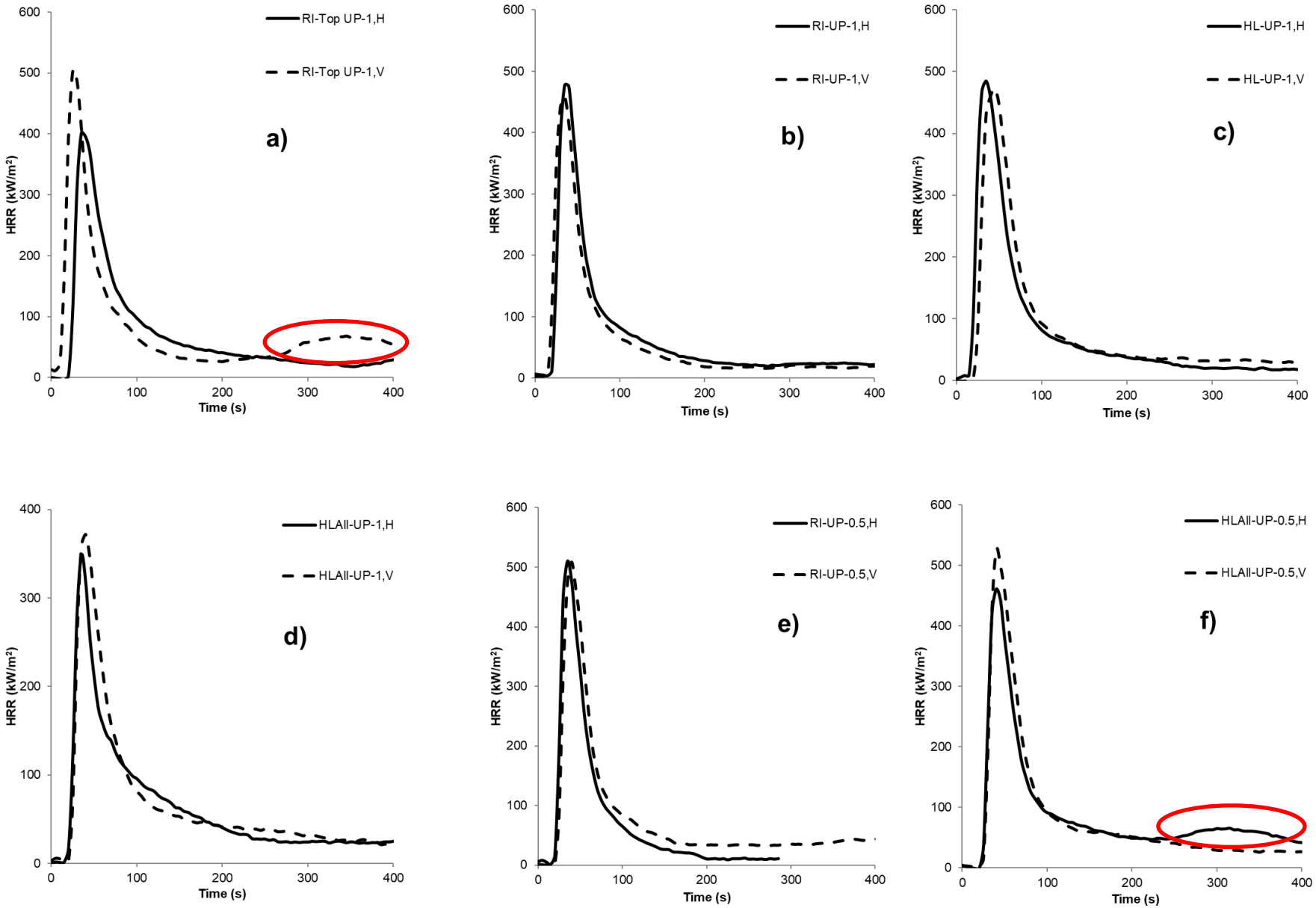

Figure 4.6: Cone calorimetric results at 50 kW/m^2 for HRR in both horizontal(H)/vertical(V) orientations versus time curves for sandwich structure composites with similar components but different compositions - (a) RI-Top UP-1, (b) RI-UP-1, (c) HL-UP-1, (d) HLAll-UP-1, (e) RI-UP-0.5 and (f) HLAll-UP-0.5

Table 4.5: Derived cone results of sandwich structures with similar components but different compositions - horizontal and vertical orientations at 50 kW/m^2 external heat flux

Sample ID	Orientation	Glass/Resin (wt%)	TTI (s)	PHRR (kW/m^2)	THR (MJ/m^2)	TSR (m^2/m^2)	Residue (wt%)
RI-Top UP-1	Horizontal	61/39	24±1	448±64	43.3±11.4	1099±291	40±4
	Vertical		14±3	451±74	41.9±8.2	1569±1032	-
RI-UP-1	Horizontal	63/37	28±2	443±49	41.9±3.7	1113±413	52±3
	Vertical		18±12	459±1	34.8±13.1	2237±1816	-
HL-UP-1	Horizontal	58/42	26±1	477±11	37.8±3.4	1109±409	54±1
	Vertical		24±9	458±20	52.3±0.3	1284±8	-
HLAll-UP-1	Horizontal	69/31	25±3	343±8	42.1±8.3	1388±776	52±1
	Vertical		18±13	368±6	33.1±10.8	2928±2799	-
RI-UP-0.5	Horizontal	67/33	29±3	508±3	27.2±8.3	969±62	63±10
	Vertical		25±12	514±6	36.7±3.7	1152±677	-
HLAll-UP-0.5	Horizontal	67/33	30±0	441±29	36.2±1.5	2653±485	55±1
	Vertical		36±1	518±10	36.4±2.0	561±31	-

Note: '-' indicates that mass loss was not recorded.

There is not much difference in the HRR curves (Figure 4.6) and similar PHRR values are observed between two orientations (Table 4.5). TTI values are slightly different, which in horizontal mode are slightly higher than the vertical, except for HLAll-UP-0.5. Although the same heat fluxes of 50 kW/m^2 were applied in both cone heater orientations, heat flux is a vector quantity, consisting of a direction and a magnitude, magnitude is same in both cases, but their cone directions are different. THR is similar in both orientations considering variation in results (Table 4.5). Large variations can be observed in TSR, however. The smoke release was analysed by the laser photometer beam when the sample is running under cone calorimetry, the ventilation system is always on during the tests, in both horizontal and vertical mode and most of the smoke release/volatiles can be drawn and collected directly through the exhaust hood and analysed. So, in theory the orientations of cone heaters for the collection in TSR should be similar or not affected. Thus, TSR in addition to being affected by the balsa wood density is sensitive to sample/cone heater orientation.

In addition, from HRR curves in Figure 4.6, the first peaks derive from when the resin on the top surface started to ignite and burn hence releasing heat, which reduced when the resin was burnt out from the top. Then the underlying wood charred (the protective char layer forms due to the thermal degradation of balsa wood), ignited, burned and released further heat. Cracking and opening of balsa wood occurred in all sandwich composites. It can be seen that in some samples there is a small second peak between 300 - 400 s as shown by red circles in Figure 4.6 (a) and (f), which could be explained that when the heat penetrates through the burnt-out top laminate and charred wood, and then the rest of the sample starts burning. Maybe in these two samples, more debonding and delamination between the top skin and charred balsa core and more gaps in blocks of balsa wood occur, leading to some flame/volatiles from the underlying wood or resin on bottom laminate coming through the foil wrapped around the sample to the top of the samples, hence showing heat release for the second peaks. Furthermore, the second peak HRR was delayed and reduced compared with those of balsa wood only due to the presence of laminate on the top.

In a previous work [13,14] the calibration of the cone calorimetry in two orientations was performed on a standard flammable material in which blocks of wood samples (whole blocks of hardwood with no gaps) were chosen and tested at heat flux of 50 kW/m^2. This test was performed in horizontal and vertical orientations. It was demonstrated that in vertical orientation the PHRR was slightly higher than in the horizontal orientation, the difference though was still within the error range of cone tests (10%). There was no significant effect on the mass loss rate. From these results it can be concluded that in these samples, such as those containing wood, which are flammable, there is not much effect of the orientation on their flammability properties [13,14]. Here in this work, it can be concluded that there is more difference in fire performances for sandwich composites between cone heater orientations, which is not unexpected, because both resins and balsa wood are flammable, the balsa core contained in sandwich composites

also has gaps, which could affect burning behaviours of whole samples, but results were still within acceptable experimental error range. Depending upon the end-use, appropriate orientation can be chosen. In the next section of the work, vertical orientation was selected to conduct temperature profile measurement, because it is the same orientation as in propane burner testing and much easier to setup on the sample holder.

4.3.2 Effect of thicknesses of core materials

The effect of thickness of the balsa core in UP/Glass – Balsa composite samples, prepared with the same sample preparation technique, i.e. hand lay-up sandwich structure in one go (samples 25.4 mm (1”), HLAll-UP-1 and 12.7 mm (0.5”), HLAll-UP-0.5) on cone calorimetric tests is shown in Figure 4.7. For simplicity, they are hereafter called 1” and 0.5” samples.

Resin contents in both 0.5” and 1” thick samples are similar. From the HRR curve shown in Figure 4.7 (a), for ignition to occur, the top skin needs to heat up. It can be seen that TTI for two different thicknesses of balsa core is similar, which is not unexpected, because the same type and similar resin content are in the top skin of both samples. The sample with 0.5” of core, HLAll-UP-0.5 shows higher PHRR compared with HLAll-UP-1 (441 *vs.* 343 kW/m^2) probably due to slightly different resin content (Table 4.5) on the top skin. The ignition and burning behaviours of polymer and wood products with different thicknesses are dependent on physical thickness. Thin samples (0.5”) usually show higher PHRR [15-18]. Usually if physical thickness is more than 10 mm, it is ranked as thermally thick, i.e., the opposite side does not heat up but remains at the ambient temperature when the specimen ignites, confirmed from Figure 4.7 (c), where the heat transfer from the back surface temperatures of both samples does not rise until around 80 s. Hence both 0.5” and 1” samples are considered as thermally thick. In addition, it can be noticed that 0.5” sample shows two peaks in the HRR curve, one pronounced and followed by a small second peak in the red circle, which could be related to the second PHRR in balsa wood, where probably some small flame comes to the top surface from edge of wrapped aluminium foil in HLAll-UP-0.5 (with 0.5” core) sandwich composites, hence producing the second small peak here.

THR for 1” sample is higher than for 0.5” as can be expected due to the greater wood content in thick samples, which burns and smoulders for a longer time. From the mass loss curve (Figure 4.7 (b)), the 0.5” sample shows higher mass loss rate than that for 1”, as expected, burning more rapidly than the 1” one. Residue remained after the test was similar in both samples, 52 - 55% (Table 4.5), which is mainly the glass fabric and charred balsa wood.

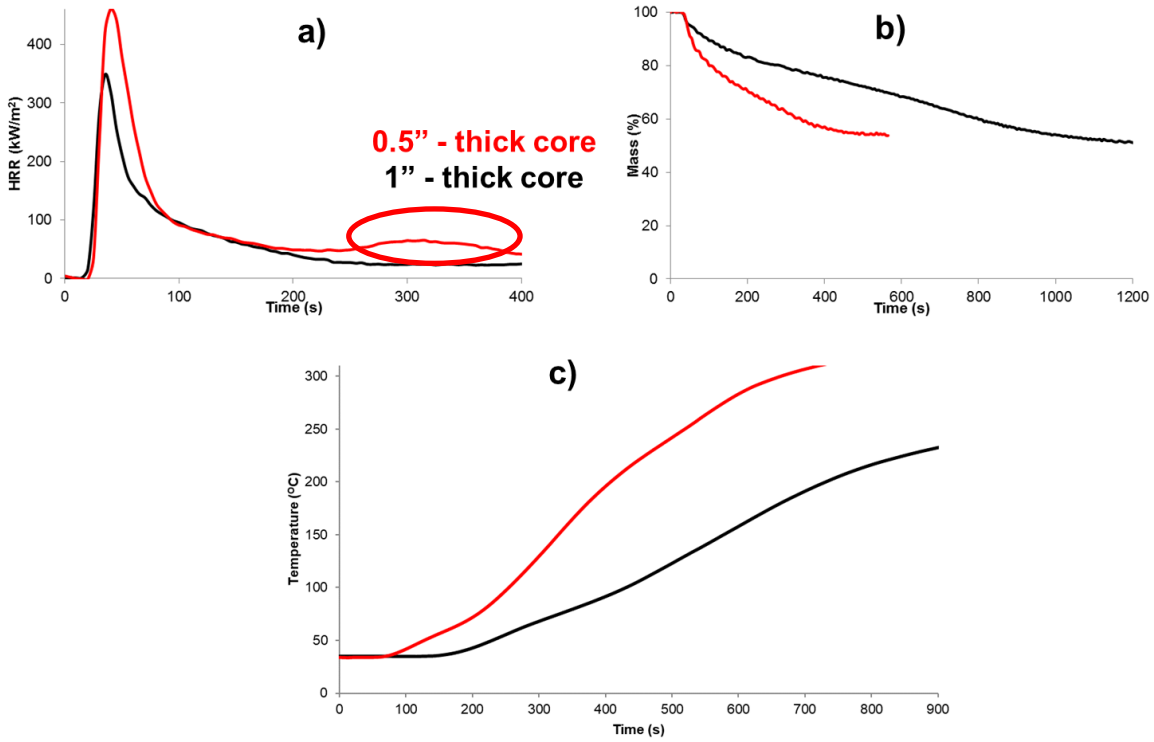

Figure 4.7: Cone calorimetric results at 50 kW/m^2 for (a) HRR, (b) mass loss versus time curves in horizontal orientation and (c) back surface temperature versus time curves in vertical mode for the effect of thicknesses of core for sandwich structure composites with similar components but different compositions

As can be seen in Figure 4.8, the back-surface temperature versus time curves from cone calorimetry and propane burner testing, propane burner curves (dash lines) showed that the 0.5” sample takes only around one third time to burn through the whole sample compared with that of the 1” sample. As explained in Section 4.1.3 that in propane burner tests, the whole sample was regarded as burn-through when the back-surface temperature reached 300 °C, the test at that stage was stopped manually. However, for the 0.5” thick samples in the propane burner test burn-through time was observed at 250 °C due to a more rapid heat transfer for the thinner core sandwich panel sample, hence 250 °C has been used for the results reported in Table 4.6. It can also be observed from Figure 4.8 that for the 1” sample, propane burner and cone results show similar temperature profiles despite different incident heat fluxes. The 0.5” sample does not show that trend; in the propane burner test the temperature on the back surface increased very rapidly, whereas in cone calorimetry the temperature profiles increased slowly compared with that of respective propane burner tests. This can be explained based on physical and thermal thickness of the 1” sample, where larger volumes of the charred wood provided a better thermal barrier effect. Another possible reason could be due to different types of k-type thermocouples used in both tests. In order to analyse thermal barrier effect of different thicknesses of balsa core, time to reach different back surface temperatures (100 - 300 °C) and maximum temperature – T_{max} in both tests are given in Table 4.6. It can be noticed that physically thin samples take shorter times to reach selected certain temperatures, and with the same sample, temperatures in propane burner tests are higher at all times compared with those corresponding values in cone tests due to higher heat fluxes and hence more intensive

penetration through the thickness of same sample under propane tests, especially for the 0.5” sample.

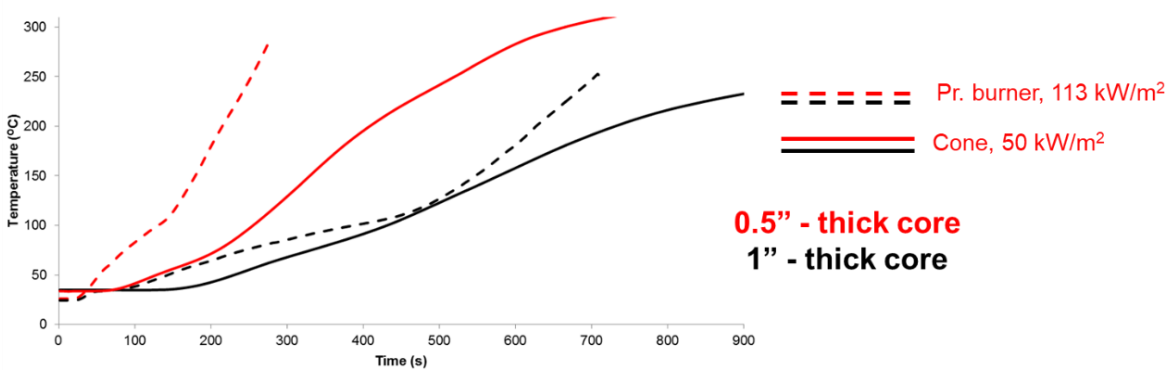

Figure 4.8: Back surface temperature versus time curves from cone calorimetry and propane burner testing for effects of thicknesses of core for sandwich structure composites with similar components but different compositions

Table 4.6: Times to reach different back surface temperatures (100 - 300 °C) and maximum temperature – T_{max} during the cone calorimetry and propane burner testing for sandwich composites with different thicknesses of the balsa core

Sample ID	Time to reach									
	100 °C (s)		200 °C (s)		250 °C (s)		300 °C (s)		T_{max} (s, °C)	
	C	P	C	P	C	P	C	P	C	P
HLAll-UP-1	430	388	730	627	-	705	-	-	900, 233	709, 252
HLAll-UP-0.5	254	130	407	215	519	253	664	-	722, 310	278, 291

Note: C - Cone calorimetry, P - Propane burner, ‘-’ in the table indicated maximum temperature during the testing did not reach the certain temperature.

4.3.3 Effect of composite laminates on one side or both sides

Composite laminates of sandwich structures on one side or on both sides with same thicknesses of balsa core and sample preparation techniques, i.e. resin infused laminates (Top side) 25.4 mm (1”), RI-Top UP-1 and resin infused laminates (Both sides) 25.4 mm (1”), RI-UP-1, given in Figures 4.9, 4.10 and Table 4.7, are compared to study the effect of the composite laminate skin.

From the cone calorimetric results of HRR and mass loss curves shown in Figure 4.9 (a) and (b), RI-Top UP-1 and RI-UP-1 do not show big differences for PHRR (448 *vs.* 443 kW/m^2), which is as expected as the PHRR is dependent on the resin content on the surface, which is similar in both samples. TTI is similar as well because both samples are using the same type of resin as matrix of the skin. In RI-Top UP-1 sample, there is a small second peak of heat release as shown in the red circle, probably due to the reason that more debonding between the burnt top skin and charred core in this sample occurred and possibly some flame or volatiles came to the front surface hence raising the heat release again as explained previously in detail (Section

4.3.1). THR and TSR are similar for both samples as well. Moreover, it can be observed from the mass loss curves for both samples, there is not much difference for first 200 s, and then the RI-Top UP-1 sample burned much quicker than RI-UP-1, i.e., a higher mass loss rate of the former. When the laminate is present on the reverse side, although the resin burns, the glass fabric reduces the rate of burning, which is reflected by the more gradual, slow, mass loss rate compared with sharper mass loss rate in the sample with skin only on the top side, shown in mass loss curve in Figure 4.9 (b). Residual mass after the cone tests is more in sample RI-UP-1 (52%) than in RI-Top UP-1 (40%); within the former all resin within the top laminate was burnt out exposing glass fabric layers, but the bottom layer had some charred residue, unburnt resin, and charred residue of balsa wood, whereas the latter consisted mainly of glass fabric on the top side and charred balsa wood.

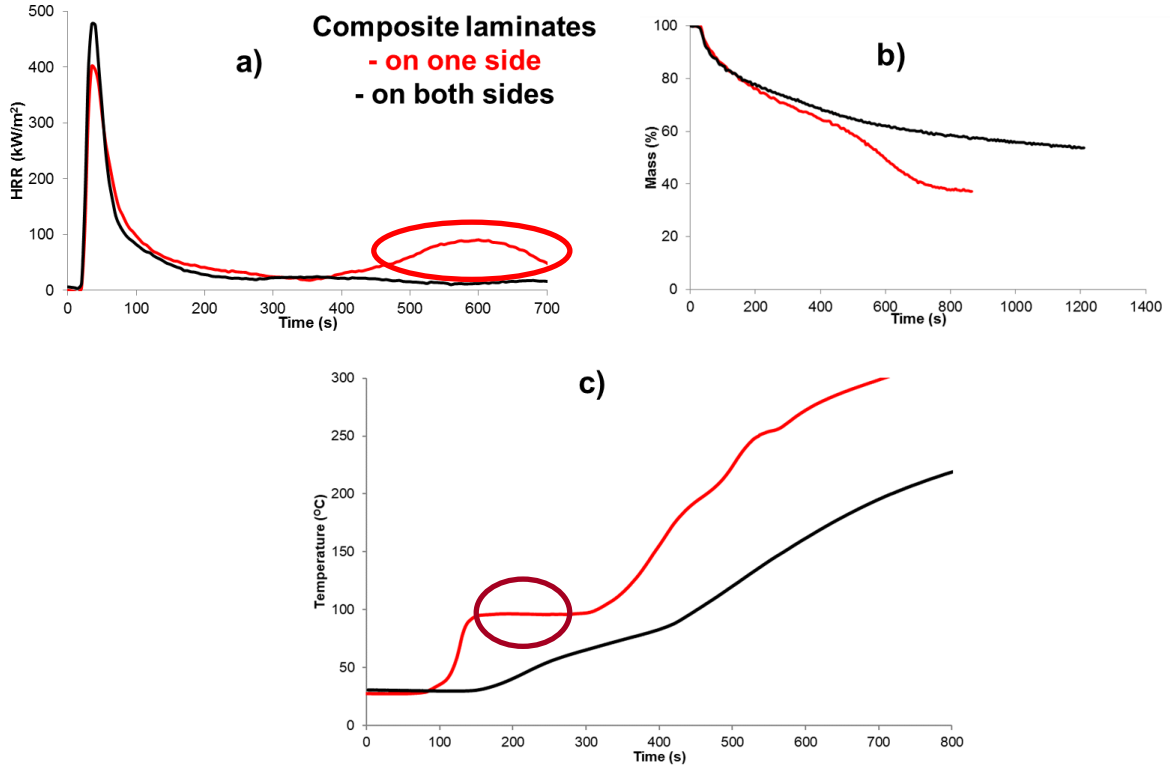

Figure 4.9: Cone calorimetric results at 50 kW/m^2 for (a) HRR, (b) mass loss versus time curves in horizontal orientation and (c) back surface temperature versus time curves in vertical mode for effects of composite laminates on one/both sides for sandwich structure composites with similar components but different compositions

From the cone calorimeter temperature profiles (Figure 4.9 (c)), it can be seen that there is a delay in the temperature rise at the beginning of the tests up to ~85 s and after that, the temperature of RI-Top UP-1 sample rises much quicker than that of RI-UP-1. Cone temperature profiles of RI-UP-1, are much slower, smooth and indicating much better thermal barrier effects and performances than that of RI-Top UP-1. It should be noted that for the cone temperature profiles of RI-Top UP-1, there is a steady state at temperature of 100 °C from 150 - 300 s (dark red circle in Figure 4.9 (c)). The reason could be due to the loss of water moisture in balsa because in this sample the opposite side is without laminate hence wood directly exposed to air

ambient atmosphere in the laboratory, probably adsorbed and absorbed more water than RI-UP-1 sample.

From the back-surface temperature versus time curves obtained from the propane burner testing shown in Figure 4.10, on comparing samples of RI-Top UP-1 and RI-UP-1 (curves with dashes in red and black), it can be observed that there is not much difference in performance until 5 minutes when flame burns through the former, whereas the latter withstands flame until 10 minutes (329 *vs.* 630 s to reach 250 °C).

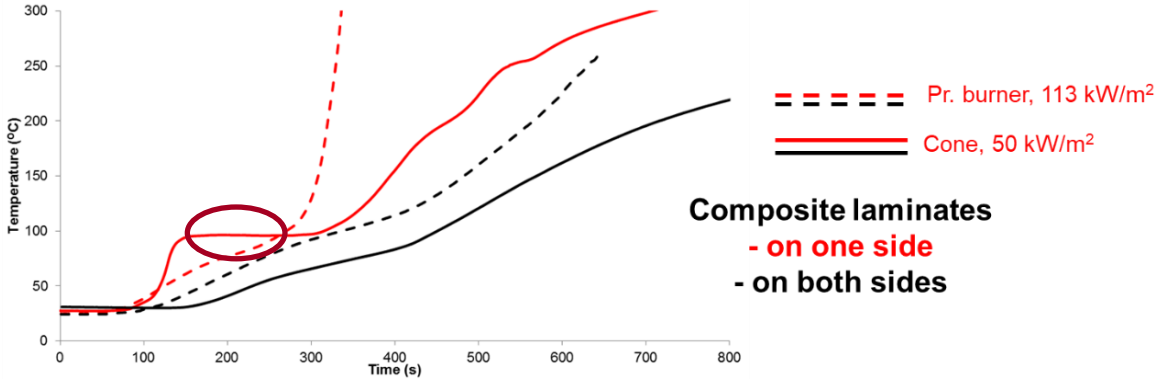

Figure 4.10: Back surface temperature versus time curves from cone calorimetry and propane burner testing for effects of composite laminates on one/both sides for sandwich structure composites with similar components but different compositions

It can be seen from the results compiled in Table 4.7 that RI-Top UP-1 sample takes a much shorter time to reach certain temperatures selected at all times than RI-UP-1 in both cone calorimetric and propane burner testing methods, revealing that RI-UP-1 sample shows a better thermal barrier effect.

Table 4.7: Times taken to reach different back surface temperatures (100 - 300 °C) and maximum temperature – T_{max} during the cone calorimetry and propane burner testing for sandwich composites with composite laminates on one/both sides

Sample ID	Time to reach									
	100 °C (s)		200 °C (s)		250 °C (s)		300 °C (s)		T_{max} (s, °C)	
	C	P	C	P	C	P	C	P	C	P
RI-Top UP-1	316	270	465	320	536	329	707	336	707, 300	336, 300
RI-UP-1	450	337	715	565	-	630	-	-	800, 219	646, 261

Note: C - Cone calorimetry, P - Propane burner, '-' in the table indicated maximum temperature during the testing did not reach the certain temperature.

4.3.4 Effect of different sample preparation techniques

UP/Glass – Balsa composite samples with the same thicknesses of 25.4 mm (1") core prepared by three different techniques i.e. resin infused laminates (both sides) [RI-UP] versus hand lay-up laminates [HL-UP] versus hand lay-up sandwich structure: in one go [HLAll-UP], are compared in Figures 4.11, 4.12 and Table 4.8.

From the HRR curve (Figure 4.11 (a)) it can be seen that TTI in all three samples prepared by different techniques are quite similar. Both RI and HL techniques give almost the same PHRR (443 *vs.* 477 kW/m^2) whereas HLALL gives slightly lower PHRR (343 kW/m^2), due to lower resin content 31% in the composite laminate versus ~40% in other samples (see Table 4.5). It could also be possible that with this technique some of the resin could be infused into the balsa core, leaving even less resin on the surface. Both THR and TSR values are similar among all samples prepared with different techniques. From the mass loss curve shown in Figure 4.11 (b), it can be seen that for both RI and HL mass loss trends are similar and their mass loss rates are slightly higher than for HLALL, because the former contains higher resin contents and hence burn faster and more intensely than HLALL. The amount of residue remaining after the cone test was similar in all three samples, 52 - 54% (Table 4.5), which is mainly the glass fabric and charred balsa wood.

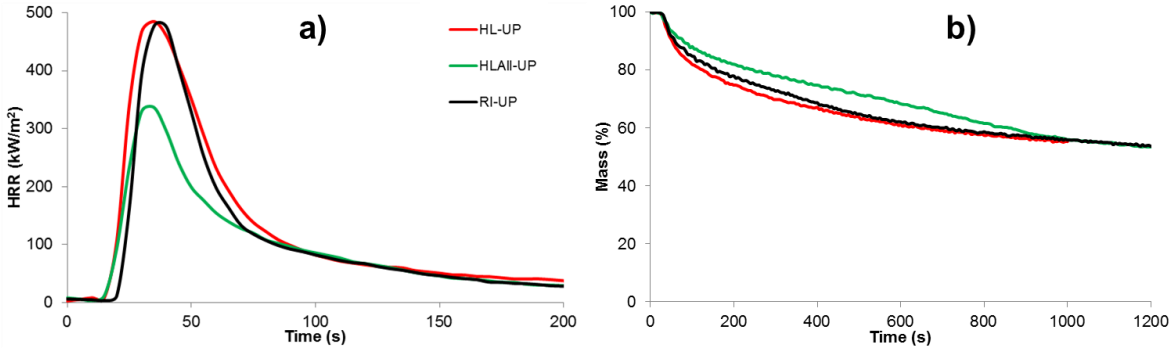

Figure 4.11: Cone calorimetric results at 50 kW/m^2 for (a) HRR and (b) mass loss versus time curves in horizontal orientation for sandwich structure composites with similar components but with different compositions prepared by different techniques

As can be observed from Figure 4.12 (a) and (b), there is no significant difference in the back-surface temperature profiles in both propane burner testing and cone calorimetric testing in the vertical orientation, also confirmed by compiled results in Table 4.8, indicating their similar thermal barrier properties of sandwich composites using two different testing methods exposed to different heat fluxes and fire conditions, no matter which sample preparation technique was used among them.

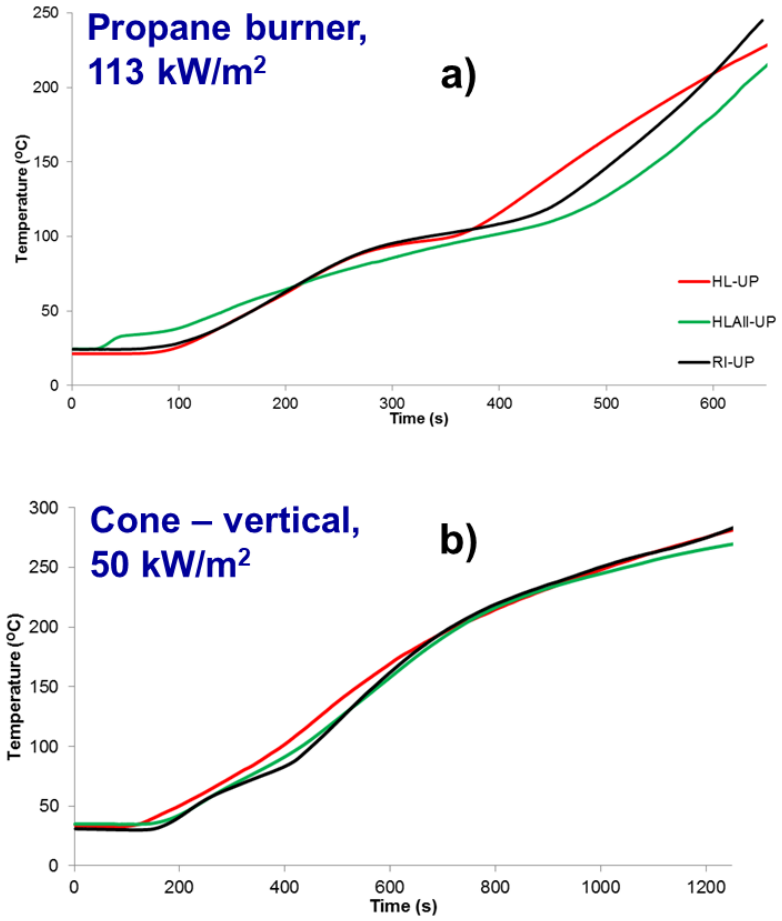

Figure 4.12: Back surface temperature versus time curves from (a) propane burner testing and (b) cone calorimetry for effects of different sample preparation techniques for sandwich structure composites with similar components but different compositions

Table 4.8: Times taken to reach different back surface temperatures (100 - 300 °C) and maximum temperature – T_{max} during the cone calorimetry and propane burner testing for sandwich composites prepared by different techniques

Sample ID	Time to reach									
	100 °C (s)		200 °C (s)		250 °C (s)		300 °C (s)		T_{max} (s, °C)	
	C	P	C	P	C	P	C	P	C	P
RI-UP	450	334	715	587	997	-	-	-	1200, 275	650, 247
HL-UP	395	357	721	578	1013	-	-	-	1200, 275	650, 228
HLAII-UP	432	387	730	627	1046	-	-	-	1200, 266	650, 215

Note: C - Cone calorimetry, P - Propane burner, '-' in the table indicated maximum temperature during the testing did not reach the certain temperature.

4.4 Conclusions

Due to the varied density of the balsa wood (150 ± 45 kg/m^3), burning behaviours of balsa core varied among different specimens and also within two different thicknesses. Two peaks of HRR were observed for those samples, presenting a typical behaviour of wood burning. Physically thick samples (25.4 mm (1") thick balsa wood) performed lower heat transfer through the sample in the cone calorimeter to slow down burning than that of relatively thinner samples (12.7 mm

(0.5”) thick one). On comparing the burning behaviour of the resin as a neat resin, in a composite laminate and in a sandwich structure, TTI and PHRR were similar in the composite laminate and the sandwich structure, which is as expected. THR and TSR values of the sandwich structure, however, are much higher than those of the composite laminate. The effect of cone orientation on the fire performance of sandwich composites showed not much difference in PHRR values between two orientations, TTI was slightly higher in the horizontal than the vertical mode, THR was similar in both orientations, though the results were still within the acceptable experimental error range of the cone data due to gaps in the wood blocks. On comparing the samples with skins on both sides or just the top side, the former shows lower heat transfer. There is no significant difference for sandwich composites prepared by different techniques in fire performance and thermal behaviours. Based on that, hand lay-up sandwich structure: in one go technique (HLAll) will be used for sample preparation of the next chapter because of shortest time consumption and easiest handling.

4.5 References

[1] “BS 476-15:1993, ISO 5660-1:1993: Fire tests on building materials and structures. Method for measuring the rate of heat release of products.” British Standards Institution, 1993.

[2] *ISO 2685:1998(E) Aircraft — Environmental test procedure for airborne equipment — Resistance to fire in designated fire zones*. International Organization for Standardization, 1998.

[3] T. Goodrich, N. Nawaz, S. Feih, B. Y. Lattimer, and A. P. Mouritz, “High-temperature mechanical properties and thermal recovery of balsa wood,” *Journal of Wood Science*, vol. 56, no. 6, pp. 437–443, 2010.

[4] T. Sebio-Puñal, S. Naya, J. López-Beceiro, J. Tarrío-Saavedra, and R. Artiaga, “Thermogravimetric analysis of wood, holocellulose, and lignin from five wood species,” in *Journal of Thermal Analysis and Calorimetry*, 2012, vol. 109, no. 3, pp. 1163–1167.

[5] L. Tranvan, V. Legrand, and F. Jacquemin, “Thermal decomposition kinetics of balsa wood: Kinetics and degradation mechanisms comparison between dry and moisturized materials,” *Polymer Degradation and Stability*, vol. 110, pp. 208–215, 2014.

[6] R. H. White and K. Sumathipala, “Cone Calorimeter Tests of Wood Composites,” *Proceedings of the Fire and Materials 2013 Conference*, pp. 401–412, 2013.

[7] B. Moghtaderi and D. F. Fletcher, “Flaming Combustion Characteristics of Wood-Based Materials,” *International Association for Fire Safety Science*, pp. 209–219, 1988.

[8] J. Kim, J.-H. Lee, and S. Kim, “Estimating the fire behavior of wood flooring using a cone calorimeter,” *Journal of Thermal Analysis and Calorimetry*, vol. 110, no. 2, pp. 677–683, Nov. 2012.

[9] M. A. Dietenberger, O. Grexa, and R. H. White, “Reaction-to-fire of wood products and other building materials: Part II, Cone calorimeter tests and fire growth models,” Research Paper FPL-RP-670, Madison, WI: U.S. Department of Agriculture, Forest Service, Forest Products Laboratory, pp. 1–58, 2012.

[10] L. Tsantaridis, “Reaction to fire performance of wood and other building products - Cone Calorimeter results and analysis,” PhD thesis, KTH Royal Institute of Technology, Stockholm, 2003.

[11] T. J. Shields, G. W. Silcock, and J. J. Murray, “Evaluating ignition data using the flux time product,” *Fire and Materials*, vol. 18, no. 4, pp. 243–254, 1994.

[12] L. Lowden and T. Hull, “Flammability behaviour of wood and a review of the methods for its reduction,” *Fire Science Reviews*, vol. 2, no. 1, p. 4, 2013.

[13] A. Alkhazaleh, “Thermal energy storage and fire safety of building materials,” PhD thesis, the University of Bolton, UK, 2018.
[14] B. K. Kandola, A. Alkhazaleh, and G. J. Milnes, “The fire behaviour of gypsum boards incorporating phase change materials for energy storage in building applications,” in *15th International Conference and Exhibition on Fire and Materials 2017*, 2017, pp. 517–527.
[15] B. K. Kandola, P. Luangtriratana, S. Duquesne, and S. Bourbigot, “The effects of thermophysical properties and environmental conditions on fire performance of intumescent coatings on glass fibre-reinforced epoxy composites,” *Materials*, vol. 8, no. 8, pp. 5216–5237, 2015.
[16] P. Luangtriratana, B. K. Kandola, S. Duquesne, and S. Bourbigot, “Quantification of Thermal Barrier Efficiency of Intumescent Coatings on Glass Fibre-Reinforced Epoxy Composites,” *Coatings*, vol. 8, no. 10, p. 347, 2018.
[17] S. Nazaré, B. Kandola, and A. R. Horrocks, “Use of cone calorimetry to quantify the burning hazard of apparel fabrics,” *Fire and Materials*, vol. 26, no. 4–5, pp. 191–199, 2002.
[18] T. Ohlemiller and J. Shields, “One- and two-sided burning of thermally thin materials,” *Fire and Materials*, vol. 17, no. 3, pp. 103–110, 1993.

Chapter 5: Designing sandwich composite structures with different resin types and combinations

In this chapter, effects of different resin types and their blends in the skins of sandwich composite structures on the latters' fire performances have been investigated. Resins were selected based on their properties, namely their commercial use in marine applications, morphology, thermal stability and fire performances as discussed in Chapter 3. Selected resins include two unsaturated polyesters (UP); two vinyl esters (VE) - an epoxy based (VE-Ep) and novolac based (VE-Nov); one epoxy (Ep); one thermoplastic resin, Elium; two resole phenolics - Durez and Methylon. Three sets of sandwich composites were prepared with skins made of four layers of glass fabrics impregnated with following resin variations:

Set 1. Different resin types: two UP types (UP and UP-R, chemically similar but different styrene contents and hence, viscosities), VE-Ep, VE-Nov, Ep, Elium. Samples with both phenolics could not be prepared due to high viscosities of the resins.

Set 2. Blends of UP and VE with two phenolic resole resins, Durez and Methylon. A tertiary blend of UP/VE/PH-Res of 35/35/30 wt% ratio was also prepared.

Set 3. UP or UP/VE based composites with top layer of Methylon.

Balsa wood with a thickness of 25.4 mm (1 inch) was used as a core material in all samples, this thickness was used because physically thick samples show a better thermal barrier effect than the 12.7 mm (0.5 inch) one as already demonstrated in Chapter 4, Section 4.3.2. Different sample preparation techniques for sandwich structure samples studied in Section 4.3.4 did not show an apparent difference in cone and propane burner test results, hence the hand lay-up sandwich structure in one go technique (HLAll), owing to its shortest time consumption and easiest handling, was used. The details of optimized curing conditions used for this chapter's sandwich composite structures are given in Appendix 2, Table A2-1.

The fire performances were evaluated with cone calorimetry at 50 kW/m^2 and propane burner testing at 113 kW/m^2 heat fluxes similar to those in Chapter 4. It has been demonstrated in Chapter 4 that not much difference is observed in cone heater orientation (horizontal or vertical), hence here the cone heater in a horizontal orientation was used. During both cone and propane burner tests, thermocouples were inserted at various locations throughout the samples from which apparent thermal conductivity and resistivity values for each component (front and back face composite laminate skins and balsa wood) as well as the sandwich composites have been calculated and discussed in detail in the following section. This study gives insight into thermal barrier properties of the chars from different resin types.

5.1 Fire performance of sandwich composites with skins of different resin types

5.1.1 Cone calorimetry

Cone calorimetric tests were undertaken for 2 specimens of each sample until the samples were completely burnt out and for 1 specimen, the test was performed until 10 minutes only. Plots of heat release rate (HRR) and mass loss *vs*. time for 30 minutes are shown in Figure 5.1.

As can be seen from Figure 5.1 (a), all samples ignited, with an intense peak heat release and after the flame went out the heat release was reduced, getting to minimum and a plateau after about 300 s. This is also seen as a sharp mass loss up to ~300 s in Figure 5.1 (b). Balsa wood then burnt with very small flame, re-igniting other parts where cracks in the wood were obvious, this resulted in a second very broad peak of low intensity (red circle in Figure 5.1(a)). In some samples and their specimens there was no increase in a second PHRR. In all of the samples though there was gradual mass loss due to burning/charring of the balsa wood.

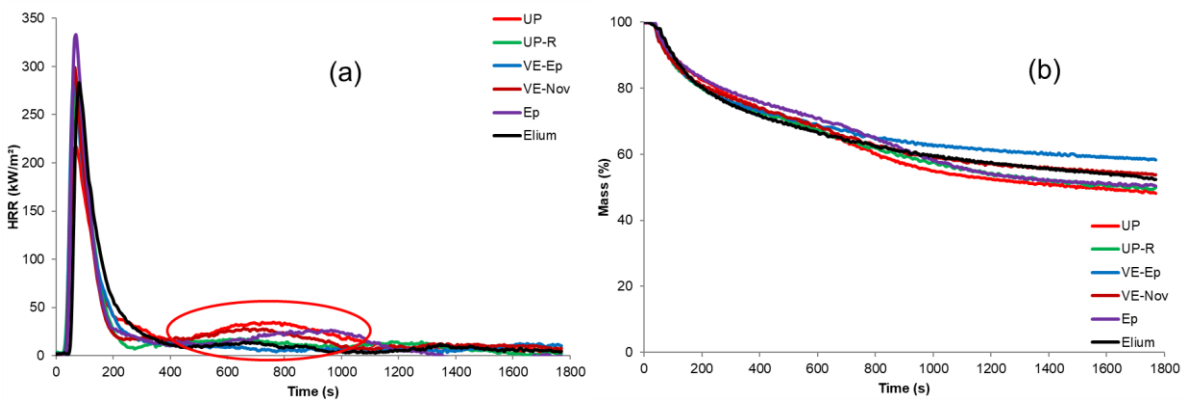

Figure 5.1: Plots of (a) heat release rate (HRR) and (b) mass loss *vs*. time for 30 minutes

For more clarity, plots of heat release rate, mass loss and smoke release for times of interest (up to 200 s for HRR and smoke release and 600 s for mass loss) are replotted in Figure 5.2 (a, b and c). All derived results are given in the Table 5.1, in which THR and TSR are reported until HRR gets to minimum/plateau after first peak and after 30 minutes duration, whereas residue, after 10 (major mass loss due to burning of resin and burning/smouldering of balsa wood) and 30 minutes (end of test) are given.

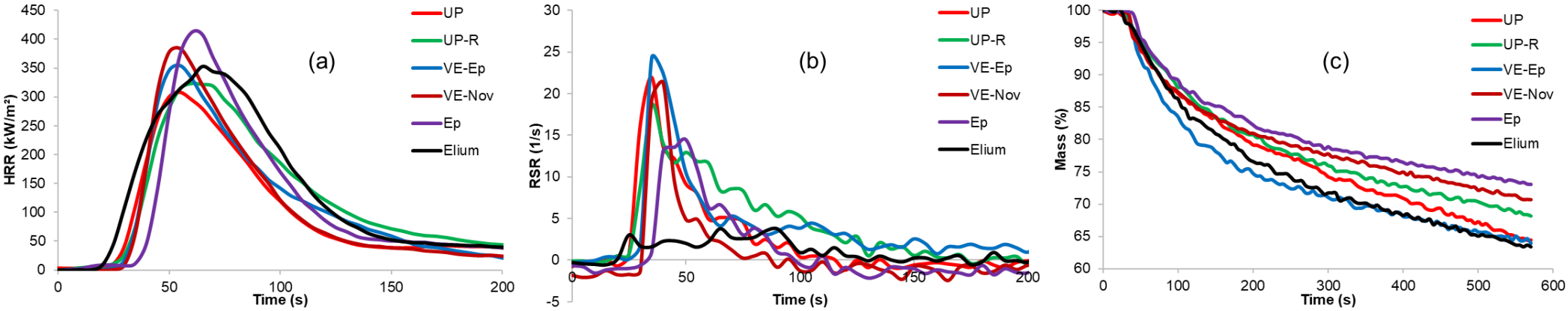

Figure 5.2: Plots of (a) HRR, (b) RSR and (c) mass loss *vs*. time for sandwich composites with skins of different resin types

Table 5.1: Derived cone calorimetric results of sandwich composites with skins containing different resin types – UPs, VEs, Ep and Elium

Sample ID	TTI (s)	FO (s)	PHRR (kW/m^2)	THR (MJ/m^2)		TSR (m^2/m^2)		Residue [b] (wt%)	
				5 mins [a]	30 mins	5 mins [a]	30 mins	10 mins	30 mins
UP	24	1296	294	23.5	46.5	554	1121	67 (34)	48 (17)
UP-R	26	1338	282	28.6	38.9	879	1153	68 (39)	49 (15)
VE-Ep	29	854	326	24.2	36.1	1009	1717	71 (33)	60 (22)
VE-Nov	29	1092	322	23.3	41.8	345	711	71 (38)	54 (21)
Ep	38	1187	375	26.1	41.9	431	1173	73 (43)	54 (22)
Elium	18	1233	341	30.5	47.1	245	2594	63 (27)	53 (19)

Notes:

TTI = time-to-ignition, FO = time-to-flame-out, PHRR = peak heat release rate, THR = total heat release, TSR = total smoke release. The reproducibility in cone parameters was ±5%.

The variation in values for different parameters are as: TTI = ±3; FO = ±289; PHRR = ±55; THR = ±4.5; TSR = ±593; Residue = ±4.

a: End of first peak was defined for the initial 300 s of cone tests to be more comparable for all samples while the first peak decreased to a minimum and constant state from the specimen tested up to 10 minutes.

b: For residue (wt%), values in the parentheses are after compensating for glass content (8 layers of glass fabric, 4 on each side of top and bottom skins).

Unsaturated polyester resins:

As can be seen from Figure 5.2 (a) and Table 5.1, both UP resins ignited around 24 - 26 s. Both have similar PHRR (282 - 294 kW/m^2), UP-R showed a higher THR for the end of first peak but a lower THR up to 30 minutes, and also a slightly higher TSR until the end of first peak but similar TSR up to 30 minutes (1153 *vs*. 1121 m^2/m^2), indicating that the flammability of both composites from UP and UP-R resins is similar. The cone results of cast resin plaques discussed in Chapter 3 (Section 3.4.2.1) showed lower PHRR, THR and TSR for UP than for UP-R. This trend for THR and TSR until the end of the first peak can be observed for the composites as well, which could be explained because during the initial period of the cone test, THR and TSR values were mainly due to burning of the resin of the top laminate, whereas later on balsa wood also started to burn and smoulder, releasing heat and smoke. The burning was erratic due to the gaps within the wooden blocks, hence THR and TSR do not show expected trends. Both samples leave similar residues of 15 - 17% at the end of the test. Digital images of the residue after the cone test are shown in Table 5.2. Resin on the top surface of the composite was completely burnt out for both samples, as shown in an exemplar image in Figure 5.3. The top laminate delaminated and balsa core thicknesses reduced for all samples. It can be noticed that gaps were shown to be present from the top view in all samples (Table 5.2, image (b)) that is because balsa wood sample received was made of small blocks, stuck together on a very thin glass fabric layer during manufacturing stage, balsa wood sheet was used as received. Gaps were tried to be avoided by pushing the balsa blocks tightly together during the sandwich structure composite preparation processes. In Table 5.2, image (a) represents the side view of char residue, where it can be seen that in this specimen of UP-R the balsa wood was damaged/collapsed resulting in gap between the top skin and the core. This effect though was random depending on the inconsistency of the balsa wood blocks in different samples and specimens. Image (b) represents the top view of the core after removing the glass fabric of the top burnt composite laminate layer; charred balsa wood can be seen. In image (c) the back surface of the burnt composite structure is shown where some charred resin and unburnt resin can be seen. It can be seen that UP-R resin gives slightly more charred residue than the UP.

Figure 5.3: Digital images of sandwich composites with skins of UP resins: the top view of a burnt sandwich composite

Table 5.2: Digital images of sandwich composites with skins of different resin types, selected one side to represent the char residue after cone calorimeter testing, top view after taking off top burnt composite laminate layers, and back surface laminates of burnt sandwich composite structures

Sample ID	Side view (a)	Top view after taking top laminates (b)	Back surface (c)
UP	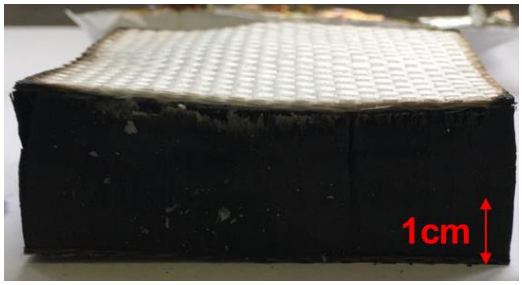		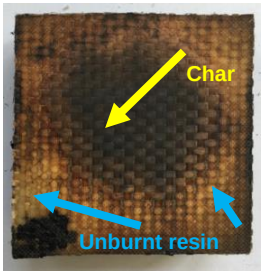
UP-R	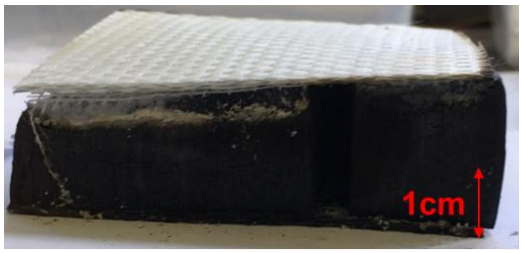	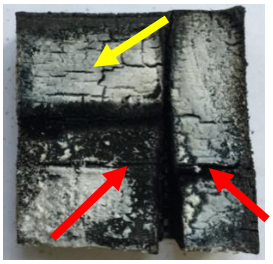	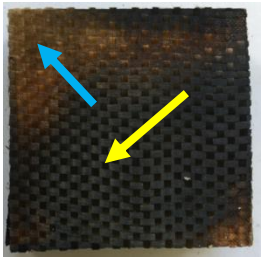
VE-Ep		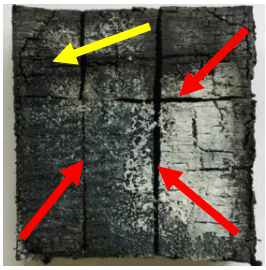	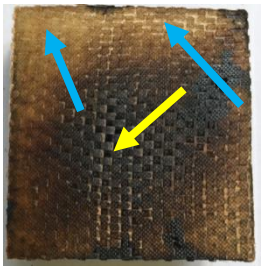
VE-Nov	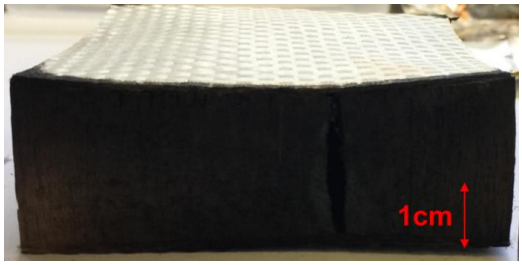	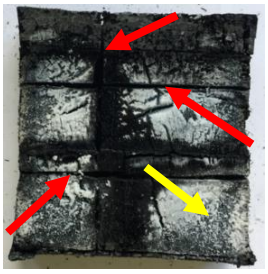	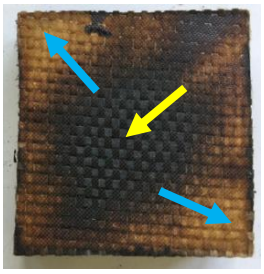
Ep		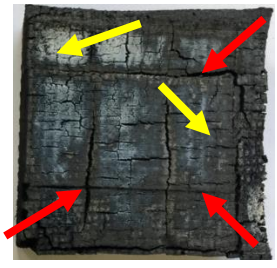	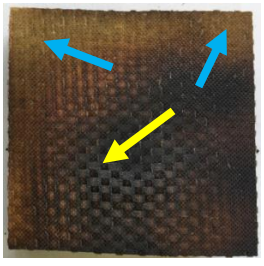
Elium	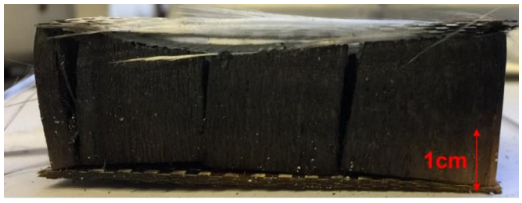	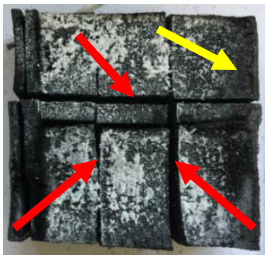	

Vinyl ester resins:

Both VE resins ignited at 29 s, similar to UP resins (24 - 26 s), which is consistent with TTI values as demonstrated by cast resins results, 42 - 46 s for the VE resins and 37 - 40 s for the UP resins (Table 3.4). As could be observed from cone results for cast resins (Section 3.4.2.1), VE-Ep showed higher PHRR, THR, TSR than that of VE-Nov, indicating its higher flammability. VE-Nov also showed higher charring tendency. And this is reflected here in cone tests of the composite structures. While PHRR values are similar (322 *vs.* 326 kW/m^2), VE-Nov showed slightly lower THR (23.3 MJ/m^2), TSR (345 m^2/m^2) until the end of first peak and higher char residue (38%) for 10 minutes compared to those of VE-Ep (24.2 MJ/m^2, 1009 m^2/m^2 and 33%, respectively). These results for composite structures are similar to cone results from cast resins because these values are more dependent on the resin content of the top surface and resin types as explained in UP section earlier. Composite skins of both VE-Ep and VE-Nov resins seem to be slightly more flammable than those of UP and UP-R resins, having higher PHRR values, producing slightly less THR but more smoke up to 30 minutes, especially for VE-Ep (Table 5.1), which could be due to different styrene contents in the two different resin types as explained earlier. Both VE samples leave similar residues (21 - 22%) at the end of the test, which are higher than those for UP resins. It can be seen from the images in Table 5.2, that for specimens of both VE-Ep and VE-Nov, the balsa wood was slightly damaged leading to some gaps between the top skin and the core (Table 5.2 (a)) but not as noticeable as in the UP-R one. It can be seen that the amount of charred resin and unburnt resin is similar for both VE resins as observed from the back surface of the burnt composite structure.

Epoxy resin:

Ep has slightly higher TTI (38 s) than UPs and VEs, which is as expected from TTI values from the cone results for cast resins (58 s *vs.* 37 - 46 s). Also, from the cast resin results, Ep indicated highest PHRR, THR and moderate TSR (Table 3.4). It is reflected here that the Ep composite shows the highest PHRR (375 kW/m^2), relatively high THR until end of first peak and up to 30 minutes, and leaves 43 and 22% of residue after 10 and 30 minutes, respectively, highest among all neat resins as skins. From the digital images of residue (Table 5.2), for Ep resins, the burnt and charred balsa wood is different from those observed for the other samples. In Ep sample, charred balsa wood blocks are more intact, without gaps within them and a thin charred layer on their surface (Table 5.2 (b)), which is apparently different from the other charred woods. This may be due to higher flammability of Ep resin, because the Ep resin on the top laminate burnt quickly and intensively and changed the burning behaviour of the underlying wood, causing less damage to the wood. The amount of charred resin and unburnt resin is high after 10 minutes (43%, Table 5.1) but similar to those of both VE resins after 30 minutes, which can also be observed in images of the back surface of the burnt composite structure in Table 5.2.

Phenolic resins:

As mentioned before, composite structures with Durez and Methylon, could not be prepared due to the high viscosity of phenolics. Based on the flammability results of cast resins given in Table 3.4, Section 3.4.2.1, with low PHRR, THR and high char residue, it is expected that the composites from these two resins should have lowest flammability among all samples with neat resins as skins.

Elium resin:

Composites of Elium resin have a lowest TTI (18 s), which is as expected because TTI from cone results of cast resin showed similarly the lowest TTI value among all cast resins (20 s, see Table 3.4). And also, a relatively high mass loss rate among all neat resins as can be seen in Figure 5.2 (c) and Table 5.1. Compared to both UPs and VEs, Elium shows slightly higher PHRR, THR, and TSR values and leaves 27% of residue after 10 minutes indicating low charring tendency of this thermoplastic resin. It can be seen from the digital images of residue and char, that for this composite of Elium, the balsa wood was badly damaged/collapsed leaving large gaps between the top skin and the core (Table 5.2 (a)) and also large gaps between separate balsa wood blocks can be observed in (b). All the resin burnt and left no char on the back surface of the burnt composite structure.

5.1.2 Heat transfer (thermal gradients) during cone tests

To study thermal gradients through the thickness of the sandwich composite structures during cone calorimetric experiments, in one specimen of each sample thermocouples were inserted at different locations as shown in Figure 5.4. The positions of thermocouples were on the surface of the top skin (TC_1), underneath the top skin (TC_2), within the centre of the core material (balsa wood) (TC_3), underneath the core material (TC_4) and underneath the bottom skin (TC_5).

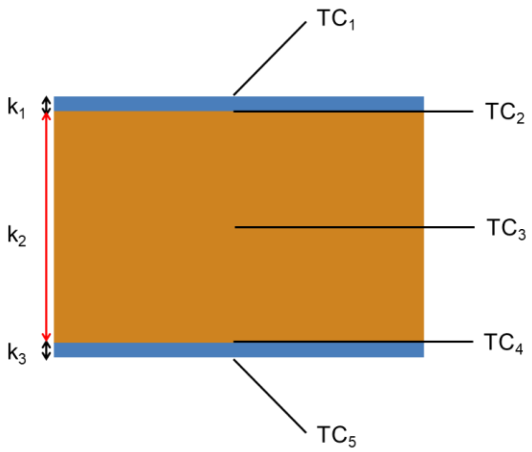

Figure 5.4: Thermocouple setup in sandwich structures for temperature measurements during cone calorimetric experiments and their corresponding thermal conductivities

Temperature *vs.* time profiles obtained from these thermocouples were monitored during the whole process of cone tests. Results for UP sample as an example are shown in Figure 5.5.

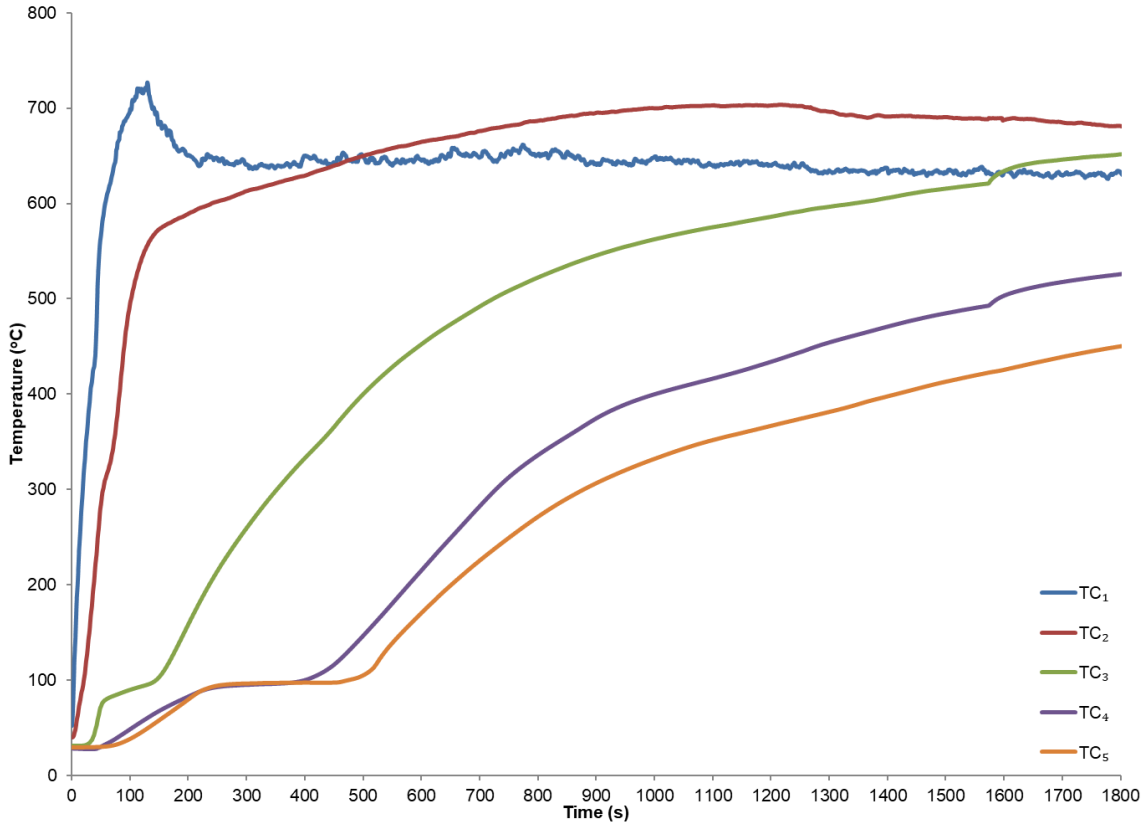

Figure 5.5: Temperature *vs.* time profiles at different locations through the thickness of the composite sandwich structure based on UP

As discussed in Chapter 4, the structural integrity of a composite material in fire is a complex problem and depends on many variables. The overall temperature profiles at different locations through the sandwich composites can be described as follows: In the initial stage of fire, the radiant heat from the cone heater is partially absorbed and then conducted through the composite. The rate of heat conduction is determined by the incident heat flux (source of heat, 50 kW/m^2 in cone tests) and the thermal conductivity of the composite. As the composite heats-up, the heat transfer from the surface through the thickness of the laminate will depend on the thermal conductivities of the resin and the reinforcing fibre. The temperature eventually reaches the decomposition temperature of the resin of the matrix, releasing volatiles on the top surface, and causing the ignition of the sample. The decomposition temperature of a resin depends on its chemical composition. Most organic resins used in structural composites (e.g. polyesters, vinyl esters, epoxies) decompose over the temperature range of 250 - 500 °C as discussed in detail in previous sections. The decomposing resin then ignites and the composite starts burning. Hence TC_1 increases rapidly, getting to maximum due to the ignition of tested sample and then decreases and stabilizes to a relatively steady state. TC_2, increases and then becomes equal to TC_1, before becoming higher than TC_1 due to the thermal feedback from the underlying balsa

wood. The rate of burning depends on the resin type, the external heat flux and the oxygen content in the fire. The heat transfer from the composite laminate (top (heat exposed) skin of the sandwich structure) to the balsa wood will then depend on the temperature dependent thermal conductivity values of the resin's char and the fibre. With heat, balsa wood will also decompose, ignite, burn and char. The heat transfer through this part will also depend on the temperature-dependent thermal conductivity of the char, which determines the increase in TC_3. TC_3, increases sharply and then reaches around 100 °C within a short period of time and attains a steady state. This steady-state stage could be due to evaporation of the water moisture in the balsa core. With the increase in heat transfer from the top layer, the temperature starts increasing sharply again due to the combination of ignition, burning and smouldering of the balsa wood. TC_4 and TC_5, both increase and then stabilize at 100 °C until 400 - 500 s for a longer period compared to TC_3, then showing similar temperature increasing trends as in TC_3 but at a lower temperature. It can also be noted that the thermal gradients through the thickness of the sandwich composite structure (TC_1 - TC_5) are as expected. While the bottom skin layer of the sandwich structure should have the same thermal properties as the top layer, due to the thermal gradient in the structure, the bottom layer will have lower heat exposure than the top surface. Hence, from the behaviour of the bottom skin, better insight into the thermal properties of a particular resin can be gained, which will be discussed in more detail later in Section 5.1.3. Heat-induced cracking within the skins (e.g. delamination and matrix cracking) will change the heat transfer behaviour, making it more complex. It was noticed in Section 4.1.3, (Chapter 4) that the temperature increased due to cracking within the balsa core, accelerating the egress rate of flammable gas.

Top and bottom skins' back surface temperature, TC_2 and TC_5, versus time curves for all samples are plotted in Figure 5.6 (a) and (b), respectively. To investigate the heat transfer through sandwich composites in more depth, different temperatures were chosen for top and bottom skins according to the following rationales. For the top skin: (i) 300 and 400 °C, these two temperatures were selected because the different resins decompose roughly around the temperature range of 300 - 400 °C, the exact temperature depending on the resin type (which can be estimated from the temperature of onset of thermal degradation, i.e.$T_{10\%}$ values from TGA results, Table 3.2) (ii) 400 - 500 °C, to capture different stages when resin ignites and burns and (iii) maximum temperature reached at the back surface of the top skin. Whereas for the bottom skin, the following temperatures were chosen: (i) 100 °C, at which the loss of all moisture occurs, (ii) 300 - 400 °C, resin decomposition similar to as the top skin. 300 °C is important, as for the propane burner test this temperature was also chosen to represent burn-through properties (iii) 400 - 500 °C, representing resin ignition and burning. The time to reach 100 (only for bottom skins), 300, 400, 500 °C and maximum temperature (T_{max}) for both skins' back surfaces during the test are reported in Table 5.3.

Figure 5.6 (a) shows that the temperature of the top skin's back surface of the composite (TC_2) exposed to the heat flux of 50 kW/m^2 increased rapidly with time over the initial 100 - 400 s

heating period. Beyond this period the surface temperature reached a relatively steady state and a maximum temperature. The maximum temperature was in the range 650 - 720 °C for different resins, Elium reached highest maximum temperature of 721 °C in 30 minutes. This is corroborated by the cone results (Table 5.1), in which the Elium based composite has the highest THR, relatively low charred residue, and large cracking and gaps between charred wood which probably accelerate the burning of the wood (Table 5.2). In addition, from the top skin's back surface temperature curves shown in Figure 5.6 (a), not too much difference can be seen at 30 minutes when the cone tests were stopped because the temperature at that time is relatively constant, due to resin having been burnt off in the top skin, temperature monitored on the back surface is actually the temperature of the glass fabric.

For the bottom skin's back surface temperature, temperature increased at the beginning up to 100 °C, and then there was a steady/constant state for almost all samples for 200 to 500 s, which represents stabilization after loss of all the moisture in tested samples. VE-Ep took the shortest time to reach 100 °C, whereas UP took the longest. The temperature rose rapidly after this steady state, when the heat conducted from the charring balsa wood reached the back surface of the bottom skin (and composite). By comparing the time to reach certain temperatures taken from the top and bottom skins' back surfaces, the thermal gradients can be observed as expected, this could be due to high thermal insulating barrier effects of combined skins and charred balsa core. Also, the maximum back surface temperature of the bottom skin did not reach even 470 °C (Table 5.3), whereas for the top skin they were all above 650 °C. VE-Ep and Ep showed slightly better thermal barrier (low heat transfer) effects than the rest of the resins (T_{max} for bottom skin being less than 400 °C), which is corroborated by lower THR values up to 30 minutes in the cone results shown in Table 5.1.

T_{max} on the back surface of the bottom skin (and the composite) was used to rank the thermal performances of different sandwich composites as this can give a good indication of the thermal barrier effect of any char formed, the trend in terms of thermal barrier effect from high to low being:

VE-Ep > Ep > VE-Nov > UP-R > UP > Elium.

On comparing with cone results in Table 5.1, there is not a direct relationship between back surface temperature and PHRR values, which is as expected as the PHRR is dependent on the resin type and content on the top surface, whereas, the back surface temperature relies on the thermal conductivity of the combination of the glass fibre, charred resin and also charred balsa wood. But there is a good correlation/agreement with THR from cone results up to 30 minutes (Table 5.1), i.e., the higher THR values in cone calorimetric results, the higher the maximum (T_{max}) back surface temperature of the bottom skin.

The differences in maximum temperatures of back surfaces of top (T) and bottom (B) skins of all samples, ΔT values, are also given in Table 5.3. The temperature of the top skin was typically around 250 - 290 °C hotter than the bottom skin, the difference being due to the thermal

insulating properties of glass fibre, and residual char of the resin (if any) and the balsa. Sandwich composites with skins of VE-Nov resin displayed the largest temperature difference (293 °C) between top and bottom skin surface, revealing better thermal barrier effect of its char compared to the chars from other resins.

5.1.3 Thermal barrier performance evaluation from cone experiments

From the temperature versus time curves in Figures 5.5 and 5.6, time - dependent thermal conductivities (k) and thermal resistivities (r) of samples were calculated.

Theory: Measurement of thermal barrier properties in cone calorimetric experiments

During the conduction of heat in solids, if the thermal environment of a solid has been constant for a sufficient time (i.e. the boundary conditions have not changed in value), it achieves a steady temperature distribution [1]. According to Rockett and Mike [1] in a solid plate of thickness h, if the two surface temperatures, T_0 and T_b are known, the heat flux per unit area (Q'') through the plate will be

$$Q'' = (T_0 - T_b)\, k / h \qquad \text{(Equation 5.1)}$$

Equation 5.1, can be written as:

$$k = \frac{Q''\, h}{T_0 - T_b} \qquad \text{(Equation 5.2)}$$

where k is the apparent thermal conductivity.

This equation was used to calculate apparent thermal conductivity values of different components of the sandwich structure. The heat flux per unit area is 50 kW/m^2 for cone calorimetry. The thermal boundary condition applied to the hot skin is assumed to be constant. The back skin and all sides of sandwich structures were covered by aluminium foil and the surface of the back skin laid on ceramic wool, hence all sides except the top surface are assumed to be insulated. Assuming that all heat supplied by the cone heater is passing through the sandwich composite, thermal conductivities of different components within a sandwich composite can be calculated. Since all the experiments were conducted under similar conditions, and in order to obtain significantly comparable data, the difference in temperatures of the first and second, second and fourth, fourth and fifth thermocouples were used to define the individual thermal conducting behaviour of the top laminate (k_1), balsa core (k_2) and bottom laminate (k_3), respectively. Thicknesses (h) of each component in the sandwich structure are assumed to be identical in each sample, where h is 1.1 mm, 25.4 mm and 1.1 mm for corresponding top laminate, core and bottom laminate.

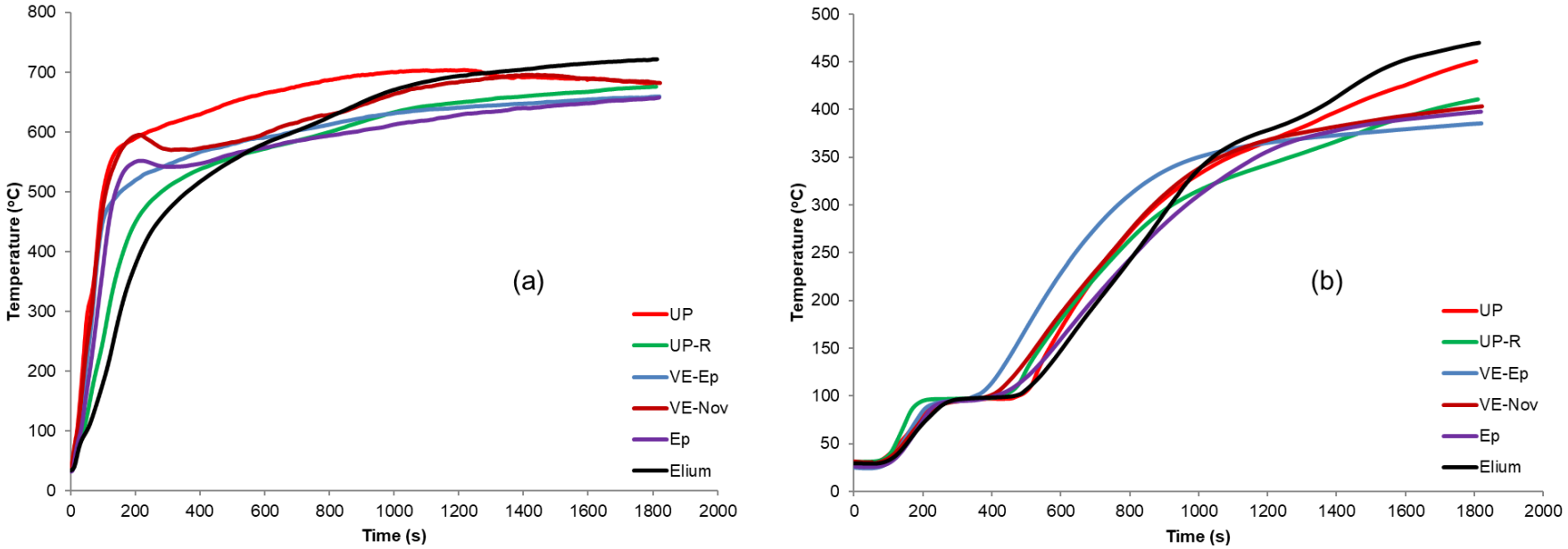

Figure 5.6: Plots of (a) top skin, TC_2 and (b) bottom skin's (TC_5) back surface temperature *vs*. time for sandwich composites with skins of different resin types

Table 5.3: Time to reach different temperatures and maximum temperature (T_{max}) of top and bottom skins' back surfaces during the cone calorimetric testing among sandwich composites with skins of different resin types

Sample ID	Time to reach back surface temperature (s) of									Maximum Temperature T_{max} (°C)		ΔT (T-B) (°C)
	Top skin				Bottom skin							
	$t_{300\ °C}$	$t_{400\ °C}$	$t_{500\ °C}$	t_{Tmax}	$t_{100\ °C}$	$t_{300\ °C}$	$t_{400\ °C}$	$t_{500\ °C}$	t_{Tmax}	T	B	
UP	53	81	101	1218	476	878	1415	-	1800	704	450	254
UP-R	118	163	281	1800	427	923	1678	-	1800	676	410	266
VE-Ep	69	86	155	1800	351	765	-	-	1800	659	385	274
VE-Nov	65	83	110	1409	392	869	1739	-	1800	696	403	293
Ep	84	107	139	1800	408	964	-	-	1800	656	397	259
Elium	154	218	361	1800	465	917	1341	-	1800	721	469	252

Notes: T - Top skin's back surface, B - bottom skin (and composite)'s back surface, '-' in the table indicated maximum temperature during the testing did not reach the certain temperature.

ΔT (T-B) - Maximum back surface temperature difference between top and bottom skins

Thermal resistivity:

Thermal resistivity, *r*, is a measure of resistance to heat flow through a given thickness of material and is the reciprocal of the thermal conductivity, *k*.

$$r = \frac{l}{k} \qquad \text{(Equation 5.3)}$$

where *l* is the thickness of the material in metres and *k* is the thermal conductivity in W/mK, hence the *r*-value is measured in metres squared Kelvin per Watt (m^2K/W)

From apparent thermal conductivity values calculated for each component of sandwich structures as discussed above, apparent thermal resistivity values were also calculated.

5.1.3.1 Thermal barrier performance of individual components

Temperature *vs.* time profiles obtained from these thermocouples were monitored as mentioned in Section 5.1.2 during the whole process of cone tests, the temperature profiles of centre of balsa core material (TC_3) was also monitored, but was not used for the calculations. The results for the UP-based composite as an example are replotted and shown in Figure 5.7.

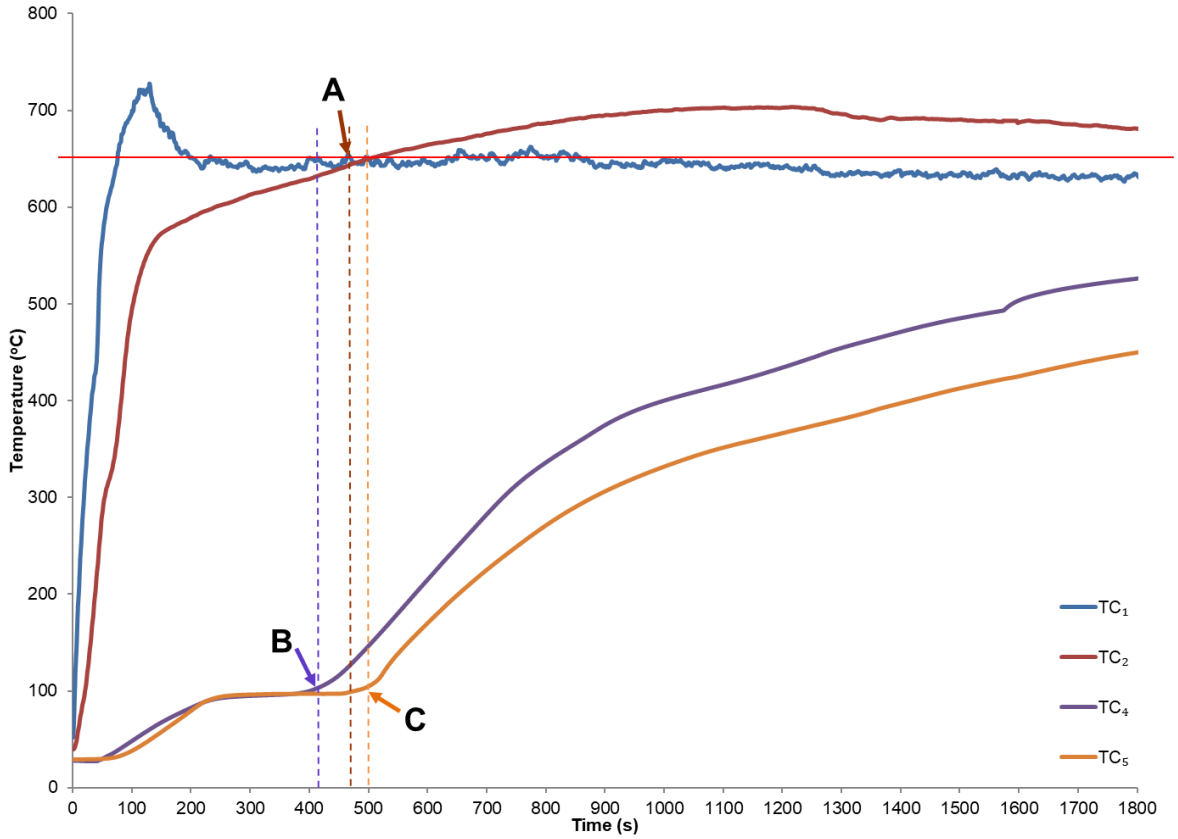

Figure 5.7: Temperature *vs.* time profiles at different locations through the thickness of the composite sandwich structures and indication of criteria set for each thermocouple reading for the calculation and plotting of apparent thermal conductivity *vs.* time curves

Criteria used for the time range selection and temperature of each component within a sandwich composite were set as follows:

- For the top skin, the surface temperature (T_0 in Equation 5.1) was taken as the value when the temperature becomes maximum and is constant for a period of time, shown as horizontal red line in Figure 5.7. The surface temperature was assumed to be constant throughout the test, as an example the value for UP sample (Figure 5.7) is 650 °C. TC_2 was taken as the back face temperature of the top skin of the composites (T_b in Equation 5.1) for calculation of k values for the top skin. For the top skin thermal conductivity was measured up to point A, when $TC_1 = TC_2$, i.e., the temperature of the top upper surface is equal to the temperature of the back surface (just underneath the top skin). As an example, point A was 474 s for this sample. Up to point A, the heat has already conducted through the top skin, after this TC_2 becomes higher than TC_1, which can be explained as due to the thermal feedback from a combination of burning, charring, smouldering etc. of the underlying balsa wood. TC_1 on the other hand remains relatively stable because the resin in the matrix on the top surface has burnt out and the thermocouple is measuring the temperature of the glass fabric. The time taken to get to point A was also noted for each sample and is reported in Table 5.4.

- For the core, the surface temperature (T_0 in Equation 5.1) was taken as TC_2, which is variable as opposed to the one taken for top skin. The back surface temperature (T_b in Equation 5.1) was taken as TC_4. As seen from Figure 5.7 and already discussed, TC_4 temperature increased in the beginning up to 100 °C, followed by a steady state, representing stabilization during evaporation of all the moisture. The temperature rose rapidly after this steady state, when the heat conducted through the charring balsa wood reached the back surface of the core (point B), which for this sample is at 420 s. The starting time for measurement of thermal conductivity of the balsa (core component) was taken as point B.

- For the bottom skin, the surface temperature (T_0 in Equation 5.1) was taken as TC_4 and the back surface temperature (T_b in Equation 5.1) was taken as TC_5. The starting point for thermal conductivity measurement was taken when TC_5 temperature started increasing after the steady state at 100 °C (point C), which is 515 s for UP-based sample.

Based on these criteria, temperature dependent apparent thermal conductivity versus time curves of each component in a sandwich structure were obtained and are shown in Figure 5.8. Apparent thermal conductivity values of top skin at 60 s and both balsa core and bottom skin at 600 and 1000 s were selected to be presented in Table 5.4. For the top skin 60 s was selected because at this time the back surface temperature of top skin (TC_2 in Figure 5.4) has risen enough indicating heat transfer, but is well below the point when the temperature is equal to the top surface temperature ($TC_1 = TC_2$), where the heat has completely transferred through the top skin. In the case of the balsa core and bottom skin, 600 s and 1000 s were selected to represent

the heating, smouldering and/or burning, and charring stages of balsa wood and resin in the bottom skin. As can be seen from Table 5.3, the back surface temperature reaches 300 °C at about 1000 s, in all samples. This temperature is discussed here because it is very important in the propane burner test, representing the burn through point. Since all tested samples are of almost same original thicknesses (26.9 - 27.6 mm, Table 2.5) and all other experimental conditions are the same, the thermal resistivity values (*r*) can be directly compared. Thermal resistivity values for each component for all samples calculated at 60 s for top skin and 600 s for both balsa core and bottom skin are given in Figure 5.9.

As can be seen from Figure 5.8 and Table 5.4, the apparent thermal conductivity curves and values of the top skin for all samples are similar, the only exception is UP where time taken to get to point A ($TC_1 = TC_2$) is shorter, resulting in the difference between *k* value at a particular time. This most probably is due to the erratic initial burning of the sample, resulting in more than expected increase in TC_2, due to non-availability of the sample and time limitations, this test could not be repeated. Apart from TC_2 readings, all other temperature readings are as expected. Apparent thermal conductivity values of the top skins calculated at 60 s for both UP and UP-R as given in Table 5.4 are similar. This is not unexpected as the top skins are very thin (1.1 mm), they also behave as thermally thin layers, i.e., for the thermally thin body, the temperature gradient within the body is minimal [2,3]. For top skin at 60 s, both VE resins have slightly higher values than Ep and Elium samples. For more clarity their thermal resistivity (reciprocal to thermal conductivity) values are plotted in Figure 5.9, where expected differences between all samples can be seen. Also, values of thermal conductivities calculated here for the top skin (Table 5.4) are similar. In order to see whether these are within reasonable expected ranges, the thermal conductivities of composite skins (K_{Comp}) at room temperature have been calculated from the rule of mixtures using literature values for polyesters, vinyl esters, epoxy and phenolics of 0.2, 0.2, 0.1, 0.35 kW/m.K × 10^{-3}, respectively [4-12] and of glass fibre 1.04 kW/m.K × 10^{-3} [13] as: K_{UP} = 0.602, K_{VE} = 0.606, K_{Ep} = 0.574, K_{PH} = 0.733 kW/m.K × 10^{-3}, respectively (see Appendix 3, Table A3-1). These values are very different from those seen in Figure 5.8 even at the start of the experiment, which is expected considering that the apparent thermal conductivities are from measured temperatures and ignore all other factors. It has also been reported in the literature [14] that the experimental and theoretical values (calculated using the rule of mixtures) for thermal conductivity values do not match.

The behaviour of balsa wood is expected to be same in all the samples. Results shown in Figure 5.8 and Table 5.4 show that these are similar, except for some slight variations, which can be explained due to the fact that all samples were prepared by hand lay-up in one go and during curing under vacuum some resin would have diffused into the balsa wood, resulting in differences in burning behaviours. Moreover, balsa wood was in blocks, stuck together, and the variation in the location of gaps due to joints will change the burning behaviours as well as heat transfer. Thermal resistivities of these samples shown in Figure 5.9 (b) also display an expected trend, i.e., inverse of that shown for *k* values.

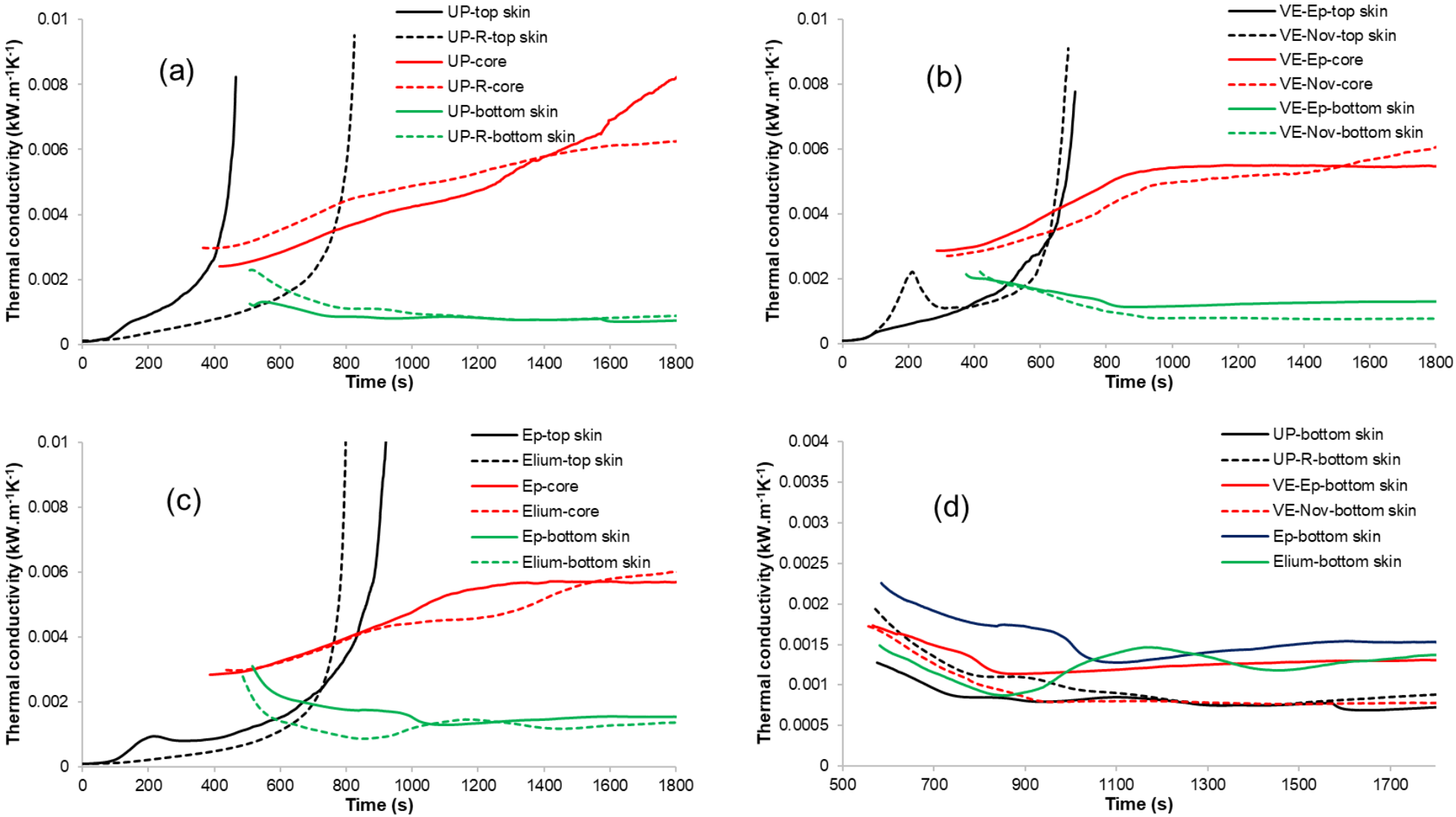

Figure 5.8: Calculated apparent thermal conductivity curves for each component in a sandwich composite of (a) UPs (b) VEs (c) Ep and Elium resins as skins and (d) bottom skins for all neat resin samples

Table 5.4: Time to reach $TC_1=TC_2$ and temperature, the calculated apparent thermal conductivity values for neat resins as skins in a sandwich structure under cone calorimetry at 50 kW/m^2 heat flux

Sample	Top surface temperature [a] (°C)	Time to reach $TC_1=TC_2$ [b] (s)	Temp. when $TC_1=TC_2$ [b] (°C)	Apparent thermal conductivity, *k* of components (kW/m.K × 10^{-3})					Apparent thermal conductivity, *k* of composite (kW/m.K × 10^{-3})	
				Top skin (60 s)	Balsa core		Bottom skin		600 s	1000 s
					600 s	1000 s	600 s	1000 s		
UP	650	474	645	0.2	2.8	4.2	1.2	0.8	2.8	4.2
UP-R	610	862	611	0.1	3.5	4.9	1.8	1.0	3.1	4.5
VE-Ep	610	702	602	0.2	3.9	5.4	1.7	1.2	3.5	5.1
VE-Nov	620	813	630	0.2	3.4	5.0	1.6	0.8	3.1	4.7
Ep	610	1014	614	0.1	3.3	4.8	2.2	1.5	2.9	4.4
Elium	630	851	637	0.1	3.2	4.4	1.4	1.2	2.8	4.5

a = Cone calorimetry - Taken as when surface temperature, TC_1 becomes constant

b = Top upper surface = just underneath the upper surface

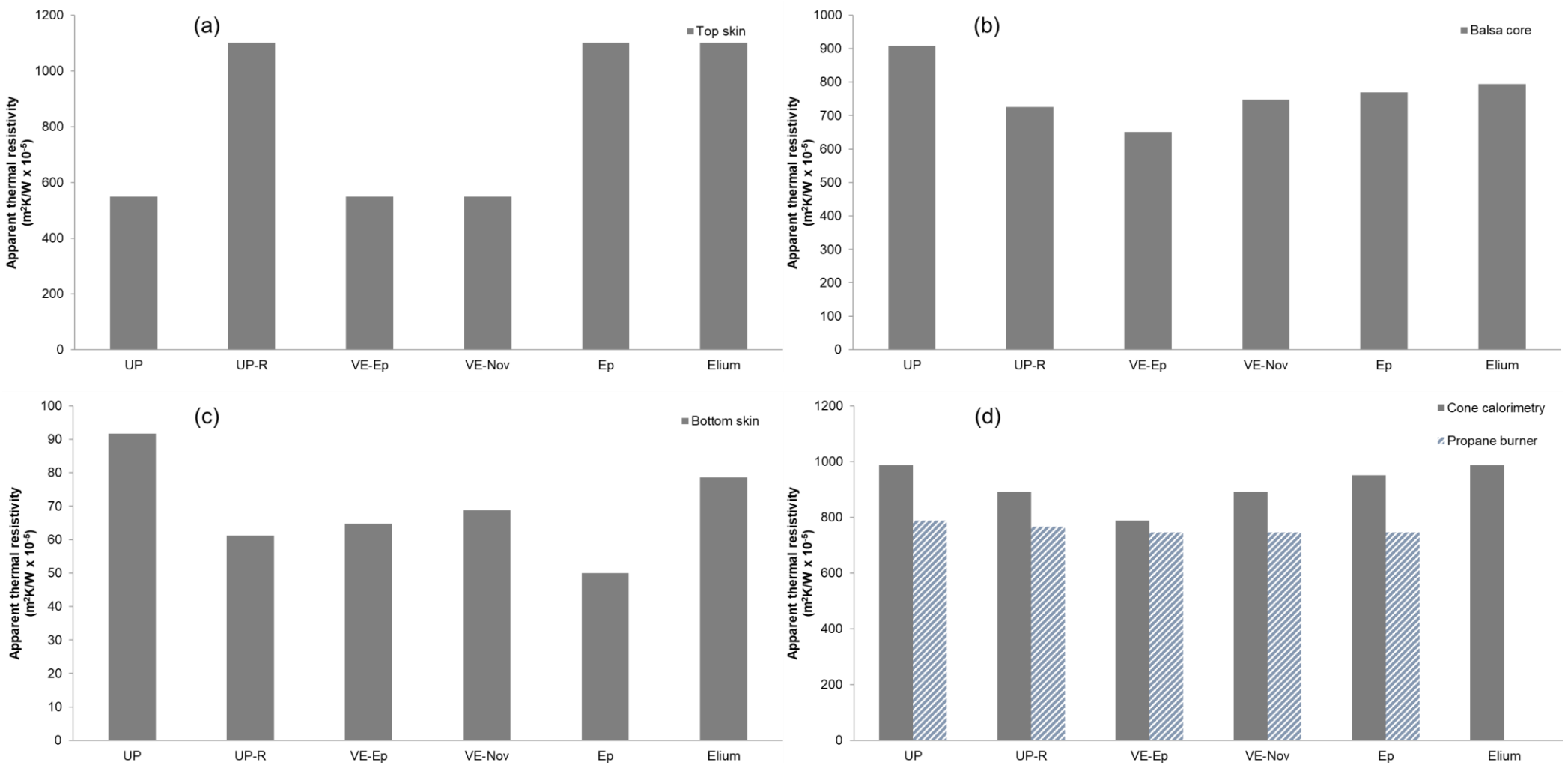

Figure 5.9: Apparent thermal resistivities of (a) top skins, (b) balsa core layer, (c) bottom skins and (d) sandwich composite structures with all resin types [combined results from cone calorimetry and propane burner tests]

The bottom skin of the composite shows a higher thermal gradient as seen from Figure 5.7 than the top skin because the top surface of the bottom skin is exposed to much lower heat than the corresponding surface of the top skin. This also results in char formation in the bottom skin (see Table 5.2 (c)). Hence there is more variation in apparent thermal conductivity values for different samples, from which the effects of different resin types can be evaluated. As seen from Table 5.4, UP has much lower thermal conductivity than UP-R and VE resins at 600 s. Among UP and VE resins, UP and VE-Nov show lower thermal conductivity at 1000 s. From the digital images of their chars on the back surface (Table 5.2), not much difference can be seen, except for UP-R, which apparently formed more char than the other three, showing a slightly higher thermal conductivity value (Table 5.4) than UP, indicating that it has a more thermally conducting char compared to UP. Epoxy resin though shows a higher value but also shows more char/similar amount of char compared with both VE resins in Table 5.2 (c), indicating char's conductive nature. In the Elium sample where all resin has burnt, it has lowest thermal conductivity value, which may be because all resin has burnt away, leaving only glass layers. Thermal resistivity results shown in Figure 5.9 (c) show the above effect in a clearer manner, from which it can be seen that UP and Elium containing show relatively better thermal insulating properties than the other samples, most probably due to the reason that when all the resin has burnt, the glass layers have separated and the gap between them helps in insulation.

5.1.3.2 Thermal barrier performance of composite structures

Since there are too many variables which affect the thermal conductivity of each layer of the composites, the global value for each composite sample was also calculated by taking the surface temperature (T_0 in Equation 5.1) from TC_1 and back face temperature (T_b in Equation 5.1) from TC_5 (see Figure 5.4) and calculating k using Equation 5.2. Apparent thermal conductivity *vs.* time curves for all samples are plotted in Figure 5.10 and values at 600 and 1000 s are presented in Table 5.4. Thermal resistivity values calculated at 600 s for sandwich composite structures for all samples are given in Figure 5.9 (d).

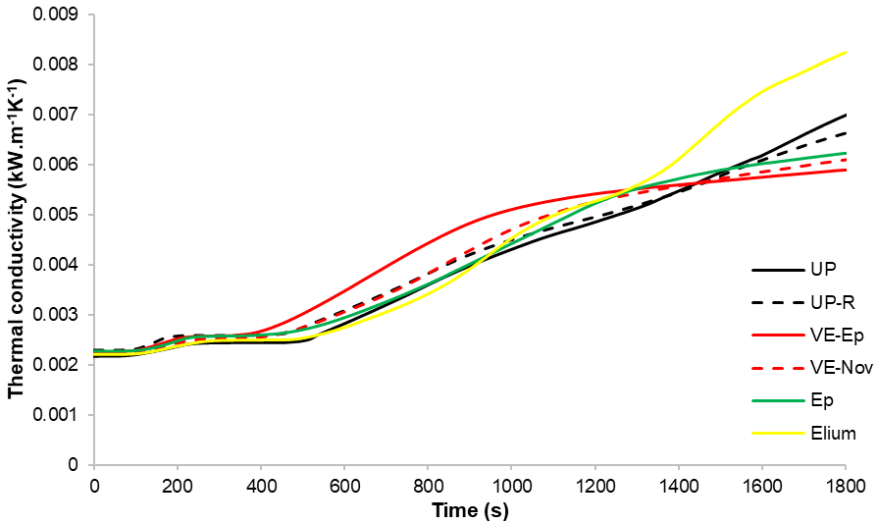

Figure 5.10: Calculated apparent thermal conductivity curves of different neat resins as skins in sandwich composites

It can be seen from the results (Figure 5.10 and Table 5.4), that VE-Ep based composite showed the highest thermal conductivities at both 600 and 1000 s (Table 5.4). UP, Ep and Elium composites showed relatively lower values overall for composites, whereas for each component in sandwich composites, not too much difference for both top and bottom skins can be seen (Table 5.4); the differences derived from the balsa core parts of the different samples. While balsa char is expected to have the same thermal conductivity in all samples, it could be that resin infusion in the balsa wood was more in certain samples than other, resulting in different burning behaviour and the char structure, the latter affecting the thermal conductivity values.

In addition, thermal resistivities of all sandwich composite structures are shown in Figure 5.9 (d), and, as expected, show an inverse trend to the *k* values.

5.1.4 Propane burner testing

The radiant heat (external heat flux of 113 kW/m^2) emitted by the flame in the propane burner test is partially absorbed and then conducted through the composite. The rate of heat conduction is determined by the incident heat flux and the thermal conductivity of the composite. Top surface temperatures for all samples are given in Table 5.5.

Table 5.5: Top surface temperatures for composites with skins containing neat resins under propane burner tests at 113 kW/m^2 heat flux

Sample	Top surface temperature * (°C)
UP	1000
UP-R	975
VE-Ep	980
VE-Nov	950
Ep	945
Elium	-

Notes:

* = In propane burner tests, while TC_{front} becomes constant.

- = Test not performed

In propane burner tests, thermocouples were inserted only on the front and back surfaces of the sandwich structures as shown schematically in Figure 5.11. TC_{front} was placed and maintained 10 mm away from the hot surface because of the high heat flux of the propane flame (~1000 °C), otherwise it would have been affected by the burning through of the front face of the laminate. The temperature changes at the back surface of the samples were continuously monitored by two thermocouples ($TC_{back1,2}$) placed and glued using epoxy adhesive resins (Araldite® 2014) on the rear centre face of the samples and fully insulated by Kaowool. Thicknesses (*h*) of all sandwich composites were in the range 26.9 to 27.6 mm.

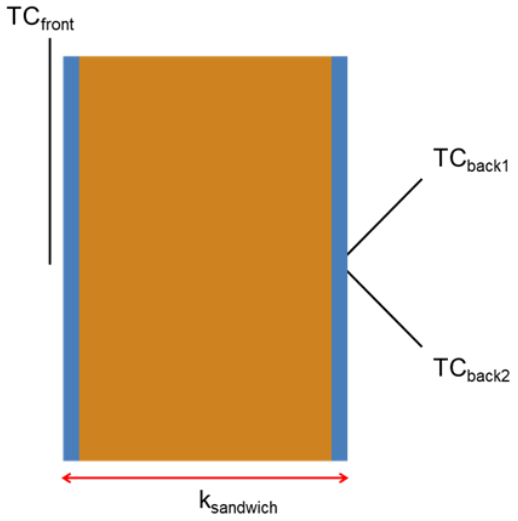

Figure 5.11: Thermocouple setup for temperature measurements in vertical orientation in propane burner tests of sandwich structures and their corresponding thermal conductivities

Temperature *vs.* time profiles obtained from these thermocouples as demonstrated in Figure 5.11 were monitored during the whole process of propane burner testing. Results for UP-R sample as an example are shown in Figure 5.12.

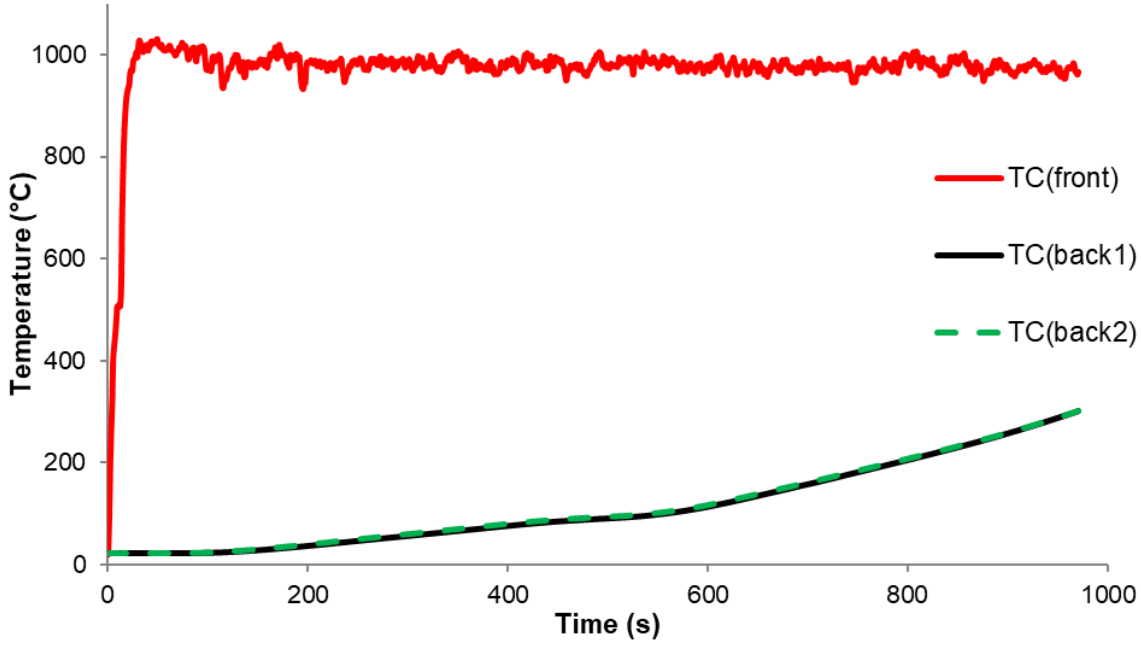

Figure 5.12: Temperature *vs.* time profiles at front and back surface of a composite sandwich structure based on UP-R under propane burner tests

As an exemplar for UP-R resin as skins, where all of three thermocouples were inserted and monitored, temperature profiles during propane burner tests are shown in Figure 5.12 from which it can be seen that the reproducibility of the back-surface temperatures is good. Due to the limited sample size prepared, only one specimen was tested for each sample. The temperature rise on the front face was due to the heat transfer from the actual propane gas flame with a high external heat flux of 113 kW/m^2 impinging directly on the front surface of the

sample, hence ignition took place causing the front temperature to rise rapidly to 975 °C for the UP-R containing sample then becoming relatively constant while the resin content on the front surface was burnt off. The temperature rise on the back is due to the heat conduction and transfer from the front through the thickness of the sandwich composite from a combination of burning of resin on the front surface and the decomposition / ignition / burning / smouldering / charring of the balsa wood core. When burning has taken place throughout the composite, the back surface reaches 300 °C. At this point, the test was stopped.

The back surface temperature versus time curves for all sandwich composite samples subjected to propane burner test are presented in Figure 5.13 and time-to-reach 300 °C values are given in Table 5.6. As can be seen from Figure 5.13, the temperature rise in all samples is similar up to about 450 s, after which some differences can be seen. UP and UP-R based composites do not show much difference until 800 s, after which the rate of temperature rise in UP is slightly slower than for UP-R but still within experimental error range considering the variations of only few seconds difference (Table 5.6) under a high heat flux of 113 kW/m^2 (1000 *vs.* 971 s to reach 300 °C).

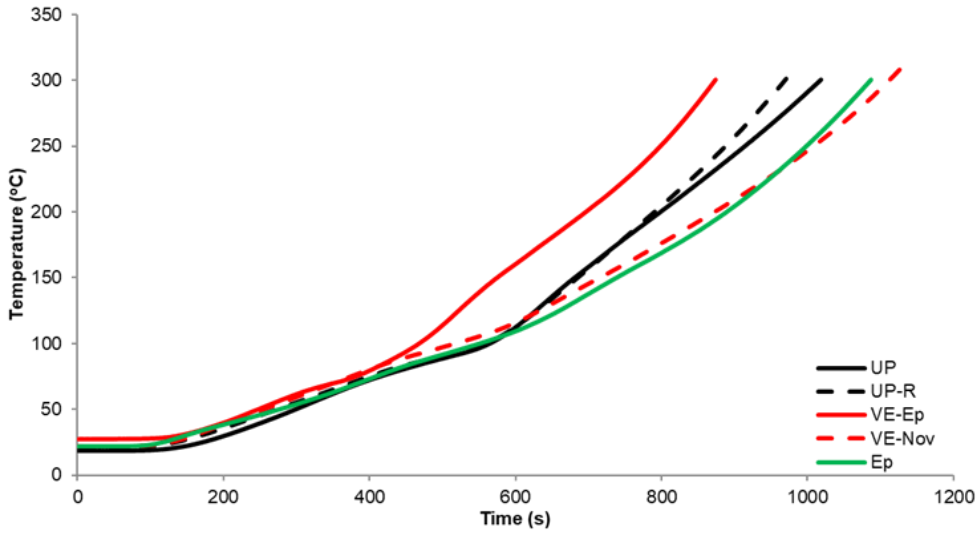

Figure 5.13: Back surface temperature versus time curves for sandwich structures with neat resins as skins obtained from propane burner testing

Table 5.6: Residues after propane burner testing and times to reach 300 °C for sandwich structures with balsa core thicknesses of 25.4 mm (1 inch) for UPs, VEs and Ep as skins

Sample	Residue (wt%)	Glass content (wt%)	Char (wt%)	Time to reach 300 °C (s)
UP	46	11	35	1000±28
UP-R	42	12	30	971±1
VE-Ep	49	15	34	865±13
VE-Nov	50	14	36	1128±21
Ep	47	10	37	1061±37
Elium	*	*	*	*

* = Test not performed

Among VE based composites, VE-Ep and VE-Nov do not show much difference until 450 s, after that temperature rise in VE-Nov is much slower than in VE-Ep. The time taken to reach 300 °C is 1128 s in VE-Nov and 865 s in VE-Ep, indicating lower flammability and charring behaviour of the former. These results are consistent with flammability results from PCFC and cone calorimetric test on cast resins (see Chapter 3) where lower PHRR and THR values and more char residue formation was observed for VE-Nov than for VE-Ep. On comparing both vinyl esters with both UP resins, it can be seen that VE-Ep shows worse performance, while VE-Nov shows better performance in terms of time to reach 300 °C (lower rate of temperature rise).

Comparing Ep composites with those of the two UPs and the two VEs, it can be seen that Ep shows very similar back surface temperature versus time curve as VE-Nov.

Comparing charring tendency within propane burner tests, both UPs and VEs form similar char residues than Ep except for UP-R which is slightly lower than the rest as shown in Table 5.6 (30, 34 - 36% *vs.* 37%). Char residues in cone results for sandwich composites (Table 5.1) at the end of test (30 minutes) show similar trends although some erratic variations can be seen but still within experimental range, which could be explained due to the fact that burning behaviours of balsa core in the samples were not very similar depending on the gaps in wood blocks, probably slightly affecting final char residue content.

From propane burner testing, the thermal barrier performances of sandwich structure composites with different neat resins as skins are ranked based on the time for the back surface temperature to reach 300 °C (s), the longer the better, as follows:

VE-Nov > Ep > UP ≈ UP-R > VE-Ep.

In general, this trend is similar to those for the back surface temperature to reach 300 °C shown in the cone experiments (see Table 5.3) though some slight variations can be observed, owing to the different external heat fluxes in the two test rigs.

5.1.5 Thermal barrier performance evaluation from propane burner test

From the above temperature versus time curves, apparent thermal conductivities (k) were calculated using Equation 5.2, by taking surface temperature TC_{front} (T_0 in Equation 5.1) as given in Table 5.5 and back surface temperature TC_{back} (T_b in Equation 5.1) from Figure 5.13. The curves are shown in Figure 5.14. As can be seen, trends of the curves are similar to those in Figure 5.8 (d) from the cone calorimetric tests, though differences among different samples are smaller in the former than the latter. In the propane burner test, the external heat flux is much higher (113 kW/m^2) compared to the cone test (50 kW/m^2), causing heat transfer and burning more intense in the former, hence temperature rises rapidly and less differences in conductivity can be observed.

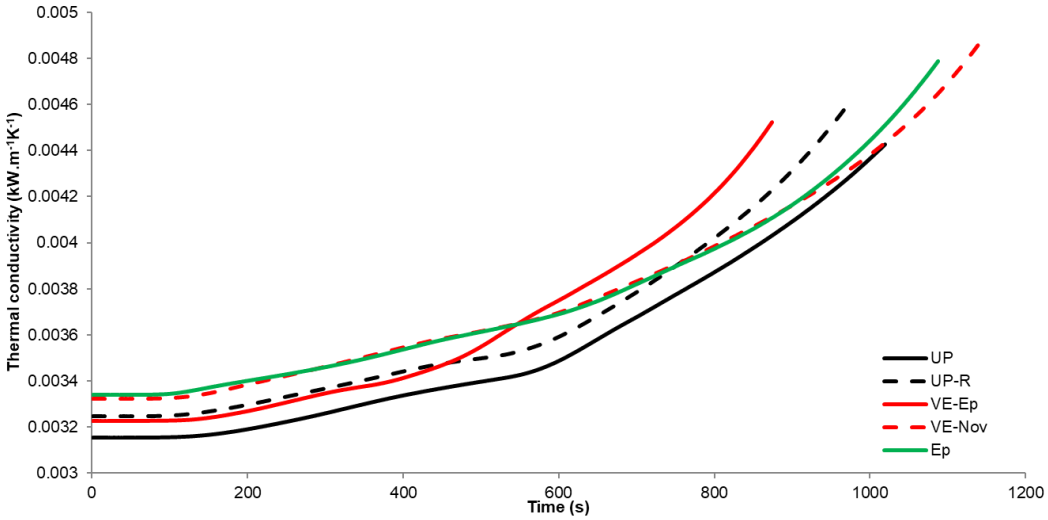

Figure 5.14: Apparent thermal conductivity versus time curves for sandwich structures with neat resins as skins obtained from propane burner testing

Table 5.7: Calculated thermal conductivities for sandwich composites with skins of different resin types at particular times from the propane burner tests

Sample	Apparent thermal conductivity, *k* of composite (kW/m.K × 10^{-3})		
	600 s	700 s	800 s
UP	3.5	3.7	3.9
UP-R	3.6	3.8	4.0
VE-Ep	3.7	3.9	4.2
VE-Nov	3.7	3.8	4.0
Ep	3.7	3.8	4.0
Elium	*	*	*

* = Test not performed

Based on the apparent thermal conductivities given in Table 5.7, values at 600 s were selected to be the representative of the composites, from which their thermal resistivities were calculated and plotted correspondingly, due to this being the same time as used in cone results for sandwich composite and hence allows better comparison, as shown in Figure 5.9 (d). Compared with those results from cone experiments (see Figure 5.9 (d)), very similar trends of apparent thermal resistivities of the sandwich composite structures with all resin types under both cone calorimetry and propane burner tests were observed, indicating that their thermal barrier performance did not change too much in spite of running via different test methods.

5.2 Fire performance of sandwich composite structures with different resin blends

In this section, fire and thermal barrier performances of sandwich composite structures from different resin blends including UP/PH-Res, VEs/PH-Res, UP/VE-Nov and UP/VE-Nov/PH-Res blends have been discussed.

5.2.1 UP or VE / phenolic resin blends

As reported in Section 2.3.3.2, Chapter 2, UP-R is incompatible with phenolic resins, hence, UP resin was used in these sandwich composites. Also, VE is not compatible with Durez, hence these blends were not prepared.

5.2.1.1 Cone calorimetry

It can be observed from Figure 5.15 and Table 5.8 that for sandwich composites with skins of UP and UP/phenolic blends, TTI is little affected by phenolic resin presence (24 s *vs.* 22 - 25 s), which is expected from the cone results of cast resins (Section 3.4.2.2). FO time for all UP/phenolic blends however, was shorter than UP. Most other cone parameters, such as PHRR, THR and TSR for the blends are reduced compared to UP resin, but not reduced as much as seen previously for cast resins (Table 3.4, Chapter 3), which could be explained due to the lower resin content in the sandwich composites. UP/Durez blends seem to perform slightly better than UP/Methylon blends, showing lower PHRR, THR and TSR values despite poor compatibility. UP/Durez:50/50 shows lower PHRR than 70/30 (159 *vs.* 185 kW/m^2) but higher THR (36.2 *vs.* 27.3 MJ/m^2) and TSR (3674 *vs.* 2623 m^2/m^2) at the end of tests. The higher THR and TSR are due to slow burning and prolonged smouldering of the underlying balsa wood. In the case of UP/Methylon 50/50, it shows a higher PHRR than 70/30 (211 *vs.* 189 kW/m^2), but considering the variation in results, this difference is negligible. Other parameters such as THR and TSR show similar trends as of UP/Durez. These trends are similar to those seen in cast resins (Section 3.4.2.2). Char residues after 30 minutes for UP/phenolic blends were similar (20 - 24%) and slightly higher than that of UP skins (17%), except UP/Durez:70/30 which showed less value (13%).

Results for sandwich composites with skins of VEs and VEs/phenolic (Methylon) blends in Figure 5.16 and Table 5.8 show that, TTI is little affected by phenolic presence (29 s *vs.* 28 - 31 s), as expected from cone results for cast resins in Section 3.4.2.2. FO times for all VEs/phenolic blends were similar as for the VEs considering the standard deviation, and varied burning behaviours of the balsa core in different samples. PHRR and THR were reduced in general for all VEs/phenolic blends. VE-Nov/Methylon blends seem to perform slightly better than VE-Ep/Methylon blends by showing more reduction in PHRR, THR and less TSR, in particular, for the 50/50% blend. The VE-Ep/Methylon:50/50 shows slightly higher PHRR than the 70/30 ratio (276 *vs.* 254 kW/m^2) as well as slightly higher THR (30.1 *vs.* 29.2 MJ/m^2) and more TSR (4733 *vs.* 955 m^2/m^2), quite similar trend can be seen in cone results for cast resins (Table 3.4) except for PHRR. The small difference in PHRR values in a sandwich composite could be due to different resin contents on the top surface. Char residues after 10 minutes of testing of VEs/phenolic blends did not show too much difference, though VE-Ep/Methylon blends resulted in slightly higher char content (38 - 40%) than that of VE-Ep skins (33%), a similar trend has been seen in cone results for cast resins (Table 3.4). However, for composite structures not much difference for char residues at the end of cone tests (30 minutes) can be seen.

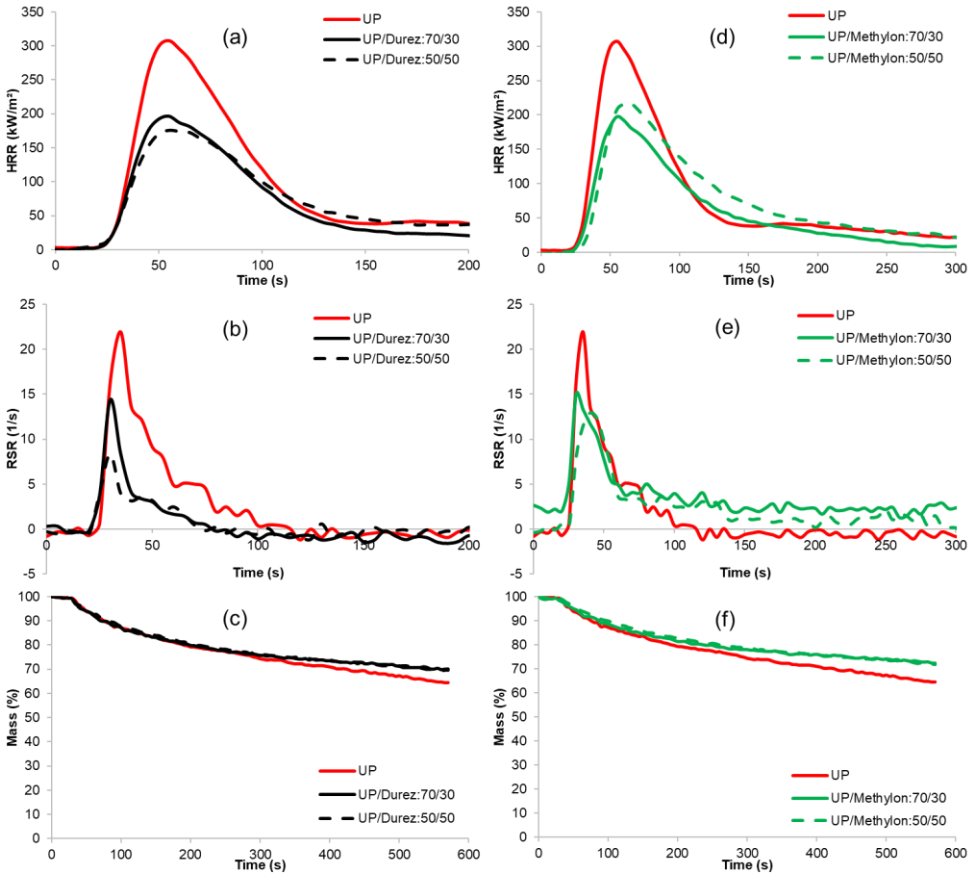

Figure 5.15: Plots of (a, d) HRR, (b, e) RSR and (c, f) mass loss *vs*. time for sandwich composites with skins of (a, b, c) UP and UP/Durez and (d, e, f) UP and UP/Methylon blends

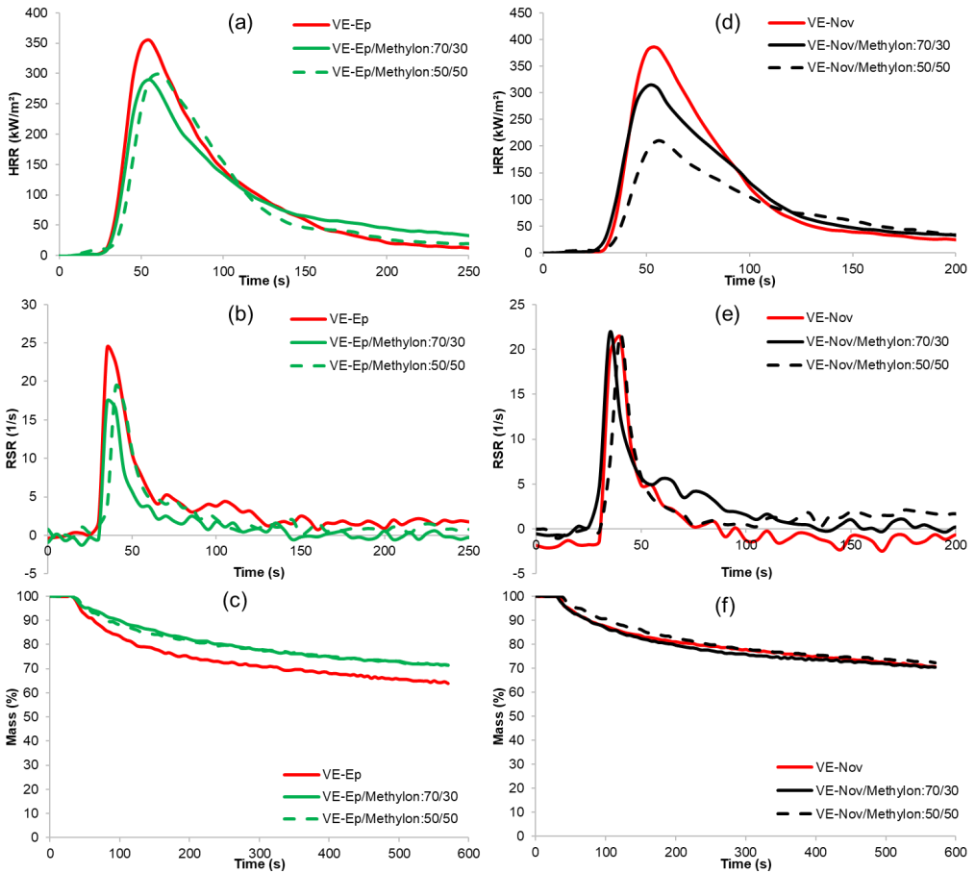

Figure 5.16: Plots of (a, d) HRR, (b, e) RSR and (c, f) mass loss *vs.* time for sandwich composites with skins of (a, b, c) VE-Ep and VE-Ep/Methylon blends and (d, e, f) VE-Nov and VE-Nov/Methylon blends

Table 5.8: Derived cone calorimetric results of sandwich composites with skins containing different resin blends – UP/Durez blends, UP/Methylon blends, VE-Ep/Methylon blends and VE-Nov/Methylon blends

Sample ID	TTI (s)	FO (s)	PHRR (kW/m^2)	THR (MJ/m^2)		TSR (m^2/m^2)		Residue [b] (wt%)	
				5 mins [a]	30 mins	5 mins [a]	30 mins	10 mins	30 mins
UP	24	1296	294	23.5	46.5	554	1121	67 (34)	48 (17)
UP/Durez:70/30	22	980	185	15.5	27.3	221	2623	70 (28)	56 (13)
UP/Durez:50/50	22	927	159	18.0	36.2	170	3674	70 (29)	58 (20)
UP/Methylon:70/30	24	972	189	17.2	26.3	1050	1350	72 (38)	60 (24)
UP/Methylon:50/50	25	965	211	22.0	40.7	703	1895	72 (40)	56 (21)
VE-Ep	29	854	326	24.2	36.1	1009	1717	71 (33)	60 (22)
VE-Ep/Methylon:70/30	28	800	254	24.2	29.2	400	955	71 (40)	53 (18)
VE-Ep/Methylon:50/50	31	1092	276	22.3	30.1	631	4733	71 (38)	52 (18)
VE-Nov	29	1092	322	23.3	41.8	345	711	71 (38)	54 (21)
VE-Nov/Methylon:70/30	28	1108	300	22.9	41	547	1138	71 (33)	59 (17)
VE-Nov/Methylon:50/50	29	1047	167	18.2	28	545	928	72 (35)	59 (21)

Notes:

TTI = time-to-ignition, FO = time-to-flame-out, PHRR = peak heat release rate, THR = total heat release, TSR = total smoke release. The reproducibility in cone parameters was ±5%.

The variation in values for different parameters of UP and UP/phenolic blends are as: TTI = ±2; FO = ±98; PHRR = ±48; THR = ±10.1; TSR = ±404; Residue = ±1.

The variation in values for different parameters of VE and VE/phenolic blends are as: TTI = ±2; FO = ±360; PHRR = ±55; THR = ±7.8; TSR = ±190; Residue = ±2.

a: End of first peak was defined for the initial 300 s of cone tests to be more comparable for all samples while the first peak decreased to a minimum and constant state from the specimen tested up to 10 minutes.

b: For residue (wt%), values in the parentheses are after compensating for glass content (8 layers of glass fabric, 4 on each side of top and bottom skins).

5.2.1.2 Thermal barrier performance during cone experiments

Temperature *vs.* time profiles obtained from thermocouples inserted underneath the top and bottom skins are shown in Figures 5.17 and 5.18. It can be observed that the temperature at the top skin's back surface of the sandwich composites of UP and UP/PH blends, VEs and VEs/PH (Methylon) blends increased rapidly with time, reaching a relatively steady state with a maximum temperature (Figures 5.17 and 5.18 (a, c)) about 660 - 700 °C (Table 5.9). However, some differences in the temperature rise could be seen in blends up to 30 minutes (when the tests were stopped). In the case of UP/Durez blends, the temperature rise is lower in the beginning than that of UP, which could be explained due to the lower flammability of the former in terms of PHRR and THR. Towards the end of the experiment, the back surface temperature of the blends is similar to the temperature of UP, that is when all the resin has been burnt and only glass layers are left behind. UP/Methylon blends, however are similar to UP in the beginning and then towards the end the temperatures for the blends are lower than that of UP. For both types of VE/phenolic blends, the temperature rise is similar in both 70/30 blends in the beginning than those of respective VE composites, but in 50/50 blends the temperatures are higher throughout the test, which could be corroborated from their high flammability seen from cone results (Table 5.8). Towards the end however, temperatures are similar to those for VE (VE-Ep or VE-Nov, respectively). From the maximum temperature values of the top skin reported in Table 5.9, VE-Ep/Methylon blends show slightly higher values than that of VE-Ep, whereas VE-Nov/Methylon blends show slightly lower temperature than VE-Nov alone, especially for 50/50 blends, which is 25 °C lower.

Significant differences in the behaviours of the back surface temperatures of bottom skins among different UP/phenolic blends and VEs/phenolic (Methylon) blends with respect to respective UP or VE samples can be observed from Figures 5.17, 5.18 (b, d). In all samples, temperature starts rising from the beginning of the experiment, reaching 100 °C, followed by a steady state. The time to reach 100 °C and duration of the steady state (200 ~ 500 s, 150 ~ 400 s for UP/phenolic and VE/phenolic blends, respectively) however, differs in all samples as can be seen from Table 5.9. This stage can be explained owing to the loss of moisture in the samples. Both UP/phenolic and VE/phenolic blends show shorter steady state periods than UP or VE alone, this could be due to the char for UP and VE/phenolic blends in the top skin being more conductive, the underlying structure heats up early, hence the temperature starts rising up early. For VE/phenolic blends, VE-Ep/Methylon:70/30 shows very similar temperature profile trend as VE-Ep alone, whereas VE-Ep/Methylon:50/50 blends show a shorter steady state and higher rate of temperature rise up to 30 minutes than the other two. By contrast, VE-Nov has lower rate of temperature rise than the other two blends until 900 s, and after that the temperature rise trend is in between the two VE-Nov/phenolic blends (Figure 5.18 (d)). As seen from cone results in Table 5.8, in VE-Ep/Methylon and VE-Nov/Methylon blends PHRR and THR are lower than respective VEs, however, the temperature profiles of the back surface of bottom skins show a reverse trend, indicating that the chars of the blends are more conductive. This can be explained based on the fact that phenolics on heating form a highly crosslinked char and this dense carbonaceous structure could be more conductive than a porous char.

In general, UP/Durez and UP/Methylon blends show lower T_{max} values on the bottom skins' back surface temperatures than that of UP. All UP/phenolic blends show shorter times to reach 100 °C ($t_{100\ °C}$), similar

times to reach 300 °C, except for UP/Durez:70/30, which has much shorter, and longer times to reach 400 °C for UP/phenolic blends (if reached). All resins have higher temperature rises than UP until ~800 s (~1100 s in UP/Durez:70/30), after which it is lower than that of UP. UP/Durez:50/50 performs a slightly better thermal barrier effect (lower rate of temperature rise) than 70/30. The images of the residues after the cone tests are given in Appendix 4 (Table A4-1), from which it can be seen that the top skins of all composites have burned completely, leaving glass layers only, similar to as shown for neat resin as skins (See Figure 5.3). The top skin delaminated and balsa core thicknesses reduced for all samples containing blended resins (Table A4-1). In UP/Durez:70/30 the collapsing of balsa wood, less unburnt resin and more darkened char on the back could be clearly seen. The conductive char could increase the thermal conductivity of this blend, and hence the relatively higher T_{max} on the bottom skin's back surface (401 *vs.* 369 - 394 °C for other UP/phenolic samples) can be seen. In the case of UP/Methylon blends, UP/Methylon:70/30 performs slightly better than the 50/50 blend after 800 s (reaching 300 °C), in terms of lower rate of temperature rise.

All VE/phenolic blends have shorter times to reach 100 °C, and then similar or slightly higher temperature rises than respective VE containing samples. VE-Ep/Methylon blends show slightly higher T_{max} on bottom skins' back surface temperatures than that of VE-Ep, whereas VE-Nov/Methylon:50/50 blend shows slightly lower T_{max}. Hence in terms of their temperature profiles VE-Ep/Methylon:70/30 has a slightly better thermal barrier effect (lower rate of temperature rise) than 50/50, whereas in the case of VE-Nov/Methylon blends the trend is other way around, i.e. VE-Nov/Methylon:50/50 shows slightly better thermal insulating properties than 70/30. This trend is same as seen from their PHRR and THR values in Table 5.8.

ΔT values, the difference in top (T) and bottom (B) skins' back surface temperatures of all samples are also given in Table 5.9. This temperature difference between two skins represents the thermal insulating properties of glass fibre, and residual char of the resin (if any) and the balsa, i.e., the higher the value, the better the thermal insulating value. ΔT values showed that chars of all UP/phenolic blends show better thermal insulating properties than that of UP (277 - 302 *vs.* 254 °C). The UP/Durez:70/30 sample does not show as much difference as the other three UP/phenolic blends (Table 5.9), but still performs better than the UP control (ΔT = 254 °C). In VEs and VEs/phenolic blends, both VE-Ep/Methylon blends display slightly better performance in terms of their increase in ΔT values than that of VE-Ep control, however VE-Nov/Methylon blends show worse performance than VE-Nov (Table 5.9).

T_{max} on the bottom skins' back surface temperature was used to rank the thermal barrier performances of different sandwich composites for UP/phenolic and VEs/phenolic (Methylon) blends, the trend in terms of thermal barrier effect from high to low being:

UP/Methylon:70/30 > UP/Methylon:50/50 > UP/Durez:50/50 > UP/Durez:70/30 > UP.

VE-Ep > VE-Nov/Methylon:50/50 > VE-Ep/Methylon:70/30 > VE-Ep/Methylon:50/50 = VE-Nov > VE-Nov/Methylon:70/30.

Comparing these to cone parameters in Section 5.2.1.1, reduced PHRR for UP/phenolic blends (Table 5.8) shows lower T_{max} than that of UP as skins, probably due to the lower thermal conductivity of the charred residue of the blends. For VE/phenolic blends, despite reductions in PHRR and THR for VEs/phenolic blends (Table 5.8), T_{max} values of the blends are higher, which gives an indication of higher thermal conductivity of the charred residue for the blends.

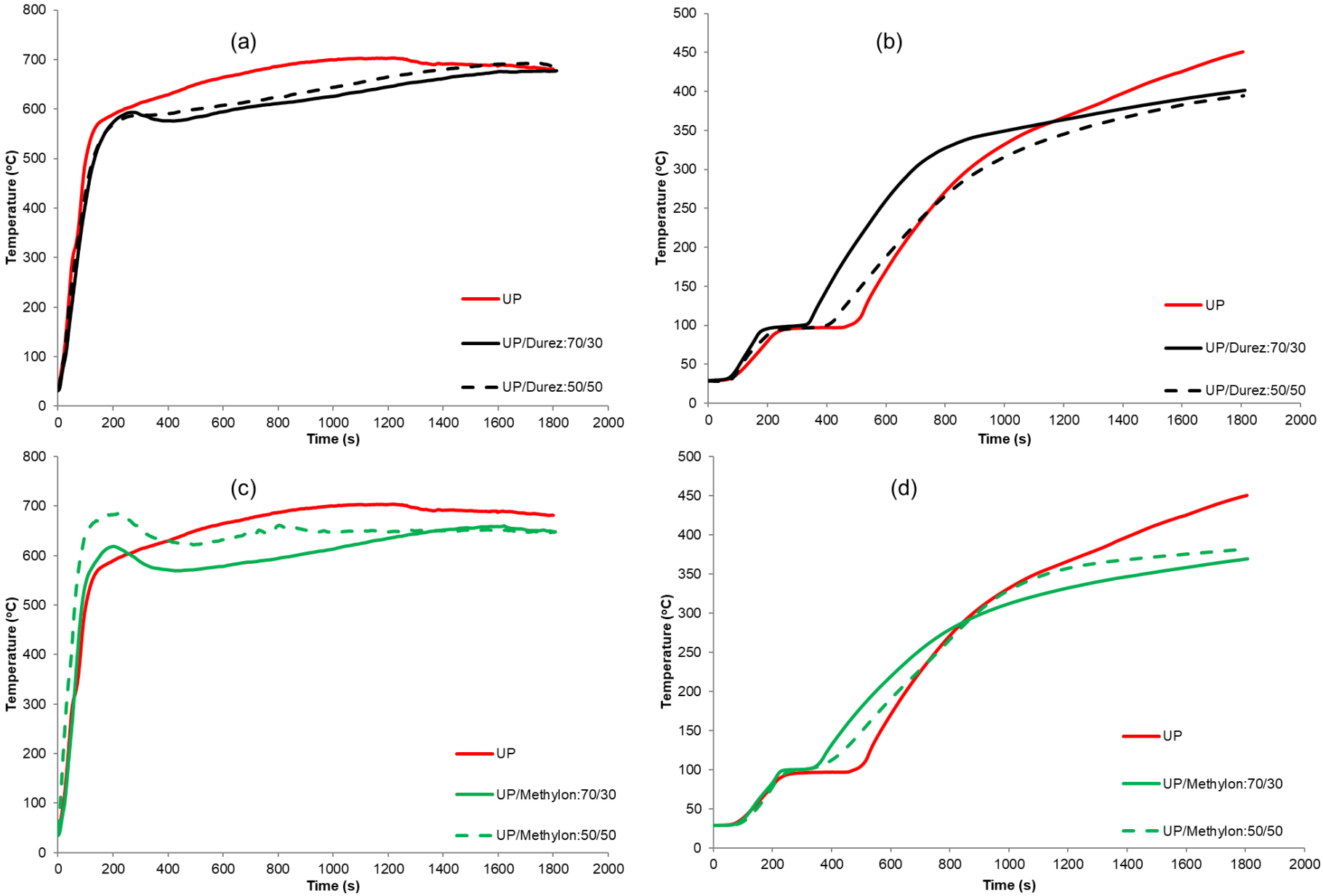

Figure 5.17: Plots of (a, c) top skin, TC_2 and (b, d) bottom skin's (TC_5) back surface temperature *vs*. time for sandwich composites with skins of (a, b) UP and UP/Durez and (c, d) UP and UP/Methylon blends

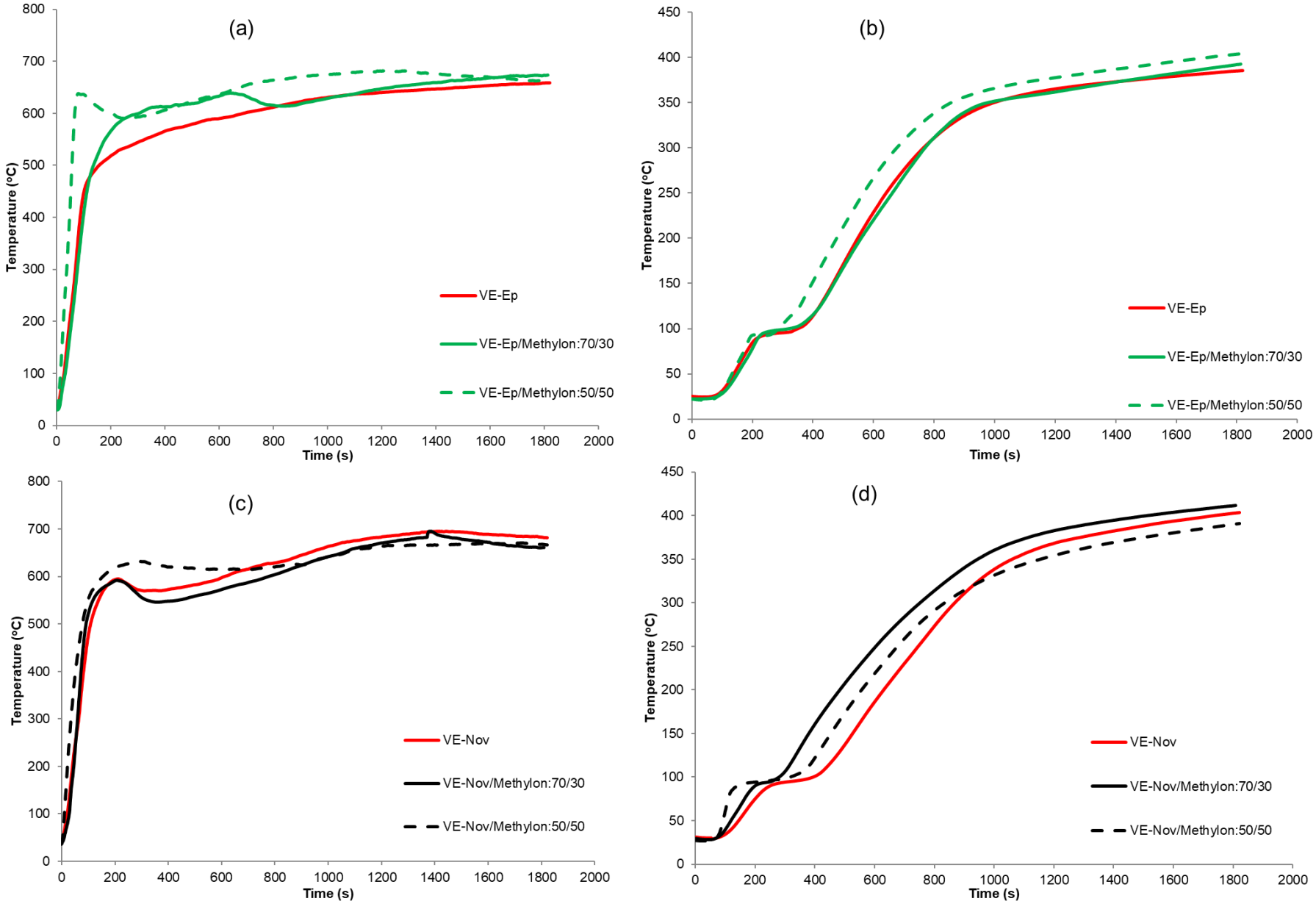

Figure 5.18: Plots of (a, c) top skin, TC_2 and (b, d) bottom skin's (TC_5) back surface temperature *vs*. time for sandwich composites with skins of (a, b) VE-Ep and VE-Ep/Methylon blends and (c, d) VE-Nov and VE-Nov/Methylon blends

Table 5.9: Time to reach different temperatures and maximum temperature (T_{max}) of top and bottom skins' back surfaces during the cone calorimetric testing among sandwich composites with skins of different resin blends – UP/Durez blends, UP/Methylon blends, VE-Ep/Methylon blends and VE-Nov/Methylon blends

Sample ID	Time to reach back surface temperature (s) of									Maximum Temperature T_{max} (°C)		ΔT (T-B) (°C)
	Top skin				Bottom skin							
	$t_{300\ °C}$	$t_{400\ °C}$	$t_{500\ °C}$	t_{Tmax}	$t_{100\ °C}$	$t_{300\ °C}$	$t_{400\ °C}$	$t_{500\ °C}$	t_{Tmax}	T	B	
UP	53	81	101	1218	476	878	1415	-	1800	704	450	254
UP/Durez:70/30	71	97	133	1769	308	692	1786	-	1800	678	401	277
UP/Durez:50/50	64	91	128	1746	400	923	-	-	1800	694	394	300
UP/Methylon:70/30	57	70	87	1620	261	911	-	-	1800	660	369	291
UP/Methylon:50/50	31	49	61	216	303	892	-	-	1800	684	382	302
VE-Ep	69	86	155	1800	351	765	-	-	1800	659	385	274
VE-Ep/Methylon:70/30	76	97	135	1766	318	771	-	-	1800	673	392	281
VE-Ep/Methylon:50/50	37	47	56	1210	288	677	1710	-	1800	683	403	280
VE-Nov	65	83	110	1409	392	869	1739	-	1800	696	403	293
VE-Nov/Methylon:70/30	61	74	92	1381	280	752	1508	-	1800	695	411	284
VE-Nov/Methylon:50/50	36	53	78	1723	312	833	-	-	1800	671	390	281

Notes: T - Top skin's back surface, B - bottom skin (and composite)'s back surface, '-' in the table indicated maximum temperature during the testing did not reach the certain temperature.

ΔT (T-B) - Maximum back surface temperature difference between top and bottom skins

Thermal barrier performance evaluation

For these composite samples from blended resins, apparent thermal conductivity values (*k*) of each component in the sandwich structure were not calculated owing to too many variables which affected the values as explained in Section 5.1.3.2 (as was the case for neat resins). Values for composites were calculated instead using the difference in top surface temperature TC_1 (T_0 in Equation 5.1) and back surface temperature TC_5 (Figure 5.4) (T_b in Equation 5.1) using equation 5.2. Apparent thermal conductivity *vs.* time curves for all samples are given in Figure 5.19 (a), (b), from which thermal conductivity values of the composite at 600 and 1000 s are presented in Table 5.10. Same methodology is to be used for the rest of blends in this chapter.

It can be observed from Figure 5.19 (a) that apparent thermal conductivity of UP/phenolic blends (both Durez and Methylon) increases quicker than that of UP. The introduction of phenolic resins slightly increases the thermal conductivity of composite samples during the combustion stage. As can be seen from Table 5.8, UP/phenolic blends have a shorter FO time than neat UP (927 ~ 980 *vs.* 1296 s), reflected here in Figure 5.19 (a) by steady increase of *k* of UP until the end of the experiment (UP sample is still burning) whereas for UP/phenolic blends, the rate of increase is much lower and is steady due to an earlier FO time. This effect is more pronounced in the case of UP/phenolic 70/30 wt% blends. Both 50/50 blends had lower thermal conductivity values and the increase in time was lower compared to respective 70/30 blends.

From Figure 5.19 (b) it can be seen that the apparent thermal conductivity of VE/phenolic (Methylon) blends increases faster compared to those of VE-Ep or VE-Nov, respectively, affecting the thermal barrier effects though better fire performances of VE/phenolic blends from cone results were seen.

It can be seen from the results in Table 5.10 that UP/phenolic blends have higher apparent thermal conductivity values than UP at both 600 and 1000 s, indicating the conductive nature of char from the phenolic component in the blends. Similarly, VE/phenolic blends showed slightly higher values than VE-Ep or VE-Nov at both 600 and 1000 s. Thermal conductivity values of 600 s were used to calculate thermal resistivity for sandwich composites, plotted as bar charts in Figure 5.20, which shows that UP has slightly better thermal insulating properties than UP/phenolic blends. i.e., the introduction of phenolic resins in the blends as skins, despite having great improvement in fire performance (cone results), lower the thermal resistivities (i.e. worse thermal insulating properties) in UP/phenolic based sandwich composites. Both VE resins show slightly better thermal insulating properties than VE/phenolic (Methylon) blends, VE-Nov/phenolic especially showing better insulating properties than VE-Ep/phenolic ones.

Table 5.10: Time to reach TC_1=TC_2 and temperature, the calculated apparent thermal conductivity values for UP resins and UP/phenolic resin blends and VE resins and VE/phenolic (Methylon) resin blends as skins in a sandwich structure under cone calorimetry at 50 kW/m^2 heat flux

Sample	Top surface temperature [a] (°C)	Time to reach TC_1=TC_2 [b] (s)	Temp. when TC_1=TC_2 [b] (°C)	Apparent thermal conductivity, *k* of composite (kW/m.K × 10^{-3})	
				600 s	1000 s
UP	650	474	645	2.8	4.2
UP/Durez:70/30	610	722	606	3.8	5.1
UP/Durez:50/50	610	506	600	3.1	4.5
UP/Methylon:70/30	590	736	589	3.6	4.8
UP/Methylon:50/50	610	394	613	3.2	4.7
VE-Ep	610	702	602	3.5	5.1
VE-Ep/Methylon:70/30	605	819	614	3.4	5.2
VE-Ep/Methylon:50/50	610	107	634	3.9	5.4
VE-Nov	620	813	630	3.1	4.7
VE-Nov/Methylon:70/30	610	842	612	3.7	5.3
VE-Nov/Methylon:50/50	605	700	615	3.4	4.9

a = Cone calorimetry - Taken as when surface temperature, TC_1 becomes constant

b = Top upper surface = just underneath the upper surface

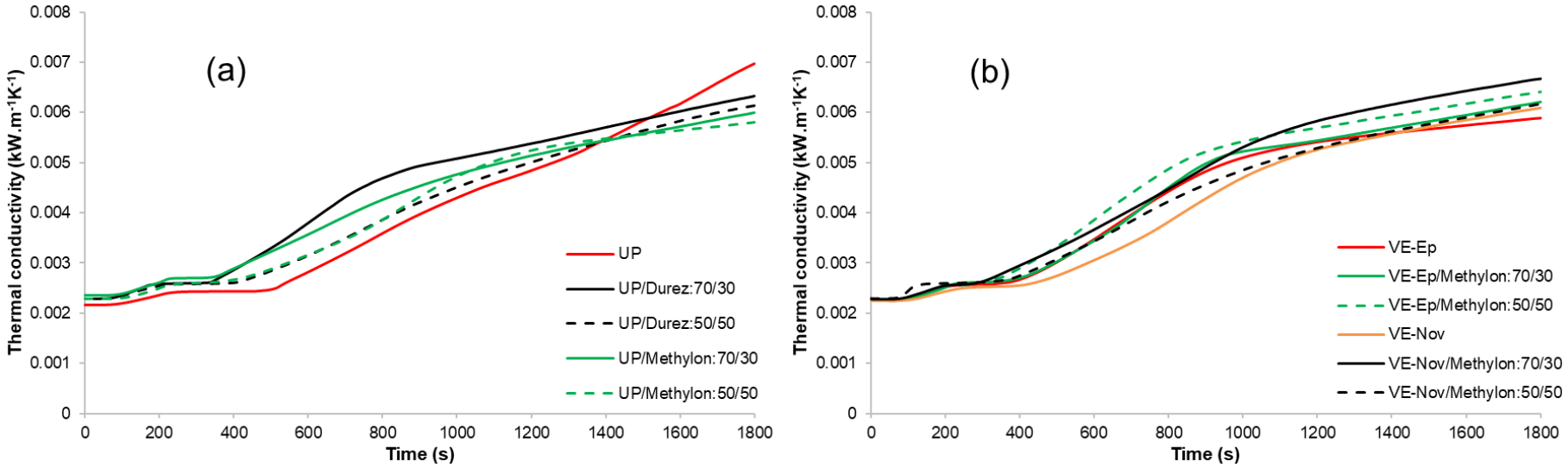

Figure 5.19: Calculated apparent thermal conductivity curves of (a) UP resins and UP/phenolic resin blends, and (b) VE resins and VE/phenolic (Methylon) resin blends as skins in sandwich composites

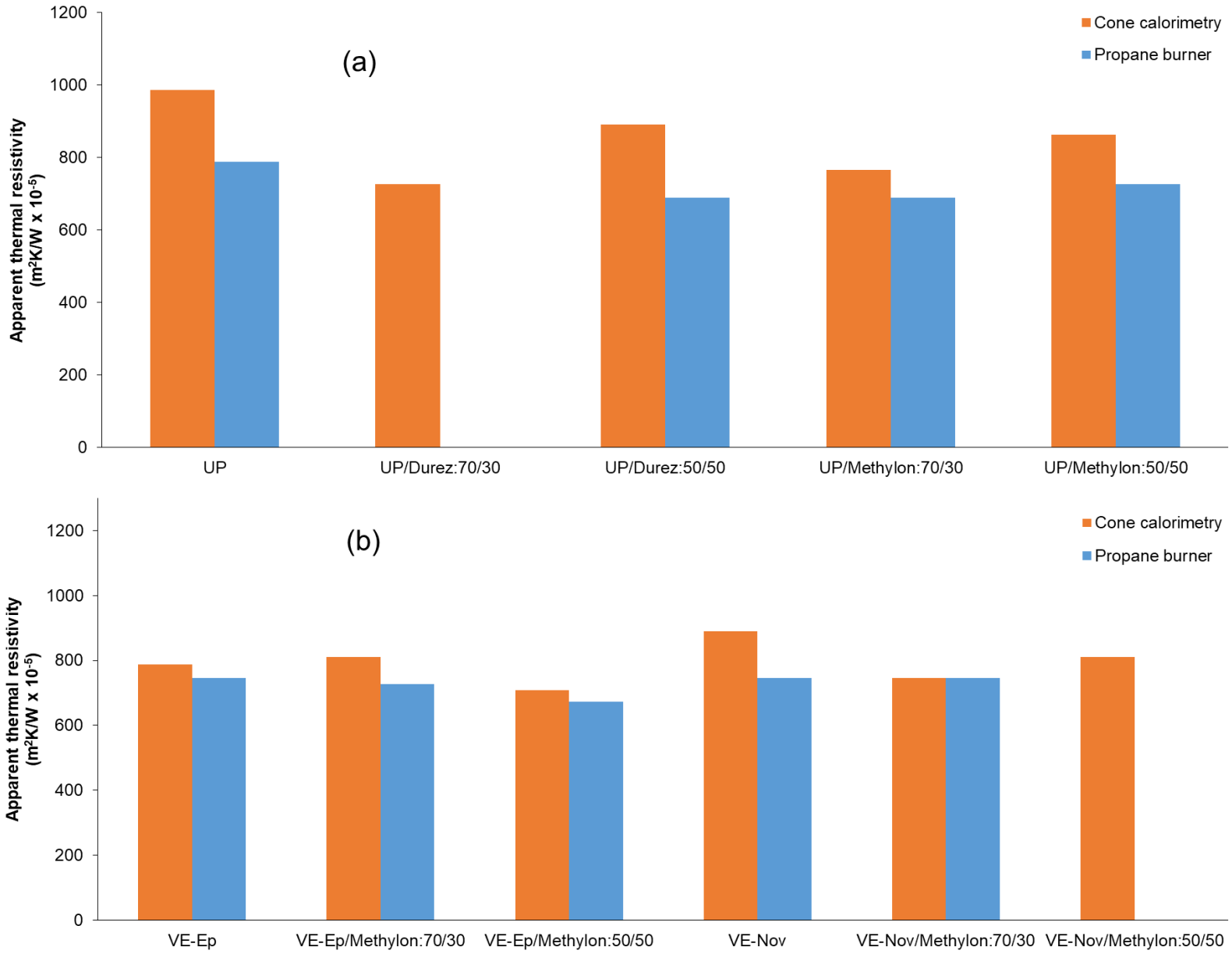

Figure 5.20: Apparent thermal resistivities of sandwich composite structures with (a) UP resins and UP/phenolic resin blends and (b) VE resins and VE/phenolic (Methylon) resin blends at 600 s under cone and propane burner tests

5.2.1.3 Propane burner testing

From the propane burner testing results for UP and UP/PH-Res blends shown in Figure 5.21 (a, b) and Table 5.11, it can be seen that UP/phenolic blends show higher rates of temperature rise than that of UP, which is a similar trend to that seen from the bottom skins' back surface temperature profiles in the cone experiments up to 800 s (Figure 5.17 (b, d)). After 800 s, the temperature profiles in the cone test have a reverse trend. In propane burner tests, due to the higher external heat flux, the heat transfer is more intense than the one in the cone calorimetry, however in the cone, the main flame is almost gone after at ~800 s, hence heat transfer is from the radiant heater only which slowed down the rate of temperature rise. Within UP/phenolic blends, UP/Durez:50/50 blend takes a longer time to reach 300 °C than UP/Durez:70/30 (858 s *vs.* 548 s), indicating much better thermal barrier performances in 50/50% blends but still not as good as for the UP resin sample (1000 s). Similarly, it can also be observed that UP/Methylon:50/50 has a slightly better thermal barrier effect than UP/Methylon:70/30 based on time to reach 300 °C values (938 s *vs.* 873 s) but again not as good as UP (1000 s), showing higher thermal conductivity of the chars of the blends (Figure 5.22 (a, b)). UP/phenolic blends form slightly more char residue than the UP control (35 - 41 *vs.* 35%), which is as expected, due to the presence of char-forming phenolic resins on the thin skins on both sides of composites. UP/Durez blends show slightly more charring tendency than UP/Methylon blends, and a similar trend can be seen in the cone results for cast resins (Section 3.4.2, Chapter 3).

In the case of VE/phenolic blends (Figure 5.21 (c, d)), similar trends for those results for UP/phenolic blends were observed, VE/phenolic blends show higher rates of temperature rise than that of VE. Also, similar trends for the temperature rise thus good agreement was noticed for temperature profiles collected in cone calorimetric results (Figure 5.18 (b, d)). For VEs and VEs/PH-Res blends, it can be observed that temperature profiles of VE-Ep, VE-Ep/Methylon:70/30 and 50/50 do not show much difference until 350 s, after that, VE-Ep and VE-Ep/Methylon:70/30 take similar times to reach 300 °C (865 s *vs.* 844 s), indicating similar thermal barrier performances for these two sandwich composites. Within VE-Nov/Methylon blends, VE-Nov/Methylon:50/50 sample could not be prepared due to lack of VE-Nov resin at that stage hence was not tested. It can also be seen that VE-Nov and VE-Nov/Methylon:70/30 do not show much difference until 400 s, and after that, VE-Nov shows much better thermal barrier effects (i.e. lower rate of temperature rise) than that of VE-Nov/Methylon:70/30 based on the time to reach 300 °C (1128 s *vs.* 895 s).

From propane burner testing, the thermal barrier performances of sandwich structure composites with UP, UP/PH-Res, VE and VE/PH-Res blends are ranked according to the time to reach 300 °C (s), the longer the better, as follows:

UP > UP/Methylon:50/50 > UP/Methylon:70/30 > UP/Durez:50/50 > UP/Durez:70/30.
VE-Nov > VE-Nov/Methylon:70/30 > VE-Ep ≈ VE-Ep/Methylon:70/30 > VE-Ep/Methylon:50/50.

A similar trend was seen from ΔT values of cone results for composites given in Table 5.9 except for UP, the probable reason has been explained in this section above.

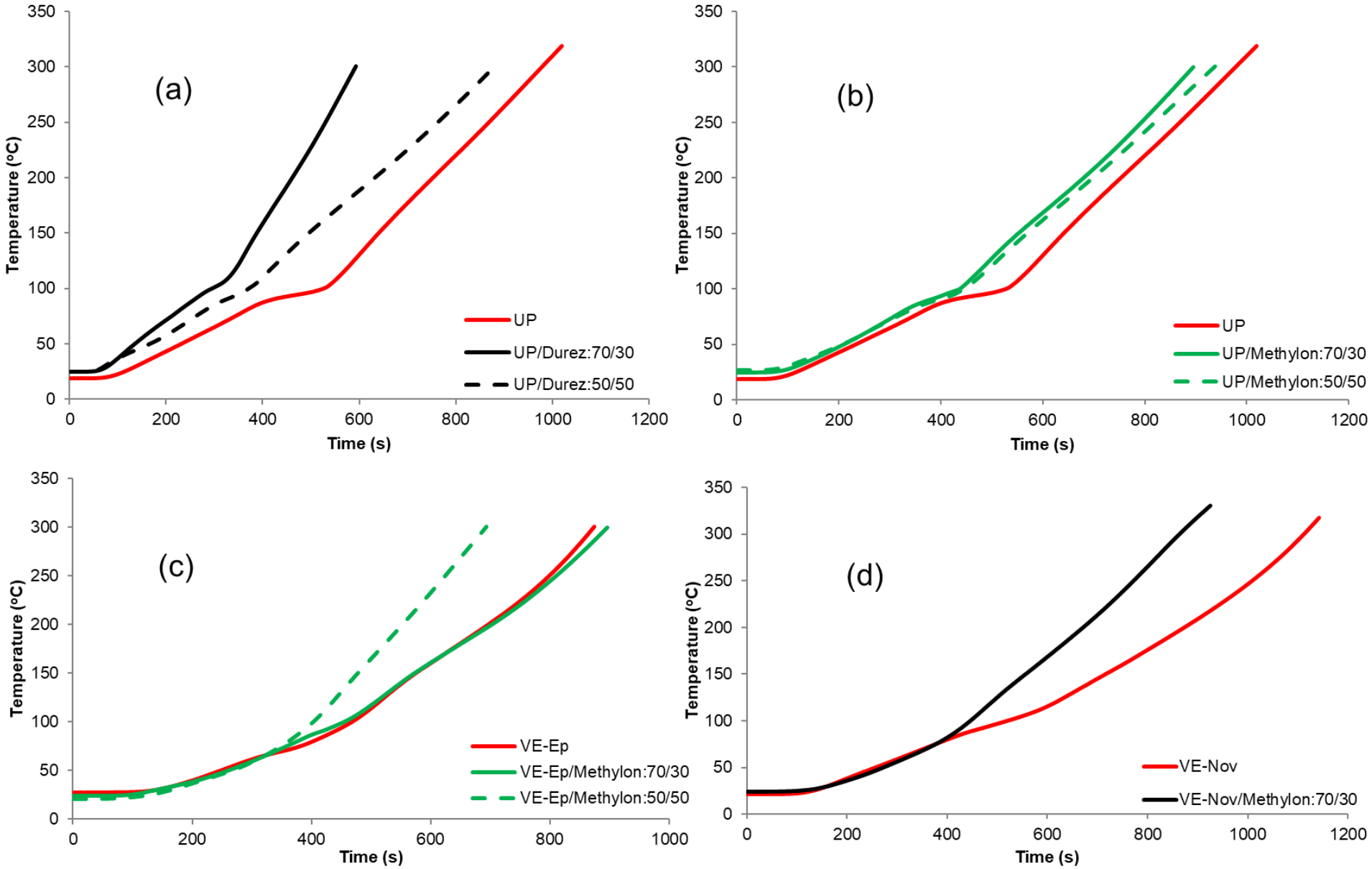

Figure 5.21: Back surface temperature versus time curves for sandwich structures among (a, b) UP and UP/PH-Res blends and (c, d) VE and VE/PH-Res blends obtained from propane burner testing

Table 5.11: Top surface temperatures, residues after propane burner testing and times to reach 300 °C for sandwich structures with balsa core thicknesses of 25.4 mm (1 inch) for UP/PH-Res and VEs/PH-Res as skins

Sample	Top surface temperature ** (°C)	Residue (wt%)	Glass content (wt%)	Char (wt%)	Time to reach 300 °C (s)
UP	1000	46	11	35	1000±28
UP/Durez:70/30	980	55	14	41	548±64
UP/Durez:50/50	955	56	16	40	858±31
UP/Methylon:70/30	940	51	16	35	873±31
UP/Methylon:50/50	975	53	17	36	938±0
VE-Ep	980	49	15	34	865±13
VE-Ep/Methylon:70/30	975	52	15	37	844±74
VE-Ep/Methylon:50/50	985	48	13	35	693±1
VE-Nov	950	50	14	36	1128±21
VE-Nov/Methylon:70/30	1000	52	18	34	895±44
VE-Nov/Methylon:50/50	-	*	*	*	*

Notes: '*' indicates that sample was not tested.

** = In propane burner tests, while TC_{front} becomes constant.

- = Test not performed

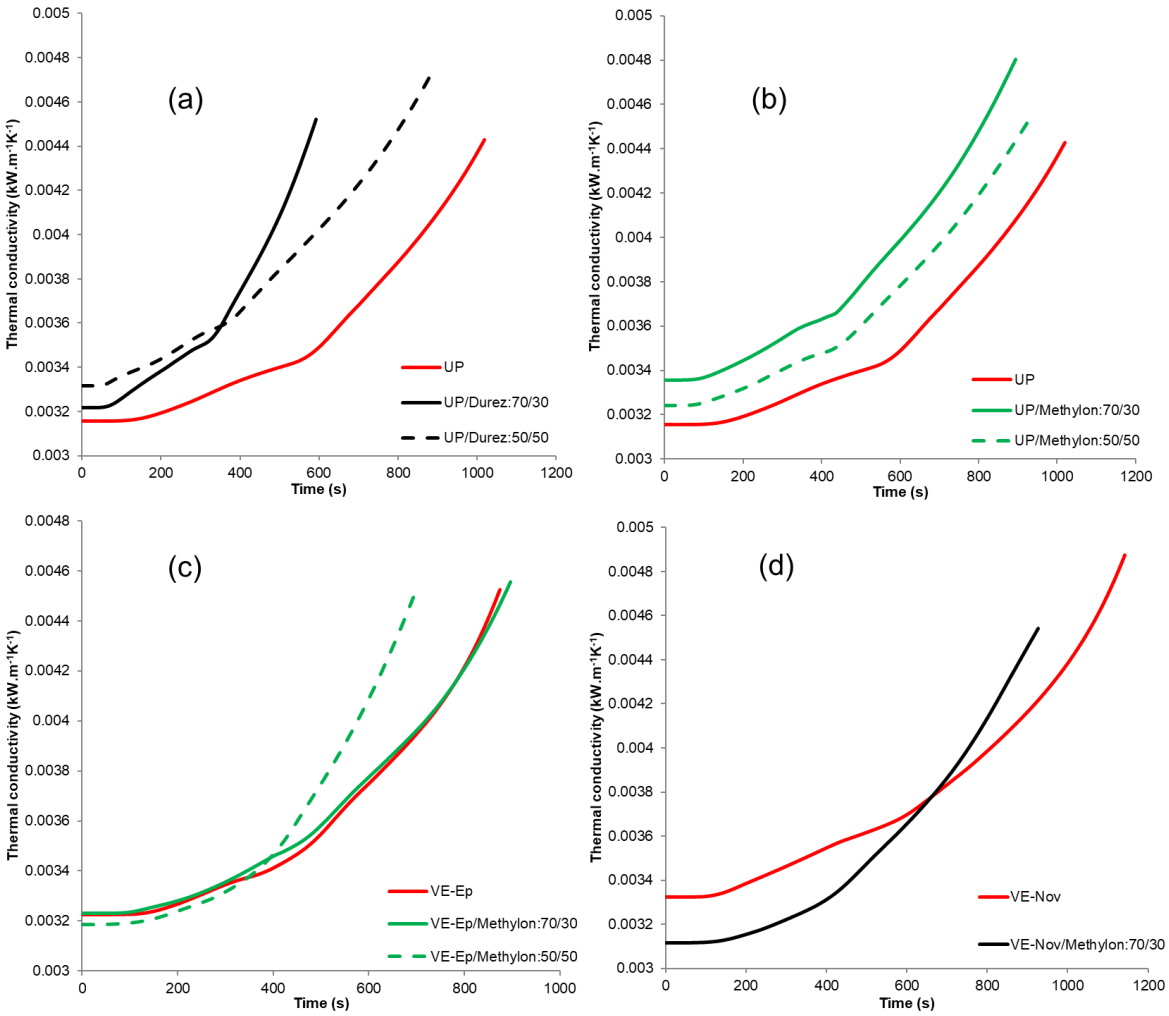

Figure 5.22: Apparent thermal conductivity versus time curves for sandwich structures among (a, b) UP and UP/PH-Res blends and (c, d) VE and VE/PH-Res blends obtained from propane burner testing

From Figure 5.22, it can be noticed that temperature dependent thermal conductivity of all samples with UP/phenolic (both Durez and Methylon) and VE/phenolic (Methylon) blends are higher than respective control samples, which could be due to the more conductive nature of phenolic resin (see Table 1.1 [9-12]) and their highly crosslinked chars. It is also reported in the literature that phenolic resins generally have higher thermal conductivity values (0.21 - 0.35 W/m.K) than UP, VE, Epoxy resins (0.1 - 0.2 W/m.K) as also reported in Section 5.1.3.1 [4-12].

Table 5.12: Calculated thermal conductivities for sandwich composites with skins of UP/Durez, UP/Methylon, VE-Ep/Methylon and VE-Nov/Methylon blends at particular times from the propane burner tests

Sample	Apparent thermal conductivity, *k* of composite (kW/m.K × 10^{-3})		
	600 s	700 s	800 s
UP	3.5	3.7	3.9
UP/Durez:70/30	-	-	-
UP/Durez:50/50	4.0	4.2	4.5
UP/Methylon:70/30	4.0	4.2	4.5
UP/Methylon:50/50	3.8	4.0	4.2
VE-Ep	3.7	3.9	4.2
VE-Ep/Methylon:70/30	3.8	4.0	4.2
VE-Ep/Methylon:50/50	4.1	--	--
VE-Nov	3.7	3.8	4.0
VE-Nov/Methylon:70/30	3.7	3.9	4.1
VE-Nov/Methylon:50/50	*	*	*

- = Test stopped prior to 600 s due to back surface temperature reached 300 °C hence its thermal conductivity for sandwich composites could not be calculated

-- = Test stopped prior to 700 s due to back surface temperature reached 300 °C hence its thermal conductivity for sandwich composites could not be calculated

* = Test not performed

The apparent thermal conductivities at 600, 700 and 800 s are calculated and given in Table 5.12. Since after 10 minutes char would have been formed in the bottom skin (if any), these values can represent the conductivity of the chars of different samples. Values at 600 s were selected to calculate and plot their respective thermal resistivities in Figure 5.20 and this time was chosen for direct comparison with results from cone calorimetry. Comparing bar chart results from both tests in Figure 5.20, similar trends of apparent thermal resistivities of sandwich composites with UP/phenolic and VE/phenolic blends can be observed. In general, apparent thermal resistivities from cone calorimetry show higher values than respective values in propane burner tests, which can be explained due to the lower heat flux used in the former (50 kW/m^2) than the latter (113 kW/m^2). With higher heat flux there is less charring tendency, since the char acts as a thermal barrier, lower char leads to lower resistivity.

5.2.2 Ternary blends – UP/VE-Nov and UP/VE-Nov/phenolic blends

Since both UP and VE resins are commercially used in the marine industry, but are equally flammable, the latter producing more smoke, it will be interesting to blend them together. VE-Nov as a cast resin shows slightly better fire performance than VE-Ep (Table 3.4) and produces

more char, this was chosen to be blended with UP with a view that the blend will have lower flammability and more char formation than UP. The introduction of phenolic (Methylon, inherently flame retardant) is expected to further reduce the flammability of ternary blends.

5.2.2.1 Cone calorimetry

From Figure 5.23 and Table 5.13 it can be seen that TTI of sandwich composites with skins of UP/VE-Nov is in between those of respective UP and VE-Nov samples (27 *vs.* 24 - 29 s). With additional presence of Methylon, TTI is reduced to a similar value to that of UP (24 s). FO time however is reduced in both samples. PHRR values of UP/VE-Nov blends were in between with those of UP and VE-Nov (301 *vs.* 294 - 322 kW/m^2), whereas with phenolic presence in UP/VE-Nov/Methylon blend, it was significantly reduced (224 kW/m^2). THR was much reduced in general for both UP/VE-Nov and UP/VE-Nov/phenolic blends compared to those individual components (30.6, 33.8 *vs.* 46.5, 41.8 MJ/m^2), hence reducing the flammability of these blends as skins. However, smoke was increased in UP/VE-Nov, but not as high as the former in UP/VE-Nov with the Methylon presence. Char residue after 10 minutes of testing though was lower than that of UP or VE-Nov, but slightly higher after 30 minutes. In general, both UP/VE-Nov and UP/VE-Nov/phenolic blends show improved fire performance, i.e., reduced flammability despite producing more smoke.

5.2.2.2 Thermal barrier performance during cone experiments

Temperature *vs.* time profiles obtained from thermocouples inserted underneath the top and bottom skins shown in Figure 5.24 demonstrate that T_{max} on the top skins' back surface reached about 665 - 675 °C (Table 5.14) for UP/VE-Nov and UP/VE-Nov/phenolic blends, which is slightly lower than those of UP and VE-Nov. The temperature is lowered with phenolic presence in UP/VE-Nov/phenolic by 10 °C. For the bottom skins' temperature, there is a steady state of temperature at 100 °C, with the duration of the steady state reduced in UP/VE-Nov blend compared to UP or VE-Nov and reducing further in UP/VE-Nov/phenolic (Figure 5.24 (b)), which may be due to different conductivities of different resin combinations. UP/VE-Nov shows a lower rate of temperature rise than UP/VE-Nov/Methylon blend before ~800 s, and after that, both blends show a very similar trend of temperature profiles up to 30 minutes. Visually it could be seen that in both UP/VE-Nov and UP/VE-Nov/Methylon samples, the bottom skins did not completely burn and delaminate (See Table A4-1). Unburnt resin could be seen on the back surface, which though had darkened, indicated that skins of blended resins provided better thermal protection than those of UP or VE-Nov. As discussed before and in Table 5.13, THR in both blends are reduced, PHRR for UP/VE-Nov is intermediate between those of UP and VE-Nov. This effect is more pronounced in the ternary blend, UP/VE-Nov/Methylon. The bottom skins' back surface temperatures of the residues of these blends are also lower than those of UP and VE-Nov samples from 800 s up to 30 minutes, indicating that the char residues of these blends are not very conductive. The lower thermal conductivity of this char could be due to the lower phenolic content compared to other blended samples.

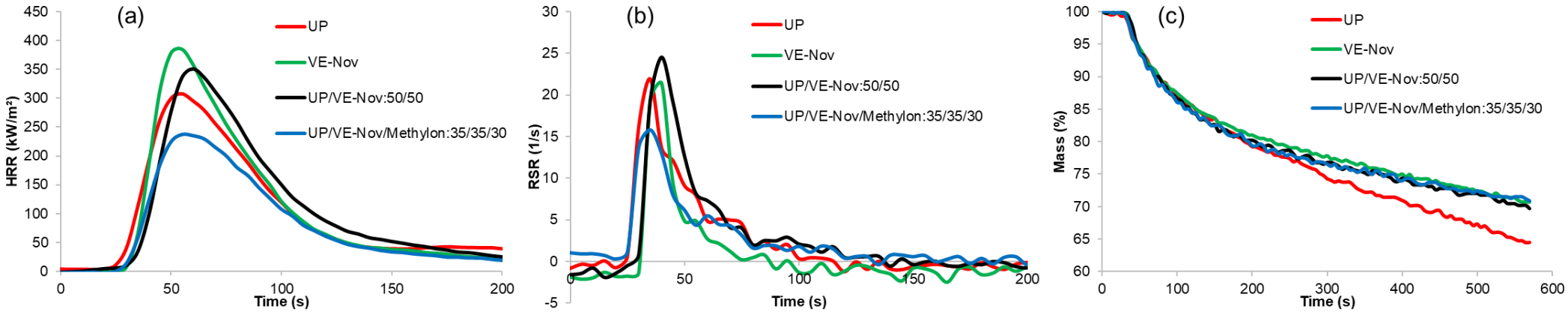

Figure 5.23: Plots of (a) HRR, (b) RSR and (c) mass loss *vs*. time for sandwich composites with skins of UP, VE-Nov, UP/VE-Nov blends and UP/VE-Nov/phenolic blends

Table 5.13: Derived cone calorimetric results of sandwich composites with skins containing different resin blends – UP, VE-Nov, UP/VE-Nov blends and UP/VE-Nov/phenolic blends

Sample ID	TTI (s)	FO (s)	PHRR (kW/m^2)	THR (MJ/m^2)		TSR (m^2/m^2)		Residue [b] (wt%)	
				5 mins [a]	30 mins	5 mins [a]	30 mins	10 mins	30 mins
UP	24	1296	294	23.5	46.5	554	1121	67 (34)	48 (17)
VE-Nov	29	1092	322	23.3	41.8	345	711	71 (38)	54 (21)
UP/VE-Nov:50/50	27	918	301	24.0	30.6	637	3394	70 (34)	55 (21)
UP/VE-Nov/Methylon:35/35/30	24	983	224	17.7	33.8	531	1893	71 (29)	59 (26)

Notes:

TTI = time-to-ignition, FO = time-to-flame-out, PHRR = peak heat release rate, THR = total heat release, TSR = total smoke release. The reproducibility in cone parameters was ±5%.

The variation in values for different parameters are as: TTI = ±3; FO = ±105; PHRR = ±55; THR = ±10.0; TSR = ±723; Residue = ±2.

a: End of first peak was defined for the initial 300 s of cone tests to be more comparable for all samples while the first peak decreased to a minimum and constant state from the specimen tested up to 10 minutes.

b: For residue (wt%), values in the parentheses are after compensating for glass content (8 layers of glass fabric, 4 on each side of top and bottom skins).

The temperature of the top skin was around 255 - 305 °C hotter than the back skin (See Table 5.14). In both UP/VE-Nov and UP/VE-Nov/Methylon the difference in top and bottom skins' back surface temperatures, ΔT, is higher than that for samples of UP and VE-Nov, indicating again that the thermal conductivity of the char of blends is lower than neat resins.

T_{max} on the bottom skins' back surface temperature was used to rank the thermal barrier performances of different sandwich composites for UP, VE-Nov, UP/VE-Nov blends and UP/VE-Nov/phenolic blends, the trend in terms of thermal barrier effect from high to low being:

UP/VE-Nov:50/50 > UP/VE-Nov/Methylon:35/35/30 > VE-Nov > UP.

Thermal barrier performance evaluation

As shown in Figure 5.25, apparent thermal conductivities of UP/VE-Nov and UP/VE-Nov/Methylon blends increase faster with time than those of UP or VE-Nov samples before ~1000 s, after that these are lower until the end of the tests. From Table 5.15, the values of apparent thermal conductivity of composites show that at 600 s, UP/VE-Nov and UP/VE-Nov/phenolic blends showed slightly higher values than that of UP or VE-Nov, however there is not much difference in the values at 1000 s probably because chars are partially or totally formed at that time. Thermal resistivities of sandwich composite structures for UP/VE-Nov and UP/VE-Nov/phenolic samples (Figure 5.26), reveal slightly better thermal insulating properties of UP or VE-Nov resins than those of UP/VE-Nov and ternary blends at 600 s, whereas as mentioned above, it would show the reverse trend (if plotted) at 1000 s.

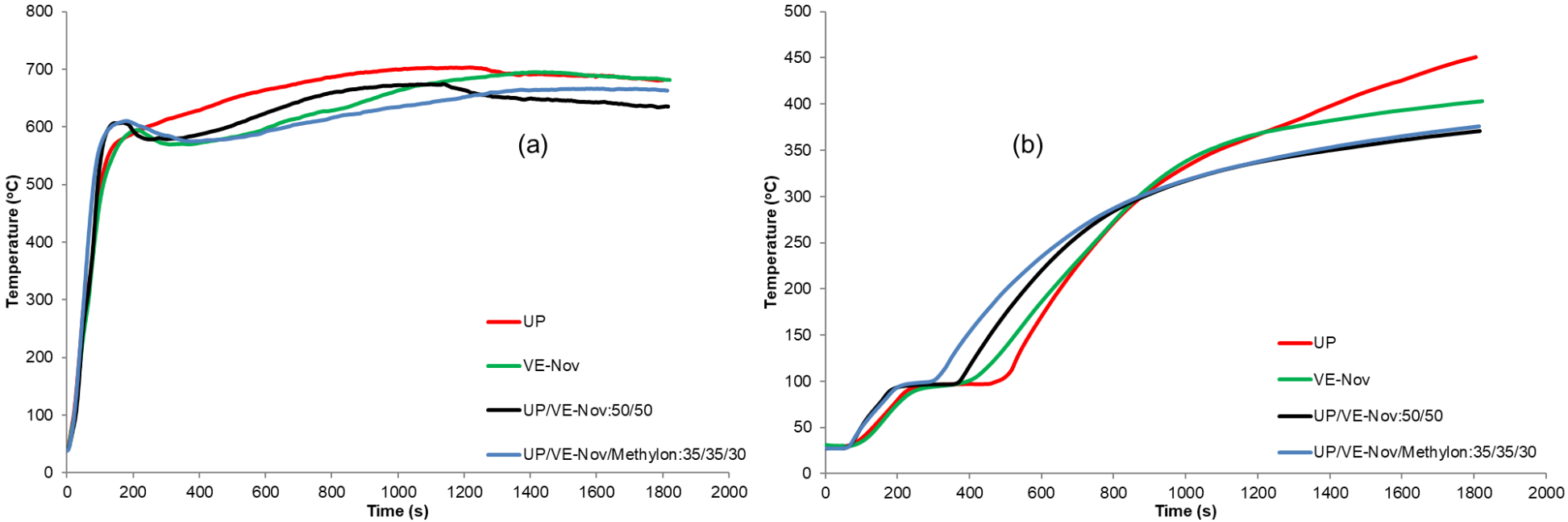

Figure 5.24: Plots of (a) top skin, TC_2 and (b) bottom skin's (TC_5) back surface temperature *vs*. time for sandwich composites with skins of UP, VE-Nov, UP/VE-Nov blends and UP/VE-Nov/phenolic blends

Table 5.14: Time to reach different temperatures and maximum temperature (T_{max}) of top and bottom skins' back surfaces during the cone calorimetric testing among sandwich composites with skins of different resin blends – UP, VE-Nov, UP/VE-Nov blends and UP/VE-Nov/phenolic blends

Sample ID	Time to reach back surface temperature (s) of									Maximum Temperature T_{max} (°C)		ΔT (T-B) (°C)
	Top skin				Bottom skin							
	$t_{300\ °C}$	$t_{400\ °C}$	$t_{500\ °C}$	t_{Tmax}	$t_{100\ °C}$	$t_{300\ °C}$	$t_{400\ °C}$	$t_{500\ °C}$	t_{Tmax}	T	B	
UP	53	81	101	1218	476	878	1415	-	1800	704	450	254
VE-Nov	65	83	110	1409	392	869	1739	-	1800	696	403	293
UP/VE-Nov:50/50	61	80	93	1138	373	883	-	-	1800	675	370	305
UP/VE-Nov/Methylon:35/35/30	51	64	80	1602	296	872	-	-	1800	666	375	291

Notes: T - Top skin's back surface, B - bottom skin (and composite)'s back surface, '-' in the table indicated maximum temperature during the testing did not reach the certain temperature.

ΔT (T-B) - Maximum back surface temperature difference between top and bottom skins

Table 5.15: Time to reach TC_1=TC_2 and temperature, the calculated apparent thermal conductivity values for UP/VE-Nov and UP/VE-Nov/phenolic resin blends as skins in a sandwich structure under cone calorimetry at 50 kW/m^2 heat flux

Sample	Top surface temperature [a] (°C)	Time to reach TC_1=TC_2 [b] (s)	Temp. when TC_1=TC_2 [b] (°C)	Apparent thermal conductivity, *k* of composite (kW/m.K × 10^{-3})	
				600 s	1000 s
UP	650	474	645	2.8	4.2
VE-Nov	620	813	630	3.1	4.7
UP/VE-Nov:50/50	605	500	603	3.4	4.6
UP/VE-Nov/Methylon:35/35/30	600	643	597	3.6	4.7

a = Cone calorimetry - Taken as when surface temperature, TC_1 becomes constant

b = Top upper surface = just underneath the upper surface

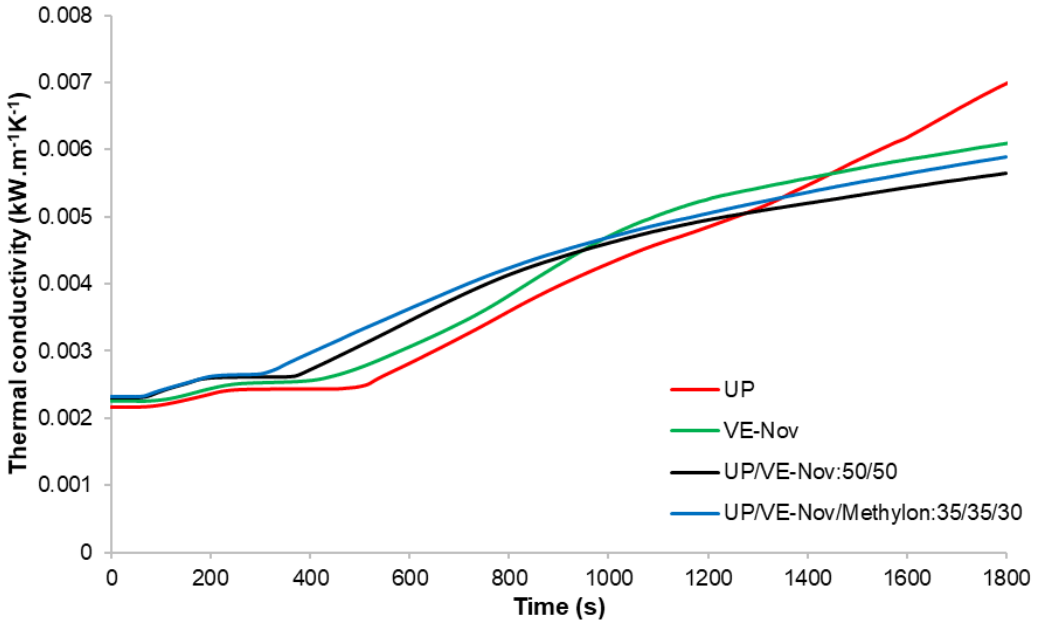

Figure 5.25: Calculated apparent thermal conductivity curves of UP/VE-Nov and UP/VE-Nov/phenolic resin blends as skins in sandwich composites

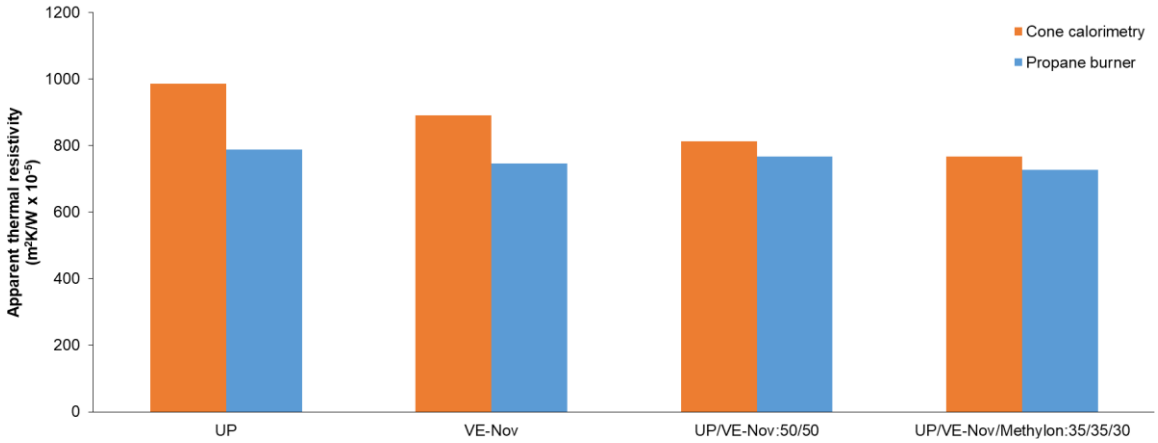

Figure 5.26: Apparent thermal resistivities of sandwich composite structures with UP/VE-Nov and UP/VE-Nov/phenolic resin blends at 600 s under cone and propane burner tests

5.2.2.3 Propane burner testing

From the results for UP, VE, UP/VE-Nov and UP/VE-Nov/phenolic blends shown in Figure 5.27 and Table 5.16, temperature profiles of UP/VE-Nov:50/50 are not much different than UP or VE-Nov until 450 s, and after that, its behaviour is similar to that of the UP sample. UP/VE-Nov:50/50 sample shows a shorter time (970 s) to reach 300 °C on the back surface than respective UP or VE-Nov, which is further reduced with phenolic presence in UP/VE-Nov/Methylon (783 s). A similar trend was observed for temperature profiles from cone calorimetric results before ~900 s (Figure 5.24 (b)). UP/VE-Nov produced slightly higher char (38%) than UP or VE-Nov (35, 36%) as shown in Table 5.16, further increasing with phenolic presence in UP/VE-Nov/phenolic sample (40%). This trend is similar to the char residue results in cone calorimetric tests (Table 5.13).

From propane burner testing, the thermal barrier performances of sandwich structure composites among UP, VE, UP/VE-Nov and UP/VE-Nov/PH-Res blends are ranked according to the time to reach 300 °C (s), the longer the better, as follows:

VE-Nov > UP > UP/VE-Nov:50/50 > UP/VE-Nov/Methylon:35/35/30.

A reverse trend was seen from the PHRR values in the cone results for sandwich composites given in Table 5.13, i.e., the lower PHRR values in cone results, the higher the temperature profiles in propane burner tests (Figure 5.27).

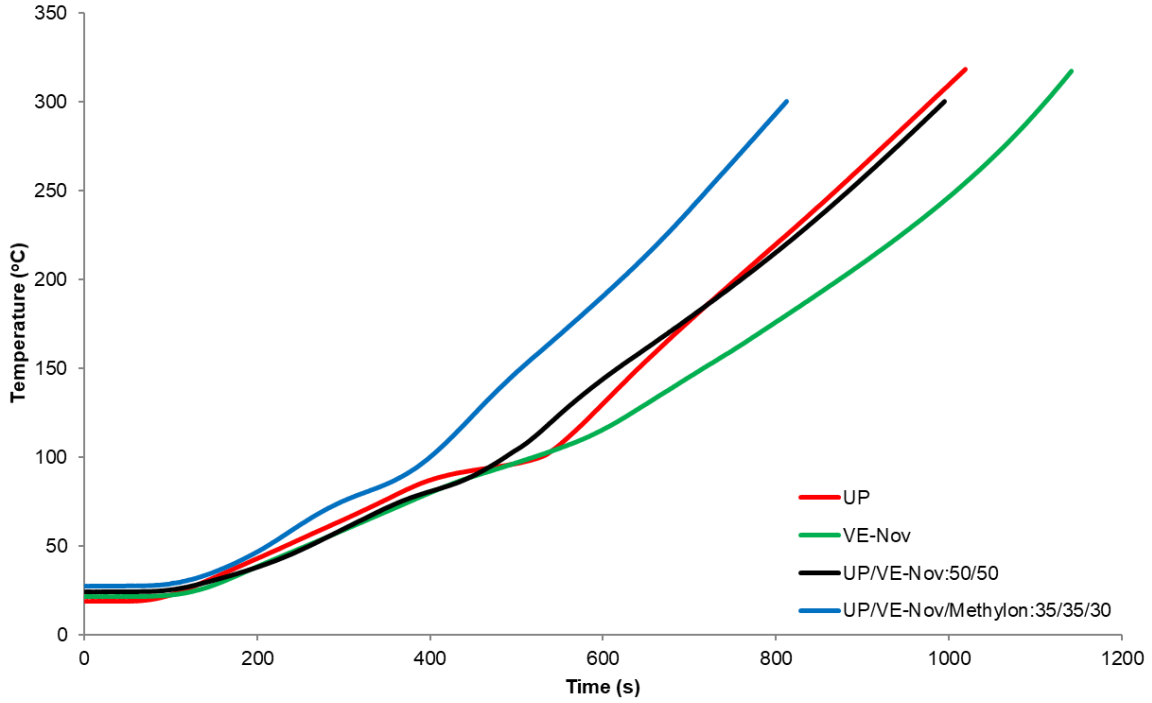

Figure 5.27: Back surface temperature versus time curves for sandwich structures among UP, VE, UP/VE-Nov and UP/VE-Nov/PH-Res blends obtained from propane burner testing

Table 5.16: Top surface temperatures, residues after propane burner testing and times to reach 300 °C for sandwich structures with balsa core thicknesses of 25.4 mm (1 inch) for UP, VE, UP/VE-Nov, UP/VE-Nov/PH-Res as skins

Sample	Top surface temperature * (°C)	Residue (wt%)	Glass content (wt%)	Char (wt%)	Time to reach 300 °C (s)
UP	1000	46	11	35	1000±28
VE-Nov	950	50	14	36	1128±21
UP/VE-Nov:50/50	1000	53	15	38	970±35
UP/VE-Nov/Methylon:35/35/30	1000	55	15	40	783±42

* = In propane burner tests, while TC_{front} becomes constant.

It can be seen from Figure 5.28 and Table 5.17 that the UP/VE-Nov blend shows intermediate thermal conductivity curves/values than those of respective UP and VE-Nov controls, whereas with additional phenolic presence in UP/VE-Nov/Methylon blend as skins, there is a noticeable increase in the thermal conductivity. This trend is similar to that seen in UP/phenolic and VE/phenolic blends in previous sections.

The apparent thermal resistivity values are plotted in Figure 5.26, where as expected their thermal insulating performances of UP/VE-Nov and ternary blends are less than UP or VE-Nov. On comparing bar chart results from cone and propane burner tests in Figure 5.26, comparable results from both tests can be seen.

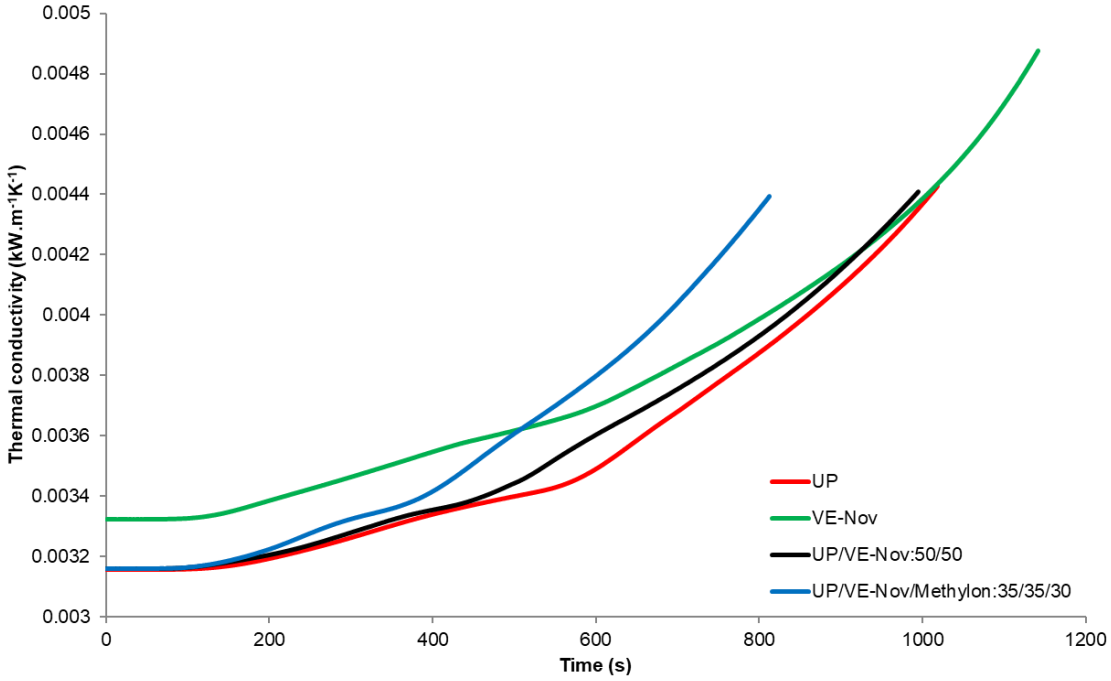

Figure 5.28: Apparent thermal conductivity versus time curves for sandwich structures among UP, VE, UP/VE-Nov and UP/VE-Nov/PH-Res blends obtained from propane burner testing

Table 5.17: Calculated thermal conductivities for sandwich composites with skins of UP/VE-Nov and UP/VE-Nov/phenolic blends at particular times from the propane burner tests

Sample	Apparent thermal conductivity, *k* of composite (kW/m.K × 10^{-3})		
	600 s	700 s	800 s
UP	3.5	3.7	3.9
VE-Nov	3.7	3.8	4.0
UP/VE-Nov:50/50	3.6	3.8	3.9
UP/VE-Nov/Methylon:35/35/30	3.8	4.0	4.4

5.3 Fire performance of sandwich composite structures with top layer of phenolic resin

In this section, fire and thermal barrier performances of sandwich composite structures with skins made of first three layers of glass fabrics impregnated with UP or UP/VE-Nov resin and the fourth (top) layer of phenolic resin (Methylon), namely 3UP1M or 3UP/VE1M, respectively, have been discussed. The rationale of applying a top layer of phenolic resin is that the top layer may act as a flame-retardant coating.

5.3.1 Cone calorimetry

From Figure 5.29 and Table 5.18, it can be seen that in composites with skins of top layer of phenolic resin, TTI of sample 3UP1M (UP with top one layer of Methylon) is slightly higher than that of UP (31 *vs.* 24 s), whereas TTI does not show much difference for 3UP/VE1M (UP/VE-Nov; top one layer of Methylon) from UP/VE-Nov (26 - 27 s). FO time is similar for both samples with top one layer of Methylon (3UP1M and 3UP/VE1M). PHRR values of both 3UP1M and 3UP/VE1M were reduced compared to respective controls UP and UP/VE-Nov (216 *vs.* 294 kW/m^2, 239 *vs.* 301 kW/m^2), indicating that one thin layer of phenolic resin is acting as a flame retarded coating in this case. In UP and 3UP1M, THR was reduced up to 30 minutes for 3UP1M (34 *vs.* 46.5 MJ/m^2) due to the presence of Methylon, but TSR was much higher than that of UP control (2103 *vs.* 1121 m^2/m^2). Methylon had a lower TSR than that of UP from cone results for cast resins (Table 3.4), but here TSR is higher. In composite samples the balsa core also burns, chars and smoulders, which releases smoke as well, and TSR is a combination of smoke released from both resin part and balsa, hence erratic variations. By contrast, in UP/VE-Nov and 3UP/VE1M, it can be seen from Table 5.18 that THR for 3UP/VE1M was reduced till the end of first HRR peak while the main burning stage took place, however an increase in THR occurred after 30 minutes (21.7 *vs.* 24.0, 35.9 *vs.* 30.6 MJ/m^2), with also a slight reduction in TSR (2992 *vs.* 3394 m^2/m^2). Not surprisingly, char residues after 10 minutes of cone tests of 3UP1M or 3UP/VE1M were higher than respective controls (37 - 43 *vs.* 34%), which could be explained due to the presence of char-forming phenolics as a top layer of the skins, i.e., because of a greater number of relatively stable aromatic benzene rings in their chemical structures. Same trend can be seen from the end of cone tests as well (30 minutes).

Both 3UP1M and 3UP/VE1M samples show better fire performances via their reductions in PHRR and THR, as well as forming slightly more charred residue, in spite of producing similar amounts of or more smoke. Due to burning and charring for both samples with one top layer of Methylon, as observed from the side view (Table A4-1), these two samples do not show pronounced gaps/break into small blocks on charred balsa and seem to have a good entity. In addition, the bottom laminate did not delaminate and still had some resin left in both samples. More unburnt resin, and less charred residue but darkened resin could be seen on the back surfaces of both samples with phenolics on the top. Thus, designing composites with top one layer of phenolics reduces flammability of the composite structure.

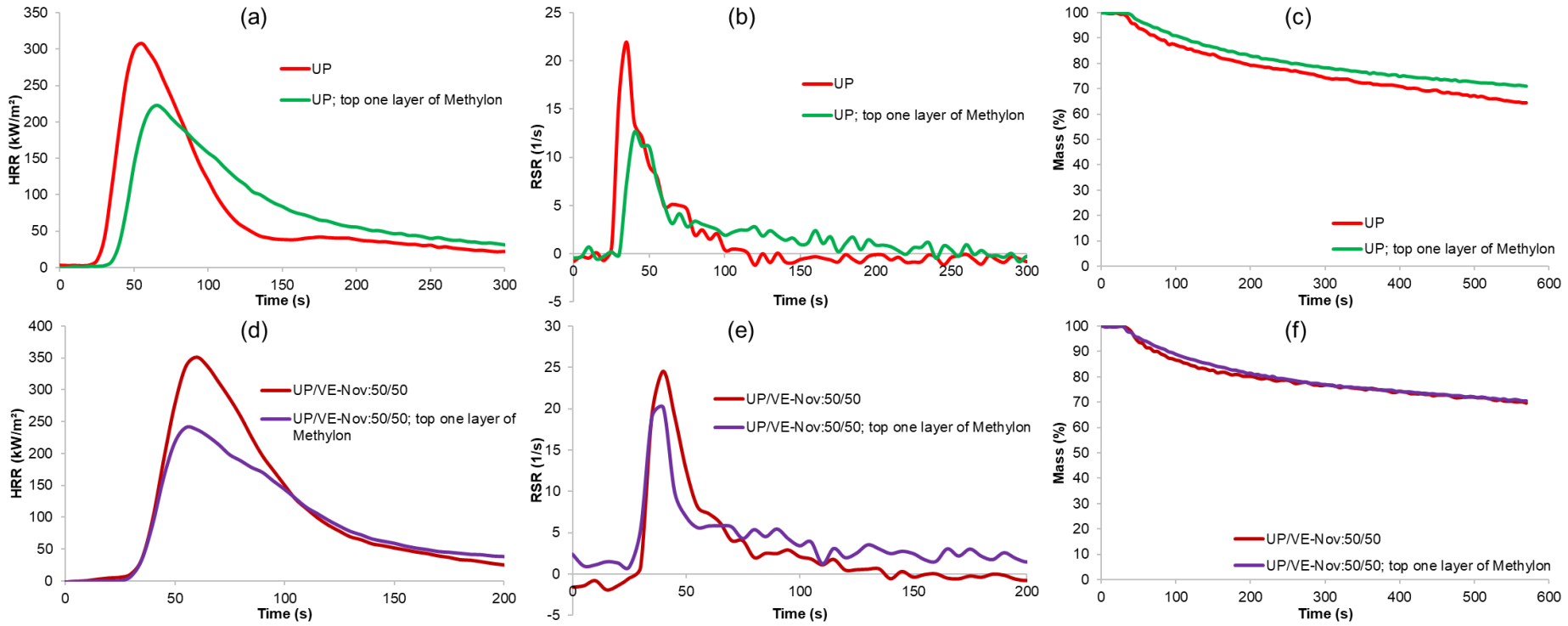

Figure 5.29: Plots of (a, d) HRR, (b, e) RSR and (c, f) mass loss *vs.* time for sandwich composites with skins of (a, b, c) UP and UP; top one layer of Methylon and (d, e, f) UP/VE-Nov and UP/VE-Nov; top one layer of Methylon

Table 5.18: Derived cone calorimetric results of sandwich composites with skins containing different resin blends – UP, UP with top one layer of Methylon, UP/VE-Nov, UP/VE-Nov blends with top one layer of Methylon

Sample ID	TTI (s)	FO (s)	PHRR (kW/m^2)	THR (MJ/m^2)		TSR (m^2/m^2)		Residue [b] (wt%)	
				5 mins [a]	30 mins	5 mins [a]	30 mins	10 mins	30 mins
UP	24	1296	294	23.5	46.5	554	1121	67 (34)	48 (17)
UP; top one layer of Methylon (3UP1M)	31	1049	216	23.9	34	596	2103	71 (43)	56 (24)
UP/VE-Nov:50/50	27	918	301	24.0	30.6	637	3394	70 (34)	55 (21)
UP/VE-Nov:50/50; top one layer of Methylon (3UP/VE1M)	26	1017	239	21.7	35.9	917	2992	71 (37)	54 (22)

Notes: TTI = time-to-ignition, FO = time-to-flame-out, PHRR = peak heat release rate, THR = total heat release, TSR = total smoke release. The reproducibility in cone parameters was ±5%. The variation in values for different parameters are as: TTI = ±2; FO = ±78; PHRR = ±44; THR = ±4.4; TSR = ±634; Residue = ±2. a: End of first peak was defined for the initial 300 s of cone tests to be more comparable for all samples while the first peak decreased to a minimum and constant state from the specimen tested up to 10 minutes. b: For residue (wt%), values in the parentheses are after compensating for glass content (8 layers of glass fabric, 4 on each side of top and bottom skins).

5.3.2 Thermal barrier performance during cone experiments

Temperature *vs.* time profiles obtained from thermocouples inserted underneath the top and bottom skins in Figure 5.30 show that T_{max} on the top skins' back surface reached about 640 - 700 °C (Table 5.19) for UP, UP/VE-Nov, 3UP1M and 3UP/VE1M. From the temperature profiles of the top skin's back surface temperature shown in Figure 5.30 (a, c), 3UP1M has a lower rate of temperature rise than that of UP shown by lower temperature at the beginning of cone temperature measurement till the end of tests (30 minutes). Whereas in the case of UP/VE-Nov:50/50 and 3UP/VE1M, these two curves do not show much difference. From T_{max} on the top skins' back surface, both 3UP1M and 3UP/VE1M samples show reduced T_{max} compared with respective controls UP or UP/VE-Nov. More pronounced effect was observed in 3UP1M sample, which is 67 °C lower than that of UP control.

From the bottom skins' back surface temperature (Figure 5.30 (b, d)), some differences were seen for samples of UP and 3UP1M, whereas similar behaviours for UP/VE-Nov and 3UP/VE1M samples were observed. There is a steady state of temperature profiles at ~100 ºC for all samples between 200 - ~500 s, UP shows the longest duration of steady state among the four, followed by UP/VE-Nov:50/50, 3UP/VE-Nov1M (both quite similar) and was further reduced in 3UP1M. Also, 3UP1M has a lower rate of temperature rise than that of UP after ~800 s up to 30 minutes, reflected by an 85 °C lower temperature of T_{max} on bottom skin (365 *vs.* 450 °C). By contrast, for samples of UP/VE-Nov and 3UP/VE1M (Figure 5.30 (d)), similar temperature profiles were seen as that for top skins' back surface temperature profiles, and not much differences can be observed from the beginning till the end of cone tests (365 - 370 °C). The T_{max} on bottom skins' back surface for 3UP1M and 3UP/VE1M is same (Table 5.19), both at 365 °C, which is lower than respective UP or UP/VE-Nov control samples, indicating the top one layer of phenolic resin on both sides of sandwich composites lowered the rate of temperature rise of charred residues.

T_{max} on the bottom skins' back surface temperature was used to rank the thermal barrier performances of different sandwich composites for 3UP1M or 3UP/VE1M, the trend in terms of thermal barrier effect from high to low being:

$$3UP1M = 3UP/VE1M > UP/VE\text{-}Nov{:}50/50 > UP.$$

Compared to those cone results given in Table 5.18, both samples with top one layer of phenolics show reduction in PHRR as well as THR, and also relatively better thermal barrier effects in terms of their temperature profiles can be observed (Figure 5.30), indicating slightly lower thermal conductivity of the charred residue for the sandwich composites with top one layer of phenolic resin (Methylon), in which it acted as a thin protective coating.

The temperature of the top skin was around 255 - 305 °C hotter than the bottom skin (Table 5.19). Also, ΔT in samples of 3UP1M or 3UP/VE1M, 3UP1M sample shows an increase (+18 °C), whereas 3UP/VE1M shows similar ΔT compared with that of respective UP or UP/VE-Nov controls.

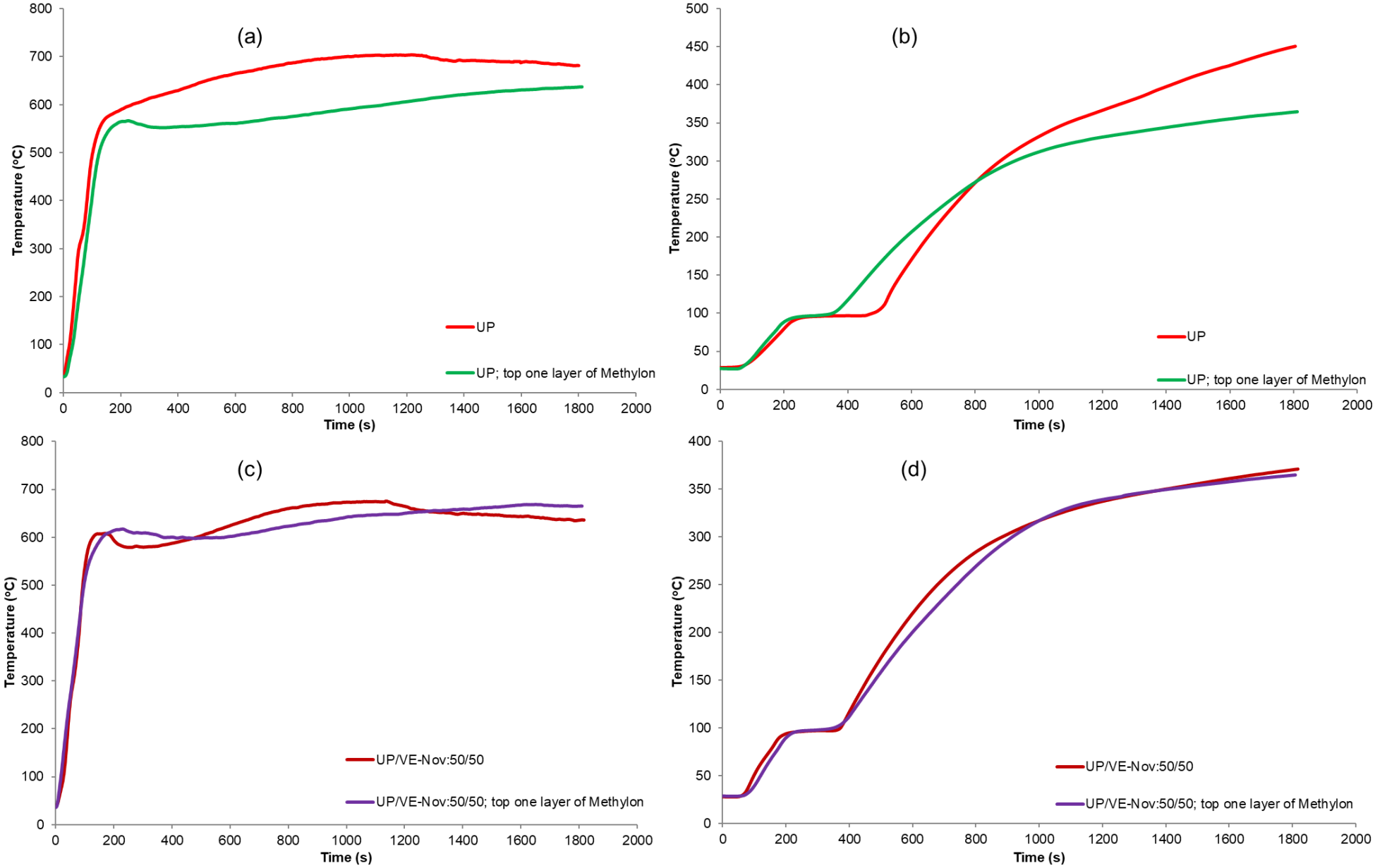

Figure 5.30: Plots of (a, c) top skin, TC_2 and (b, d) bottom skin's (TC_5) back surface temperature *vs*. time for sandwich composites with skins of (a, b) UP and UP; top one layer of Methylon and (c, d) UP/VE-Nov and UP/VE-Nov; top one layer of Methylon

Table 5.19: Time to reach different temperatures and maximum temperature (T_{max}) of top and bottom skins' back surfaces during the cone calorimetric testing among sandwich composites with skins of top layer of phenolic resin

Sample ID	Time to reach back surface temperature (s) of									Maximum Temperature T_{max} (°C)		ΔT (T-B) (°C)
	Top skin				Bottom skin							
	$t_{300\ °C}$	$t_{400\ °C}$	$t_{500\ °C}$	t_{Tmax}	$t_{100\ °C}$	$t_{300\ °C}$	$t_{400\ °C}$	$t_{500\ °C}$	t_{Tmax}	T	B	
UP	53	81	101	1218	476	878	1415	-	1800	704	450	254
UP; top one layer of Methylon	77	98	124	1800	351	923	-	-	1800	637	365	272
UP/VE-Nov:50/50	61	80	93	1138	373	883	-	-	1800	675	370	305
UP/VE-Nov:50/50; top one layer of Methylon	57	77	97	1649	348	915	-	-	1800	669	365	304

Notes: T - Top skin's back surface, B - bottom skin (and composite)'s back surface, '-' in the table indicated maximum temperature during the testing did not reach the certain temperature.

ΔT (T-B) - Maximum back surface temperature difference between top and bottom skins

Table 5.20: Time to reach TC_1=TC_2 and temperature, the calculated apparent thermal conductivity values for UP or UP/VE-Nov with top one layer of Methylon as skins in a sandwich structure under cone calorimetry at 50 kW/m^2 heat flux

Sample	Top surface temperature [a] (°C)	Time to reach TC_1=TC_2 [b] (s)	Temp. when TC_1=TC_2 [b] (°C)	Apparent thermal conductivity, *k* of composite (kW/m.K × 10^{-3})	
				600 s	1000 s
UP	650	474	645	2.8	4.2
UP; top one layer of Methylon	600	974	590	3.4	4.6
UP/VE-Nov:50/50	605	500	603	3.4	4.6
UP/VE-Nov:50/50; top one layer of Methylon	605	749	619	3.3	4.6

a = Cone calorimetry - Taken as when surface temperature, TC_1 becomes constant

b = Top upper surface = just underneath the upper surface

Thermal barrier performance evaluation

As can be seen from Figure 5.31, the apparent thermal conductivity of 3UP1M is slightly higher than UP until ~1400 s and then UP is increased significantly. 3UP/VE1M sample did not show much difference than the UP/VE-Nov. It seems that applying the top one layer of Methylon mainly does not affect the properties of chars of the underlying layers of UP or UP/VE-Nov while reducing the overall flammability of the composites in terms of reduction in PHRR and THR (cone results). From values of apparent thermal conductivity shown in Table 5.20 for composites of 3UP1M and 3UP/VE1M, both samples showed very similar values at both 600 s and 1000 s.

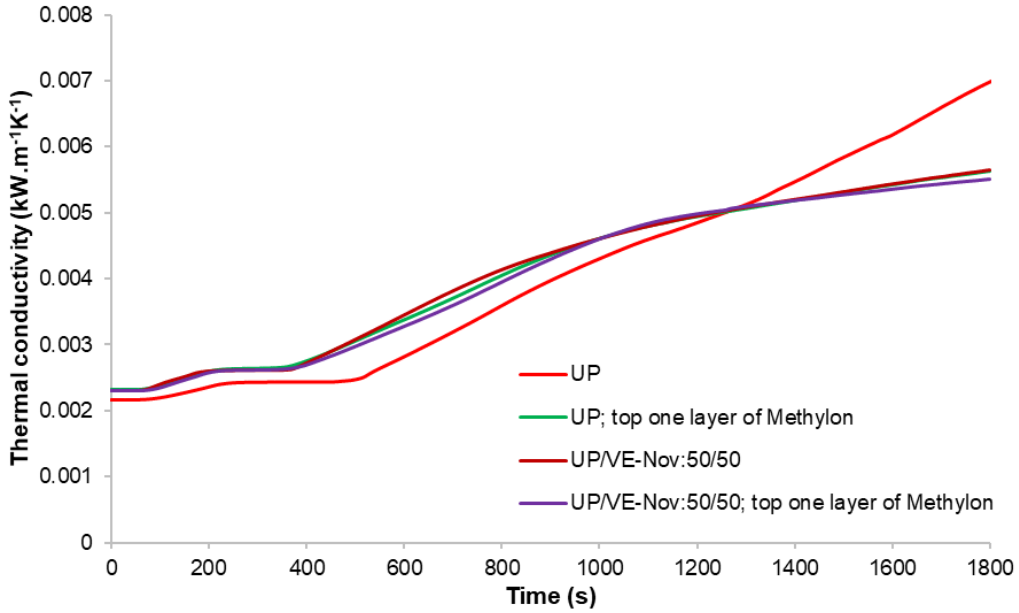

Figure 5.31: Calculated apparent thermal conductivity curves of UP or UP/VE-Nov with top one layer of Methylon as skins in sandwich composites

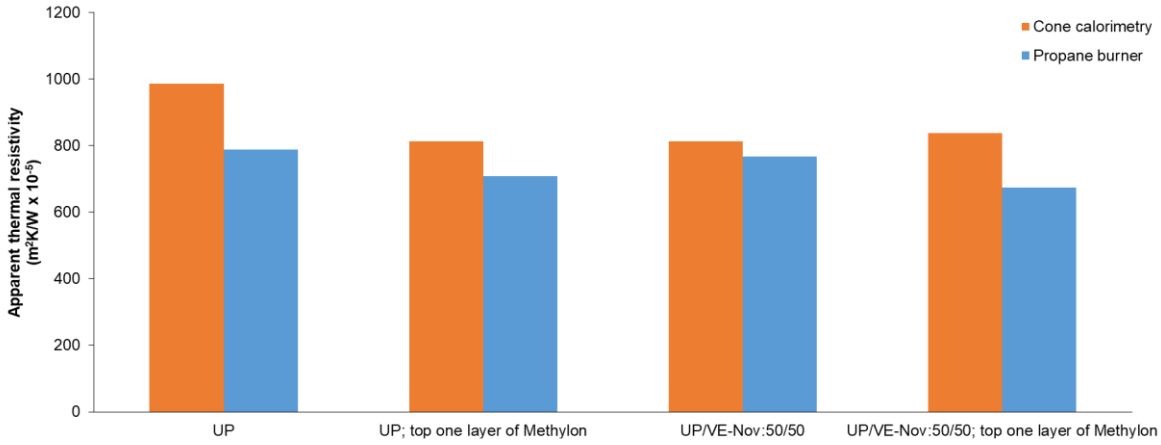

Figure 5.32: Apparent thermal resistivities of sandwich composite structures with UP or UP/VE-Nov with top one layer of Methylon at 600 s under cone and propane burner tests

5.3.3 Propane burner testing

From temperature profile results shown in Figure 5.33 and Table 5.21, it can be observed that, 3UP1M takes a similar time to reach 300 °C as UP, considering standard variation in results (985 *vs.* 1000 s). In the case of UP/VE-Nov and 3UP/VE1M, both samples do not show much difference until 200 s, and after that, the rate of temperature rise in 3UP/VE1M is much quicker than in UP/VE-Nov sample. 3UP/VE1M takes a much shorter time to reach 300 °C than respective UP/VE-Nov (612 *vs.* 970 s).

The thermal barrier performances of sandwich structure composites ranked according to the time to reach 300 °C (s), the longer the better, is as follows:

UP ≈ 3UP1M ≈ UP/VE-Nov:50/50 > 3UP/VE1M.

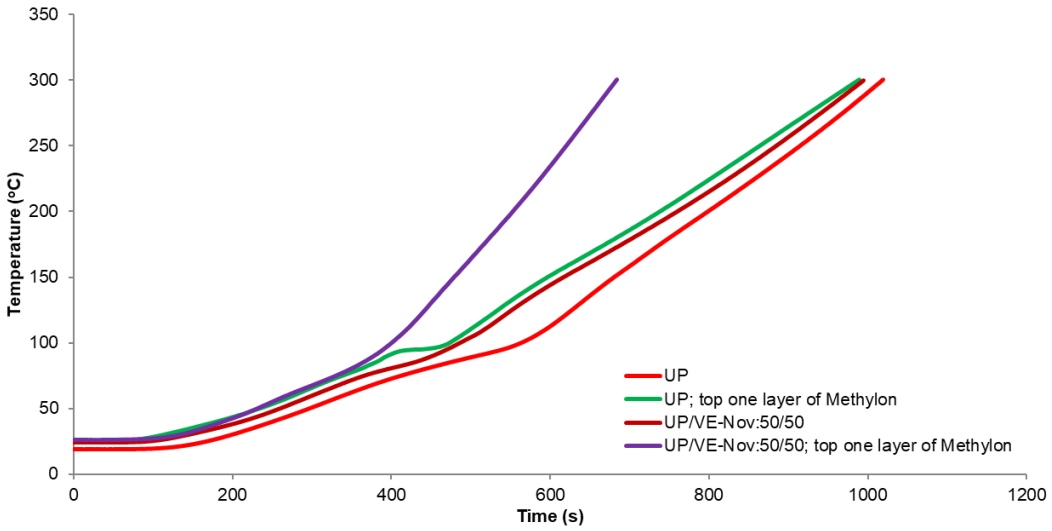

Figure 5.33: Back surface temperature versus time curves for sandwich structures between UP, UP; top one layer of PH-Res blends and UP/VE-Nov, UP/VE-Nov; top one layer of PH-Res blends obtained from propane burner testing

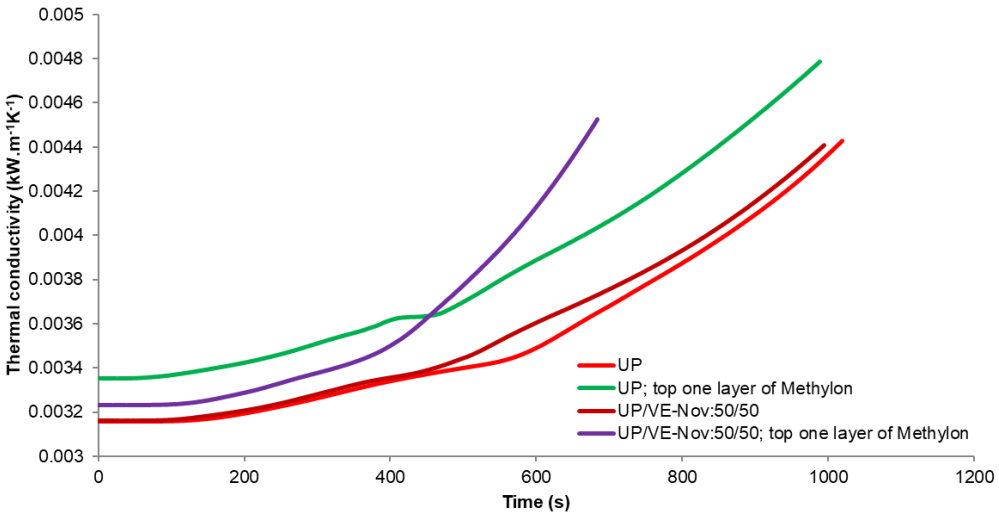

Figure 5.34: Apparent thermal conductivity versus time curves for sandwich structures between UP, UP; top one layer of PH-Res blends and UP/VE-Nov, UP/VE-Nov; top one layer of PH-Res blends obtained from propane burner testing

Table 5.21: Top surface temperatures, residues after propane burner testing and times to reach 300 °C for sandwich structures with balsa core thicknesses of 25.4 mm (1 inch) for UP, UP with top one layer of PH-Res, UP/VE-Nov, UP/VE-Nov blends with top one layer of PH-Res as skins

Sample	Top surface temperature * (°C)	Residue (wt%)	Glass content (wt%)	Char (wt%)	Time to reach 300 °C (s)
UP	1000	46	11	35	$1000_{\pm 28}$
UP; top one layer of Methylon	945	49	17	32	$985_{\pm 6}$
UP/VE-Nov:50/50	1000	53	15	38	$970_{\pm 35}$
UP/VE-Nov:50/50; top one layer of Methylon	985	48	15	33	$612_{\pm 102}$

* = In propane burner tests, while TC_{front} becomes constant.

From Figure 5.34, both 3UP1M and/or 3UP/VE1M show higher thermal conductivity than those of respective UP or UP/VE-Nov constituents. The designing of a composite by applying top one layer of Methylon, noticeably increases the thermal conductivity of sandwich composites. This behaviour in the propane burner test is similar to that seen for resin blends of UP/phenolic, VE/phenolic or UP/VE-Nov/phenolic, which could be due to the conductive nature of phenolic resin's char on the top of UP or UP/VE-Nov char.

Table 5.22: Calculated thermal conductivities for sandwich composites with skins of top layer of phenolic resin at particular times from the propane burner tests

Sample	Apparent thermal conductivity, *k* of composite (kW/m.K × 10^{-3})		
	600 s	700 s	800 s
UP	3.5	3.7	3.9
UP; top one layer of Methylon	3.9	4.1	4.3
UP/VE-Nov:50/50	3.6	3.8	3.9
UP/VE-Nov:50/50; top one layer of Methylon	4.1	-	-

- = Test stopped prior to 700 s due to back surface temperature reached 300 °C hence its thermal conductivity for sandwich composites could not be calculated

According to the apparent thermal conductivities reported in Table 5.22, 3UP1M or 3UP/VE1M show slightly higher thermal conductivity values for the composites at 600 s, more pronounced for 3UP1M at different times (700 and 800 s). In addition, compared with those results from cone experiments (see Figure 5.32), in general, similar trends of apparent thermal resistivities of sandwich composites with 3UP1M or 3UP/VE1M under both cone and propane burner tests were seen. Thermal resistivities of top one layer of phenolic (Methylon) were lowered compared to those of underlying resins (UP or UP/VE-Nov resin only) used as skins for sandwich composites as expected.

5.4 Conclusions

In this chapter, sandwich composites with different types of neat resins, resin blends and with top layer of phenolic resins have been studied. From the cone calorimetric results of sandwich composites, the flammability of samples with neat resins could be ranked as:

$$Ep \approx Elium > VE\text{-}Ep > VE\text{-}Nov > UP\text{-}R \approx UP$$

This trend for composites was similar to that seen from cone results of cast resins. The differences in maximum temperatures of back surfaces of top and bottom skins of all samples, ΔT was used as a measure of thermal gradient. The VE-Nov composite, had the highest ΔT value among all samples indicating that its char has a better thermal barrier performance than the others.

All UP or VE/phenolic blends showed lower flammability than respective control samples. The increase in phenolic content in blends generally further reduced the flammability. The application of one top layer of phenolic resin helped in reducing the flammability of the composites more than using the blends.

The temperature profiles in propane burner tests showed a higher rate of temperature rise than in cone results due to a higher heat flux and different heat source (propane gas flame) in the former as opposed to radiant heat in the latter. Apparent thermal conductivities, calculated from the differences in top and bottom surface temperatures of the composites, were higher for samples containing phenolic resins. The apparent thermal conductivity values of different components indicated that the nature of the charred residue in different layers plays an important role in determining the thermal performance of the whole sandwich composite.

5.5 References

[1] J. A. Rockett and J. A. Milke, “Conduction of heat in solids,” in *SFPE handbook of fire protection engineering*, 2nd ed., Chapter 2, National Fire Protection Association, Quincy, MA, USA, 1995, pp. 1–25.

[2] C. Zhang, *Reliability of Steel Columns Protected by Intumescent Coatings Subjected to Natural Fires*, vol. 21, no. 4. Berlin, Heidelberg: Springer Berlin Heidelberg, 2015.

[3] Q. Yuan, D. Huang, Y. Hu, L. Shen, L. Shi, and M. Zhang, “Comparison of Fire Behaviors of Thermally Thin and Thick Rubber Latex Foam under Bottom Ventilation,” *Polymers*, vol. 11, no. 1, p. 88, 2019.

[4] J. Murphy, *The reinforced plastics handbook*. Oxford: Elsevier Advanced Technology, 1998.

[5] D. Rosato and D. Rosato, *Reinforced Plastics Handbook*, 3rd ed. Oxford: Elsevier, 2005.

[6] H. Derek, *An introduction to composite materials*, 1st ed. Cambridge Solid State Science Series, Cambridge: Cambridge University Press, 1981.

[7] B. T. Lattimer, J. Ouellette, and J. Trelles, “Thermal Response of Composite Materials to Elevated Temperatures,” in *Modeling of Naval Composite Sturctures in Fire*, L. S.

Couchman and A. P. Mouritz, Eds. Cooperative Research Centre for Advanced Composite Structures, 2006, pp. 1–46.

[8] *End grain balsa core, FLEXOKORE, Property Table Data sheet*. West Walpole Street, NE33 5BY, UK: East Coast Fibreglass Supplies Ltd, 2016.

[9] "Thermal conductivity of Phenolic," 2018. [Online]. Available: https://www.makeitfrom.com/material-properties/Phenol-Formaldehyde-PF-Phenolic. [Accessed: 01-Jul-2019].

[10] J. D. Monk, E. W. Bucholz, T. Boghozian, S. Deshpande, J. Schieber, C. W. Bauschlicher, and J. W. Lawson, "Computational and Experimental Study of Phenolic Resins: Thermal–Mechanical Properties and the Role of Hydrogen Bonding," *Macromolecules*, vol. 48, no. 20, pp. 7670–7680, Oct. 2015.

[11] J. T. Mottram and R. Taylor, "Thermal conductivity of fibre-phenolic resin composites. Part II: Numerical evaluation," *Composites Science and Technology*, vol. 29, no. 3, pp. 211–232, 1987.

[12] R. D. Patton, C. U. Pittman, L. Wang, J. R. Hill, and A. Day, "Ablation, mechanical and thermal conductivity properties of vapor grown carbon fiber/phenolic matrix composites," *Composites - Part A: Applied Science and Manufacturing*, vol. 33, no. 2, pp. 243–251, 2002.

[13] H. Derek, *An introduction to composite materials*, 1st ed. Cambridge Solid State Science Series, Cambridge: Cambridge University Press, 1981.

[14] B. Mutnuri, "Thermal conductivity characterization of composite materials", MSc thesis, West Virginia University, Morgantown, West Virginia, 2006.

Chapter 6: Conclusions and recommendations for future work

The main aim of this research was to investigate the thermal properties and fire resistance of some light weight sandwich composites, that could be potentially used in marine applications. To achieve this firstly resins commonly used for marine application (unsaturated polyester (UP) and vinyl ester (VE)) were selected. To compare these with other resins, some commonly used resins for other applications and some inherently fire-resistant resins, which could be used alone or blended with UP and/or VE were selected.

Selected resins included:

- Unsaturated polyester: two resins, UP and UP-R, with similar chemical structures but different styrene contents, hence viscosities. UP-R has lower viscosity and is commercially used for resin infusion purpose.
- Vinyl ester: two resins, VE-Ep (epoxy based) and VE-Nov (novolac phenolic based).
- Epoxy: Ep, commonly used in the aerospace industry.
- Elium: a liquid thermoplastic acrylic resin.
- Phenolics: two resins, an alcohol-soluble resole (Durez) and an allyl-functionalised resole (Methylon).

The blends prepared and studied included:

- UP/phenolic: one UP with two types of phenolics; UP/Durez and UP/Methylon, in 70/30 and 50/50 wt% ratios
- VE/phenolic: two VE with two types of phenolics; VE-Ep/Durez, VE-Nov/Durez, VE-Ep/Methylon, VE-Nov/Methylon, in 70/30 and 50/50 wt% ratios
- UP/VE-Nov, 50/50 wt% ratio

Resins were cast into plaques and characterised for their physical, chemical, morphological, thermal properties and fire performances (*Chapter 3*). Then the best design for a sandwich composite and its method of preparation was established using one of the UP resins and studying the effects of different preparation techniques, lay-ups and thicknesses of core materials on the fire and thermal barrier performances. Based on the results, one type of composite structure and preparation technique were selected for further studies (*Chapter 4*). A number of sandwich composites were then prepared using different resins and resin blends/combinations as matrices for skins, using balsa core of similar thickness. Their fire and thermal barrier properties were studied and results analysed to select parameters that could be used to assess their overall fire-resistant properties (*Chapter 5*).

The main conclusions drawn from this study are presented in the following sections.

6.1 Materials properties (*Chapter 3*)

All resins and their blends were cast into plaques. The curing conditions were established based on DSC results or taken from the results of previous studies. UP, VE, Ep and Elium were cured at room temperature followed by post-curing at 80 °C for 3-6 h, however, VE-Ep needed an additional step at 140 °C for 3h. Phenolics needed curing at elevated temperatures up to 220 °C using multiple steps in order to have void-free plaques and ensure complete curing (Table 2.1, Chapter 2).

The curing conditions of all the blends were more complex (Table 2.2), the conditions had to be adjusted to cure UP or VE first and then the phenolic part.

6.1.1 Morphology and physical properties

- All neat cast resins were clear and smooth. UP, UP-R, VE-Ep, VE-Nov, Ep and Elium sample plaques were relatively flat, however both phenolic resin plaques had slightly convex top surfaces indicating shrinkage during curing. In phenolics the colour darkened probably owing to some chemical degradation and molecular rearrangement during curing.

- The glass transition temperature (T_g), an important parameter for thermosets, was measured by DMTA. Cured UP resins had lower T_g values (92 - 121 °C) than cured VE resins (116 - 157 °C). Cured Ep and Elium had relatively higher T_g values (133 and 134 °C, respectively), whereas cured phenolic resins, Durez and Methylon, had the highest T_g values (277 and 295 °C, respectively).

- In the case of resin blends, good miscibility was observed in UP/Methylon, VEs/Methylon and UP/VE-Nov blends indicated by single T_g values in the DMTA traces of the blends. On the other hand, while UP/Durez was visually clear with no signs of phase separation, relatively poorer miscibility was observed from DMTA results indicated by two T_g values. In both VE/Durez blends total phase separation was observed, both visually as well as from the DMTA results.

6.1.2 Flammability

As an indication of thermal stability and potential flammability, thermogravimetric analysis (TGA) tests were conducted on all cured resins and resin blends under nitrogen and air. The onset of decomposition temperature (T_{onset} ($T_{10\%}$), where 10% mass loss occurs) and % residue remaining at 550 °C were chosen to assess flammability in terms of their relationship with other flammability tests. For flammability, pyrolysis combustion flow calorimetry (PCFC) and cone calorimetry were carried out. The combined conclusions from these results are given below.

6.1.2.1 TGA T_{onset} data versus cone TTI

T_{onset} from TGA data can give information about the ignition. The value of T_{onset} ($T_{10\%}$) values from the TGA data under air *vs.* TTI (time to ignition) for neat resins are plotted in Figure 6.1, where it can be seen that the correlation between the two parameters is reasonable.

All UP and VE resins ignited similarly at ~40 s, Ep had a slightly higher TTI (58 s). Among the phenolics only Methylon had a higher TTI (68 s), whereas Durez ignited at 38 s. Elium had the lowest TTI, and ignited at 20 s.

The correlation between $T_{10\%}$ and TTI among resin blends was less good than that of neat resins, which could be attributed to poor compatibility of the components in some blends as demonstrated by two T_g values in the respective DMTA results. All blends showed intermediate TTI between values of the two respective components, the only exceptions were both UP/Durez blends, in which lower compatibility was indicated by the presence of two T_g values.

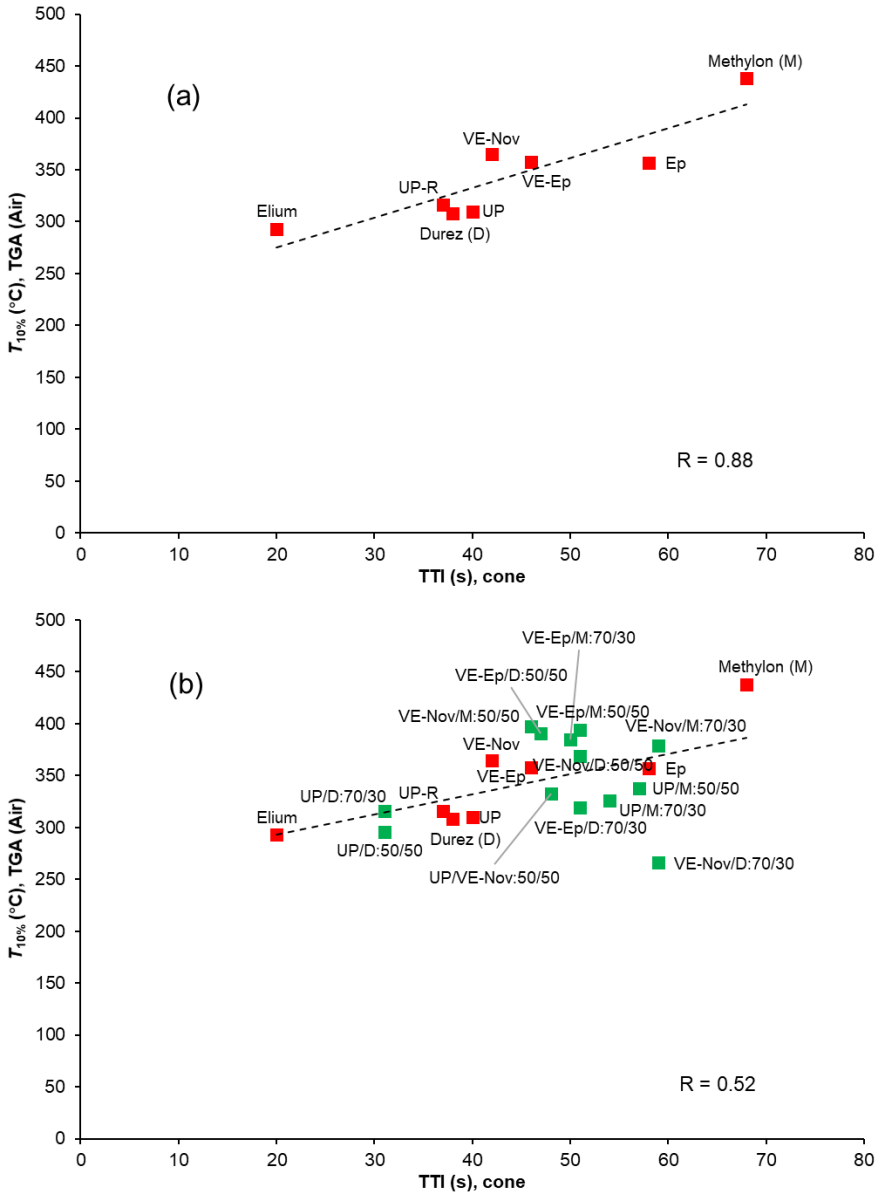

Figure 6.1: Plot of $T_{10\%}$ from TGA data under air *vs.* TTI from cone calorimetric data for (a) cured neat resins, and (b) cured neat resins and resin blends

6.1.2.2 TGA char yield in N_2 versus LOI

Char residue from TGA is an indication of the flammability of the material; the higher the value, the less flammable the material should be [1]. Limiting oxygen index (LOI), defined as the minimum concentration of oxygen required to sustain burning, is a measure of a polymer's flammability. While an LOI study was not conducted in this work, LOI data for selected UP, phenolic resins and their blends were available from previous work [2], which has been used to plot LOI against char yields from TGA in N_2 in Figure 6.2. A good correlation can be seen, as previously observed by other researchers [1,3].

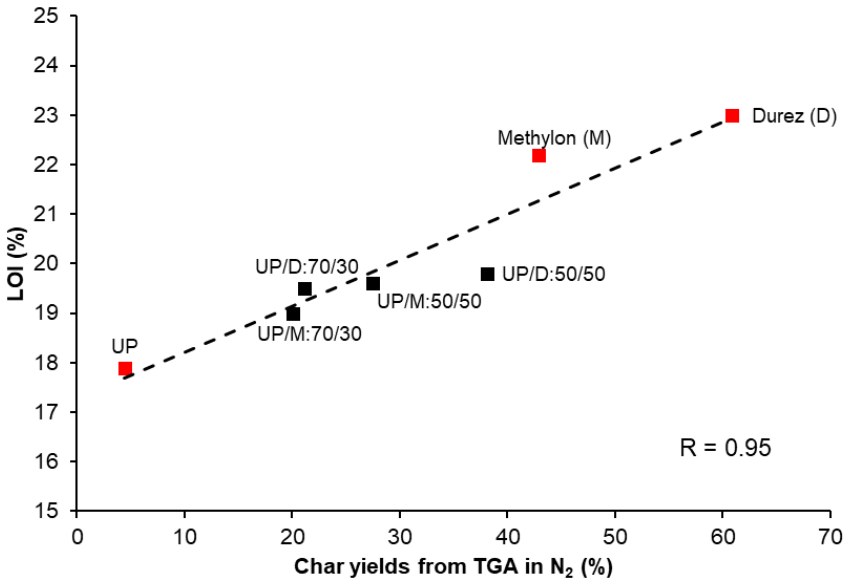

Figure 6.2: Plot of char yields from TGA in N_2 *vs.* LOI

This shows that phenolics have lower flammability than UP and flammability of the blends are in between those.

6.1.2.3 Char yield and PHRR from PCFC relationships

There is also a linear relationship between char residues from TGA under N_2 and from cone calorimetric tests as seen from Figure 6.3, particularly for neat resins. Resin blends showed less correlation than neat resins. Phenolics as expected produced more char than all other neat resins followed by VE-Nov. The amount of char produced in resin blends was in between the values of the respective two components. The overall correlation is reasonable.

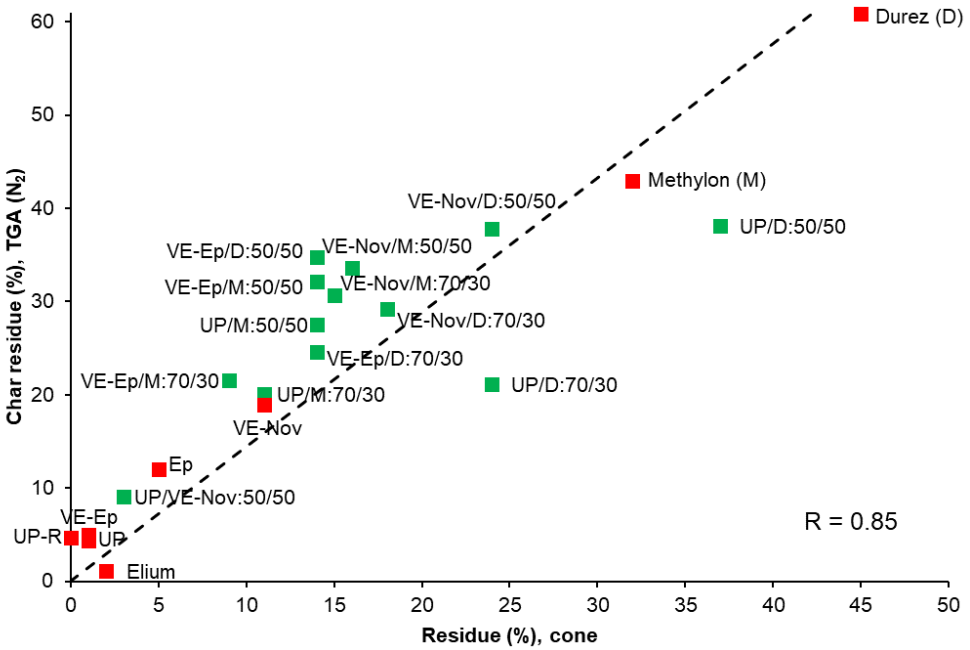

Figure 6.3: Plot of char residue from TGA under N_2 *vs.* cone calorimetry

Char yield values of blends were also used to observe any interactions between different components in a blend. The experimental and expected char residues from TGA in both atmospheres and cone calorimetry are given in Table 6.1, the expected values shown in parentheses were calculated from residue values of individual components via the rule of mixtures. In UP/Durez there is some interaction (higher degree of crosslinking) during decomposition as the experimental values are much higher than calculated ones. UP/Methylon showed less interaction than UP/Durez. Both VEs/Durez generally showed less interactions, and are considered, therefore, more likely to be physical mixtures compared to the UP/Durez blends, probably due to there being more phase separation in the VEs/Durez blends.

Table 6.1: Experimental *vs.* expected (calculated from values of individual components using the rule of mixtures, given in parentheses) char residues from TGA data under air and nitrogen atmospheres and cone calorimetry

Resin	Residue remaining at 550 °C (wt%)		Residue (wt%)
	TGA		Cone calorimetry
	Air	N_2	
UP/Durez:70/30	36.8 (18.0)	21.1 (21.3)	24 (14.2)
UP/Durez:50/50	48.7 (30.0)	38.1 (32.6)	37 (23)
UP/Methylon:70/30	20.8 (13.1)	20.1 (15.9)	11 (10.3)
UP/Methylon:50/50	19.2 (21.9)	27.5 (23.6)	14 (16.5)
VE-Ep/Durez:70/30	12.0 (18.0)	24.6 (21.8)	14 (14.2)
VE-Ep/Durez:50/50	37.9 (30.0)	34.8 (33.0)	14 (23)
VE-Nov/Durez:70/30	24.0 (23.5)	29.2 (31.5)	18 (21.2)
VE-Nov/Durez:50/50	43.0 (35.5)	37.8 (39.9)	24 (28)
VE-Ep/Methylon:70/30	24.0 (13.1)	21.6 (16.4)	9 (10.3)
VE-Ep/Methylon:50/50	35.0 (21.9)	32.1(23.9)	14 (16.5)
VE-Nov/Methylon:70/30	29.6 (18.6)	30.7 (26.1)	15 (17.3)
VE-Nov/Methylon:50/50	35.4 (27.4)	33.6 (30.9)	16 (21.5)
UP/VE-Nov:50/50	2.1 (3.6)	9.1 (11.6)	3 (6)

For the char residue difference for all blends, calculated between the % changes in experimental and calculated char from TGA and cone calorimetry, and % changes in PHRR from PCFC were calculated and presented in Table 6.2 in order to investigate the possible interactions occurring between composite components. A positive value indicates that there is some positive interaction between components in terms of char enhancement and with respect to PHRR, a negative value indicates a fire retardant promoting interaction. It is noticeable that changes in increased TGA char may correspond to a reduced PHRR in PCFC values since increased char will reduce flammable volatile formation and hence flammability. It is evident that for most samples a positive char enhancement is accompanied by a negative PHRR from PCFC trend. Conversely, a negative TGA char value despite not very common means that there is an antagonism between the components which could lead to increased PHRR in PCFC (i.e., increased flammability) values, although this effect is not observed here. It should be noted that the errors in determining char residues in TGA, cone and PHRR in PCFC values are generally within 5%, hence the difference % values of <1 or 2 % should be neglected as being within reasonable error.

Table 6.2: % Changes in experimental and expected char residues from TGA data under air and nitrogen atmospheres and cone calorimetry *vs.* % changes in PHRR values from PCFC

Resin	ΔResidue remaining at 550 °C (wt%)		ΔResidue (wt%)	ΔPHRR (%)
	TGA		Cone calorimetry	PCFC
	Air	N_2		
UP/Durez:70/30	+18.8	-0.2	+9.8	-13.2
UP/Durez:50/50	+18.7	+5.5	+14	-40.1
UP/Methylon:70/30	+7.7	+4.2	+0.7	-36.6
UP/Methylon:50/50	-2.7	+3.9	-2.5	-50.4
VE-Ep/Durez:70/30	-6	+2.8	-0.2	*
VE-Ep/Durez:50/50	+7.9	+1.8	-9	*
VE-Nov/Durez:70/30	+0.5	-2.3	-3.2	*
VE-Nov/Durez:50/50	+7.5	-2.1	-4	*
VE-Ep/Methylon:70/30	+10.9	+5.2	-1.3	-36.3
VE-Ep/Methylon:50/50	+13.1	+8.2	-2.5	-37.3
VE-Nov/Methylon:70/30	+11	+4.6	-2.3	-26.6
VE-Nov/Methylon:50/50	+8	+2.7	-5.5	-37.6
UP/VE-Nov:50/50	-1.5	-2.5	-3	-3.2

Notes:
"*" Samples were not tested due to the incompatibility in those blends.
For TGA and cone calorimetric data, "+" indicates positive and "-" negative using experimental subtract expected values.
% changes in PHRR from PCFC were calculated using results from Table 3.3 (b), (experimental - expected values)/expected values*100%; for instance, UP/Durez:70/30, (230-265)/265*100% = -13.2%.

Derived from Table 6.2, the correlations for PHRR difference (%) in PCFC data *vs.* char difference (%) from TGA in air and N_2, as well as cone calorimetry are plotted in Figure 6.4. Figure 6.4 (a) shows little or no correlation between PHRR *vs.* TGA char in air dependence; Figure 6.4 (b) shows the expected negative PHRR *vs.* char relationship with a relatively good

correlation suggesting that the TGA nitrogen condition reflects the expected relationship discussed; Figure 6.4 (c) shows a similar absence of correlation similar to that in (a). That Figure 6.4 (a) and (c) trends are similar suggests that reductions in PHRR values from PCFC experiment do not reflect the changes in TGA or cone chars in air. This is not surprising since the PCFC is generating volatiles under nitrogen whereas both TGA chars in air and cone chars in air are formed in the same atmospheric environment.

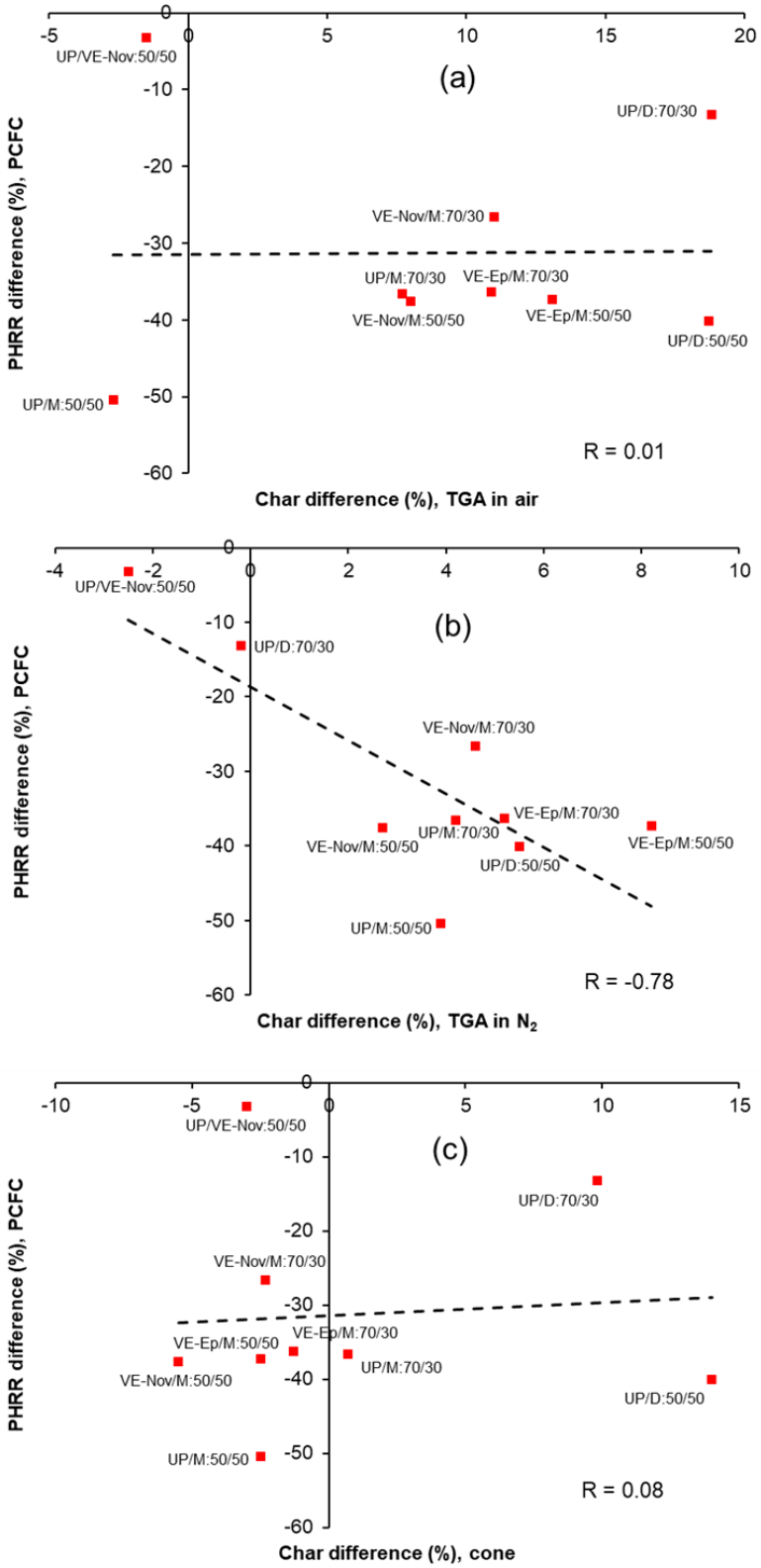

Figure 6.4: Plots of PHRR difference (%) in PCFC *vs.* char difference (%) from (a) TGA in air, (b) TGA in N2, and (c) cone calorimetry

6.1.2.4 Correlation between PCFC and cone calorimetry

In order to see if PCFC (Pyrolysis Combustion Flow Calorimetry) can be used to assess the flammability of the resins as in principle as accurately as from cone calorimetry; the correlation between important parameters from both tests were studied.

In PCFC, the main parameters of interest are HRC (Heat Release Capacity) and THR (Total Heat Release). HRC is the PHRR (Peak Heat Release Rate) divided by the heating rate; the latter is constant during tests and hence the HRC can be correlated with PHRR from cone. The HRC from PCFC and PHRR from cone, as well as THR from both tests are plotted in Figure 6.5 (a) and (b), respectively.

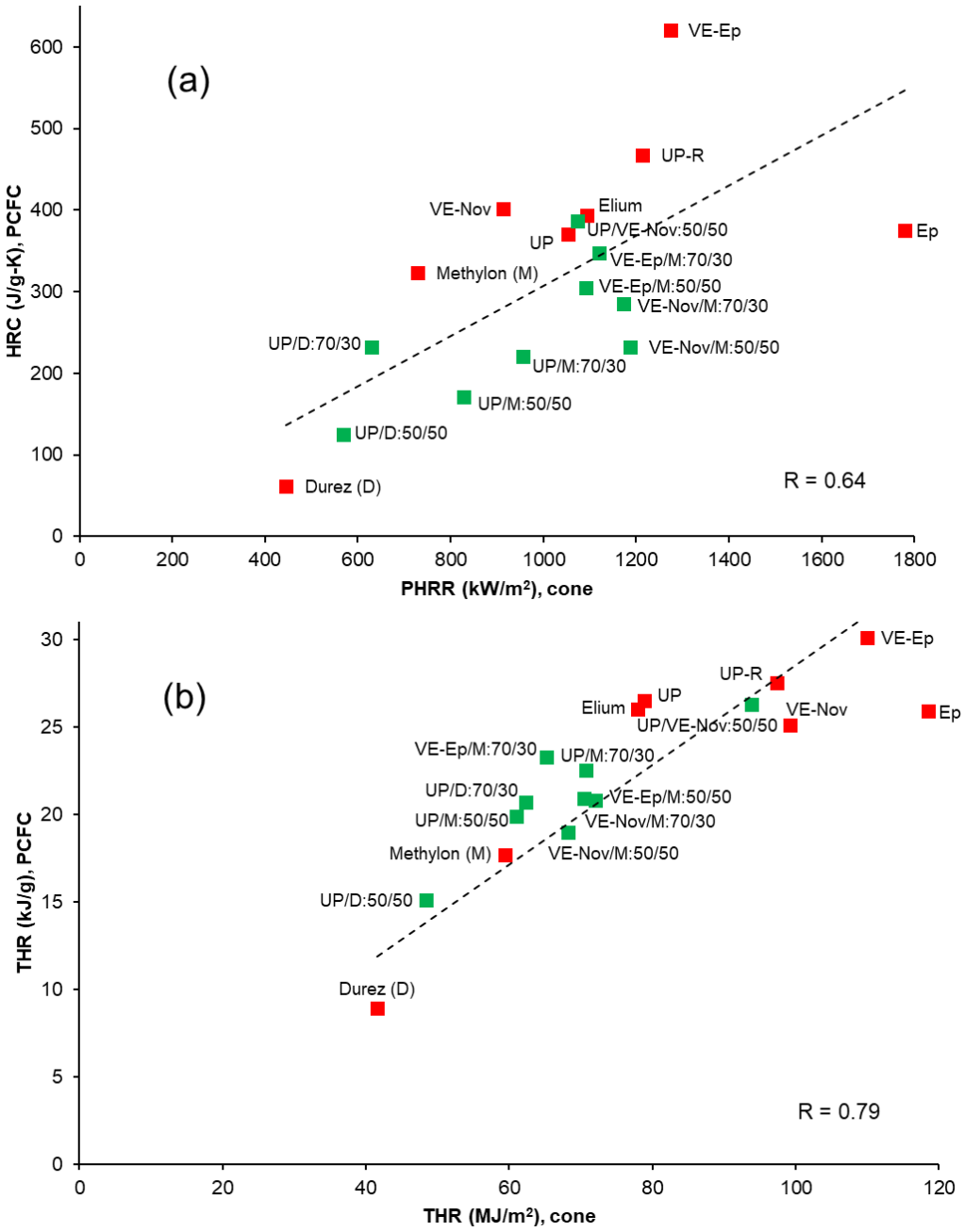

Figure 6.5: Plots of (a) HRC *vs.* PHRR and (b) THR from PCFC tests and cone calorimetric data for different cured neat resins and resin blends

THR of results between both tests showed good correlation, which is expected as THR in both tests is evaluated by the amount of heat released throughout the decomposition / combustion process based on the oxygen consumption theory. The slight deviations can be explained due to different sample geometries in both tests. However, less correlation was observed in PHRR and HRC, but considering variation in PHRR values in cone test, the correlation is satisfactory.

6.1.2.5 PCFC data versus TGA char yield in N_2

In order to investigate if the char yield from TGA in nitrogen can be related to the flammability parameters from PCFC, the char yield has been plotted against THR and HRC in Figure 6.6 (a and b). The correlation between THR and char yield is very good and is better than that between HRC and char yield.

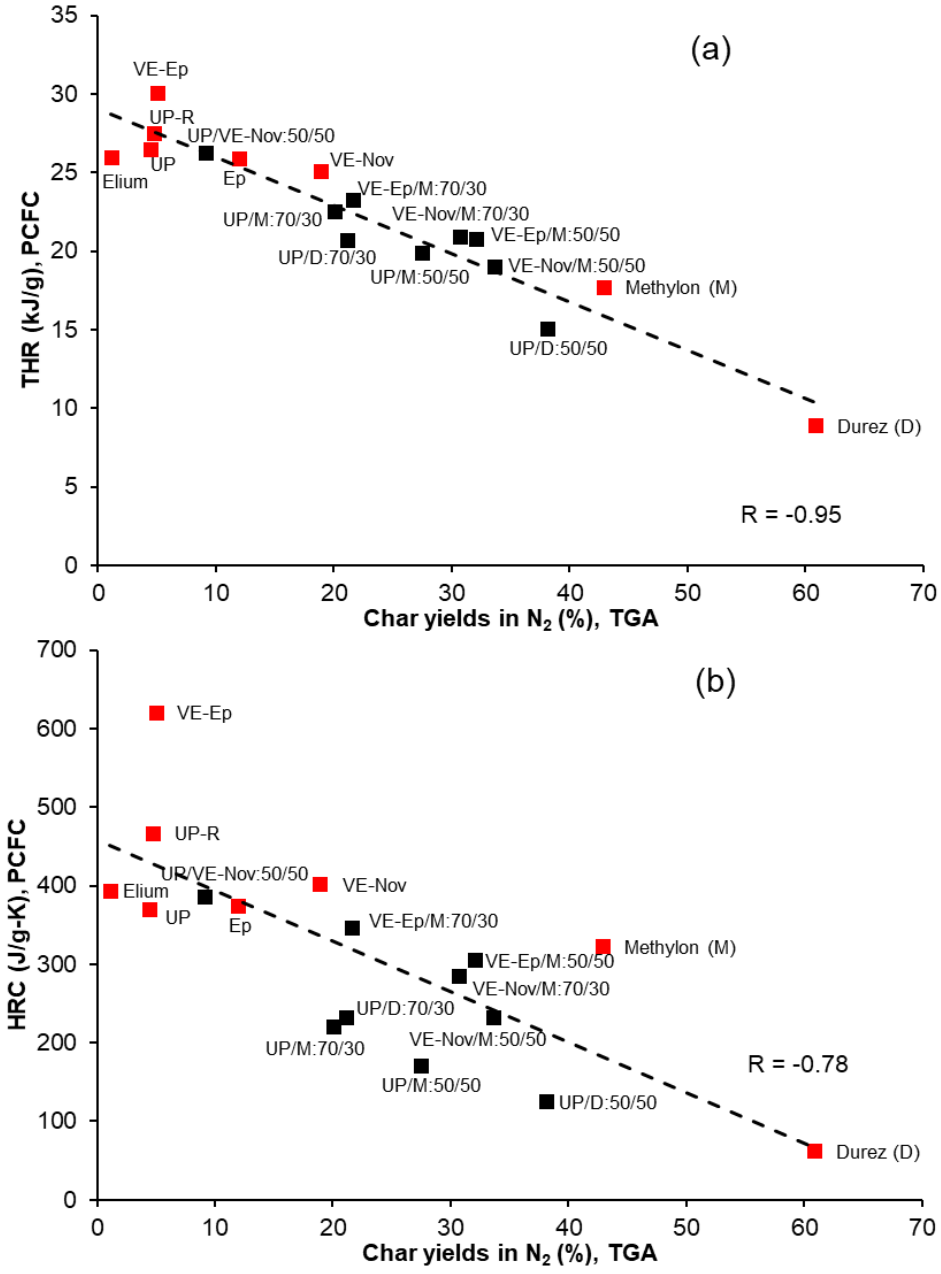

Figure 6.6: Plots of (a) THR, and (b) HRC from PCFC *vs.* char yields from TGA in N_2

Overall, this work has shown that small scale tests such as TGA and PCFC can give a good indication of the flammability of the materials. For overall flammability evaluation we need, however, a number of parameters rather than just one.

6.1.3 Fire safety of resins

Since in PCFC there are two main parameters of importance, namely HRC and THR, and in cone three, TTI, PHRR and THR, it is difficult to choose one parameter for ranking the overall performance. Hence, all critical parameters need to be taken into account. Here two fire safety diagrams are introduced based on the two tests. In Figure 6.7 (a) THR in PCFC is plotted against HRC and in Figure 6.7 (b) THR from cone tests is plotted against the flashover propensity values (calculated by dividing PHRR by TTI). Fire safe materials are expected to have low THR and HRC values in PCFC, and low THR and PHRR/TTI values under cone, meaning that they should have short fire durations and slow fire growth. Such materials should fall close to the coordinates (0;0) on a 2-D plot.

Fire safety assessment diagrams from both PCFC and cone tests show similar but not the same trends, which is expected, because in PCFC, one parameter, TTI is missing.

- Based on fire safety assessment diagrams from the cone test results, fire safety of neat resins can be ranked as:

  Durez > Methylon > UP > VE-Nov > UP-R > VE-Ep > Ep > Elium

- Fire safety of blends lies in between those of the respective components. In general, 50/50 blends showed higher fire safety than the respective 70/30 blends. UP/phenolic-based systems showed higher fire safety than respective VEs/phenolic-based ones. The general trend for fire safety from high to low among different blends is as follows:

  UP/Durez > UP/Methylon* > VE-Ep/Durez > VE-Nov/Durez > VE-Nov/Methylon > VE-Ep/Methylon* > UP/VE-Nov

  *UP and VE-Ep/Methylon samples can be termed as more fire safe in terms of ‘slow fire growth’.

  Fire safety of both VE-Ep/Durez and VE-Nov/Durez has been evaluated here, but since the blends showed phase separation, these were not studied further in this project.

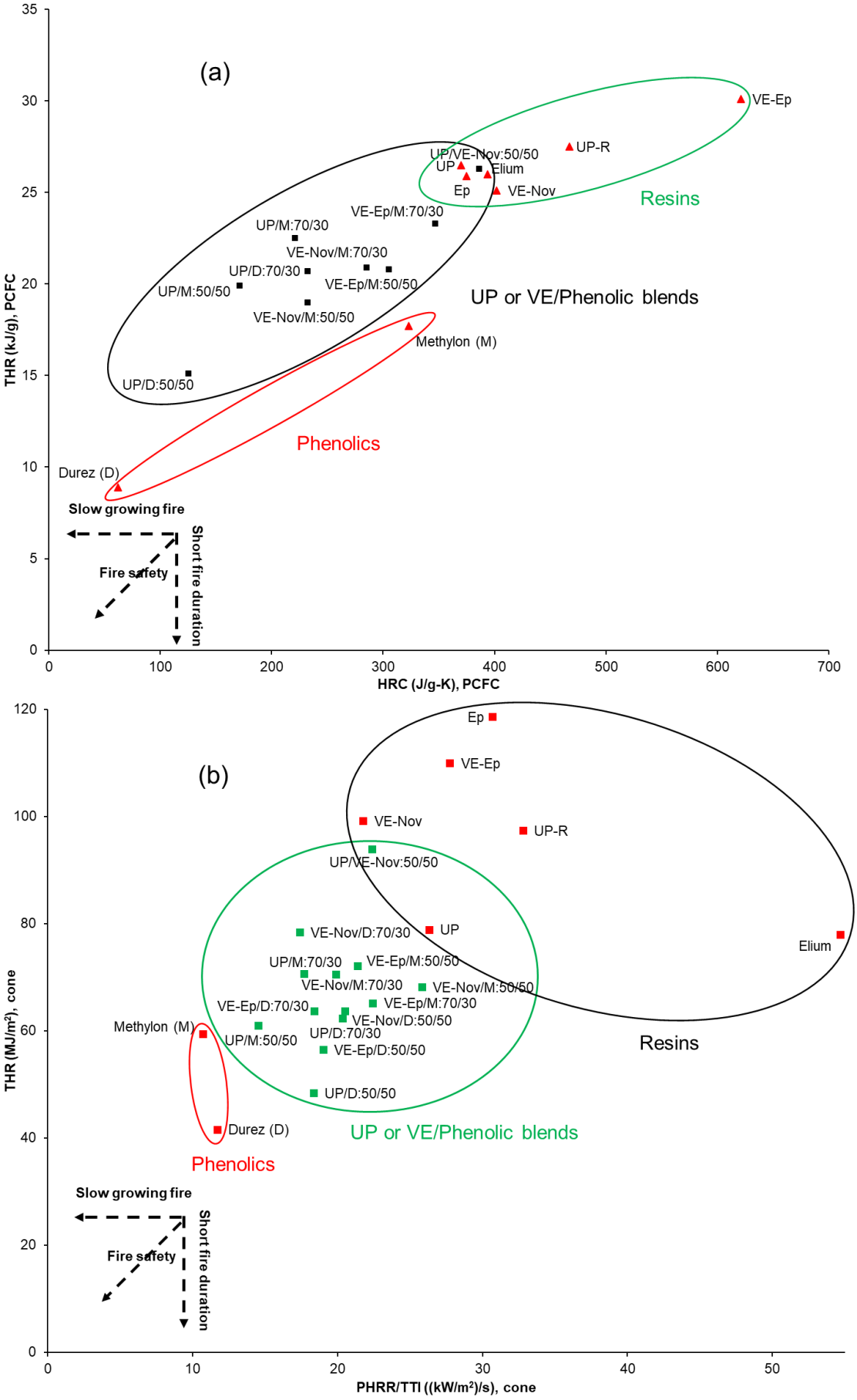

Figure 6.7: Fire safety diagrams of neat resins and resin blends (a) from PCFC, and (b) from cone calorimetry

6.2 Designing sandwich structure composites with similar components but different compositions (*Chapter 4*)

Sandwich composites with similar components (glass fibre-reinforced unsaturated polyester (UP) composite laminates as skins and balsa wood as a core) but with different compositions were prepared.

Design variables included:

(i) Cores of two different thicknesses (25.4 mm (1”) and 12.7 mm (0.5”))

(ii) Composite laminate as a skin on one side or both sides

For (i) and (ii), composite laminates for skins were prepared by the resin infusion technique

(iii) Different sample preparation techniques:

a) Resin infused laminates as skins on both sides [RI-UP]

b) Hand lay-up laminates as skins on both sides [HL-UP]

c) Hand lay-up sandwich structure in one go [HLAll-UP]

Their fire performances were evaluated by using two different standard fire tests: cone calorimetry and propane burner testing. Cone calorimetry was used in two orientations: horizontal and vertical; the latter was used because in the propane burner test the sample is in a vertical orientation. In order to understand variations in results, balsa wood on its own was also tested. Composite laminates used for skins were also tested on their own and the results compared with those of the sandwich structures and neat resins. The main conclusions drawn from this study are as follows:

- Burning behaviour of balsa wood

The cone results for balsa wood of the two different thicknesses showed a lot of variations, and also for the same thickness, the reproducibility of the results was very low. This is due to the fact that balsa wood is a natural product with variable density (150 ± 45 kg/m^3) along the same sheet. Also, balsa wood samples (as received) were made of blocks, glued together with a thin glass woven fabric on one side, while the other side had gaps. The position of these gaps varied in different samples, which may have affected their ignition and burning behaviours.

In both thick and thin samples, two peaks in the HRR were observed, while there was not much difference in the first peak, in thick samples it took much longer to reach the second peak. The mass loss rate of thick samples was slower than the thin ones due to slower degradation in the thick wood sample.

Heat transfer within each sample was measured by inserting thermocouples on the back surface during cone calorimeter and propane burner tests. The temperature profiles on the back surface at 50 kW/m^2 under cone were similar to the ones with 113 kW/m^2 heat flux in propane burner

tests. The temperature started rising after about 100 s, and after reaching 100 °C, remained steady for about 100 s under both tests, indicating the loss of moisture in the wood. The temperature rise rate then depended on the heat flux, as expected.

- Burning behaviour of resin as a neat resin, in a composite laminate and in a sandwich structure

The burning behaviours/flammability of composite laminate and the sandwich structure were very similar after taking standard variation into account. The TTI and PHRR were expected to be similar, the only difference was that the sandwich structure burned for a longer time. THR of the sandwich structure hence was much higher than that of the composite laminate due to longer burning of balsa wood in the former. The burning behaviour of the resin however was different from the other two. In general, the composite laminate and sandwich structure showed lower flammability than the individual cast resin.

- Effect of cone heater orientation

The cone heater orientation had a minimal effect on PHRR and THR values, the TTI in horizontal mode was though slightly higher than in the vertical orientation. Hence results for sandwich composites from two different cone heater orientations were comparable and still within acceptable experimental error. On comparing previous researcher's work [4,5] with this work, more differences in fire performances for sandwich composites between cone heater orientations were observed, probably due to gaps in balsa blocks, which could affect burning behaviours of the samples. Cone results from standard blocks of hardwood samples with no gaps [4,5], showed better reproducibility.

- Effect of thicknesses of core materials

UP/glass-balsa sandwich composite samples containing 1 or 0.5" thick balsa cores, i.e., HLAll-UP-1 and HLAll-UP-0.5, were tested for their fire performance. The 0.5" core sample showed higher PHRR than the 1" core sample, which arises from the physical and thermal thickness effects of the latter. THR for the 1" core sample was higher than for the 0.5" core sample due to the higher wood content of the thicker sample. The back surface temperature profiles of 1" core (physically thick) samples showed a better thermal barrier effect (lower heat transfer through the sample) than that of the 0.5" core one under both cone and propane burner tests. In addition, for 1" core samples under both tests, similar temperature profiles were seen despite different incident heat fluxes. But the 0.5" core sample did not show that trend. This could be due to the physical and thermal thickness of the 1" core sample, where the larger volume of the charred wood provided a better thermal barrier effect.

- Effect of composite laminates on one side or on both sides

Composite laminates of sandwich structures on one side or on both sides with the same thicknesses of balsa core and sample preparation techniques, i.e., RI-Top UP-1 and RI-UP-1, were investigated. Both samples gave similar results in cone tests, hence have similar flammability. For samples with skins on both sides, despite burning of the resin, the glass fabric on the rear side reduced the rate of burning, hence gave a lower mass loss rate. It has also been evident from both cone and propane burner tests that composites with laminates on both sides showed much better thermal barrier performances (lower heat transfer) than composites laminated on only one side.

- Effect of different sample preparation techniques

Cone results for UP/glass-balsa sandwich composites made with the same thickness of 25.4 mm (1") balsa core prepared by three different techniques, i.e., RI, HL and HLAll, showed that all three samples had very similar fire performances. Also trends in back surface temperature profiles under both cone and propane burner tests in vertical orientation were similar, indicating similar heat transfer within the sandwich composites.

6.3 Designing sandwich composite structures with different resin types and combinations (*Chapter 5*)

A number of sandwich composites were prepared where different resins and resin combinations were used in the skins, keeping all other composition variables constant. The latter were chosen based on the results in the above section as:

- Balsa core of 25.4 mm (1 inch) thickness
- Composite laminates with skins on both sides, each skin made of four glass fibre layers, but impregnated with different resin types
- Sample preparation technique i.e. hand lay-up sandwich structure in one go (HLAll)

Using different resin and resin combinations, the following three sets of sandwich composites were prepared:

Set 1. Different resin types: two UP types (UP and UP-R), VE-Ep, VE-Nov, Ep, Elium. Samples containing the two phenolic resins, Durez and Methylon could not be made due to the high viscosities of the resins.

Set 2. Blends of UP or VE with two phenolics:

- UP/Durez, UP/Methylon, 70/30 and 50/50 ratios
- VE-Ep/Methylon, VE-Nov/Methylon, 70/30 and 50/50 ratios
- UP/VE-Nov, 50/50 ratio
- UP/VE-Nov/Methylon, 35/35/30 ratio

Set 3. UP or UP/VE based composites with a top layer containing Methylon

- UP with Methylon in top layer (3UP1M)
- UP/VE-Nov:50/50 with Methylon in top layer (3UP/VE1M)

As in the previous section, their fire and thermal barrier performances were evaluated by cone calorimetry at 50 kW/m^2 in horizontal mode and propane burner tests at 113 kW/m^2 heat flux with thermocouples inserted at various locations in all samples. Top and bottom skin temperatures for sandwich composites under both testing methods were plotted, from which the apparent thermal conductivity and resistivity values for each component (top and bottom skins and balsa wood) as well as the sandwich composites were calculated. As with fire and thermal performances, samples with best performances in terms of improved flammability and prolonged burn-through time have been identified.

The main findings from this work are given in the following sections:

6.3.1 Fire performance of sandwich composites with skins containing different resin types

- Flammability

In the cone test, all samples ignited and times-to-ignition (TTI) were very similar (18 - 38 s), small variations though depended on the resin type, which is as expected as it is the resin in the top skin which ignites first. All samples had an intense PHRR and after the flame went out the heat release was reduced, reaching a minimum at ~120 s followed by a plateau. The sharp peak represented burning of the top skin, was accompanied by a sharp mass loss until ~120 s. This was followed then by a small flame due to burning of the balsa wood, sometimes re-igniting other parts of the wood where there were cracks in the wood, leading to a second very broad HRR peak of low intensity. In order to compare the fire performances of different resin types, here UP has been taken as control and changes in selected but significant parameters, i.e., PHRR, THR and char residue with respect to UP are presented in Table 6.3. The time taken for the back surface temperature of the sandwich composite to reach 300 °C, $t_{300\,°C}$, was used as a measure of the burn-through performance of the sandwich composite, and is also presented in Table 6.3.

Considering the fire performance of neat resins-based composites, it can be seen that both UP composites showed similar flammability, VE-Ep composite showed slightly higher flammability than that of VE-Nov, however, both VE composites were slightly more flammable than both the UP. Ep and Elium composites were more flammable than both UP and VE composites. These trends in results for composite structures were similar to the cone results for the cast resins (Chapter 3).

Table 6.3: Changes in selected cone and propane burner test parameters with respect to UP resin (selected as control)

	Cone calorimetry					Propane burner test	
	ΔPHRR (%)	ΔTHR at (%)		ΔChar at 30 mins (%)	$\Delta t_{300\ °C}$ (s)	ΔChar (%)	$\Delta t_{300\ °C}$ (s)
		5 mins	30 mins				
UP	0	0	0	0	0	0	0
UP-R	-4.1	+21.7	-16.3	-2	+45	-5	-29
VE-Ep	+10.9	+3.0	-22.4	+5	-113	-1	-135
VE-Nov	+9.5	-0.9	-10.1	+4	-9	+1	+128
Ep	+27.6	+11.1	-9.9	+5	+86	+2	+61
Elium	+16.0	+29.8	+1.3	+2	+39	*	*

Notes:
"+" indicates an increase and "-" a reduction.
* = Test not performed
$\Delta t_{300\ °C}$ = Δtime to reach 300 °C on bottom skin (s)

From this, flammability from high to low for neat resin-based composites in general could be ranked as follows:

$$Ep \approx Elium > VE\text{-}Ep > VE\text{-}Nov > UP\text{-}R \approx UP$$

- Thermal barrier performance

Thermal barrier performance of composites with different neat resins in the skins are ranked according to $\Delta t_{300\ °C}$ (the longer the better) as follows:

$$VE\text{-}Nov > Ep > UP \approx UP\text{-}R > VE\text{-}Ep.$$

This trend is similar in cone and propane burner test results, although some slight variations were observed due to different external heat fluxes in the two test rigs.

The VE-Nov containing composite sample, while showing worse flammability than UP in the cone test, showed better thermal insulating properties in the propane burner test.

- Thermal conductivities of chars

During some cone tests thermocouples were inserted at various locations throughout the samples, the temperature differences in different thermocouples were used to allow determination of the apparent thermal conductivities of the top skin, balsa core and bottom skin, respectively. In both cone and propane burner tests, the differences in top and back face temperatures were used to measure apparent thermal conductivities and resistivity values of

the whole composite's charred residue. This study gives an insight into the thermal barrier properties of the chars from different resin types.

Apparent thermal conductivities of different components:

Calculated apparent thermal conductivities for top skins containing UP and both VEs were similar, 0.2 kW/m.K × 10^{-3}, but slightly higher than the values for Ep and Elium (0.1 kW/m.K × 10^{-3}); these values are reasonably close to those reported in the literature.

The burning behaviour of balsa wood in all samples was similar, although slight variations in apparent thermal conductivities were seen. Since these composite samples were prepared by hand lay-up in one go technique, it is possible that some samples were resin rich and that during the curing stage under vacuum some resin might have diffused into the balsa wood, causing differences in burning behaviours of the wood in the different samples.

Bottom skins for the composites showed higher thermal gradients than top skins because the top surface of the bottom skin was exposed to much lower heat than the respective surface of the top skin, resulting in more char formation in the bottom skin. Hence, variations in apparent thermal conductivity values for different samples were more clearly seen. Among UP and VE composites, UP had a much lower thermal conductivity value than UP-R and both VEs at 600 s, whilst Ep had a higher value. The Elium containing sample had the lowest value, which is unexpected as it is the most flammable. However, since all the Elium resin burns away, leaving only separated glass layers, the gaps left between them assists insulation.

Overall, the UP containing composite sample displayed a better thermal insulation than the other samples.

The global value of apparent thermal conductivity for each composite was also calculated. Composites containing both UPs had lower overall thermal conductivities than those of both VE containing samples. Ep and Elium containing composites had the lowest overall thermal conductivities, whereas VE-Ep based composite had the highest value.

6.3.2 Fire performance of sandwich composite structures with different resin blends

- Flammability

In the cone calorimetric results, TTI for all blends were similar to those of the respective UP or VE controls. For comparing the fire performances of the resin blends, changes in vital parameters for each blend sample with respect to the corresponding control sample (UP, VE or UP/VE-Nov) are presented in Table 6.4.

Table 6.4: Changes in selected cone and propane burner test parameters of the blends with respect to [a]UP, [b]VEs or [c]UP/VE-Nov resins

	Cone calorimetry					Propane burner test	
	ΔPHRR (%)	ΔTHR at (%)		ΔChar at 30 mins (%)	$\Delta t_{300\ °C}$ (s)	ΔChar (%)	$\Delta t_{300\ °C}$ (s)
		5 mins	30 mins				
UP/Durez:70/30 [a]	-37.1	-34.0	-41.3	-4	-186	+6	-452
UP/Durez:50/50 [a]	-45.9	-23.4	-22.2	+3	+45	+5	-142
UP/Methylon:70/30 [a]	-35.7	-26.8	-43.4	+7	+33	±0	-127
UP/Methylon:50/50 [a]	-28.2	-6.4	-12.5	+4	+14	+1	-62
VE-Ep/Methylon:70/30 [b]	-22.1	±0	-19.1	-4	+6	+3	-21
VE-Ep/Methylon:50/50 [b]	-15.3	-7.9	-16.6	-4	-88	+1	-172
VE-Nov/Methylon:70/30 [b]	-6.8	-1.7	-1.9	-4	-117	-2	-233
VE-Nov/Methylon:50/50 [b]	-48.1	-21.9	-33.0	±0	-36	*	*
UP/VE-Nov:50/50 [a;b]	+2.4; +6.5	+2.1; +3.0	-34.2; -26.8	+4; ±0	+5; +14	+3; +2	-30; -158
UP/VE-Nov/Methylon:35/35/30 [c]	-25.6	-26.3	+10.5	+5	-11	+2	-187
UP; top one layer of Methylon (3UP1M) [a]	-26.5	+1.7	-26.9	+7	+45	-3	-15
UP/VE-Nov:50/50; top one layer of Methylon (3UP/VE1M) [c]	-20.6	-9.6	+17.3	+1	+32	-5	-358

Notes:
"+" indicates an increase and "-" a reduction.
* = Test not performed
$\Delta t_{300\ °C}$ = Δtime to reach 300 °C on bottom skin (s)

All blends showed lowered flammability than the respective control samples in terms of reduced PHRR and THR, as expected, the trends being similar to those seen for the cast resins (see Chapter 3, Table 3.4).

- Thermal barrier performance

As seen in Table 6.4, $\Delta t_{300\ °C}$ on bottom skins in propane burner tests were noticeably reduced for all resin-blended composites containing phenolics, which was unexpected, indicating that the chars from phenolic resins are more conductive.

- Thermal conductivities of chars

Apparent thermal conductivities of chars for all blends were higher than those of the respective controls in both cone and propane burner tests.

Overall, while the presence of phenolics in sandwich composites made from resin blends helped

in reducing their flammability compared to control samples in cone test, the performance in the propane burner test got worse in terms of reduction in burn-through time.

6.3.3 Fire performance of sandwich composite structures with a top layer of phenolic resin

- Flammability

Skins of sandwich composites with a single top layer of phenolic resin (3UP1M and 3UP/VE1M) showed improved fire performances in terms of reduced PHRR and THR in cone test; TTI though was not affected.

- Thermal barrier performance

As seen from Table 6.4 $\Delta t_{300\,^{\circ}C}$ on bottom skins were noticeably reduced in the propane burner test for the 3UP/VE1M composite compared with the UP/VE-Nov control, whereas, $\Delta t_{300\,^{\circ}C}$ in 3UP1M composite remained similar to UP in both tests.

- Thermal conductivities of chars

Apparent thermal conductivities of chars for 3UP1M and 3UP/VE1M were similar or slightly higher than those of the respective controls in both cone and propane burner tests.

Overall, the flammabilities of sandwich composites were reduced by applying a thin layer of phenolic resin on top of both skins, without detrimental effect to thermal barrier performance (burn-through property) of the composite. This indicates that the top phenolic layer acts as a flame retardant coating and does not adversely affect the conductivity of the underlying char.

6.4 Overall fire safety assessment of composite sandwich structures

In the sections above, the flammabilities of different resins of the composite samples in terms of their cone parameters have been evaluated and it was observed that depending on which parameters are used to assess the flammability, the ranking of samples changed. To compile important parameters, fire safety plots (THR *vs.* PHRR/TTI) were plotted, from which overall flammability of different resin types and their blends could be ranked. However, this approach does not include heat transfer through the thickness of the sample, which affects the time to burn-through in a composite.

Here to combine the fire and thermal barrier properties, a thermal barrier efficiency index is proposed, which is defined as:

$$\text{Thermal barrier efficiency index (TBI)} = \frac{\text{PHRR}}{\text{TTI} \times t_{300\,^{\circ}\text{C}}}$$

Where $t_{300\,^{\circ}\text{C}}$ is time taken for the back surface temperature to reach 300 °C in cone or propane burner test.

In Figure 6.8 THR values from cone test at 30 minutes for all composite sandwich structures are plotted against TBI values, using $t_{300\,^{\circ}\text{C}}$ from cone tests (Figure 6.8 (a)) and propane burner tests (Figure 6.8 (b)). From this, there are generally two different zones in behaviours of samples: an upper right corner of neat resins (red circles) and a lower left corner of resin blends containing phenolics (green circles) as can be seen in Figure 6.8 (a) and (b), which use cone and propane burner test results, respectively. However, among different neat resin and resin blend composites, a difference in trend is observed compared to that seen for cast resins in Figure 6.8 (b), which is unexpected. This could be due to different resin content on the surfaces of the skins of sandwich composites compared to cast resins in Figure 6.8 (b). Moreover, in sandwich composites very thin (4 plies) skin layers have been used, hence the resin content in each sample is very low, small differences may cause variations. UP-R seems to be safest. However, all resin blends performed better than neat resins. Among resin blends, UP/Methylon:70/30, VE-Ep/Methylon:70/30 ratio and 3UP1M based composites performed best.

The proposed thermal barrier efficiency index is a preferred fire safety parameter if both reaction to fire (low flammability) and low fire resistance are required criteria for a particular application. The other fire safety parameters commonly used for regulatory purposes are for reaction to fire only, for example, FIGRA (PHRR/time to PHRR) represents fire growth rate, MARHE represents maximum average rate of heat emission, and PHRR/TTI (or TTI/PHRR) represents propensity to flashover.

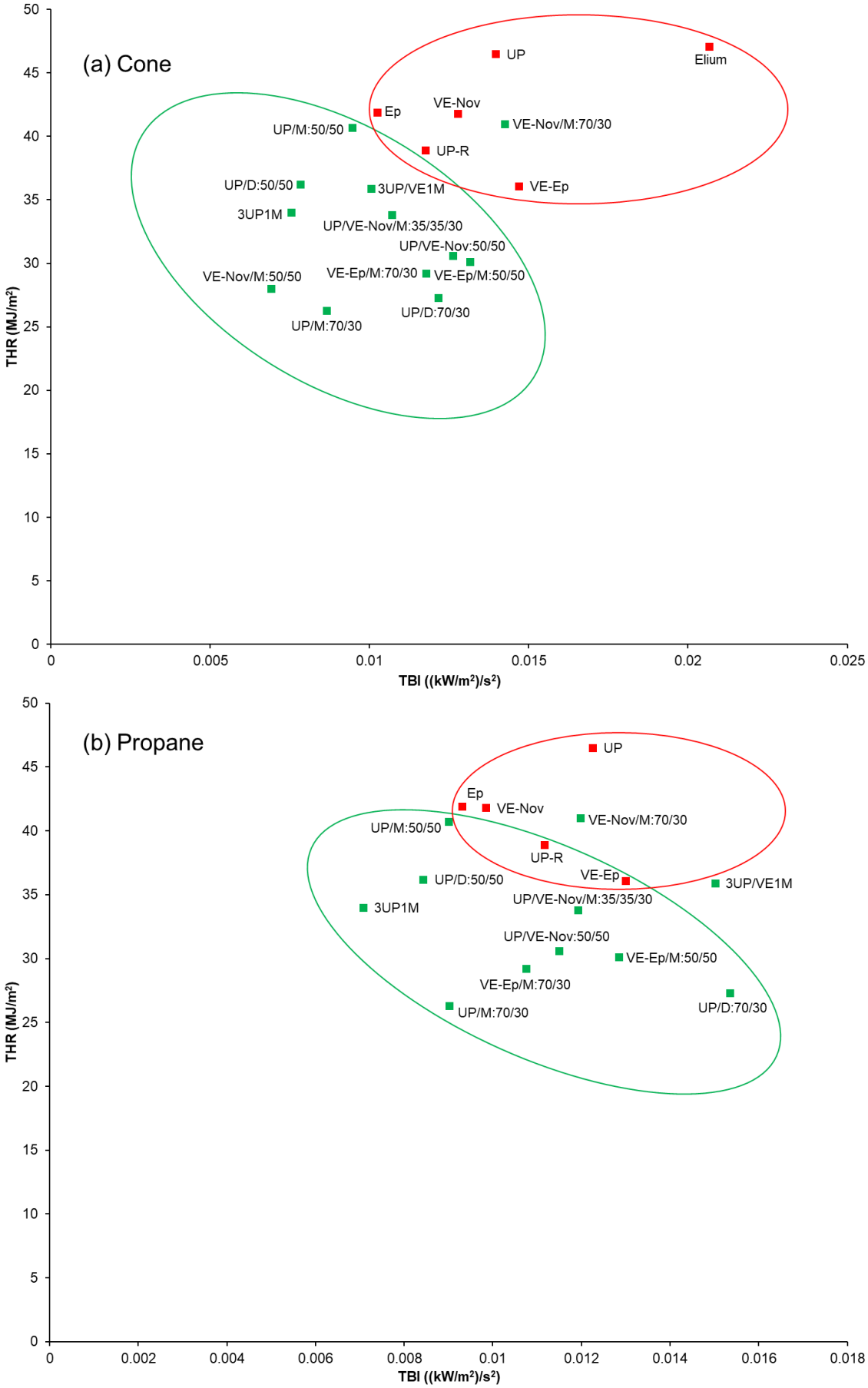

Figure 6.8: Plots of combined fire and thermal properties, THR from cone *vs.* TBI values from (a) cone calorimetry and (b) propane burner tests [sandwich composites with skins of neat resins (red circles) and resin blends containing phenolics (green circles)]

6.5 Recommendations and suggestions for future work

In this work it has been demonstrated that in thick sandwich composites, the resin type has a minimal effect on overall flammability of the composite. The potential of incorporating phenolic resins as blends with UP/VE or using one top layer of phenolic in skins of UP/VE in order to improve both fire and thermal performance of sandwich composites has been demonstrated. In order to take this research forward, the following recommendations are proposed:

1. All samples should be tested for surface flame spread according to IMO Resolution MSC.307(88) Part 5 [6] or using an equivalent small-scale test.

2. The focus of this study was on composites used mainly in the marine industry, hence only glass fabric was studied for the reinforcement. This work could be extended to usage of different types of fibres such as carbon, aramid, glass/carbon or glass/aramid hybrid fabrics or hybrid patterns for different fibre layers in the skins of the sandwich structures.

3. In this work, using phenolic resin in the top ply of the composite skin seemed to be very effective in reducing the flammability of the sandwich structure. This aspect could be further exploited by applying an additional or alternative flame-retardant coating layer on the surface so that the ignition can be greatly delayed or even prevented. Furthermore, using a blended phenolic resin for underlying plies in combination with a phenolic resin as the top ply would gain even more benefits for the fire behaviour of the skin and hence for the sandwich composites.

4. Heat transfer modelling in glass fibre reinforced composites and sandwich composite structures could be carried out to simulate temperature profiles during decomposition, ignition and charring phases under different heating scenarios. The development of computer models could enable engineers and designers to design fire safe composites specific to a particular heat scenario application.

6.6 References

[1] D.W. Van Krevelen, “Some basic aspects of flame resistance of polymeric materials,” *Polymer*, vol. 16, no. 8, pp. 615–620, 1975.

[2] B.K. Kandola, L. Krishnan, D. Deli, and J.R. Ebdon, “Blends of unsaturated polyester and phenolic resins for application as fire-resistant matrices in fibre-reinforced composites. Part 2: Effects of resin structure, compatibility and composition on fire performance,” *Polymer Degradation and Stability*, vol. 113, pp. 154–167, 2015.

[3] J. Zhang, “The flammability of acrylic fibres and polymers,” PhD thesis, University of Bolton, United Kingdom, 1992.

[4] A. Alkhazaleh, “Thermal energy storage and fire safety of building materials,” PhD thesis, the University of Bolton, UK, 2018.

[5] B. K. Kandola, A. Alkhazaleh, and G. J. Milnes, “The fire behaviour of gypsum boards incorporating phase change materials for energy storage in building applications,” in *15th International Conference and Exhibition on Fire and Materials 2017*, 2017, pp. 517–527.

[6] *IMO Resolution MSC.307(88): International Code for Application of Fire Test Procedures*. International Maritime Organization, FTP Code, 2010.

Appendix 1: Cone calorimetric results for balsa wood versus plywood

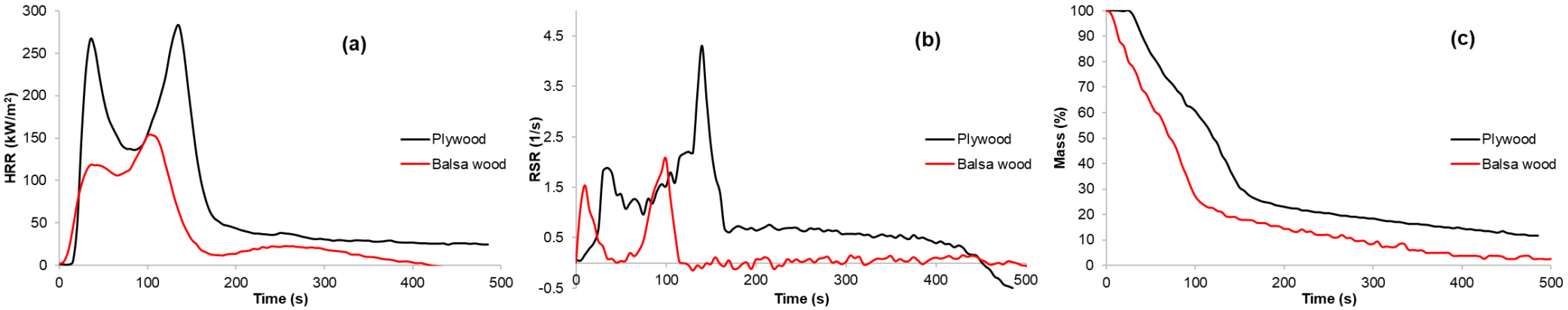

Figure A1-1: Plots of (a) HRR, (b) RSR and (c) mass loss *vs.* time for 6 mm thick plywood and 12.7 mm thick balsa wood

Table A1-1: Derived cone calorimetric results of plywood and balsa wood with thicknesses of 6 mm and 12.7 mm

Sample ID	TTI (s)	FO (s)	PHRR (kW/m^2) Peak 1	PHRR (kW/m^2) Peak 2	THR (MJ/m^2)	TSR (m^2/m^2)	Residue (wt%)
Plywood 6 mm	28 ± 4	372 ± 13	218 ± 63	274 ± 39	37.5 ± 5.5	382 ± 36	16 ± 4
Balsa wood 12.7 mm	5 ± 1	131 ± 1	130 ± 16	159 ± 6	20.8 ± 3.0	116 ± 24	2 ± 0

Notes:

TTI = time-to-ignition, FO = time-to-flame-out, PHRR = peak heat release rate, THR = total heat release, TSR = total smoke release.

The reproducibility in cone parameters was ±5% in general.

Appendix 2: Curing conditions for sandwich composites with skins of neat resins and resin blends containing phenolics

Table A2-1: Curing conditions for composite laminates and sandwich structures with skins of neat resins and resin blends containing phenolics

Sample No.	Sandwich structure samples – Skin types	Curing conditions (°C, h)
	Neat resin + Glass woven plain fabric	
1	UP	RT 24h, 80 ˚C 6h
2	UP-R	RT 24h, 80 ˚C 6h
3	VE-Ep	RT 24h, 80 ˚C 3h, 140 ˚C 3h
4	VE-Nov	RT 24h, 80 ˚C 3h
5	Ep	RT 24h, 80 ˚C 6h
6	Elium	RT 4h, 90 ˚C 6h
	Blended resins + Glass woven plain fabric	
7	UP/Durez:70/30	50 ˚C 6h, 80 ˚C 24h, 90 ˚C 9h, 130 ˚C 1h, 160 ˚C 1h, 180 ˚C 2h
8	UP/Durez:50/50	80 ˚C 24h, 100 ˚C 1h, 130 ˚C 1h, 160 ˚C 1h, 180 ˚C 2h
9	UP/Methylon:70/30	50 ˚C 6h, 80 ˚C 12h, 100 ˚C 8h, 120 ˚C 6h, 130 ˚C 6h, 150 ˚C 2h, 180 ˚C 3h
10	UP/Methylon:50/50	50 ˚C 6h, 80 ˚C 12h, 100 ˚C 8h, 120 ˚C 6h, 130 ˚C 6h, 150 ˚C 2h, 190 ˚C 3h
11	VE-Ep/Methylon:70/30	RT 2h, 80 ˚C 6h, 100 ˚C 6h, 150 ˚C 6h, 180 ˚C 6h
12	VE-Ep/Methylon:50/50	RT 2h, 80 ˚C 6h, 110 ˚C 6h, 140 ˚C 6h, 180 ˚C 6h
13	VE-Nov/Methylon:70/30	RT 2h, 80 ˚C 6h, 100 ˚C 6h, 150 ˚C 6h, 180 ˚C 6h
14	VE-Nov/Methylon:50/50	RT 2h, 80 ˚C 6h, 110 ˚C 6h, 140 ˚C 6h, 180 ˚C 6h
15	UP/VE-Nov:50/50	RT 24h, 80 ˚C 12h
16	UP/VE-Nov/Methylon:35/35/30	50 ˚C 2h, 80 ˚C 12h, 100 ˚C 6h, 120 ˚C 6h, 130 ˚C 6h, 150 ˚C 2h, 180 ˚C 4h, 190 ˚C 6h
17	UP/VE-Nov:50/50; top one layer of Methylon	RT 12h, 80 ˚C 12h, 100 ˚C 8h, 120 ˚C 6h, 130 ˚C 6h, 150 ˚C 2h, 180 ˚C 6h
18	UP; top one layer of Methylon	RT 24h, 80 ˚C 12h, 100 ˚C 8h, 120 ˚C 6h, 130 ˚C 6h, 150 ˚C 2h, 180 ˚C 6h

Appendix 3: Theoretical thermal conductivities of fibre-reinforced composite laminates

Table A3-1: Theoretical values for glass fibre-reinforced composites for thermal conductivity using the rule of mixtures

Sample	Density (g/cm^3)	V_f (%)	V_m (%)	K_{Comp} (kW/m.K × 10^{-3})
UP	1.025	47.8	52.2	0.602
VE	1.05	48.3	51.7	0.606
Epoxy	1.14	50.4	49.6	0.574
Phenolic	1.4	55.5	44.5	0.733

Rule of mixtures: $K_{Comp} = K_f V_f + K_m V_m$

Where K_{Comp} is the overall longitudinal thermal conductivity of the composite, K_f, K_m are the individual thermal conductivities of the fibre and matrix, respectively and V_f, V_m are the fibre volume fraction and matrix volume fraction of the composite.

Appendix 4: Char residue digital images of sandwich composites with skins of different resin blends

Table A4-1: Digital images of sandwich composites with skins of different resin blends, selected one side to represent the char residue after cone calorimeter testing, top view after taking off top burnt composite laminate layers, and back surface laminates of burnt sandwich composite structures

Sample ID	Side view (a)	Top view after taking top laminates (b)	Back surface (c)
UP/Durez:70/30		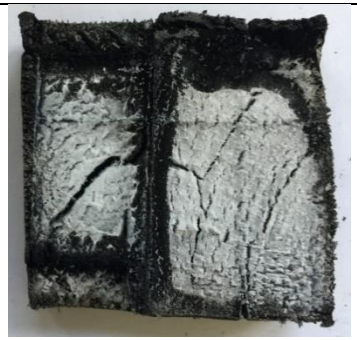	
UP/Durez:50/50			
UP/Methylon:70/30			

UP/Methylon:50/50	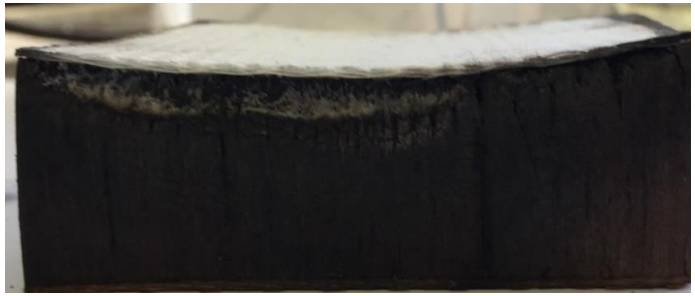		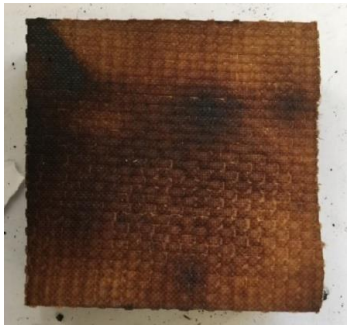
VE-Ep/Methylon:70/30			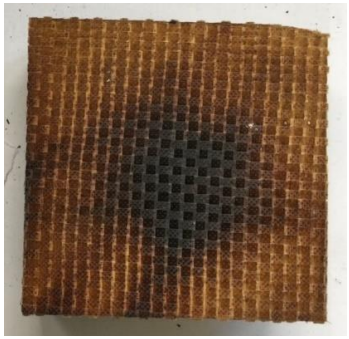
VE-Ep/Methylon:50/50			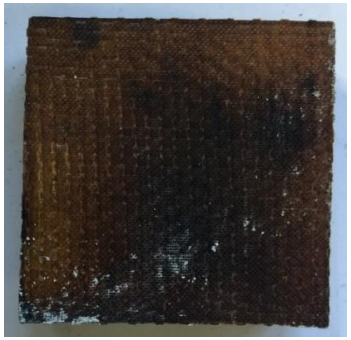

VE-Nov/Methylon:70/30			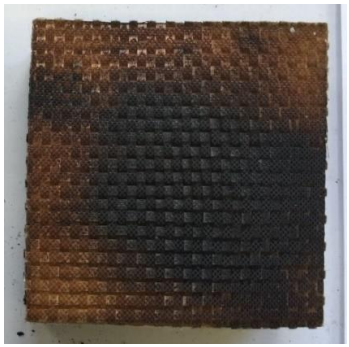
VE-Nov/Methylon:50/50			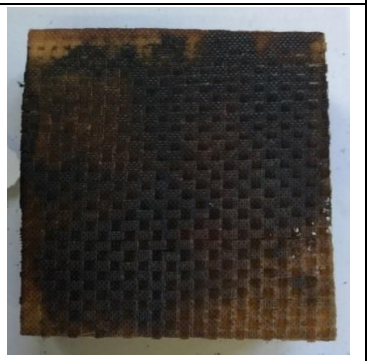
UP/VE-Nov:50/50			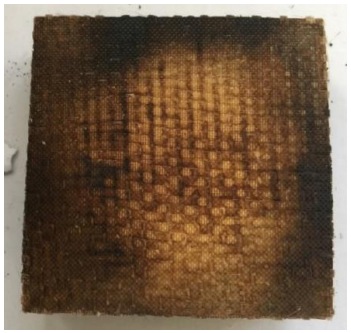

UP/VE-Nov/Methylon:35/35/30			
UP; top one layer of Methylon			
UP/VE-Nov:50/50; top one layer of Methylon